

Advances in Palladium and Nickel Catalyzed Cross-Coupling Reactions

by

Ryan S. Sawatzky

Submitted in partial fulfilment of the requirements  
for the degree of Doctor of Philosophy

at

Dalhousie University  
Halifax, Nova Scotia  
December, 2017

© Copyright by Ryan S. Sawatzky, 2017

## Table of Contents

List of Tables .....	v
List of Figures .....	vi
List of Schemes .....	vii
Abstract .....	ix
List of Abbreviations and Symbols Used .....	x
Acknowledgements .....	xiv
Chapter 1 Introduction .....	1
1.1 Introduction to Catalysis .....	1
1.1.1 Homogeneous versus Heterogeneous Catalysis .....	2
1.2 Modern Homogeneous Transition Metal Catalysis .....	3
1.2.1 General Mechanism of Palladium Catalyzed Reactions and Ligand Effects .....	4
1.3 Overview of Thesis Research .....	6
Chapter 2 Palladium Catalyzed C-O Coupling at Room Temperature .....	8
2.1 Background: Formation of Alkyl Aryl Ethers Using Aliphatic Alcohols .....	8
2.2 Palladium Catalyzed C-O Cross-Coupling Using Aliphatic Alcohols .....	9
2.3 Results and Discussion .....	13
2.4 Summary .....	18
2.5 Experimental .....	18
2.5.1 General Considerations .....	18
2.5.2 General Procedures .....	19
2.5.3 Characterization Data for Isolated Materials .....	23
Chapter 3 Microwave-Assisted Nickel-Catalyzed Synthesis of Aryl Amines from Aryl Halides and Ammonium Salts .....	28
3.1 Buchwald-Hartwig Amination (BHA) .....	28
3.1.1 Catalytic Mechanism of Buchwald-Hartwig Amination .....	29
3.1.2 Buchwald-Hartwig Amination using Ammonia .....	32
3.2 Development of First Row Transition Metal Catalysts .....	32
3.2.1 Nickel Catalyzed Amination Reactions .....	36

3.3	Microwave-Assisted Catalysis .....	39
3.3.1	Microwave Effects .....	40
3.4	Results and Discussion.....	43
3.5	Results and Discussion.....	48
3.6	Summary .....	52
3.7	Experimental .....	53
3.7.1	General Considerations.....	53
3.7.2	General Procedure .....	54
3.3.2	Characterization Data for Isolated Materials.....	58
Chapter 4 Nickel-Catalyzed Cross-coupling of Secondary Amines/Azoles Using a Wide Bite Angle Ligand.....		66
4.1	Utility of Wide Bite Angle Ligands in Transition Metal Catalysis .....	66
4.1.1	Proposed Application to Nickel-Catalyzed C-N Cross-Coupling .....	70
4.2	Results and Discussion.....	71
4.3	Summary .....	78
4.4	Experimental .....	78
4.4.1	General Considerations.....	78
4.4.2	General Procedures.....	79
4.4.3	Characterization of Isolated Materials .....	82
Chapter 5 (DPEphos)Ni(mesityl)Br: An Air-Stable Pre-Catalyst for Suzuki-Miyaura Cross-Couplings Yielding Biheteroaryls .....		89
5.1	Nickel catalyzed Suzuki-Miyaura Cross-Coupling Reactions .....	89
5.2	Results and Discussion.....	91
5.3	Summary .....	98
5.4	Experimental .....	99
5.4.1	General Considerations.....	99
5.4.2	General Procedures.....	100
5.4.3	Characterization of isolated products.....	101
Chapter 6 Conclusions and Future Work.....		114
6.1	Chapter 2: Palladium Catalyzed C-O Cross-Coupling.....	114
6.2	Chapter 3: Microwave Assisted Monoarylation of Ammonium Salts .....	115
6.3	Chapter 4: Wide Bite Angle Ligands in Nickel-Catalyzed C-N Cross-Coupling.....	116

6.4 Chapter 5: Suzuki-Miyaura Cross-Coupling using (DPEphos)Ni(mesityl)Br .....	116
References .....	118
Appendix .....	A1
Chapter 2 Characterization Data .....	A1
Chapter 3 Characterization Data .....	A13
Chapter 4 Characterization Data .....	A32
Chapter 5 Characterization Data .....	A64

## List of Tables

<b>Table 2-1:</b> (Hetero)aryl halide scope with optimal ligand reported.....	14
<b>Table 2-2:</b> Alcohol scope with optimal ligand reported.....	16
<b>Table 2-3:</b> Examples of C-O coupling with structurally diverse mesylates.....	17
<b>Table 3-1:</b> Select examples of bisphosphines used in cobalt catalyzed asymmetric hydrogenation of alkenes.....	34
<b>Table 3-2:</b> Examples of copper catalyzed asymmetric hydroamination.....	35
<b>Table 3-3:</b> Select examples of nickel-catalyzed amination of aryl chlorides.....	37
<b>Table 3-4:</b> Ligand complex <b>C3-3</b> used by Hartwig and examples of nickel-catalyzed ammonia monoarylation.....	39
<b>Table 3-5:</b> Scope of nickel catalyzed ammonia monoarylation using ammonium acetate under microwave conditions.....	50
<b>Table 3-6:</b> Nickel catalyzed aminations using MeNH <sub>3</sub> Cl and EtNH <sub>3</sub> Cl using microwave heating.....	51
<b>Table 4-1:</b> Ligand screen for nickel catalyzed C-N cross-coupling.....	73
<b>Table 4-2:</b> Scope of C(sp <sup>2</sup> )-N cross-coupling using <b>C4-1</b> .....	76
<b>Table 5-1:</b> Optimization of Conditions and Pre-Catalyst Screening.....	93
<b>Table 5-2:</b> Suzuki-Miyaura Cross-Couplings Using <b>C4-1</b> .....	94
<b>Table 5-3:</b> Optimization of Conditions for Pyridinyl Boronic Acids Using <b>C4-1</b> .....	96
<b>Table 5-4:</b> Suzuki-Miyaura Cross-couplings of Pyridinyl Boronic Acids Using <b>C4-1</b> .....	98

## List of Figures

<b>Figure 1-1:</b> General mechanisms for the Suzuki and Heck reactions.....	5
<b>Figure 2-1:</b> Examples of drugs containing the aryl alkyl ether moiety.....	9
<b>Figure 2-2:</b> General palladium catalyzed C-O cross-coupling mechanism and some useful ligands used in such reactions.....	10
<b>Figure 2-3:</b> Ligands used in catalytic screening for palladium-catalyzed C-O coupling...	12
<b>Figure 3-1:</b> General mechanism for Buchwald-Hartwig aminations.....	30
<b>Figure 3-2:</b> Examples of state-of-the-art ligands used in BHA chemistry.....	31
<b>Figure 3-3:</b> Complexes and ligands used by Buchwald and Hartwig for nickel-catalyzed amination reactions.....	37
<b>Figure 3-4:</b> The PAd-Dalphos ligand developed by the Stradiotto group.....	46
<b>Figure 4-1:</b> The bite angle ( $\varphi$ ) for a bidentate ligand.....	67
<b>Figure 4-2:</b> <i>Cis</i> and <i>trans</i> geometries in square planar metal complexes.....	67
<b>Figure 4-3:</b> Examples of wide bite angle ligands.....	68
<b>Figure 4-4:</b> Xantphos variants to be synthesized.....	71
<b>Figure 4-5:</b> Wide bite angle ligand variants tested in nickel-catalyzed C-N cross-coupling.....	72
<b>Figure 4-6:</b> Single-crystal X-ray structure of <b>C4-1</b> .....	75

## List of Schemes

<b>Scheme 1-1:</b> Examples of palladium catalyzed C-C cross-coupling reactions.....	4
<b>Scheme 2-1:</b> Generic reaction schemes for Williamson ether synthesis and Chan-Lam coupling.....	10
<b>Scheme 2-2:</b> General reaction conditions for palladium-catalyzed C-O cross-coupling reactions.....	11
<b>Scheme 2-3:</b> C-O coupling with aryl sulfonates.....	17
<b>Scheme 3-1:</b> Amine synthesis through sequential Mitsunobu and Staudinger reactions...	29
<b>Scheme 3-2:</b> General scheme of BHA.....	29
<b>Scheme 3-3:</b> Derivative of the pharmaceutical Cinacalcet synthesized through copper catalyzed asymmetric hydroamination.....	35
<b>Scheme 3-4:</b> General nickel catalyzed monoarylation of ammonia.....	39
<b>Scheme 3-5:</b> Examples of palladium-catalyzed Heck reaction performed under microwave heating and their comparison to conventional heating methods.....	42
<b>Scheme 3-6:</b> General scheme of the palladium-catalyzed Suzuki coupling using the phosphadadamantane ligand ( <b>L3-16</b> ).....	45
<b>Scheme 3-7:</b> Synthesis of PAd-Dalphos ( <b>L3-17</b> ) and the corresponding precatalyst ( <b>C3-4</b> ).....	46
<b>Scheme 3-8:</b> Nickel-catalyzed monoarylation of ammonia using microwave heating.....	48
<b>Scheme 4-1:</b> General hydroformylation reaction showing linear and branched products..	68
<b>Scheme 4-4:</b> Proposed synthesis of known and new Xantphos variants, variants of DPEphos to be synthesized in similar fashion.....	72
<b>Scheme 4-5:</b> Synthesis of the air-stable precatalyst <b>C4-1</b> .....	74
<b>Scheme 4-2:</b> General nickel catalyzed hydrocyanation showing linear and branched products.....	69

<b>Scheme 4-3:</b> Sequential aminations to give asymmetric aryl amines using Xantphos.....	71
<b>Scheme 5-1:</b> Electrophile Selectivity in Suzuki-Miyaura Cross-couplings Using <b>C4-1</b> ....	95
<b>Scheme 6-1:</b> Example of potential 2-step cross-coupling enabled by selective Suzuki-Miyaura cross-coupling with <b>C4-1</b> .....	117



## Abstract

Homogeneous organometallic complexes have become an indispensable tool as they are employed as catalysts for a large number of chemical transformations. Ancillary ligands, organic molecules that bind to the metal center, are critical for fine tuning the performance of these catalysts. The initial portion of this thesis describes a comparative survey of several state-of-the-art ligands for Pd catalyzed C-O cross-coupling reactions. As part of this survey two sets of conditions are employed: reactions carried out at 90 °C, using 1 mol % Pd, and room temperature reactions, using 7 mol % Pd. In these comparisons, it was found that Rockphos was the ligand of choice for reactions at room temperature, as well for electron rich electrophiles. The Josiphos variant, CyPF-*t*Bu, was the optimal ligand for reactions at elevated temperatures, as well as for activated electrophiles.

Many ligands that have found use in Pd chemistry have been repurposed for use in Ni catalysis. While this an effective strategy, it is not necessarily ideal. The bisphosphine PAd-Dalpos has been tailored for Ni catalyzed monoarylation of ammonia, and primary amines. Here, ammonium, methylamine, and ethylamine salts are successfully used as cross-coupling partners employing microwave heating. High yielding reactions, utilizing as little as 1 mol % Ni can be completed in as little as 5 minutes under these conditions.

In an effort to establish trends of reactivity in Ni catalysis, the complex (DPEphos)Ni(mesityl)Br was developed for both C-N, C-C cross-coupling reactions. This complex was first established in the cross-coupling of secondary amines, and azoles with activated aryl chlorides. The observation of PhB(OH)<sub>2</sub> required as a catalyst activator lead to the development of this complex as a catalyst for C-C cross-coupling using unstable 5-membered heterocyclic boronic acids for challenging biheteroaryl formation. Here reactions conducted at room temperature were found to be comparable to the previous state-of-the-art Ni catalysis. In addition, 3-pyridinyl-boronic acids were also successfully employed. While the scope of reactivity with such challenging substrates was modest, the work herein represents a step forward as only a small handful of examples exist for Ni catalyzed reactions.

## List of Abbreviations and Symbols Used

$\alpha$	alpha position, first carbon adjacent to a carbonyl group or metal
$\beta$	beta position, second carbon adjacent to a carbonyl group or metal
$\delta$	chemical shift
$\eta$	hapticity (contiguous donor atoms)
$\kappa$	hapticity (non-contiguous donor atoms)
1-Ad	1-adamantyl
Ar	aryl
Bippyphos	Ligands containing the 1',3',5'-triphenyl-1'-H-[1,4]bipyrazole core
BINAP	2,2'-bis(diphenylphosphino)-1,1'-binaphthalene
BHA	Buchwald-Hartwig amination
Bn	benzyl
Boc	tert-butoxycarbonyl
catASium MNN(R)	(-)-4,5-bis[(2R,5R)-2,5-dimethylphospholanyl](1,2-dimethyl-1,2-dihydropyridazine-3,6-dione
cataCXium A	di(1-adamantyl)- <i>n</i> -butylphosphine
<i>cis</i>	adjacent donor atoms in a square planar complex
CgPH	2,4,6-trioxa,1,3,5,7-tetramethyl-8-phosphaadamantane
COD	1,5-cyclooctadiene

Cp	cyclopentadienyl, $\eta$ -5C <sub>5</sub> H <sub>5</sub>
CPME	cyclopentyl methyl ether
Cy	cyclohexyl
CyPF- <i>t</i> Bu	(R)-(-)-1-[(S)-2-(dicyclohexylphosphino)ferrocenyl]ethyl-di- <i>tert</i> -butylphosphine
d	doublet
DEAD	diethyl azodicarboxylate
DcPPF	1,1-bis(dicyclohexylphosphino)ferrocene
DiPPF	1,1'-bis(diisopropylphosphino)ferrocene
DME	dimethoxyethane
DMF	dimethylformamide
DPEphos	bis[(2-diphenylphosphino)phenyl] ether
DPPF	1,1'-bis(diphenylphosphine)ferrocene
ESI	electrospray ionization
GP	General Procedure
h	hour(s)
HRMS	high-resolution mass spectrometry
i.d.	internal diameter
IPr	1,3-bis(2,6-diisopropylphenyl)imidazole-2-ylidene

L	neutral 2-electron donor
L <sub>n</sub>	general ligand set
M	mol/L or molecular ion or generic metal
m	multiplet
<i>m/z</i>	mass to charge ratio
Mor-Dalpos	<i>N</i> -[2-di(1-adamantyl)phosphino]phenylmorpholine
nd	not detected
<i>n</i> Bu	<i>n</i> -butyl
NBS	<i>N</i> -bromosuccinimide
NHC	<i>N</i> -heterocyclic carbene
NMR	nuclear magnetic resonance
OAc	acetate
OMs	mesylate
<i>ortho</i>	adjacent position on an aromatic ring
OTs	tosylate
PAd-Dalpos	1,3,5,7-tetramethyl-8-(2-di- <i>o</i> -tolylphosphinophenyl)-2,4,6-trioxa-8-phosphaadamantane
PEPPSI	pyridine-enhanced precatalyst preparation stabilization initiation
PTFE	poly(tetrafluoroethylene)

Ph	phenyl
q	quartet
Rockphos	2-di( <i>tert</i> -butyl)phosphino-2',4',6'-triisopropyl-3-methoxy-6-methylbiphenyl
s	singlet
(S)-DTBM-SEGPPOS	(S)-(+)-5,5'-bis[di(3,5-di- <i>tert</i> -butyl-4-methoxyphenyl)phosphino]-4,4'-bi-1,3-benzodioxole
SM	Suzuki-Miyuara
<i>s</i> Bu	<i>sec</i> -butyl
t	triplet
( <i>S,S',R,R'</i> )-Tangphos	(1 <i>S</i> ,1 <i>S'</i> ,2 <i>R</i> ,2 <i>R'</i> )-1,1'-di- <i>tert</i> -butyl-(2,2')-diphospholane
<i>t</i> Bu	<i>tert</i> -butyl
TCT	2,4,6-trichloro-1-3-5-triazine
TMEDA	<i>N,N,N',N'</i> -tetramethylethylenediamine
<i>trans</i>	donor atoms opposite each other in a square planar complex
X	halide substituent or anionic ligand
Xantphos	4,5-bis(diphenylphosphino)-9,9-dimethylxanthene

## Acknowledgements

I would like to thank the Stradiotto group members (past and present) whose aid has made this work possible. I would like to thank Breanna Hargreaves for her help with the palladium catalyzed C-O project. I extend my greatest appreciation to my supervisor, Dr. Mark Stradiotto for the guidance, assistance and direction during my research to date.

I would also like to thank Dr. Mike Lumsden (NMR3) for assistance with NMR experiments, Mr. Xiao Feng (Dalhousie) for the collection of all mass spectrometry data, and Drs. Robert McDonald and Michael Ferguson (Alberta X-ray Crystallography Lab) for the collection, and refinement of X-ray data.

Dr. Laura Turculet, and her group are also acknowledged for helpful discussions, as well as help around the lab.

Lastly, I wish to thank all my friends, and family who have made this work possible. Through all the late nights, and conversations when events did not turn out as planned. Your help has been invaluable.

# Chapter 1 Introduction

## 1.1 Introduction to Catalysis

Catalytic chemistry has become an integral part of synthetic chemistry. Reactions that employ catalysts have enabled chemists to achieve transformations that would otherwise be impossible by using traditional methods. Current research in the area of catalytic chemistry focuses on the development of new and improved catalysts with the aim of synthesizing complex, high-value molecules from the simplest, most abundant materials possible. Not only is the goal to develop new methods, but to improve upon traditional synthetic chemistry, thereby making reactions “greener” by using more environmentally friendly reaction conditions and reagents.

A catalyst is defined as a substance that increases the rate of reaction, but is not consumed, and is regenerated in the process. Catalysts operate by lowering the activation barrier of a reaction; in doing so they provide a lower energy reaction pathway, allowing the reaction to proceed.<sup>[1]</sup> Nature has evolved enzymatic catalysts, which are involved in a diverse number of biological processes. These catalysts, while extremely efficient, are often very selective with respect to their target substrates. Many enzymes cease to function if the target molecule is modified even in small ways.<sup>[2]</sup> In contrast, traditional synthetic chemical methods often employ the use of acids or bases as catalysts for reactions. The use of these catalysts can be applied to a large variety of reactions types, as well as a large number of substrates. The drawback in this case is that these reactions are not always

selective, with undesired side reactions, or poor selectivity occurring as a result. Bridging these two catalyst types are transition metal catalysts. Reactions employing appropriately designed transition metal catalysts can be applied to a wide substrate scope, while still maintaining good selectivity.

### **1.1.1 Homogeneous versus Heterogeneous Catalysis**

Catalysts can be broadly classified in two categories: heterogeneous and homogeneous. Heterogeneous catalysts operate in a separate phase than the reaction. Typically, these catalysts are solids acting on a liquid or gas phase reaction. Catalysts of this type have the advantages of being very robust, and are often capable of operating under high pressures and temperatures. Furthermore, these catalysts are easily separated from reaction mixture and can be recovered for reuse in further reactions. However, these catalysts are difficult to study as their active site is not easily characterized. As a consequence, the mechanisms of reactions employing heterogeneous catalysts are not easily studied, this results in the inability to fine tune the catalyst to suit the target reaction. A common example of a heterogeneous catalyst is the catalytic converter in automobiles. This catalyst is a solid monolith comprised of multiple platinum-group metals (i.e. Ru, Os, Rh, Ir, Pd, Pt) supported on a main group oxide. As the exhaust from the engine is passed over this catalyst, the catalyst transforms many toxic molecules to comparatively more benign forms, such as the conversion of carbon monoxide to carbon dioxide.



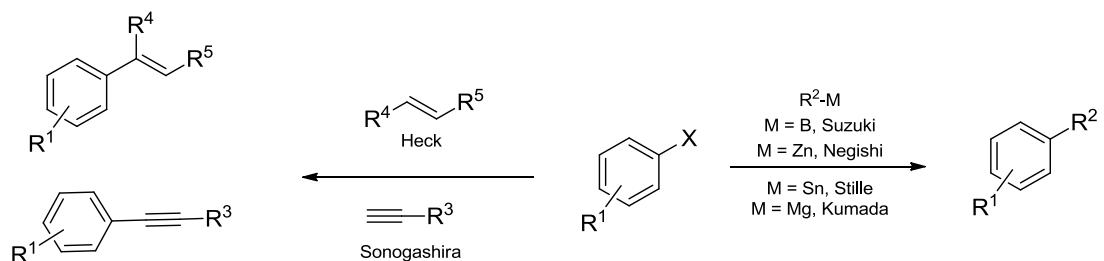
Homogeneous catalysts operate in the same phase as the reactants. These catalysts operate under milder conditions and often decompose under the more forcing conditions that are used with more robust heterogeneous catalysts. Also, as these catalysts are in the same phase as the reactants, their separation from the products is not as easy. Recovery is also problematic; in many cases homogeneous catalysts are not reused in multiple reactions. What makes homogeneous catalysts attractive is the well-defined nature of the active site. Since these catalysts can be easily characterized, their role in the reaction can be studied. Once the mechanism is understood, the catalyst can be tuned by modification of the supporting ligands. The structure of these ligands is an important contributor toward the performance of these catalysts. Changing one functional group on the ligand can have a profound effect on the reactivity of the catalyst, imparting improvement in rates and selectivity. The focus of this document will be on the application of homogeneous transition metal catalysts.

## **1.2 Modern Homogeneous Transition Metal Catalysis**

The development of modern homogeneous transition metal catalysts began in the latter half of the twentieth century. The catalysts developed during this time have been recognized by the awarding of the Nobel Prize in Chemistry in 2001, 2005, and 2010. The prize in 2001 was awarded to Noyori, Knowles, and Sharpless for their contributions to asymmetric catalysis.<sup>[3]</sup> The 2005 prize was given to Schrock, Grubbs, and Chauvin for the development of olefin metathesis reactions.<sup>[4]</sup> The prize most related to the work described in this document is the 2010 award, which was given to Suzuki, Heck, and Negishi for their

work on palladium catalyzed C-C bond forming reactions. Suzuki, and Negishi coupling reactions use organoboron<sup>[5]</sup> and organozinc reagents,<sup>[6]</sup> respectively, as coupling partners for aryl and alkyl electrophiles, such as organohalides. The Heck reaction involves the coupling of aryl electrophiles with substituted alkenes to yield more complex alkene molecules.<sup>[7]</sup> In all three of these reactions sub-stoichiometric amounts of palladium, with respect to the electrophile, are used as the catalyst (**Scheme 1-1**).

Since these initial breakthroughs, multiple new palladium catalyzed C-C bond forming methodologies have been developed. Kumada coupling uses organomagnesium reagents as coupling partners for aryl or alkyl electrophiles.<sup>[8]</sup> Stille coupling involves the use of organostannanes as coupling partners with aryl halides to afford substituted arenes.<sup>[9]</sup> Sonogashira reactions couple aryl halides with terminal alkynes to form functionalized aryl alkynyl products.<sup>[10]</sup> Each of these represents a useful synthetic protocol for use by industrial and academic chemists. Furthermore, continued reaction development has allowed heteroatomic coupling partners to be used, yielding highly functionalized C-O, C-N, C-P and C-S products.



**Scheme 1-1:** Examples of palladium catalyzed C-C cross-coupling reactions, employing a generic electrophile.

### 1.2.1 General Mechanism of Palladium Catalyzed Reactions and Ligand Effects

The aforementioned C-C coupling reactions can be represented by a catalytic cycle with several elementary steps (**Figure 1-1 a**). The first step, known as oxidative addition, occurs when the metal center ‘inserts’ into the C-X (X is either a halide or pseudohalide) bond of the aryl electrophile. Removal of the halide and concomitant addition of a carbon nucleophile (R) to the metal center represents the transmetalation step. Finally, the C-C bond forming step, reductive elimination, occurs which releases the product and regenerates the catalyst. There are deviations from this cycle; the Heck reaction,<sup>[11]</sup> for example has some notable differences (**Figure 1-1 b**). Oxidative addition occurs first, followed by olefin coordination and subsequent migratory insertion, rather than transmetalation. The product is released via abstraction of a  $\beta$ -hydride to give the substituted alkene. The catalyst is regenerated by base-promoted extraction of HX during or following the reductive elimination step.

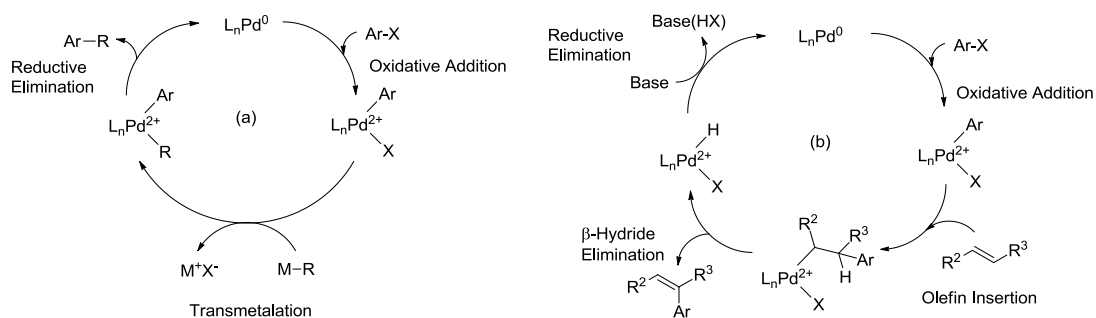


**Figure 1-1:** (a) General mechanism for Suzuki and related cross-couplings, (b) general mechanism for the Heck reaction.

The supporting ligands have a profound impact on each of these elementary mechanistic steps, whereas their influence can promote some steps while hindering others.<sup>[12]</sup> Strong electron donation to the metal center can make oxidative addition more favorable, while disfavoring reductive elimination. Conversely, ligands that are less donating of electron

density to the metal center, or  $\pi$ -accepting ligands, favor reductive elimination while disfavoring oxidative addition. Steric effects also play an integral part in each of these steps. Large bulky ligands tend favor reductive elimination while hindering oxidative addition, transmetalation, and substrate coordination steps; however bulky ligands can aid by keeping the metal center monoligated, which facilitates oxidative addition. Balancing of all these factors is critical to the design of effective catalysts.<sup>[12]</sup>

### **1.3 Overview of Thesis Research**

Chapter 2 of this document describes my work in palladium-catalyzed C-O cross-coupling. My goal in this area was to expand the scope of these reactions and to identify a catalyst which exhibits desirable performance at ambient temperatures. To this end, head-to-head comparison reactions of established palladium catalysts with “Dalphos” ligands, developed by the Stradiotto group, were conducted.

Chapter 3 outlines my work in microwave-assisted nickel-catalyzed aminations using ammonium salts. This work focuses on a new ligand designed by the Stradiotto group specifically for use in nickel-catalyzed amination reactions. The use of ammonium salts as coupling partners allows for the easy handling of reagents that would otherwise be found in gaseous form or in commercial stock solutions of pre-determined concentration. This work also makes use of microwave heating, both to reduce reaction times as well as to enable challenging reactions to be completed.

Chapter 4 describes my work in the development of a highly effective DPEphos nickel precatalyst for the use in C-N cross-coupling of activated aryl halides with secondary amines and azoles. The main purpose of this work was to diversify the catalysts for these reactions, adding to the synthetic chemist's toolbox. In addition, this work also aids in establishing trends in reactivity, allowing for the more rational design of catalyst systems in the future.

Chapter 5 describes my work using the DPEphos precatalyst developed in Chapter 4 in challenging nickel catalyzed Suzuki-Miyaura cross-coupling reactions to afford biheteroaryls. Furthermore, this catalyst is able to accommodate pyridine boronic acids, which have been a particular challenge in these transformations.

Finally, Chapter 6 outlines potential avenues of future study arising from my thesis research.

## Chapter 2 Palladium Catalyzed C-O Coupling at Room Temperature

### 2.1 Background: Formation of Alkyl Aryl Ethers Using Aliphatic Alcohols

Alkyl aryl ethers are common moieties found in many synthetic and pharmaceutical products. Among the top five selling pharmaceuticals in 2013, three contain this functionality (**Figure 2-1**). Traditionally this moiety is synthesized through either the Williamson ether synthesis (**Scheme 2-1**) or nucleophilic (aromatic) substitution. Both of these methods tend to require harsh reaction conditions, with the Williamson synthesis using either alkali metals or strong bases, and nucleophilic substitution requiring an acidic or basic reaction medium. Additional challenges exist in that if the alkyl halide is too hindered, the alkoxide will act as a base yielding the elimination product and the alcohol. Alternative copper mediated methods which include Ullmann coupling<sup>[13]</sup> and Chan-Lam<sup>[14]</sup> coupling are also available. However, Ullmann coupling uses stoichiometric amounts or high loadings of copper which is not ideal.<sup>[15]</sup> Chan-Lam coupling uses catalytic amounts of copper to couple aryl boron reagents with aliphatic alcohols to yield alkyl aryl ethers;<sup>[16]</sup> while effective, the drawback to this method is the availability of required boron reagents.

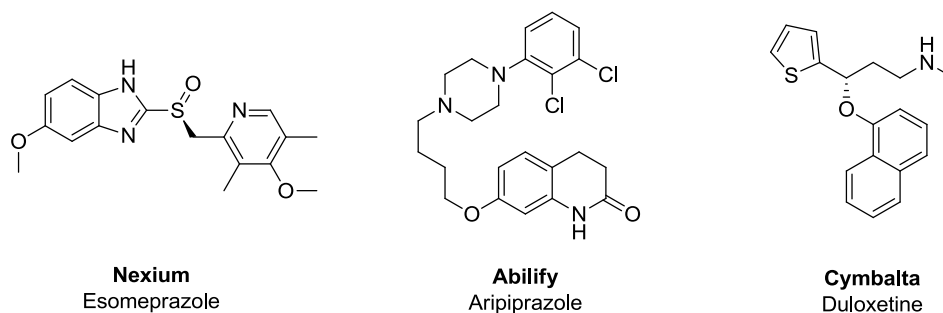
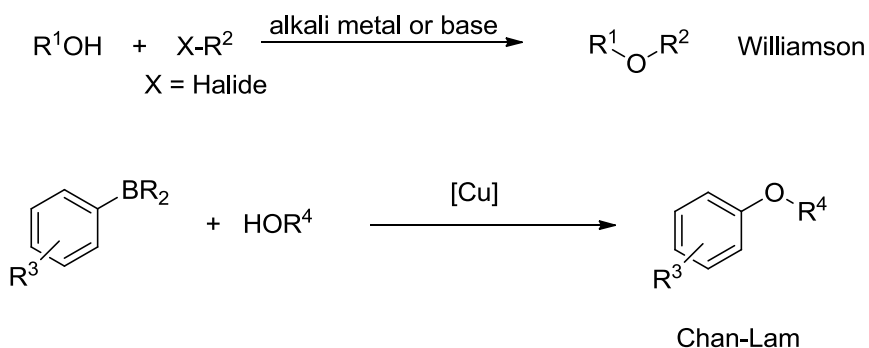


**Figure 2-1:** Examples of drugs containing the aryl alkyl ether moiety.

## 2.2 Palladium Catalyzed C-O Cross-Coupling Using Aliphatic Alcohols

The first reports of palladium catalyzed C-O coupling using primary and secondary aliphatic alcohols as coupling partners was reported by Buchwald in 2001<sup>[17]</sup> and 2005<sup>[18]</sup> respectively. While effective, there was substrate dependence with respect to the optimal ligand for such reactions, and the coupling of electron-rich aryl halides was not achieved. Despite mechanistic similarities to other palladium catalyzed cross-couplings (**Figure 2-2**), much less progress has been achieved in the C-O cross-coupling of primary and secondary alcohols with aryl electrophiles. This is due to  $\beta$ -hydride elimination of the metal alkoxide intermediate being very favorable,<sup>[19]</sup> ultimately leading to the formation of the corresponding ketone or aldehyde, and the dehalogenated aryl species. Palladium-catalyzed coupling of tertiary alcohols<sup>[20]</sup> and phenols,<sup>[21]</sup> which lack  $\beta$ -hydrogen atoms do not suffer from this problem; as such, several protocols exist for the use of these coupling partners. In 2001, Buchwald reported the first example of C-O coupling of alcohols featuring  $\beta$ -hydrogen atoms with aryl bromides and chlorides.<sup>[17-18]</sup> This early work was limited in that unactivated aryl halides required *ortho*-substitution to drive reductive

elimination. Relatively little work has been done to improve upon these initial methods. The current state-of-the-art in palladium-catalyzed C-O coupling is represented by the work of Beller,<sup>[19]</sup> Buchwald,<sup>[22]</sup> and Maligres (Merck)<sup>[23]</sup> using Ad-Bippyphos, Rockphos and CyPF-*t*Bu ligands respectively (**Scheme 2-2**).<sup>[24]</sup>



**Scheme 2-1:** Generic reaction schemes for Williamson ether synthesis and Chan-Lam coupling.

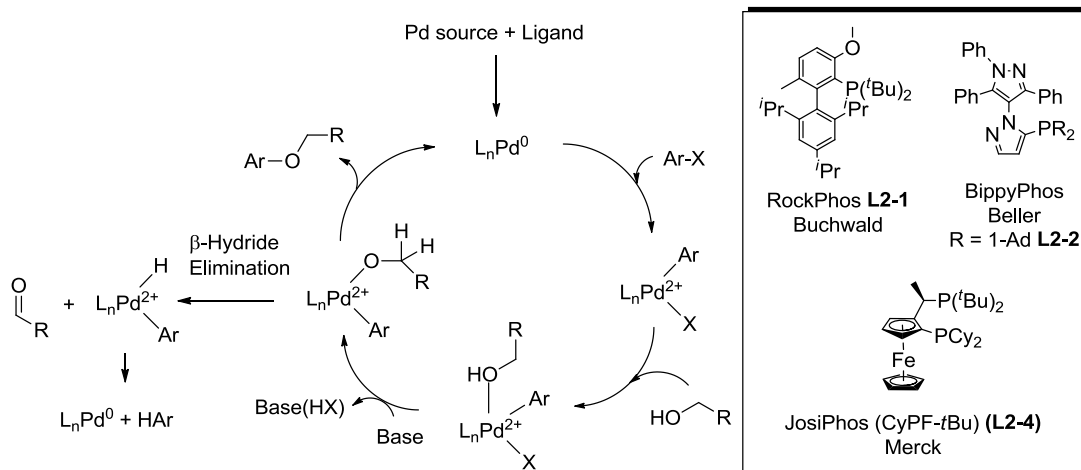
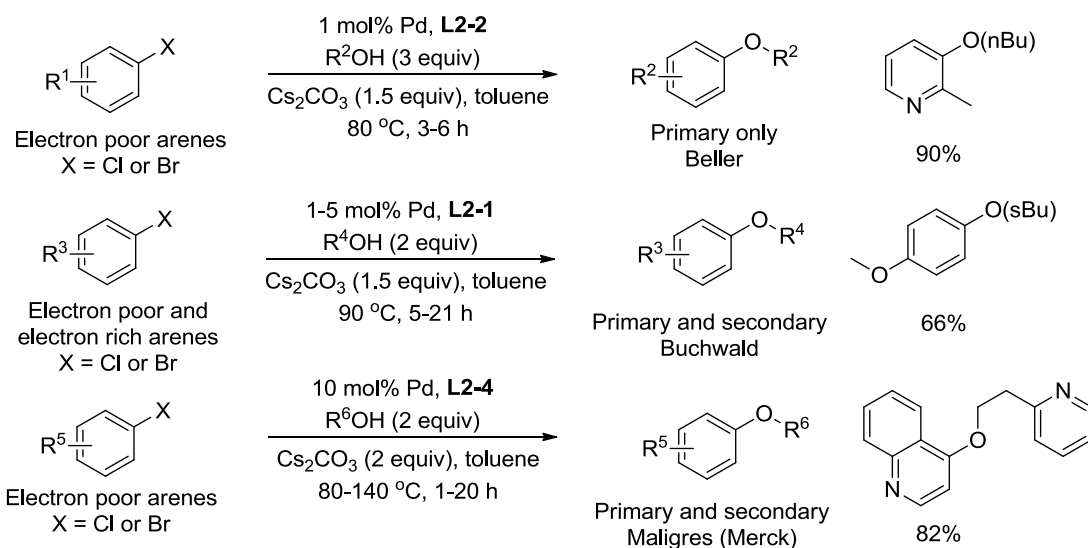


**Figure 2-2:** General palladium catalyzed C-O cross-coupling mechanism and some useful ligands used in such reactions.

The combined aforementioned work of Beller and Buchwald display a fairly large substrate scope with respect to the aryl halide electrophile, with Beller's catalyst featuring **L2-2** being unable to accommodate electron-rich electrophiles. Furthermore, the work of Beller focuses solely on a very limited number of linear primary alcohols, almost



exclusively 1-butanol.<sup>[19]</sup> Buchwald's work using **L2-1** is similar in scope, with the exception that a small number of secondary alcohols, mostly 2-butanol, are also employed. Buchwald's catalyst system also requires the addition of 4 Å molecular sieves, and the use of triethylamine as the solvent is required in many cases to achieve good yields.<sup>[25]</sup> This report was the first to use deactivated electrophiles; however, these substrates have diminished yields when bearing *ortho*-substitution or when coupled with secondary alcohols. While the report from Maligres using **L2-4** shows an impressive alcohol scope, only activated aryl halides are successfully employed. These methods all suffer as the use of high catalyst loadings, and elevated temperatures are required to force these reactions to completion. This work is summarized in **Scheme 2-2**.



**Scheme 2-2:** General reaction conditions for palladium-catalyzed C-O cross-coupling reactions by Beller, Buchwald and Maligres with select examples shown.

Together, the reports from Beller, and Buchwald have established reasonable aryl halide scope in palladium-catalyzed C-O cross-coupling, including examples of electron rich aryl halides; but these are lacking in the alcohol scope and in the case of the report from Buchwald, additional additives were required to achieve reasonable yields. The report from

Maligres and co-workers featured a good selection of alcohol coupling partners, but activated aryl halides and high loadings were required to achieve good yields. One major drawback to these reports is that the ligands employed are expensive; the ligands used in the Maligres and Buchwald papers, Josiphos (**L2-4**) and Rockphos (**L2-1**) respectively, cost over \$600/g (**Figure 2-2**). The Stradiotto group previously reported a palladium catalyst system based on Mor-Dalpos (**L2-5**, **Figure 2-3**) that exhibits similar or superior reactivity in selective palladium-catalyzed C-N couplings,<sup>[26]</sup> relative to Josiphos (**L2-4**). As a part of my thesis research, I became interested to see if the analogous reactivity is applicable in C-O chemistry, providing a cheaper alternative to the previous catalyst systems, and perhaps expanding the substrate scope. Furthermore, I sought to identify catalysts that might operate at ambient temperature, so as to avoid the use of forcing conditions, especially when using volatile aliphatic alcohols. The ligands examined in my reaction survey are presented in **Figure 2-3**.

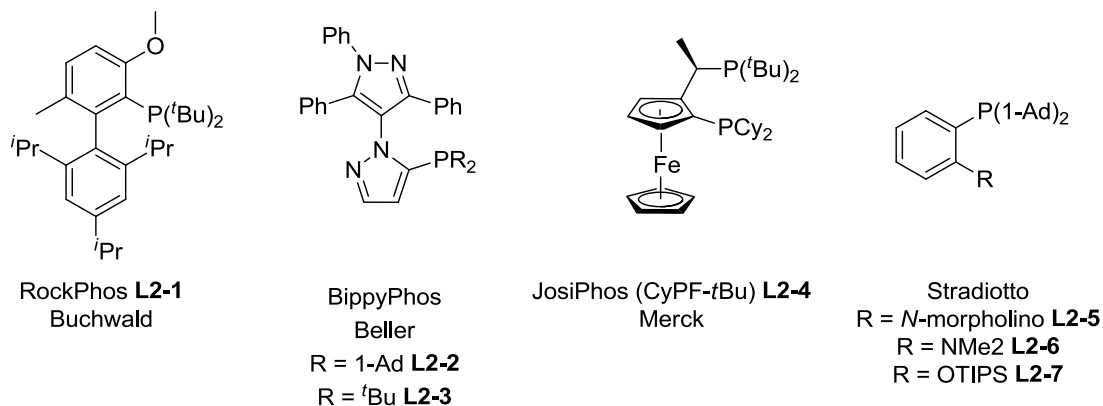


**Figure 2-3:** Ligands used in catalytic screening for palladium-catalyzed C-O coupling.

## 2.3 Results and Discussion

As the Maligres report already contained an extensive ligand screen,<sup>[23]</sup> the catalytic behavior of high-performing ligands in challenging palladium-catalyzed C-O couplings was compared to that of several Dalphos variants (**Table 2-1**). Representative commercially available substrates were employed using optimized conditions reported previously,<sup>[22-23]</sup> including the choice of base and solvent. In initial test reactions at 90 °C (1 mol% Pd) using 4-chloroquinoline and 2-phenylethanol as coupling partners (**2-2a**) it was observed that Ad-Bippyphos (**L2-2**), Josiphos (**L2-4**), Rockphos (**L2-1**) and Mor-Dalphos (**L2-5**) performed equally well. *t*Bu-Bippyphos (**L2-3**) performed comparably in this reaction giving an estimated 80% conversion to product; however, the other two Dalphos variants performed poorly (**L2-6** and **L2-7**) in these reactions, showing less than 20% conversion. In an attempt to separate out a superior system, the same reactions were conducted at ambient temperature. Higher catalyst loadings (7 mol % Pd) were required to achieve excellent reactivity under these conditions, with Ad-Bippyphos (**L2-2**), Josiphos (**L2-4**), Rockphos (**L2-1**), and Mor-Dalphos (**L2-5**) affording complete conversion to **2-2a** (**Table 2-1**). In an effort to differentiate these ligands and to ascertain trends in reactivity, the survey was expanded to other substrates. The results of this catalytic survey are presented in **Tables 2-1** and **2-2**, with the best-performing ligand at 90 °C ([A] 1 mol% Pd) and at 25 °C ([B] 7 mol% Pd) as indicated.

Reactivity surveys such as this are quite rare in the literature, as many reports only have ligand comparisons as part of a reaction optimization survey, typically involving a single

test reaction. Only the optimal ligand/catalyst system is brought forward to explore the reaction scope, even if several ligands showed desirable reactivity in the initial test reaction. While this strategy is certainly cost effective with respect to the number of reactions needed to be run, gaps in reactivity are often left as only one ligand/catalyst is thoroughly tested. This can lead to more work for those interested in applying these methods in their own systems, as reactivity trends are not always obvious by reading multiple reports from different research groups.

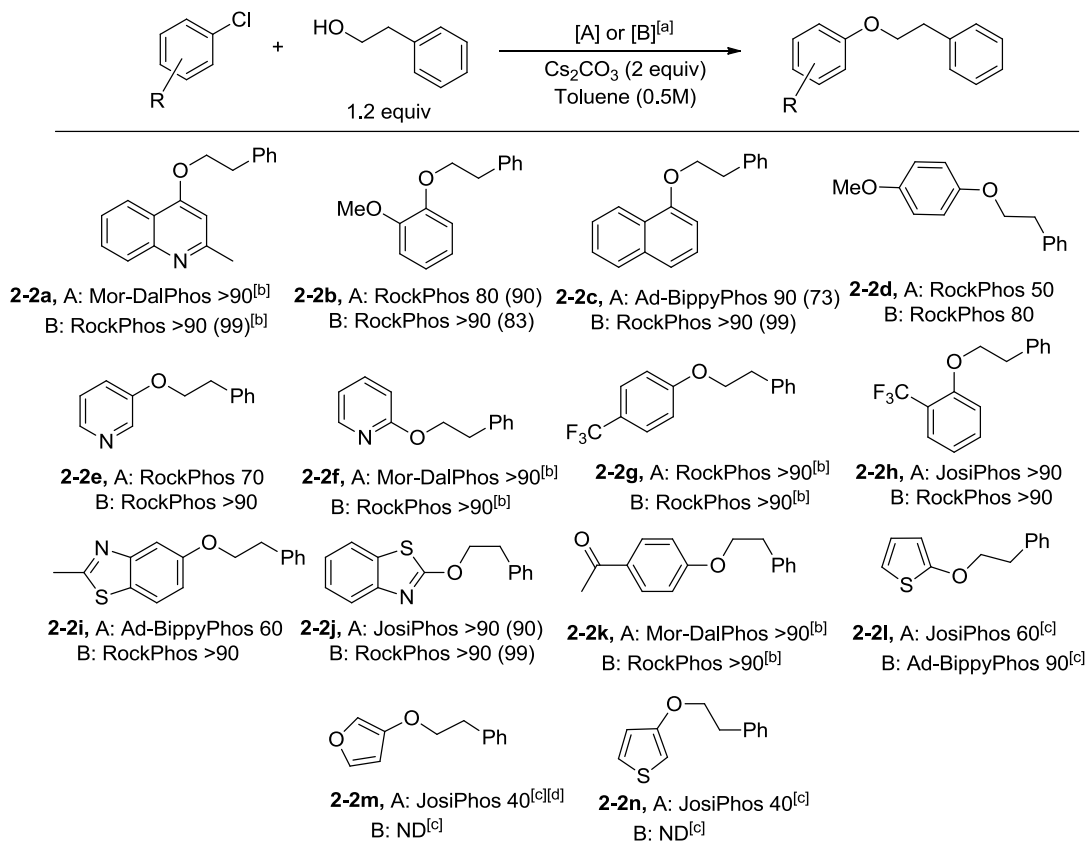


**Table 2-1:** (Hetero)aryl halide scope with optimal ligand reported. GC conversions, isolated yields in parentheses [a] Reaction conditions : [A]  $[\text{Pd}(\text{cinnamyl})\text{Cl}]_2$  0.5 mol%, ligand 1.5 mol%, 90 °C; [B]  $[\text{Pd}(\text{cinnamyl})\text{Cl}]_2$  3.5 mol%, ligand 11.5 mol%, 25 °C. [b] multiple ligands performed equally well [c] 48 h [d] aryl bromide was used. ND = not detected

It is important to note that in this survey no considerations were taken as to the order of addition, nor were any additives used. This is important, as both of these features were

shown previously by the Buchwald group to affect reactivity in the case of Rockphos.<sup>[22]</sup> From the aryl halide scope (**Table 2-1**) it can be seen that multiple ligands work well for activated arenes (leading to **2-2a**, **2-2g**, **2-2k**) at both room temperature and at 90 °C. Rockphos (**L2-1**) was the ligand of choice for electron rich-arenes; surprisingly optimal reactivity was achieved at room temperature. This is thought to be due to the fact that while Rockphos is an extremely active catalyst, at elevated temperatures ligand displacement, competing  $\beta$ -hydride elimination or hydrodehalogenation may become more facile. This can be seen in examples **2-2d**, and **2-2e**, where Rockphos is the optimal choice under both conditions but performs better at ambient temperature. Only for activated arenes did any other ligands show comparable activity at room temperature. This represents an important step forward, as the only previous room temperature reactions of this type involved the use of methanol or ethanol.<sup>[27]</sup> While Rockphos proved to be superior in a large number of cases, relatively poor reactivity was seen with 2-haloheteroarenes (as in the formation of **2-2f**), especially pyridines. In this case, the nitrogen may also coordinate to the metal center deactivating the catalyst. For these substrates, chelating ligands proved to be the most competent. This could be due to the large chelating ligands disfavoring heteroatom coordination while favouring reductive elimination to the desired product. At elevated temperatures, there was some substrate dependence as to the most effective ligand for heteroaryl halides, but in most cases Josiphos (**L2-4**) proved to be the optimal choice. Josiphos was the only ligand capable of enabling the palladium-catalyzed cross-coupling of alcohols with pendant groups capable of metal coordination (**2-2x**).

Coupling reactions with secondary alcohols proved to be more challenging. Presumably bulky alcohols have difficulty coordinating to the metal leading to sluggish reactivity; in

many cases no reactivity was observed under ambient conditions. Five-membered heterocycles proved to be the most challenging electrophilic substrates. Long reaction times were needed to achieve only modest conversions, with bulky alcohols showing no reactivity after 48 hours.

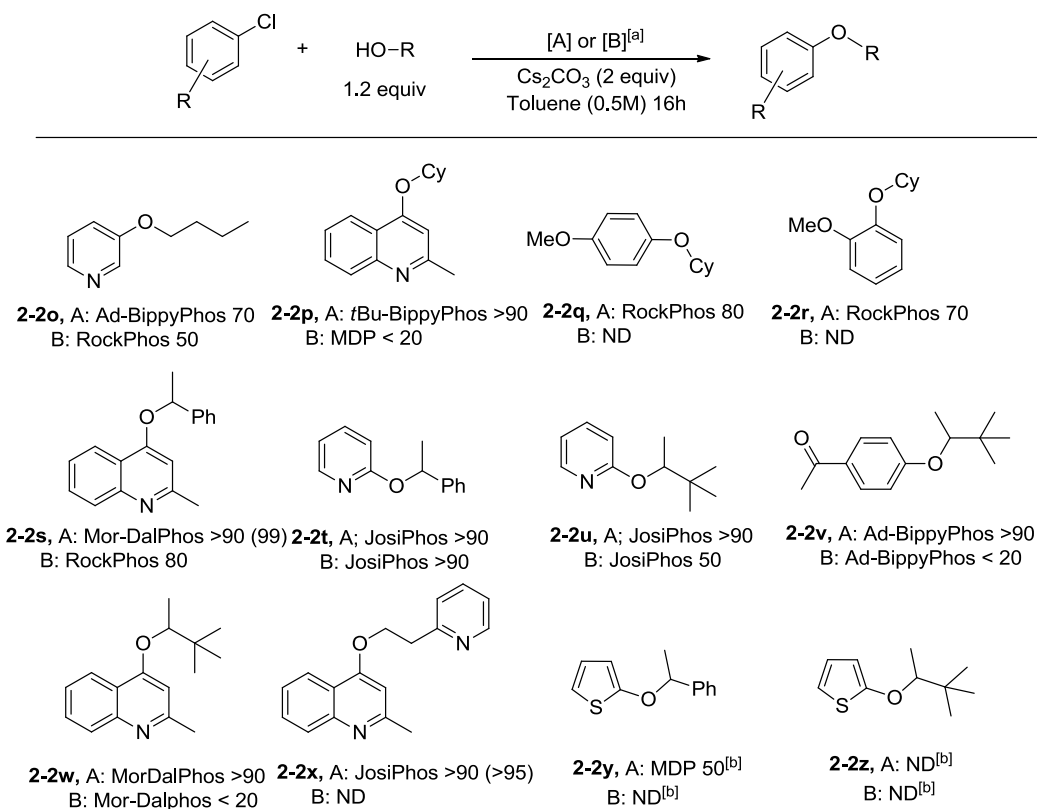
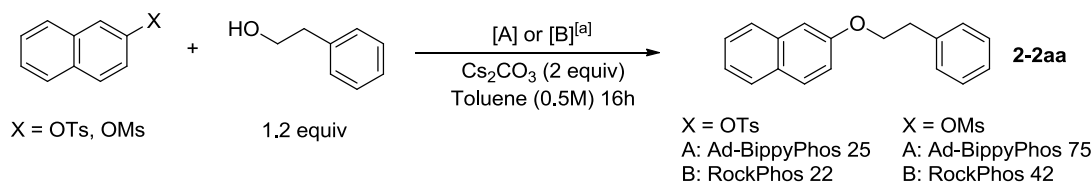


**Table 2-2:** Alcohol scope with optimal ligand reported. GC conversions, isolated yields in parentheses. [a] Reaction conditions : [A] [Pd(cinnamyl)Cl]<sub>2</sub> 0.5 mol%, ligand 1.5 mol%, 90 °C; [B] [Pd(cinnamyl)Cl]<sub>2</sub> 3.5 mol%, ligand 11.5 mol%, 25 °C. [b] 48 h ND = not detected

Reactivity with aryl sulfonates was also of interest, especially mesylates as they are a part of the microbial sulfur cycle and are treated in waste water.<sup>[28]</sup> Additionally aryl sulfonates are easily prepared from the corresponding phenols, allowing access to substrates that may have complimentary substitution to available (hetero)aryl halides. The test reaction used herein involved both the tosylate and mesylate prepared from 2-naphthol. Surprisingly mesylates gave superior yields over tosylates (**Figure 2-2**), with the mesylate

reaction at elevated temperature being higher-yielding compared to the reaction at room temperature. Using the superior conditions at elevated temperatures, a small number of structurally diverse mesylates were tested (**Table 2-3**). Gratifyingly, respectable yields were obtained for both electron-rich and electron poor-substrates. Notably, these represent the first examples of palladium catalyzed C-O coupling using aryl mesylates. It should be noted that reactions of this type with phenol derived electrophiles would not necessarily be considered optimal over traditional methods, especially where nucleophilic substitution of the phenol with the appropriate alkyl halide would be preferred. However, this method would find use in cases where the alkyl halide or phenol is unavailable or where traditional methods fail.



**Scheme 2-3:** C-O coupling with aryl sulfonates. Isolated yields. [a] Reaction conditions : [A] [Pd(cinnamyl)Cl]<sub>2</sub> 0.5 mol%, ligand 1.5 mol%, 90 °C [B] [Pd(cinnamyl)Cl]<sub>2</sub> 3.5 mol%, ligand 11.5 mol%, 25 °C.

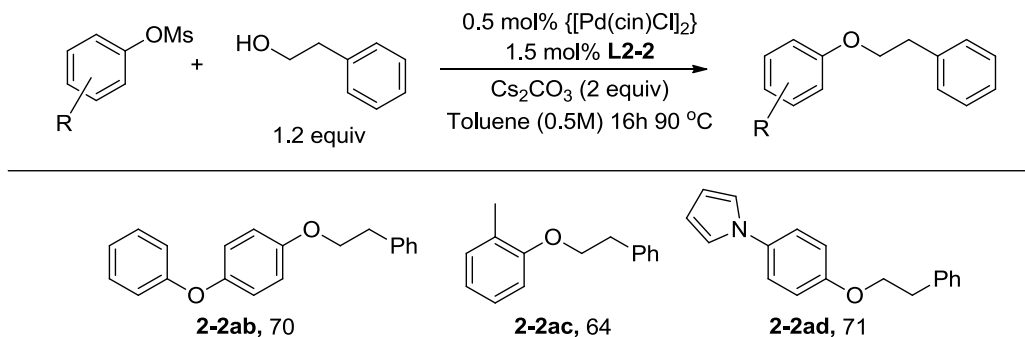


**Table 2-3:** Examples of C-O coupling with structurally diverse mesylates (isolated yields shown).

## 2.4 Summary

Although the initial goal of establishing Mor-Dalphos as a cost-efficient and broadly useful ligand alternative in palladium catalyzed C-O coupling was not met, head-to-head ligand competition studies allowed for the identification of optimal ligands for use under both heating and room temperature conditions. At elevated temperatures, Josiphos proved to be the most effective at coupling activated aryl halides, while Rockphos was optimal for electron-rich substrates. New reactivity was established by performing reactions at room temperature; such conditions employing Rockphos holds promise for the use of volatile substrates. Lastly, proof-of-principle experiments established, for the first time, that such cross-couplings can be extended to aryl mesylates.

## 2.5 Experimental

### 2.5.1 General Considerations

All reactions were set up inside a nitrogen atmosphere glovebox (unless stated otherwise) and products were isolated using standard benchtop conditions. Toluene used in the glovebox was purified by sparging with nitrogen followed by passage through a double column purification system equipped with one alumina packed column and one copper-Q5 packed column. Solvents used in the glovebox were stored over 4 Å molecular



sieves. Mor-Dalphos, and  $[\text{Pd}(\text{cinnamyl})\text{Cl}]_2$  were prepared according to procedures outlined in the literature.<sup>[26b]</sup> Mesylates and tosylates were prepared from their corresponding alcohols using known methods from the literature.<sup>[29]</sup> All other reagents, solvents and materials were used as received from commercial sources (unless stated otherwise). Product purification was performed by column chromatography over Brockmann I, activated, neutral alumina as indicated. All  $^1\text{H}$  NMR and  $^{13}\text{C}$  NMR spectra were recorded using a Bruker AV-500 spectrometer at 300 K. Chemical shifts are expressed in parts per million (ppm) using the residual  $\text{CHCl}_3$  solvent peak ( $^1\text{H}$  7.26 ppm,  $^{13}\text{C}$  77.1 ppm) as an internal reference. Coupling constants ( $J$ ) are reported in Hertz (Hz). Splitting patterns are described as follows: br, broad; s, singlet; d, doublet; t, triplet; q, quartet; m, multiplet. Mass spectra were obtained using ion trap instruments using electrospray ionization, in positive ion mode. GC data was obtained using an instrument equipped with a SGE BP-5, 30 m, 0.25 mm internal diameter column.

## 2.5.2 General Procedures

### General Ligand Screening Procedure for the Formation of Alkyl Aryl Ethers at 25 °C (GP 2-1)

In a dinitrogen atmosphere glovebox:  $[\text{Pd}(\text{cinnamyl})\text{Cl}]_2$  (3.75 mol%, 5.8 mg), ligand (11.25 mol%),  $\text{Cs}_2\text{CO}_3$  (0.6 mmol, 196 mg), and toluene (0.6 mL) were added to a glass vial equipped with a magnetic stir bar. The vial was sealed with a screw cap fitted with a PTFE/silicone septum and removed from the glovebox. Aryl halide (0.30 mmol) and

alcohol (0.36 mmol) were then added via micro syringe. Reaction vials were then placed on a stir plate and the solutions were stirred magnetically for 16 h. After 16 hours samples were taken and filtered through a small plug of silica with dichloromethane. GC analysis of these samples was performed and relative yield estimates were obtained by comparison of starting material peaks to the product peak.

**General Ligand Screening Procedure for the Formation of Alkyl Aryl Ethers at 90 °C (GP 2-2)**

In a dinitrogen atmosphere glovebox: [Pd(cinnamyl)Cl]<sub>2</sub> (0.5 mol%, 1.6 mg), ligand (1.5 mol%), Cs<sub>2</sub>CO<sub>3</sub> (1.2 mmol, 391 mg), and toluene (1.2 mL) were added to a glass vial equipped with a magnetic stir bar. The vial was sealed with a screw cap fitted with a PTFE/silicone septum and removed from the glovebox. Aryl halide (0.60 mmol) and alcohol (0.72 mmol) were then added via micro syringe. Reaction vials were then placed on a temperature-controlled aluminum plate set to 90 °C, and the solutions were stirred magnetically for 16 h. After 16 hours, the reaction vials were removed from the heating block and cooled to room temperature. Samples were taken and filtered through a small plug of silica with dichloromethane. GC analysis of these samples was performed and relative yield estimates were obtained by comparison of starting material peaks to the product peak.

### **General Procedure for Formation and Isolation of Alkyl-Aryl Ethers at 25 °C (GP 2-3)**

In a dinitrogen atmosphere glovebox: [Pd(cinnamyl)Cl]<sub>2</sub> (3.75 mol%, 11.6 mg), ligand (11.25 mol%), Cs<sub>2</sub>CO<sub>3</sub> (1.2 mmol, 196 mg), and toluene (1.2 mL) were added to a glass vial equipped with a magnetic stir bar. The vial was sealed with a screw cap fitted with a PTFE/silicone septum and removed from the glovebox. Aryl halide (0.60 mmol) and alcohol (0.72 mmol) were then added via micro syringe. Reaction vials were then placed on a stir plate and the solutions were stirred magnetically for 16 h. After 16 hours, the reaction was filtered through an alumina and Celite filter with dichloromethane. The product was concentrated via rotary evaporation and purified by column chromatography.

### **General Procedure for Formation and Isolation of Alkyl-Aryl Ethers at 90 °C (GP 2-4)**

In a dinitrogen atmosphere glovebox: [Pd(cinnamyl)Cl]<sub>2</sub> (0.5 mol%, 1.6 mg), Ligand (1.5 mol%), Cs<sub>2</sub>CO<sub>3</sub> (1.2 mmol, 391 mg), and toluene (1.2 mL) were added to a glass vial equipped with a magnetic stir bar. The vial was sealed with a screw cap fitted with a PTFE/silicone septum and removed from the glovebox. Aryl halide (0.60 mmol) and alcohol (0.72 mmol) were then added via micro syringe. Reaction vials were then placed on a temperature-controlled aluminum plate set to 90 °C and the solutions were stirred magnetically for 16 h. After 16 hours, the reaction vials were removed from the heating block and cooled to room temperature. The reaction mixture was then filtered through an

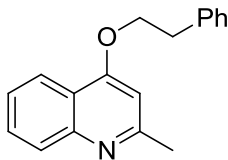
alumina and Celite filter with dichloromethane. The product was concentrated via rotary evaporation and purified by column chromatography.

**General Procedure for Formation and Isolation of Alkyl-Aryl Ethers at 90 °C using aryl mesylates and tosylates (GP 2-5)**

In a dinitrogen atmosphere glovebox: [Pd(cinnamyl)Cl]<sub>2</sub> (0.5 mol%, 2.6 mg), ligand (1.5 mol%), Cs<sub>2</sub>CO<sub>3</sub> (2.0 mmol, 652 mg), and toluene (2.0 mL) were added to a glass vial equipped with a magnetic stir bar. The vial was sealed with a screw cap fitted with a PTFE/silicone septum and removed from the glovebox. Aryl halide (1.0 mmol) and alcohol (1.2 mmol) were then added via micro syringe. Reaction vials were then placed on a temperature-controlled aluminum plate set to 90 °C and the solutions were stirred magnetically for 16 h. After 16 hours, the reaction vials were removed from the heating block and cooled to room temperature. The reaction mixture was then filtered through an alumina and Celite filter with dichloromethane. The product was concentrated via rotary evaporation and purified by column chromatography.

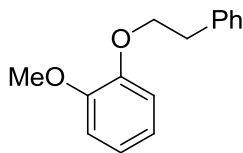
### 2.5.3 Characterization Data for Isolated Materials

2-Methyl-4-phenethoxyquinoline (**2-2a**).



Following **GP 2-3 (L2-1** 31.6 mg, aryl halide 121  $\mu$ L, alcohol 86.2  $\mu$ L), the title product was isolated as a white solid (90%).  $^1\text{H}$  NMR (500 MHz,  $\text{CDCl}_3$ ):  $\delta$  8.17 (d,  $J = 8.5$  Hz, 1H), 7.97 (d,  $J = 8.5$  Hz, 1H), 7.68 (t,  $J = 7.5$  Hz, 1H), 7.47 (t,  $J = 7.5$  Hz, 1H), 7.38-7.39 (m, 4H), 7.28-7.33 (m, 1H), 6.63 (s, 1H), 4.41 (t,  $J = 7$  Hz, 2H), 3.29 (t,  $J = 7$  Hz, 2H), 2.70 (s, 3H);  $^{13}\text{C}\{^1\text{H}\}$  NMR (125.8 MHz,  $\text{CDCl}_3$ ):  $\delta$  161.6, 160.2, 149.0, 138.0, 129.9, 129.2, 128.8, 128.2, 126.9, 124.9, 121.8, 120.0, 101.3, 69.1, 35.7, 26.1;  $m/z$  ESI+ found 264.1383  $[\text{M}+\text{H}]^+$  calculated for  $\text{C}_{18}\text{H}_{18}\text{NO}$  264.1344.

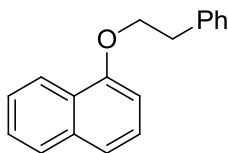
1-Methoxy-2-phenethoxybenzene (**2-2b**).



Following **GP 2-3 (L2-1** 31.6 mg, aryl halide 76.2  $\mu$ L, alcohol 86.2  $\mu$ L) the title product was isolated as a colorless oil (83%).  $^1\text{H}$  NMR (500 MHz,  $\text{CDCl}_3$ ):  $\delta$  7.33-7.40 (m, 4H), 7.27-7.32 (m, 1H), 6.94-7.00 (m, 4H), 4.28 (t,  $J = 7.6$  Hz, 2H), 3.92 (s, 3H), 3.28 (t,  $J = 7.6$  Hz, 2H);  $^{13}\text{C}\{^1\text{H}\}$  NMR (125.8 MHz,  $\text{CDCl}_3$ ):  $\delta$  150.0, 148.7, 138.5, 129.5, 128.9, 126.9, 121.6, 121.3, 113.9, 122.5, 70.3, 56.4, 36.2;  $m/z$  ESI+ found 229.1223  $[\text{M}+\text{H}]^+$  calculated

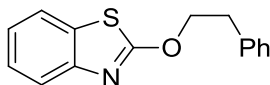
for C<sub>15</sub>H<sub>17</sub>O<sub>2</sub> 229.1184. Following **GP 2-4 (L2-1** 6.0 mg, aryl halide 76.2 μL, alcohol 86.2 μL) the title product was isolated as a colorless oil (90%).

1-Phenethoxynaphthalene (**2-2c**).



Following **GP 2-3 (L2-1** 31.6 mg, aryl halide 81.7 μL, alcohol 86.2 μL) the title product was isolated as a light brown solid (>95%). <sup>1</sup>H NMR (500 MHz, CDCl<sub>3</sub>): δ 8.31 (d, J = 8.0 Hz, 1H), 7.83 (d, J = 8.0 Hz, 1H), 7.48-7.54 (m, 2H), 7.46 (d, J = 8.5 Hz, 1H), 7.36-7.43 (m, 5H), 7.27-7.31 (m, 1H), 6.85 (d, J = 7.6 Hz, 1H), 4.41 (t, J = 6.9 Hz, 2H), 3.30 (t, J = 6.9 Hz, 2H); <sup>13</sup>C{<sup>1</sup>H} NMR (125.8 MHz, CDCl<sub>3</sub>): δ 154.8, 138.7, 134.7, 129.3, 128.7, 127.6, 126.7, 126.5, 126.0, 125.9, 125.3, 122.3, 120.4, 104.9, 69.1, 36.2; m/z ESI+ found 249.1274 [M+H]<sup>+</sup> calculated for C<sub>18</sub>H<sub>17</sub>O 249.1235. Following **GP 2-4 (L2-2** 6 mg, aryl halide 81.7 μL, alcohol 86.2 μL) the title product was isolated as a light brown solid (73%).

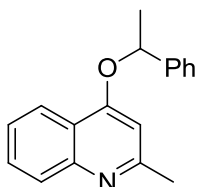
2-Phenethoxybenzo[d]thiazole (**2-2j**).



Following **GP 2-3 (L2-1** 31.6 mg, aryl halide 78.1 μL, alcohol 86.2 μL) the title product was isolated as a white solid (>95%). <sup>1</sup>H NMR (500 MHz, CDCl<sub>3</sub>): δ 7.72 (d, J = 8.1, 1H), 7.67 (d, J = 7.9 Hz, 1H), 7.32-7.42 (m, 5H), 7.24-7.31 (m, 2H), 4.82 (t, J = 7.1 Hz, 2H), 3.22 (t, J = 7.0 Hz, 2H); <sup>13</sup>C{<sup>1</sup>H} NMR (125.8 MHz, CDCl<sub>3</sub>): δ 172.9, 149.6, 137.6, 132.1, 129.2, 128.7, 126.9, 126.1, 123.6, 121.4, 121.0, 72.3, 35.4; m/z ESI+ found 256.0791

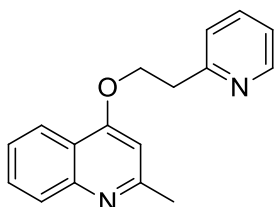
[M+H]<sup>+</sup> calculated for C<sub>15</sub>H<sub>14</sub>N<sub>1</sub>O<sub>1</sub>S<sub>1</sub> 256.0751. Following **GP 2-4 (L2-4** 47.2 mg, aryl halide 78.1 μL, alcohol 86.2 μL) the title product was isolated as a white solid (90%).

2-Methyl-4-(1-phenethoxy)quinoline (**2-2s**).



Following **GP 2-4 (L2-5** 4.2 mg, aryl halide 121 μL, alcohol 86.9 μL) the title product was isolated as a colorless oil (>95%). <sup>1</sup>H NMR (500 MHz, CDCl<sub>3</sub>): δ 8.31 (d, J = 8.3 Hz, 1H), 7.97 (d, J = 8.5 Hz, 1H), 7.70 (t, J = 7.1 Hz, 1H), 7.51 (t, J = 7.5 Hz, 1H), 7.37-7.41 (m, 2H), 7.43-7.47 (m, 2H), 7.30-7.35 (m, 1H), 6.51 (s, 1H), 5.61 (q, J = 6.5 Hz, 1H), 2.60 (s, 3H), 1.82 (d, J = 6.5 Hz, 3H); <sup>13</sup>C{<sup>1</sup>H} NMR (125.8 MHz, CDCl<sub>3</sub>): δ 160.6, 160.0, 149.1, 142.1, 129.8, 129.0, 128.3, 128.1, 125.5, 124.9, 122.0, 120.4, 103.1, 76.5, 26.1, 24.4; m/z ESI+ found 264.1383 [M+H]<sup>+</sup> calculated for C<sub>18</sub>H<sub>18</sub>NO 264.1344.

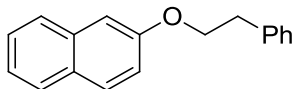
2-Methyl-4-(2-(pyridin-2-yl)ethoxy)quinoline (**2-2x**).



Following **GP 2-4 (L2-4** 4.7 mg, aryl halide 121 μL, alcohol 81.1 μL) the title product was isolated as a brown solid (>95%). <sup>1</sup>H NMR (500 MHz, CDCl<sub>3</sub>): δ 8.60-8.62 (m, 1H), 8.09 (d, J = 8.3 Hz, 1H), 7.96 (d, J = 8.5 Hz, 1H), 7.64-7.70 (m, 2H), 7.43 (t, J = 7.4 Hz, 1H), 7.36 (d, J = 7.8 Hz, 1H), 7.18-7.22 (m, 1H), 6.51 (s, 1H), 4.63 (t, J = 7.4 Hz, 2H), 3.45 (t,

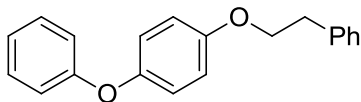
J = 7.4 Hz, 2H), 2.71 (s, 3H);  $^{13}\text{C}\{^1\text{H}\}$  NMR (125.8 MHz,  $\text{CDCl}_3$ ):  $\delta$  161.6, 160.3, 158.2, 149.7, 148.9, 136.7, 129.9, 128.1, 124.9, 123.9, 122.0, 121.8, 120.0, 101.4, 67.6, 37.9, 26.0; m/z ESI+ found 265.1335  $[\text{M}]^+$  calculated for  $\text{C}_{17}\text{H}_{17}\text{N}_2\text{O}$  265.1344.

#### 2-Phenethoxynaphthalene (**2-2aa**).



Following **GP 2-5** (**L2-2** 10.0 mg, aryl mesylate 222.3 mg, alcohol 144  $\mu\text{L}$ ) the title product was isolated as a white solid (75%).  $^1\text{H}$  NMR (500 MHz,  $\text{CDCl}_3$ ):  $\delta$  7.74-7.83 (m, 3H), 7.48 (t, J = 7.3 Hz, 1H), 7.36-7.42 (m, 5H), 7.29-7.34 (m, 1H), 7.18-7.23 (m, 2H), 4.36 (t, J = 7.1 Hz, 2H), 3.23 (t, J = 7.1 Hz, 2H);  $^{13}\text{C}\{^1\text{H}\}$  NMR (125.8 MHz,  $\text{CDCl}_3$ ):  $\delta$  157.0, 138.4, 134.7, 129.5, 129.2, 128.7, 127.8, 126.9, 126.7, 126.5, 123.8, 119.1, 106.9, 68.9, 36.0; m/z ESI+ found 249.1274  $[\text{M}+\text{H}]^+$  calculated for  $\text{C}_{18}\text{H}_{17}\text{O}$  249.1235. Following **GP 2-5** (**L2-1** 31.6 mg, aryl mesylate 133.4 mg, alcohol 86.2  $\mu\text{L}$ ) the title product was isolated as a white solid (42%).

#### 1-Phenethoxy-4-phenoxybenzene (**2-2ab**).

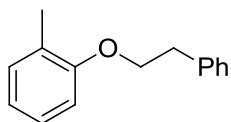


Following **GP 2-5** (**L2-2** 10.0 mg, aryl mesylate 264.3 mg, alcohol 144  $\mu\text{L}$ ) the title product was isolated as a light yellow oil (70%).  $^1\text{H}$  NMR (500 MHz,  $\text{CDCl}_3$ ):  $\delta$  7.33-7.46 (m, 7H), 7.14 (apparent t, J = 7.4 Hz, 1H), 7.04-7.09 (m, 4H), 6.96-7.00 (m, 2H), 4.26 (t, J = 7.1 Hz, 2H), 3.21 (t, J = 7.1 Hz, 2H);  $^{13}\text{C}\{^1\text{H}\}$  NMR (125.8 MHz,  $\text{CDCl}_3$ ):  $\delta$  158.6, 155.2,



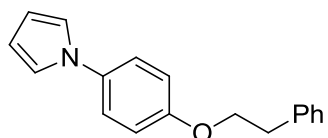
150.3, 138.3, 129.7, 129.1, 128.6, 126.6, 122.5, 120.9, 117.7, 115.7, 69.3, 36.0; m/z ESI+ found 291.1380 [M+H]<sup>+</sup> calculated for C<sub>20</sub>H<sub>19</sub>O<sub>2</sub> 291.1340.

1-Methyl-2-phenethoxybenzene (**2-2ac**).



Following **GP 2-5** (**L2-2** 10.0 mg, aryl mesylate 200.3 mg, alcohol 144  $\mu$ L) the title product was isolated as a colorless oil (64%). <sup>1</sup>H NMR (500 MHz, CDCl<sub>3</sub>):  $\delta$  7.40-7.45 (m, 4H), 7.33-7.37 (m, 1H), 7.22-7.26 (m, 2H), 6.96 (t, J = 7.4 Hz, 1H), 6.89-6.92 (m, 1H), 4.28 (t, J = 6.9 Hz, 2H), 3.22 (t, J = 6.9 Hz, 2H), 2.33 (s, 3H); <sup>13</sup>C{<sup>1</sup>H} NMR (125.8 MHz, CDCl<sub>3</sub>):  $\delta$  157.0, 138.7, 130.7, 129.2, 128.4, 126.9, 126.8, 126.5, 120.4, 111.0, 68.7, 36.1, 16.3; m/z ESI+ found 235.1093 [M+Na]<sup>+</sup> calculated for C<sub>15</sub>H<sub>16</sub>NaO 235.1099.

1-(4-Phenethoxyphenyl)-1H-pyrrole (**2-2ad**).

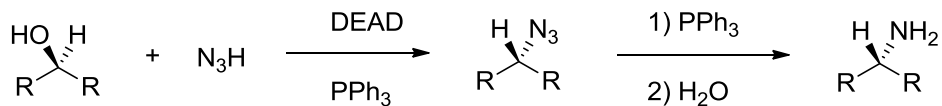


Following **GP 2-5** (**L2-2** 10.0 mg, aryl mesylate 237.3 mg, alcohol 144  $\mu$ L) the title product was isolated as a white solid (71%). <sup>1</sup>H NMR (500 MHz, CDCl<sub>3</sub>):  $\delta$  7.27-7.39 (m, 7H), 7.02-7.04 (m, 2H), 6.96-7.00 (m, 2H), 6.35-6.37 (m, 2H), 4.24 (t, J = 7.1, 2H), 3.16 (t, J = 7.1, 2H); <sup>13</sup>C{<sup>1</sup>H} NMR (125.8 MHz, CDCl<sub>3</sub>):  $\delta$  156.9, 138.1, 134.6, 129.0, 128.5, 126.5, 122.1, 119.7, 115.3, 109.8, 69.1, 35.8; m/z ESI+ found 264.1383 [M+H]<sup>+</sup> calculated for C<sub>18</sub>H<sub>18</sub>NO 264.1344.

## Chapter 3 Microwave-Assisted Nickel-Catalyzed Synthesis of Aryl Amines from Aryl Halides and Ammonium Salts

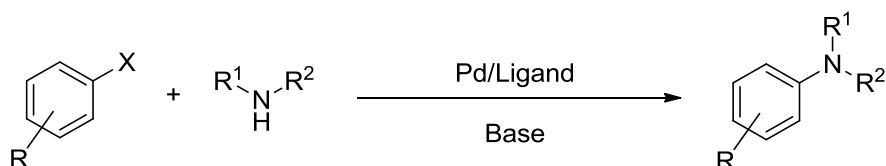
### 3.1 Buchwald-Hartwig Amination (BHA)

The palladium-catalyzed cross-coupling of (hetero)aryl (pseudo)halides and N-H substrates (Buchwald-Hartwig amination, BHA) represents a versatile methodology for the synthesis of substituted (hetero)anilines.<sup>[30]</sup> Previous to the development of BHA, limited methods were known for the formation of aryl amines. Traditional methods were limited to a small number of reaction types including electrophilic aromatic substitution, involving installation of a nitro group, followed by reduction to the corresponding amine, reactions involving benzyne intermediates, as well as Ullmann-type coupling using stoichiometric amounts of copper. Alternative methods for the synthesis of alkylamines exist, such as the Mitsunobu synthesis followed by a Staudinger reduction (**Scheme 3-1**). These more conventional methods are limited, as the number of amines that can be synthesized is relatively small, and often require more than one step to reach the desired amine product. Early palladium-catalyzed C-N couplings, inspired by C-C bond forming catalysts (see Chapter 1), preceded BHA. These reactions were similar to Suzuki and Stille reactions, using amino boron, and amino stannanes<sup>[31]</sup> respectively. However, these reactions were still not optimal as they required boron and toxic tin reagents.



**Scheme 3-1:** Amine synthesis through sequential Mitsunobu and Staudinger reactions (DEAD = diethyl azodicarboxylate).

Palladium-catalyzed amination of aryl halides with amines was discovered independently by both the Buchwald and Hartwig groups in 1995.<sup>[32]</sup> This initial work was limited in that only secondary amines and aryl bromides could be used. Subsequently, Buchwald, Hartwig, as well as other groups have vastly improved the reaction scope via optimization of base, solvent, and ancillary ligands employed to include a wide variety of nitrogen nucleophiles as well as the use of a diverse group of (hetero)aryl electrophiles, including aryl chlorides and sulfonates.<sup>[30, 33]</sup> These substrates are attractive as the chlorides are both cheap and abundant, while the sulfonates are easily prepared from the corresponding phenols. The general scheme for BHA is shown in **Scheme 3-2**.



**Scheme 3-2:** General scheme of Buchwald-Hartwig amination.

### 3.1.1 Catalytic Mechanism of Buchwald-Hartwig Amination

The mechanism of BHA is closely related to previously discussed palladium-catalyzed C-C, and C-O bond forming reactions (**Figure 3-1**). Firstly, the presumptive Pd<sup>0</sup> catalyst

must be formed to enter the catalytic cycle. This is done in one of two ways: the reduction of a  $\text{Pd}^{2+}$  source to  $\text{Pd}^0$ , or through *in situ* formation of the catalyst by the binding of the ligand to a  $\text{Pd}^0$  source (e.g.,  $\text{Pd}(\text{PPh}_3)_4$ ). Once the active  $\text{L}_n\text{Pd}^0$  catalyst is formed (the number of ligands,  $n$ , varies on the basis of the ligand used) oxidative addition of the aryl electrophile can occur, followed by amine binding. Base promoted abstraction of the anion, and deprotonation of the bound amine gives the palladium amido intermediate. Reductive elimination and release of the amine product and regenerates the catalyst. Ideally the catalyst is composed of a 1:1 ratio of ligand and metal; however, the addition of small excess of ligand relative to the metal can aid in catalyst stabilization by trapping any undesired ligand-free palladium that may occur under catalytic conditions. This strategy was employed in the C-O cross-coupling chemistry discussed in Chapter 2.

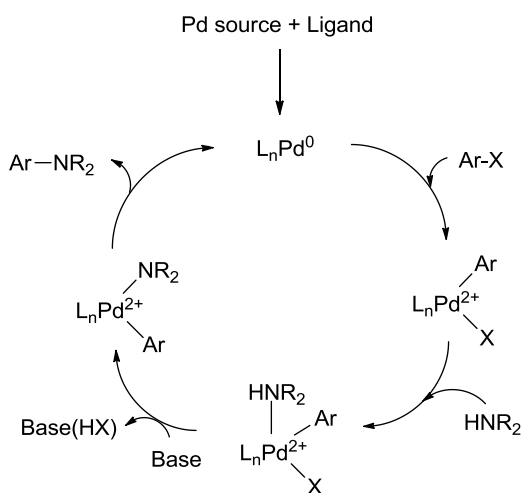


**Figure 3-1:** General mechanism for Buchwald-Hartwig aminations.

The early reports of BHA involved the use of tri(ortho-tolyl)phosphine as the supporting ligand,<sup>[32a]</sup> however, more complex ligands were found to enable the inclusion of a larger substrate scope. Buchwald-type catalysts now include functionalized biaryl

phosphines,<sup>[34]</sup> while Hartwig employed CyPF-*t*Bu of the Josiphos ligand family developed by Solvias.<sup>[35]</sup> Other ligands were designed to address other reactivity challenges in BHA. These include, but are not limited to, Bippyphos, cataCXium<sup>®</sup> A, the *N*-heterocyclic carbene (NHC) PEPPSI catalyst system, and Mor-Dalphos, developed by Singer,<sup>[36]</sup> Beller,<sup>[37]</sup> Organ<sup>[33a]</sup> and Stradiotto<sup>[26a]</sup> respectively (**Figure 3-2**). These ligands feature strongly electron donating phosphine atoms, except the NHC which features a strongly donating carbene. Such ligands help facilitate oxidative addition, which in most cases is rate limiting in BHA reactions of aryl chlorides. These ligands also have large bulky moieties, which helps with reductive elimination as well as affording selectivity.

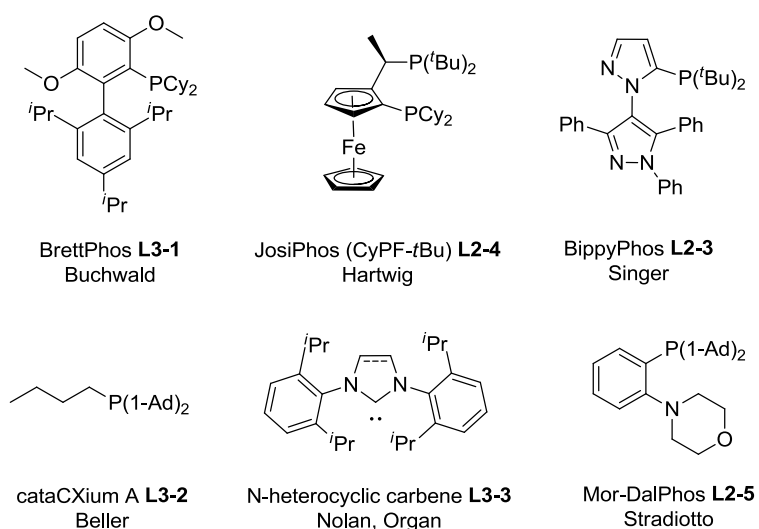


**Figure 3-2:** Examples of state-of-the-art ligands used in BHA chemistry.

### 3.1.2 Buchwald-Hartwig Amination using Ammonia

The primary (hetero)aniline moiety is seen in many pharmaceuticals, natural, and synthetic products. The use of ammonia as a reaction partner is the most direct way to access such products; ammonia is also cheap and abundant, being one of the largest industrial products worldwide.<sup>[38]</sup> Several challenges exist with the use of ammonia in BHA, including that the aniline product is often a better substrate than ammonia for most BHA catalysts which can lead to undesired diarylation byproducts. The first example of BHA using ammonia was reported by Hartwig in 2006 using the aforementioned CyPF-*t*Bu Josiphos ligand (**L2-4**).<sup>[39]</sup> Rapid improvement has been achieved by multiple groups since that initial report. Notably the Stradiotto group using Mor-Dalphos (**L2-5**) reported the first examples of room temperature monoarylation of ammonia.<sup>[26a]</sup>

### 3.2 Development of First Row Transition Metal Catalysts

Recent advances in transition metal catalysis has seen the movement away from traditionally employed second and third row platinum-group metals to the more Earth-abundant first row metals. First row metals have the advantage of being much cheaper than their platinum-group counterparts; for example, nickel is approximately 60 times cheaper than palladium per gram based on their dichloride salts. However, first row metals do suffer from a few drawbacks. Firstly, many catalytic precursors are not particularly stable. A commonly used nickel source, bis(1,5-cyclooctadiene)nickel(0), is thermally unstable as

well as being air-sensitive. Furthermore, many first row transition metals have more easily accessible oxidation states compared to second and third row metals in the same group. Comparing nickel to palladium, nickel is often found in oxidation states of 0 through 3+ whereas palladium tends to prefer 0, 2+ and 4+.<sup>[40]</sup> The result is that first row metals are prone to single-electron reactions, which can lead to uncontrolled chemistry. Despite these challenges, many groups have begun to utilize first row metals to do the work typically done by platinum-group metals, through the use of appropriate ancillary ligands.

In 2013, Chirik and co-workers reported the use of cobalt catalysts in the asymmetric hydrogenation of alkenes (**Table 3-1**).<sup>[41]</sup> In this work they compare a large variety of common bisphosphines using high throughput screening methods. Multiple cobalt sources and transmetallating activators were tested;  $\text{Co}(\text{OBn})_2$  with  $\text{LiCH}_2\text{SiMe}_3$  gave the highest yields and best selectivities. Drastic differences in yield and selectivity were observed between each ligand and even between ligand variants of the same family, thereby highlighting the fact that ancillary ligand effects are still poorly understood for the first-row transition metals.

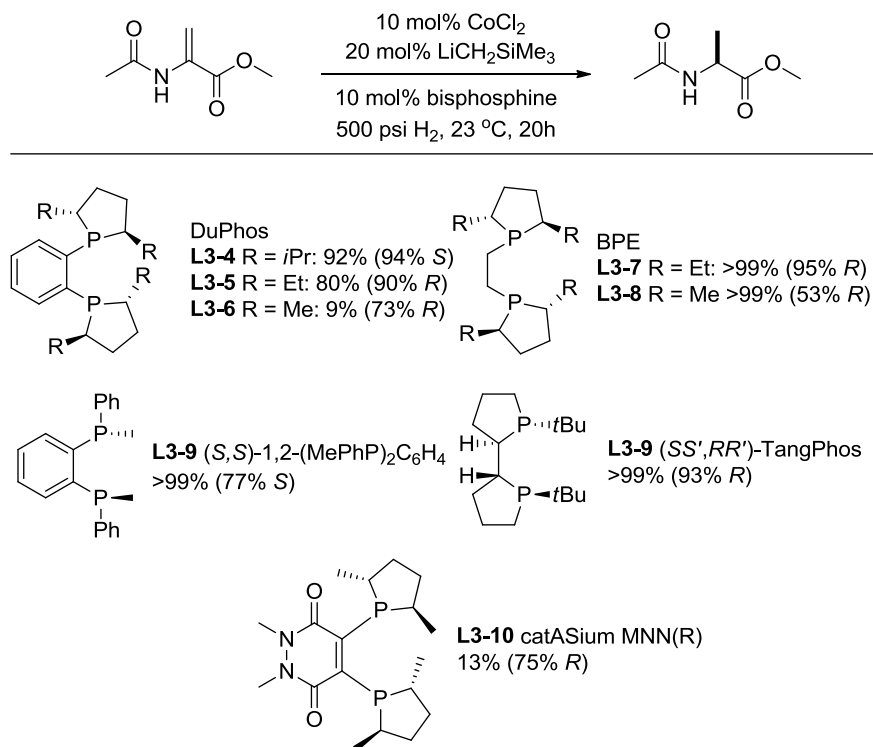


**Table 3-1:** Select examples of bisphosphines used in cobalt-catalyzed asymmetric hydrogenation of alkenes.

Another recent example of first-row metal catalysis leading to C-N bond-formation is the copper-catalyzed asymmetric hydroamination of internal alkenes reported by Buchwald and co-workers (**Table 3-2**).<sup>[42]</sup> Unactivated internal alkenes are major industrial products, and as such are attractive building blocks in synthetic chemistry. This report features the use of such feedstock chemicals and hydroxylamine esters as coupling partners to afford chiral alkyl amines in good yields with excellent selectivity. It was noted that the substitution in the 4-position on the phenyl ring of the hydroxylamine ester had a strong impact on the yields; with no substitution in this position, test reactions performed poorly (<40% yield), with diethyl amine being the optimal substituent. Using this method, the authors prepared several pharmaceutical derivatives, further proving the competency of this system (**Scheme 3-3**). One limitation of this method is the exclusive use of secondary



amines and the use of hydroxylamine ester precursors. These reagents are not readily available and are prepared by a three-step procedure. This method, if extended to other amine precursors could prove invaluable to both industrial and academic synthetic chemists.

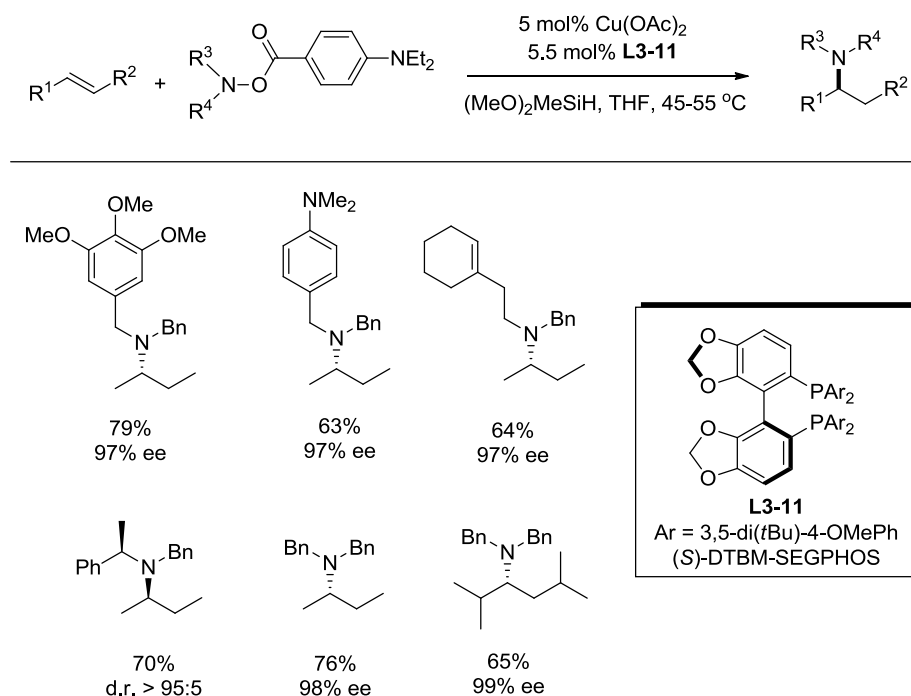
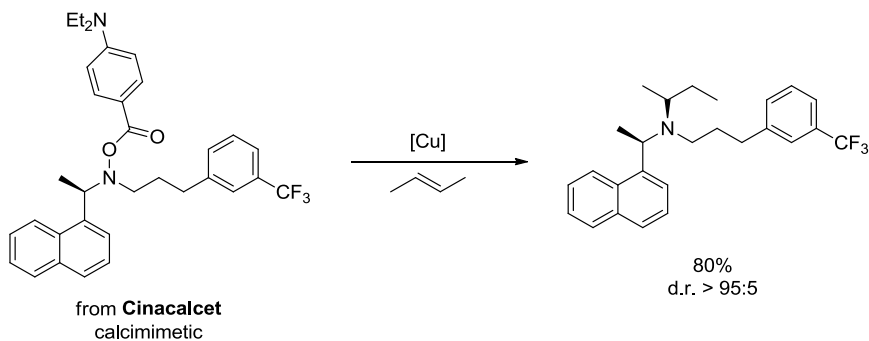


**Table 3-2:** Examples of copper-catalyzed asymmetric hydroamination.



**Scheme 3-3:** Derivative of the pharmaceutical Cinacalcet synthesized through copper catalyzed asymmetric hydroamination.

These selected recent reports highlight the fact that repurposing ligands designed in the context of platinum-group metal catalysis in some case can prove to be quite effective in developing useful base-metal catalysts. However, much research in the area of understanding ancillary ligand effects is needed to fully exploit first-row metal catalysts. To this end new ligands need to be designed to confer desirable catalytic properties, including activity and selectivity, to first-row metals.

### 3.2.1 Nickel Catalyzed Amination Reactions

The first report of nickel-catalyzed amination reactions analogous to BHA was by Wolfe and Buchwald in 1997.<sup>[43]</sup> This work sought to address challenges in similar palladium-catalyzed reactions, specifically the use of aryl chlorides, which were a limitation in palladium chemistry at the time. To this end, appropriately ligated nickel proved to be an effective catalyst, coupling a variety of aryl chlorides with several anilines and amines (**Table 3-3**). One limitation, as mentioned, is that the amine coupling partners were limited to a handful of primary amines, cyclic secondary amines, and anilines (both primary and secondary). Two ligands were found to be effective (**L3-12** and **L3-13**), and it was shown that there was substrate dependence as to the optimal ligand choice. It was also demonstrated that a complex made from nickel(II) chloride and the ligand can be an effective alternative to Ni(COD)<sub>2</sub>; reactions using this complex however, required the use of an external reductant (methylmagnesium bromide) to produce the active catalytic species. Relatively little work has been done in this field since this pioneering report, as

advances in palladium-catalyzed aminations quickly proved to be more effective with a larger substrate scope.

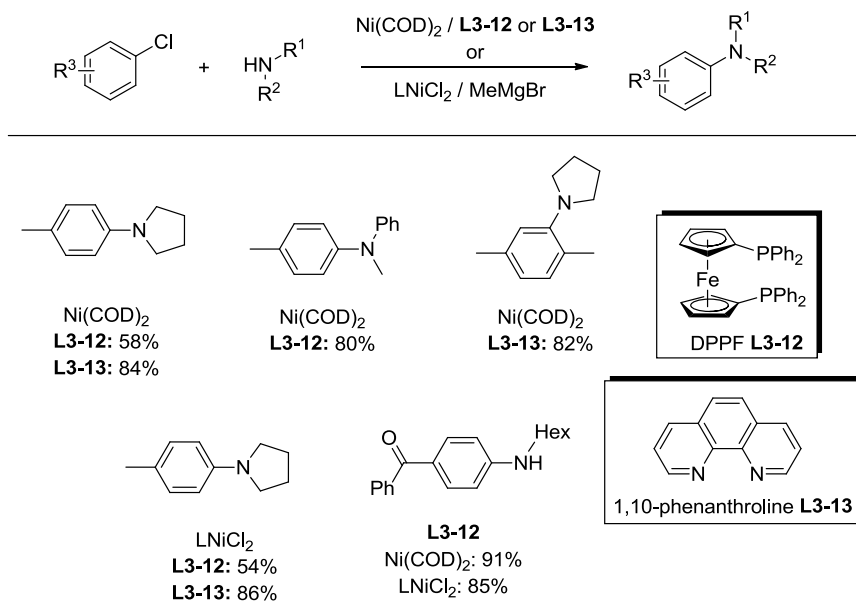


**Table 3-3:** Select examples of nickel-catalyzed amination of aryl chlorides.

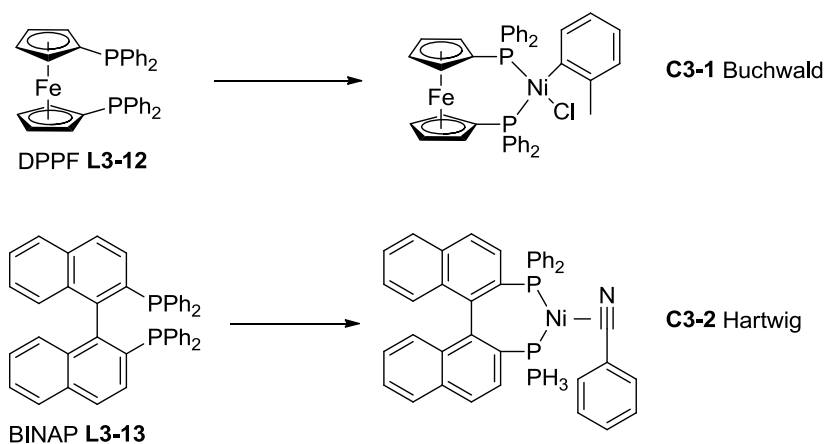


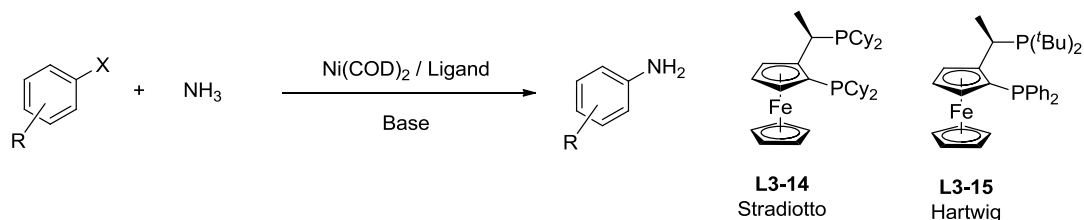
**Figure 3-3:** Complexes and ligands used by Buchwald and Hartwig for nickel-catalyzed amination reactions.

Nickel catalyzed amination reactions returned to the spotlight in 2014, with notable reports coming from the groups of Buchwald<sup>[44]</sup> and Hartwig.<sup>[45]</sup> Buchwald again made use

of DPPF (**L3-12**), but in this report an air-stable nickel(II) complex (**C3-1**) that does not require an external reductant is used. Conversely, Hartwig used a nitrile-stabilized nickel(0) complex (**C3-2**) with BINAP (**L3-13**) as the supporting ligand (**Figure 3-3**). These first reports involved the arylation of primary and secondary amines, for the most part with activated aryl halides or substrates featuring *ortho*-substitution. Yields suffered for electron-rich aryl halides that lack any *ortho* functionality. While these systems proved to be quite effective for the coupling of primary and secondary amines, with a noteworthy range of electrophile leaving groups in the case of **C3-1**, the analogous reactions with ammonia remained elusive.

The first nickel-catalyzed aryl aminations using ammonia were reported by the Stradiotto group in 2015.<sup>[46]</sup> This report highlighted the use of both ammonia stock solutions as well as gaseous ammonia. Concomitantly, Hartwig published a similar paper on nickel catalyzed ammonia coupling.<sup>[47]</sup> Hartwig employed the use of ammonium salts in addition to ammonia stock solutions. These papers both featured a catalyst using different members of the Josiphos family of ligands (**L3-14**, **L3-15**, **Scheme 3-4**). These ligands are quite expensive, owing to a lengthy synthesis and unneeded chirality. Hartwig made use of the nitrile-stabilized nickel(0) complex (**C3-3**), while Stradiotto used the simple combination of ligand and Ni(COD)<sub>2</sub>. While both of these systems performed well, the substrate scope was larger in the report by Stradiotto, especially with respect to heteroaryl halides. Additionally, few examples of electron-rich aryl halides lacking *ortho*-substitution exist. Notwithstanding such progress, the challenge circa 2016 was to find an inexpensive ligand for nickel-catalyzed C-N cross-coupling that was able to accommodate ammonia, as well as being effective in transformations of electron-rich aryl halides. Further

advances to extend reactivity to milder conditions (e.g. ambient temperature), as well as to expand the scope of amine substrates beyond ammonia (i.e., alkyl amines, anilines, indoles, and amides) are highly sought after.



**Scheme 3-4:** General nickel catalyzed monoarylation of ammonia.

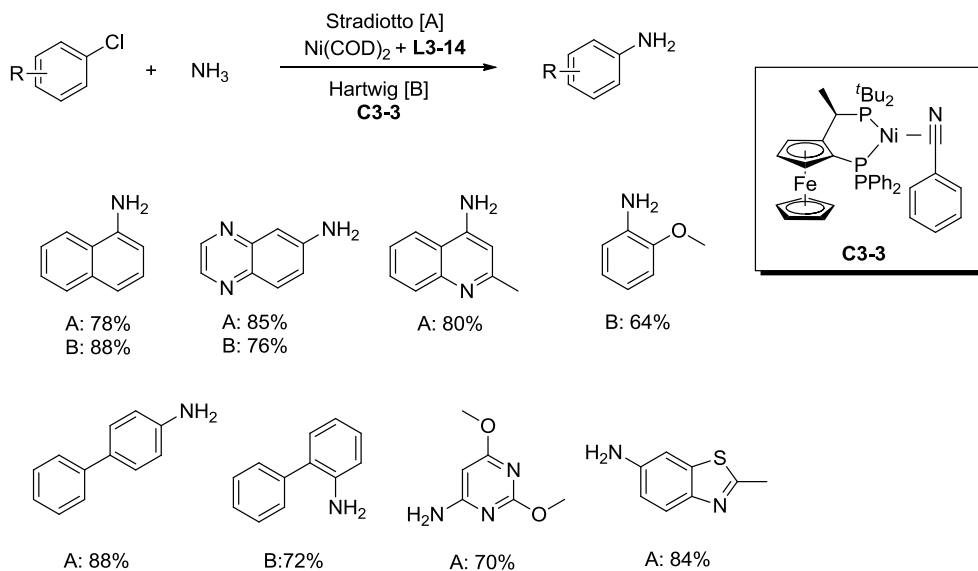


**Table 3-4:** Ligand complex **C3-3** used by Hartwig and examples of nickel-catalyzed ammonia monoarylation.

### 3.3 Microwave-Assisted Catalysis

The use of microwave reactors in synthetic chemistry was first reported in 1986.<sup>[48]</sup> The initial uptake of this heating method was slow as the lack of understanding of microwave

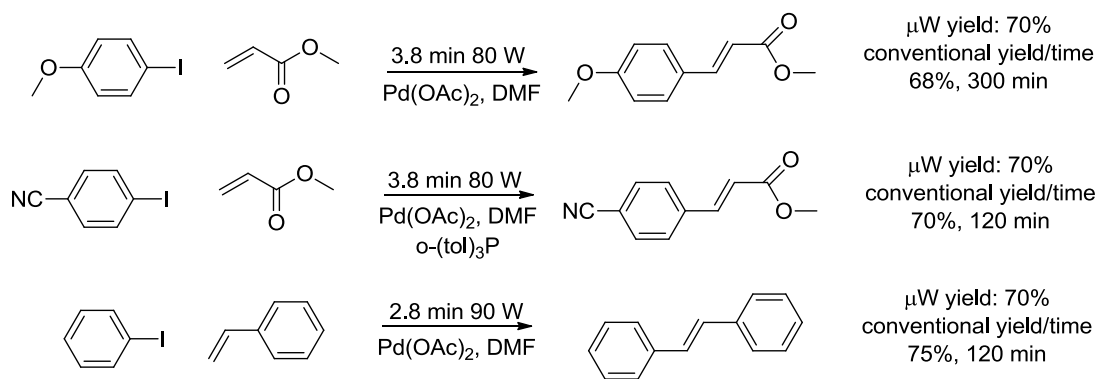
heating, with respect to chemical synthesis, lead to uncontrolled reactions and irreproducibility. New instrumentation and better understanding of the heating mechanism has seen an increase uptake of this method, since the late 1990s.

Microwaves fall within the frequency range of 0.3-300 GHz. Microwave reactors operate much like a conventional kitchen microwave oven. Both have a set frequency of 2.45 GHz, which corresponds to a wavelength of 12.24 cm; this wavelength is too low in energy to induce chemical reactions directly. Microwave heating works by a process known as dielectric heating where dipoles (induced or permanent) or ions interact with electric component of the photon.<sup>[49]</sup> The dipole or ion attempts to reorient itself in alignment with the oscillating electric field and heating occurs due to molecular friction and dielectric losses. For efficient heating, the frequency needs to be low enough to allow the molecule to attempt to realign but high enough so that it cannot realign perfectly. Fortunately, the frequency of 2.45 GHz satisfies these conditions allowing for the efficient heating of chemical reactions. Several reports of transition metal catalysis using microwave methods exist, including but not limited to Suzuki,<sup>[50]</sup> Stille,<sup>[50]</sup> Negishi<sup>[51]</sup> and BHA<sup>[52]</sup> cross-couplings.

### **3.3.1 Microwave Effects**

In several cases reactions run under microwave conditions have afforded increased yields or different product distributions when compared to conventionally heated reactions run at similar temperatures. In 1996, Hallberg showed that palladium-catalyzed Heck

reactions can be completed in a fraction of the time with similar or improved yields compared to traditional heating methods (**Scheme 3-5**).<sup>[53]</sup> These differences are generally accepted as being purely thermal/kinetic effects. Reactions conducted in a highly polar medium can be rapidly heated, with increases greater than 200 °C over the span of several seconds being known for extreme cases such as heating in ionic liquids. Since microwave heating heats the reaction solution itself, no temperature gradient is formed compared to conventional heating in which heat must be transferred through the reaction vessel to the reaction mixture.<sup>[54]</sup> Rapidly heating the reaction mixture in sealed vessels allows for reaction temperatures to be accessed that are difficult to achieve using standard refluxing conditions. Temperatures that are double the boiling point of the solvent are common, although considerations regarding the considerable pressure that can develop must be made for low-boiling point solvents. Reactions can be accelerated under these conditions according to the Arrhenius law ( $k = Ae^{-E_a/RT}$ ),<sup>[55]</sup> with reactions that would take several days under ambient conditions being completed in minutes under microwave heating. Shorter reaction times can aid in transition metal-catalyzed reactions in the sense that the shorter the reaction times diminish catalyst decomposition process that can occur with prolonged heating.



**Scheme 3-5:** Examples of palladium-catalyzed Heck reaction performed under microwave heating and their comparison to conventional heating methods.

Reactions can also be effectively heated in solvents that are nearly microwave transparent, such as 1,4-dioxane, toluene and hexane. Here, polar or ionic solids/solutes are selectively heated which transfer heat to the mixture.<sup>[56]</sup> This can effectively create ‘molecular radiators’ and local hotspots, by certain reagents in the reaction mixture being selectively heated. These types of interactions have been proposed to account for rate and selectivity differences observed between microwave and conventional heating. It should be noted while these effects can be considered as microwave-specific effects, they are still thermal effects. Non-thermal effects have been suggested and are highly debated. For example, it has been suggested that the attempted alignment of the molecules to the microwaves could lead to orientational ordering,<sup>[57]</sup> which in turn cause other rate or selectivity increases. Even though the effects of microwave heating are not fully understood, the method of microwave heating has proven invaluable in synthetic chemistry.



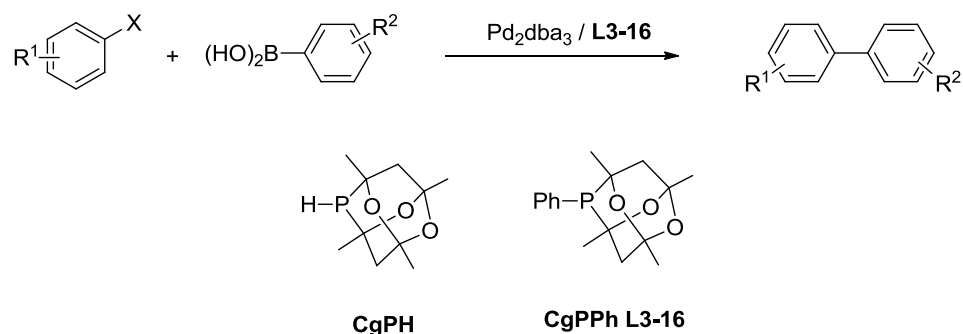
### 3.4 Results and Discussion

As mentioned above, (hetero)aryl amines are valuable synthetic targets as they appear in many natural products, pharmaceuticals and synthetic molecules; of particular interest are functionalized anilines, which can be formed in BHA reactions by using ammonia as the coupling partner. As noted in Section 3.1.2, the monoarylation of ammonia is a particular challenge as the resulting aniline product is often a better nucleophile than ammonia itself, leading to polyarylated products. One of the ways to attempt to circumvent this problem is to simply add excess ammonia so that the product aniline is statistically disfavoured to reenter the catalytic cycle. This method is not without problems. Even though ammonia is not as good of a substrate compared to aniline for most catalytic systems, it is sufficiently nucleophilic enough that a large excess can poison the catalyst.

Since the first report of the monoarylation of ammonia from the Hartwig group appeared in 2006,<sup>[39]</sup> much work has been done to improve the scope and move to more mild and user-friendly conditions. Recent work has shown that nickel could be a good replacement for palladium in C-C and C-heteroatom bond forming reactions.<sup>[25, 58]</sup> Nickel being in Group 10 with platinum and palladium has similar reactivity, but costing about 3000, and 2000 times less respectively, based on current bulk metal prices. Nickel has a smaller atomic radius and is less electronegative compared to palladium and platinum. Given this, one would expect that oxidative addition of aryl chlorides to Ni(0) would proceed more slowly compared to similar Pd(0) and Pt(0) complexes; however it has been shown that the reverse is true, and Ni(0) oxidative addition of aryl chlorides is more rapid compared to Pd(0) and Pt(0).<sup>[59]</sup> As mentioned earlier nickel has more easily accessible

oxidation states, resulting in radical and single electron transfer mechanisms being more facile compared the other group 10 metals.<sup>[60]</sup> Despite this difference nickel-catalyzed aminations have been shown to be mechanistically similar to palladium, with an analogous Ni(0)/Ni(II) catalytic cycle similar to BHA being viable, but not exclusively observed.<sup>[40, 61]</sup>

In designing a new ligand for use in the nickel-catalyzed C-N cross-coupling, the Stradiotto group envisioned the use of a bulky, relatively electron poor bisphosphine to facilitate the reductive elimination step as nickel can, as mentioned previously, more easily undergo oxidative addition of aryl chloride to Ni(0) relative to Pd(0). Notably this design approach differs from that employed for palladium in BHA (Section 3.1). In this vein, Chris Lavoie, a Ph.D. student in the Stradiotto group was able to identify an alternative to the Josiphos family of ligands. This bisphosphine ligand was based on the 1,3,5,7-tetramethyl-2,4,8-trioxa-6-phosphaadamantane moiety (i.e., **CgPH**). This core structure was first synthesized by Epstein and Buckler in 1961,<sup>[62]</sup> by reacting 2,4-pentanedione with phosphine under acidic conditions. However the first use of such ligands in cross-coupling catalysis (with palladium) was disclosed by Capretta in 2003 (**Scheme 3-6**).<sup>[63]</sup> This report described the palladium-catalyzed Suzuki coupling to form functionalized bi(hetero)aryls. As the phosphorus is located within the adamantyl core, the steric demands are accentuated; studies show that this phosphaadamantane core is similar in size to di-tert-butylphosphine ( $P^tBu_2$ ) and a relatively poor electron donor much like phosphinites ( $P(OR)_2$ ).<sup>[64]</sup>



**Scheme 3-6:** General scheme of the palladium-catalyzed Suzuki coupling using the phosphadamantane ligand (**L3-16**), as well as the secondary phosphine (**CgPH**).

The Stradiotto group thought the properties of the **CgP** fragment would make an ideal choice for a bisphosphine ligand with applications in nickel-catalyzed C-N coupling. Several different alkyl and aryl phosphines were tested as the second phosphine; it was found that an *ortho*-phenylene ligand containing both the **CgP** as well as a di(*ortho*-tolyl)phosphino moiety, which was named PAd-Dalpos (**L3-17**, **Figure 3-5**), was the optimal choice in test reactions focusing on ammonia monoarylation. It was found that the most active catalyst system was achieved by the use of a precatalyst that resembles an oxidative addition complex (**C3-4**, **Scheme 3-7**). This air stable complex is synthesized from the more stable  $\text{NiCl}_2 \cdot \text{DME}$ , forgoing the use of the more traditionally used, but unstable  $\text{Ni}(\text{COD})_2$ . After the ligand **L3-17** is bound to the metal center, one of the chlorides is replaced with an *o*-tolyl from the corresponding Grignard reagent. This square planar complex is added directly to the reaction mixture without the need for an external reductant, in contrast to the previously employed (Josiphos) $\text{NiCl}_2$  complex.<sup>[46]</sup>

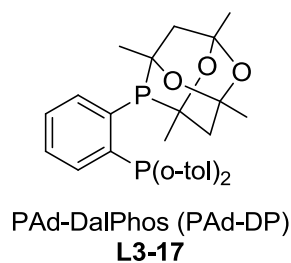
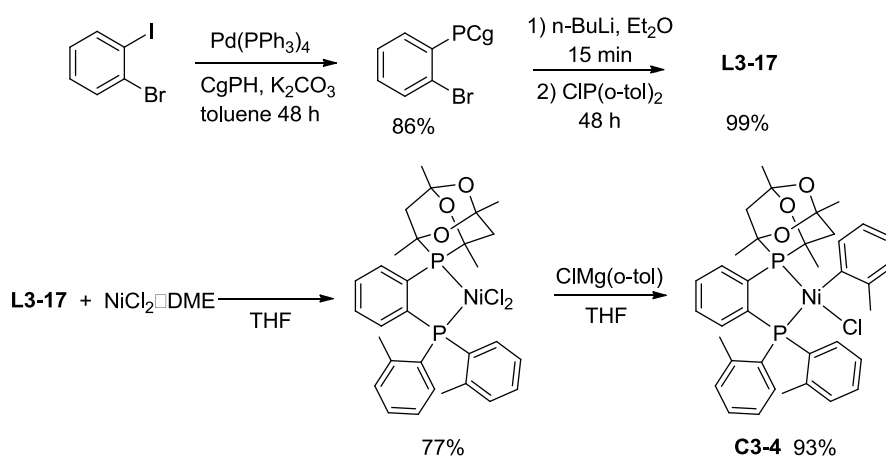


**Figure 3-4:** The PAd-DalPhos ligand developed by the Stradiotto group.



**Scheme 3-7:** Synthesis of PAd-DalPhos (**L3-17**) and the corresponding precatalyst (**C3-4**).

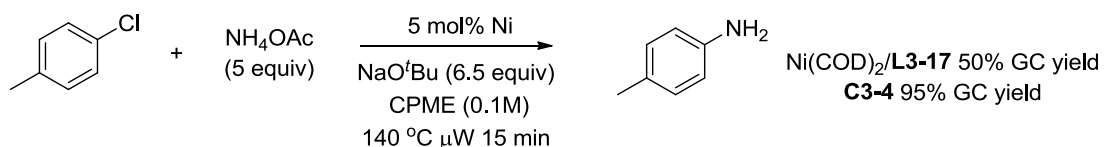
The focus of my thesis research in this area was to explore the use of microwave methods for the monoarylation of ammonia and other small nitrogen nucleophiles. The goal of microwave heating, as mentioned previously, is to reduce reaction times from hours to minutes and to provide access to difficult substrates not usable by conventional heating. The previous report on nickel-catalyzed ammonia monoarylation from the Stradiotto group employed **L3-14** involved the use of ammonia from stock solutions as well as the use of gaseous ammonia (**Section 3.2.1**). Gaseous ammonia is practically not suitable for microwave reactions and initial test reactions with ammonia solutions proved ineffective.

However, the report of nickel-catalyzed ammonia monoarylation from the Hartwig group featured the use ammonium salts, in addition to the use of ammonia solutions.<sup>[47]</sup> In this context, I sought to combine the use of ammonium salts with microwave methods for the first time, using **LC3-4**.

Ammonium salts provide an easier-to-handle alternative to solution and gaseous reagents for academic chemists as gaseous ammonia requires the use of specialized equipment, and solutions of ammonia are sold only in predetermined concentrations. The counter ion with the ammonium salt is also important, as it allows for the tuning of the effective amine concentration through solubility. The first report of the use of ammonium salts for ammonia monoarylation was reported by Panahi in 2014.<sup>[65]</sup> This report involved the use of a nickel(II) chloride catalyst with DPPF (**L3-12**) as the ancillary ligand. This methodology is limited, in that it employs phenols with the activator 2,4,6-trichloro-1,3,5-triazine (TCT), and examples of the monoarylation of ammonia were limited as well, with only a handful of substrates reported. This report was closely followed by a similar report from Hartwig, featuring the use of the palladium-Josiphos (**L2-4**) catalyst system.<sup>[45]</sup> This work made use of ammonium sulfate as the ammonia source, as well as methyl and ethyl ammonium chloride which would otherwise have low boiling points (MeNH<sub>2</sub>, bpt -6.3 °C; EtNH<sub>2</sub>, bpt 16.6 °C) as neutral amines. As mentioned previously, Hartwig also incorporated the use of ammonium salt in his nickel-catalyzed ammonia monoarylation report.<sup>[47]</sup> Building on this work, my thesis work focused on advancing this chemistry (i.e., lower catalyst loadings, shorter reaction times, broader scope) through the combined use of **C3-4** with microwave heating.

### 3.5 Results and Discussion

Inspired by previous work, test reactions were completed with several ammonium salts ( $\text{NH}_4\text{Cl}$ ,  $(\text{NH}_4)_2\text{SO}_4$ , and  $\text{NH}_4\text{OAc}$ ) and it was found that ammonium acetate was the optimal choice for the monoarylation of ammonia as outlined in **Scheme 3-8**. It was noted that an increase in pressure of approximately 3 bar occurred when the reaction temperature reached the melting point of  $\text{NH}_4\text{OAc}$  ( $T = 110\text{-}112\text{ }^\circ\text{C}$ ). This increase in pressure is likely from a greater amount of free ammonia generation caused by a greater interaction between two liquid phases compared to liquid-solid interaction from higher melting point ammonium salts. It was observed that a larger excess of base is required relative to analogous cross-couplings using ammonia stock solution; that is understandable given that base is needed both to first to generate free ammonia from the ammonium salt, then to deprotonate the nickel-coordinated ammonia as part of the cross-coupling catalytic cycle. It was also seen that the precatalyst **C3-4** provided superior reactivity compared to the combined use of  $\text{Ni}(\text{COD})_2$  and **L3-17**. Efficient formation of the monoarylated product was achieved in just 15 minutes by use of **C3-4**, where typical reaction times required by conventional heat are between 3-16 hours. This represents the first example of the monoarylation of ammonia under microwave conditions by use of any catalyst.



**Scheme 3-8:** Nickel-catalyzed monoarylation of ammonia using microwave heating.

From the scope presented in **Table 3-5**, it can be seen that efficient coupling using ammonium salts under microwave heating can be achieved in moderate to excellent yields. In most cases polyarylated products account for the remainder of the aryl halide mass balance as evidenced by gas chromatography analysis. The exception to this is the case of electron-rich aryl halides (leading to **3-3g**), where small amounts of the starting material were also recovered. Heteroaryl halides (leading to **3-3b**) as well as activated aryl halides (leading to **3-3d**) have proven to be challenging, as the more reactive substrates are more prone to polyarylation. Substrates with *ortho* substitution are also challenging as seen by the diminished yields with said substrates. Substrates that contain *diortho*-substitution were unreactive, as was also seen in previous reports.<sup>[46-47]</sup> Also of note is that the **C3-4** catalyst system is capable of coupling aryl halides and ammonia salts at room temperature, affording **3-3a**. This represents the first monoarylation of ammonia with ammonium salts at ambient temperature. Similar reactivity was extended to the use of methyl and ethylammonium salts (**Table 3-6**), which is practically useful given the gaseous nature of these reagents. Alkylamines are better nucleophiles compared to ammonia, and the coupling products are disubstituted, which decreases the possibility of diarylation; as such increased yields were observed relative to reactions using ammonium acetate. Using these alkylammonium coupling partners leads to excellent yields of the target anilines with activated heteroaryl halides.

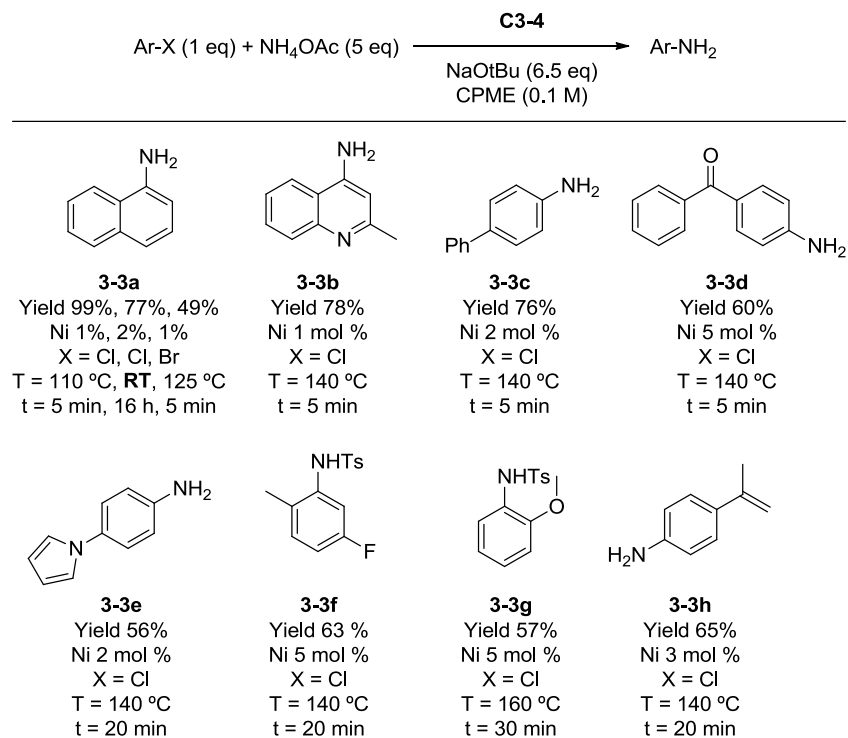


**Table 3-5:** Scope of nickel catalyzed ammonia monoarylation using ammonium acetate under microwave conditions. Isolated yields are given.



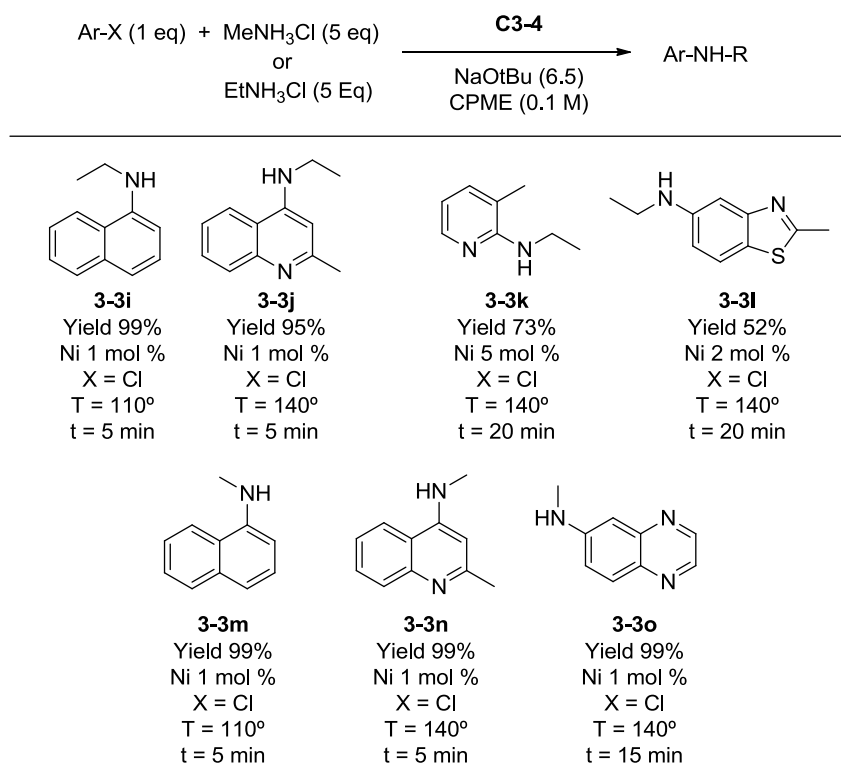


**Table 3-6:** Nickel catalyzed aminations using MeNH<sub>3</sub>Cl and EtNH<sub>3</sub>Cl using microwave heating. Isolated yields are given.

From these reactions using ammonium salts under microwave conditions, comparisons to previously reported catalytic systems can be drawn. In terms of catalyst loading, the **C3-4** system is comparable to similar Pd and Ni systems, in which 0.5-5 mol % catalyst is standard.<sup>[12, 44, 46-47, 61, 65]</sup> Heteroaryl substrates have proven challenging using this system, as the activated nature of these substrates can lead to undesired polyarylated products, especially in the case of ammonium acetate. Also missing in the scope are substrates containing aldehydes, and ketones with  $\alpha$ -protons. These substrates are capable of being deprotonated by *tert*-butoxide bases and  $\alpha$ -arylation of the ketone, which is a known reaction for nickel, likely competes with the desired C-N cross-coupling. For example, numerous products were observed in reactions involving 4-chloroacetophenone, as evidenced by both gas chromatography and thin layer chromatography. Tuning of the

reaction conditions and the use of milder bases, such as carbonates and phosphates, would allow for the inclusion of these substrates. The drawback of using ammonium salts as coupling partners is the need for additional base to generate free ammonia that is able to enter the catalytic cycle. While the use of these solid amine source provides a more user-friendly approach compared to commercial stock solutions, the large excess of base required could prove problematic, especially for base-sensitive substrates. Perhaps the largest advantage to this system can be found in the use of microwave heating. This method can reduce reaction times that can range from 2-24 hours down to 5-30 minutes, depending on the substrate, thereby allowing for the rapid synthesis of the target aniline.

### 3.6 Summary

The work presented herein shows the new ligand PAd-Dalpos (**L3-17**) to be an effective alternative to the Josiphos ligand family in the nickel catalyzed monoarylation of ammonia. Microwave irradiation was employed as a heating method to rapidly conduct reactions, providing the aminated products in minimal amount of time. The hydrochloride salts of the small alkylamine nucleophiles, methylammonium and ethylammonium, were also used successfully. Challenges still remain in this chemistry, such as the selective ammonia monoarylation with strongly activated (hetero)aryl halides. Successful cross-couplings with *diortho* substituted electrophiles also remain elusive.

## 3.7 Experimental

### 3.7.1 General Considerations

All reactions were set up in a dinitrogen atmosphere glovebox and products were isolated using standard benchtop techniques. Anhydrous cyclopentyl methyl ether (CPME) was purchased from Sigma, subjected to three standard freeze-pump-thaw cycles, and was stored in the glovebox. THF, and diethyl ether were distilled from sodium, and benzophenone. Other solvents used in the glovebox were purified by sparging with nitrogen followed by passage through a double column purification system equipped with one alumina packed column and one copper-Q5 packed column. Solvents used in the glovebox were stored over 4 Å molecular sieves. Other reagents were purchased from commercial sources and used as received. All  $^1\text{H}$  NMR and  $^{13}\text{C}$  NMR spectra were recorded using a Bruker AV-300 spectrometer at 300 K. Chemical shifts are expressed in parts per million (ppm) using the residual  $\text{CHCl}_3$  solvent peak ( $^1\text{H}$  7.26 ppm,  $^{13}\text{C}$  77.1 ppm) as an internal reference. Coupling constants ( $J$ ) are reported in Hertz (Hz). Splitting patterns are described as follows: br, broad; s, singlet; d, doublet; t, triplet; q, quartet; m, multiplet. GC data were obtained using an instrument equipped with a SGE BP-5, 30 m, 0.25 mm internal diameter column.

### 3.7.2 General Procedure

#### General Procedure for Microwave Reactions with Ammonium Salts (GP 3-1)

In a dinitrogen glovebox; (PAd-DP)Ni(o-tol)Cl (**C3-4**), ammonium salt (5 equiv, 5 mmol), NaOtBu (6.5 equiv, 6.5 mmol) and substrate (1 mmol), if solid, were weighed into an oven dried 10-20 mL microwave vial with stir bar. Substrate (1 mmol), if liquid, was added followed by 10 mL cyclopentyl methyl ether (CPME). The vial was sealed with an aluminum crimp cap featuring a PTFE/silicone septum, and was removed from the glovebox. Reaction was then heated to the specified temperature in a Biotage Initiator<sup>+</sup> microwave reactor for the given time, using fixed hold time. Upon completion, the reaction mixture was cooled to room temperature, taken up in ca. 50 mL dichloromethane and washed with 3x50 mL distilled water. The organic layer was dried over anhydrous sodium sulfate, filtered and concentrated via rotary evaporation. The crude mixture was purified via column chromatography as indicated.

**1,3,5,7-tetramethyl-2,4,6-trioxaphosphaadamantane-phenylbromide (A).** To a glass screw-capped vial containing a magnetic stir bar was added 2-bromoiodobenzene (0.73 mL, 5.7 mmol, 1.05 eq), toluene (9.0 mL), Pd(PPh<sub>3</sub>)<sub>4</sub> (0.330 g, 0.285 mmol), K<sub>2</sub>CO<sub>3</sub> (1.571 g, 11.4 mmol, 2.0 eq), and 1,3,5,7-tetramethyl-2,4,8-trioxaphosphaadamantane (1.14 g, 5.3 mmol). The vial was sealed with a PTFE-lined cap and was removed from the glovebox. The vial was placed in an oil bath set to 110 °C and magnetic stirring was initiated. After 48 h (unoptimized) the reaction mixture was cooled, diluted with CH<sub>2</sub>Cl<sub>2</sub> (50 mL), and

washed with distilled water (3 x 50 mL). The organic layer was dried over anhydrous Na<sub>2</sub>SO<sub>4</sub>, filtered, and the collected eluent solution was concentrated under reduced pressure by use of a rotary evaporator. The resulting yellow oil was filtered through an alumina plug (ca. 50 g) eluting with 90% hexanes/CH<sub>2</sub>Cl<sub>2</sub>; the solvent was then removed from the collected eluent under reduced pressure by use of a rotary evaporator. The resulting yellow solid was purified by flash chromatography over silica, eluting with 10% ethyl acetate/hexanes to afford **A** as a white solid (1.69 g, 86 % yield). <sup>1</sup>H NMR: (CDCl<sub>3</sub>, 500 MHz) 8.29 (d, *J* = 7.7, 1H), 7.66-7.64 (m, 1H), 7.37 (apparent t, *J* = 7.5 Hz, 1H), 7.25 (apparent t, *J* = 7.6 Hz, 1H), 2.14 (m, 1H), 2.02-1.89 (m, 2H), 1.55-1.44 (m, 13H). <sup>13</sup>C{<sup>1</sup>H} NMR: (CDCl<sub>3</sub>, 125.8 MHz) 135.3 (d, *J* = 22.6 Hz), 135.2, 133.8 (d, *J* = 2.5 Hz), 133.2 (d, *J* = 37.7 Hz), 131.0, 127.5, 97.0, 96.2, 74.5 (d, *J* = 10.1 Hz), 73.9 (d, *J* = 25.2 Hz), 45.8 (d, *J* = 20.1 Hz), 36.5, 28.7 (d, *J* = 18.9 Hz), 28.2, 27.9, 26.7 (d, *J* = 11.3 Hz). <sup>31</sup>P{<sup>1</sup>H} NMR: (CDCl<sub>3</sub>, 202.5 MHz) -29.6. HRMS-ESI (m/z) Calcd for C<sub>16</sub>H<sub>20</sub><sup>79</sup>BrNaO<sub>3</sub>P [M+ Na]: 393.0226; Found: 393.0214.

**Synthesis of PAD-Dalphos L3-17.** Compound **A** and diethyl ether (~0.3 M in **A**) were added to a glass screw-capped vial containing a magnetic stir bar. The vial was sealed with a cap featuring a PTFE septum. The solution was then cooled to -33 °C and magnetic stirring was initiated, followed by drop-wise addition of *n*-butyllithium (1.5 eq, 2.5 M in hexanes) via syringe. The resulting mixture was left to stir for 30 minutes while warming to ambient temperature. At this point a solution of chlorodi(*o*-tolyl)phosphine (1.2 equiv) in diethyl ether (~0.5 M) was added dropwise via syringe with continued stirring. The resulting mixture was left to stir for 48 h (unoptimized) at ambient temperature, after which

the crude reaction mixture was opened to air on the benchtop and was filtered through a short Celite plug; the collected eluent was concentrated by use of a rotary evaporator. The residue was adsorbed onto silica and was then concentrated to dryness by use of a rotary evaporator. The so-formed silica dry pack was added to a silica plug (ca. 50 g), and 10% EtOAc/hexanes (ca. 300 mL) was passed through the plug. The collected eluent was then concentrated to dryness by use of a rotary evaporator, was washed with cold pentane (3 x 1.5 mL), and was then dried in vacuo to afford the desired bisphosphine as a white solid (80%). Note that the NMR spectral assignments was rendered complex by: the  $C_1$ -symmetric nature of these species owing to the chiral (racemic) phosphadamantane group; second-order coupling; dynamic behavior; and possibly in the case of **C3-4** dynamic equilibria involving rotamers and/or between tetrahedral and square planar species.  $^1\text{H}$  NMR: ( $\text{CDCl}_3$ , 300 MHz) 8.32 (m, 1H), 7.39 (m, 1H), 7.29-7.21 (m, 5H), 7.11-7.04 (m, 2H), 6.89-6.87 (m, 1H), 6.79 (dd,  $J = 7.2, 3.1$  Hz, 1H), 6.64 (m, 1H), 2.42 (s, 3H), 2.36 (s, 3H), 2.14-1.79 (m, 3H), 1.57-1.21 (m, 13H).  $^{13}\text{C}\{^1\text{H}\}$  NMR: ( $\text{CDCl}_3$ , 125.8 MHz) 142.7-142.2 (m), 134.2, 133.5, 130.3-130.0 (m), 128.8-128.6 (m), 126.4, 125.8, 97.2, 96.3, 74.5-74.2 (m), 46.1 (d,  $J = 18.9$  Hz), 36.6, 28.4-28.0 (m), 26.3 (d,  $J = 11.3$  Hz), 21.7, 21.5.  $^{31}\text{P}\{^1\text{H}\}$  NMR: ( $\text{CDCl}_3$ , 202.5 MHz, 298K) -24.1 (broad m), -37.7 (d,  $J = 166$  Hz).  $^{31}\text{P}\{^1\text{H}\}$ R: ( $\text{CDCl}_3$ , 121.5 MHz, 223K) -23.8 (d,  $J = 160$  Hz, major species), -30.2 to -33.0 (broad m, minor species), -38.8 (d,  $J = 177$  Hz, minor species), -39.4 (d,  $J = 160$  Hz, major species). HRMS-ESI (m/z) Calcd for  $\text{C}_{30}\text{H}_{34}\text{NaO}_3\text{P}_2$  [ $\text{M}+\text{Na}$ ]: 527.1881; Found: 527.1875. Anal. Calcd for  $\text{C}_{30}\text{H}_{34}\text{O}_3\text{P}_2$ : C, 71.42; H, 6.79. Found: C, 71.12; H, 6.84.

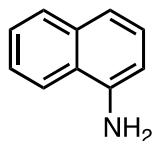
**Synthesis of (L3-17)NiCl<sub>2</sub>.** In a dinitrogen filled glovebox, a 100 mL oven dried round bottom flask containing a magnetic stir bar was charged with NiCl<sub>2</sub>(DME) (1.78 g, 8.10 mmol) and L3-17 (PAd-Dalpos) (4.54 g, 9.00 mmol, 1.1 eq). The solid mixture was dissolved in ca. 90 mL of THF and the resulting solution was stirred magnetically at room temperature for 1 h. The crude reaction mixture was poured directly onto a glass frit and was washed with pentane (5 x 30 mL). The remaining solid on the frit was dissolved by passing CH<sub>2</sub>Cl<sub>2</sub> through the frit (ca. 50 mL), followed by collection of the eluent. The solvent was removed *in vacuo* affording the desired product as a dark purple paramagnetic solid (3.93 g, 77 %). Anal. Calcd for C<sub>30</sub>H<sub>34</sub>Cl<sub>2</sub>NiO<sub>3</sub>P<sub>2</sub> C, 56.82; H, 5.40. Found: C, 56.72; H, 5.65. A single crystal suitable for X-ray diffraction analysis was prepared by slow evaporation of pentane into a solution of CH<sub>2</sub>Cl<sub>2</sub> at room temperature.

**Synthesis of C3-4.** (L3-17)NiCl<sub>2</sub> (3.90 g, 6.15 mmol) and THF (62 mL) were added to an oven-dried 100 mL round-bottom flask containing a magnetic stir bar. Magnetic stirring was initiated and *ortho*-tolylmagnesium chloride was then added drop-wise (7.40 mL, 7.40 mmol, 1.2 eq, 1.0 M in THF) to the heterogeneous mixture, resulting in an immediate color change from red to orange. The reaction mixture was allowed to stir at room temperature for 2 h. The reaction mixture was subsequently treated with MeOH (5 mL) in air, and then was reduced to dryness *in vacuo*. The residue was treated with cold MeOH (0 °C, 15 mL), and the crude reaction mixture was then filtered through a glass frit, affording a retained orange solid that was washed with additional cold MeOH (0 °C, 3 x 10 mL), followed by pentane (3 x 50 mL). The orange solid on the frit was then dissolved *via* addition of CH<sub>2</sub>Cl<sub>2</sub> (50 mL). Collection of the eluent followed by removal solvent afforded (L3-17)Ni(o-

tolyl)Cl, **C3-4**, as an orange solid (3.95 g, 93 % yield). The existence of a major and minor diastereomers (ca. 2:1) in solution is suggested on the basis of  $^{31}\text{P}\{^1\text{H}\}$  NMR data.  $^1\text{H}$  NMR: ( $\text{CDCl}_3$ , 500 MHz) 8.74 (m, 1H), 7.59-7.09 (m, 10H), 6.86-6.67 (m, 5H), 3.33-2.59 (m, 9H), 1.98-1.93 (m, 1H), 1.59-1.53 (m, 6H), 1.42 (s, 3H), 1.10-0.92 (s, 6H).  $^{13}\text{C}\{^1\text{H}\}$  NMR: ( $\text{CDCl}_3$ , 125.8 MHz) 145.9 (m), 145.8 (m), 143.4-143.2 (m), 136.7-133.1 (m), 132.0-130.9 (m), 129.6-128.6 (m), 126.3-125.8 (m), 124.7 (m), 123.8 (m), 122.7, 97.8-96.2 (m), 40.2-39.6 (m), 28.8-24.2 (m).  $^{31}\text{P}\{^1\text{H}\}$  NMR: ( $\text{CDCl}_3$ , 202.5 MHz) 32.6 (d,  $J = 4.3$  Hz, minor species), 31.5 (d,  $J = 4.6$  Hz, major species), 27.6 (d,  $J = 4.6$  Hz, major species), 26.5 (d,  $J = 4.3$  Hz, minor species). On the basis of the observed positional disorder associated with the Ni-bound *ortho*-tolyl fragment within the X-ray structure of **C3-4**, arising from Ni-C(tolyl) bond rotation (80:20 occupancy ratio), we interpret the major and minor species as being rotamers of this type. Anal. Calcd for  $\text{C}_{37}\text{H}_{41}\text{ClNiO}_3\text{P}_2$  C, 64.42; H, 5.99. Found: C, 64.11; H, 5.84. A single crystal suitable for X-ray diffraction analysis was prepared by slow evaporation of pentane into a solution of  $\text{CH}_2\text{Cl}_2$  at room temperature.

### 3.3.2 Characterization Data for Isolated Materials

Naphthalen-1-amine (**3-3a**)

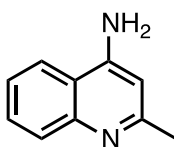


Following **GP 3-1**: (1 mol % **C3-4**, 110 °C, 5 minutes) the title compound was isolated in



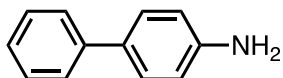
99% yield from the corresponding chloride. Purified by column chromatography (10:1, hexanes/EtOAc) to yield as a purple solid in 89% yield from the corresponding chloride.  $^1\text{H}$  NMR (500 MHz,  $\text{CDCl}_3$ ):  $\delta$  7.88-7.84 (m, 2H), 7.51-7.49 (m, 2H), 7.36-7.29 (m, 2H), 6.82 (m, 1H), 4.17 (br s, 2H);  $^{13}\text{C}\{^1\text{H}\}$  NMR (125.8 MHz,  $\text{CDCl}_3$ ):  $\delta$  142.3, 134.6, 128.8, 126.5, 126.0, 125.1, 123.9, 121.0, 109.1. Agrees with data previously reported in the literature.<sup>[46]</sup>

#### 4-Aminoquinoline (**3-3b**)



Following **GP 3-1**: (0.5 mmol ammonium acetate, 1 mol% **C3-4**, 140 °C, 5 minutes) the title compound was isolated in 78% yield. Purified by column chromatography (7:2:1, hexanes/EtOAc/ $\text{NH}_4\text{Pr}_2$ ) to yield a light yellow solid in 87% yield from the corresponding chloride.  $^1\text{H}$  NMR (500 MHz,  $\text{CDCl}_3$ ):  $\delta$  7.92 (d,  $J = 8.5$  Hz, 1H), 7.72-7.70 (m, 1H), 7.63-7.59 (m, 1H), 7.40-7.36 (m, 1H), 6.50 (s, 1H), 4.68 (br s, 2H), 2.58 (s, 3H);  $^{13}\text{C}\{^1\text{H}\}$  NMR (125.8 MHz,  $\text{CDCl}_3$ ):  $\delta$  159.5, 149.8, 18.9, 129.6, 129.3, 124.3, 120.2, 117.6, 25.5. Agrees with data previously reported in the literature.<sup>[46]</sup>

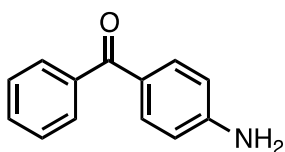
#### 4-Phenylaniline (**3-3c**)



Following **GP 3-1**: (2 mol % **C3-4**, 140 °C, 5 minutes) the title compound was isolated in 76% yield from the corresponding chloride. Purified by column chromatography (10:1,

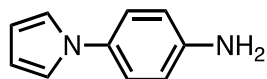
hexanes/EtOAc) to yield a beige yellow solid in 63% yield from the corresponding bromide.  $^1\text{H}$  NMR (300 MHz,  $\text{CDCl}_3$ ):  $\delta$  7.58-7.56 (m, 2H), 7.46-7.40 (m, 4H), 7.32-7.28 (m, 1H), 6.80-6.77 (m, 2H), 3.72 (br s, 2H);  $^{13}\text{C}\{^1\text{H}\}$  NMR (75.5 MHz,  $\text{CDCl}_3$ ):  $\delta$  145.8, 141.2, 131.6, 128.7, 128.0, 126.4, 126.3, 115.4. Agrees with data previously reported in the literature.<sup>[46]</sup>

#### 4-Aminobenzophenone (**3-3d**)



Following **GP 3-1**: (5 mol% **C3-4**, 140 °C, 5 minutes). Purified by column chromatography (0% EtOAc/100% hexanes to 50/50% EtOAc/hexanes gradient) to yield a white solid in 60% yield from the corresponding chloride.  $^1\text{H}$  NMR (300 MHz, DMSO):  $\delta$  7.57-7.62 (m, 3H), 7.54-7.56 (m, 1H), 7.51-7.52 (m, 2H), 7.48-7.50 (m, 1H), 6.57-6.64 (m, 2H), 6.14 (br s, 2H);  $^{13}\text{C}\{^1\text{H}\}$  NMR (75.5 MHz, DMSO):  $\delta$  193.3, 153.7, 139.0, 132.5, 130.9, 128.7, 128.1, 123.6, 112.5. Agrees with data previously reported in the literature.<sup>[47]</sup>

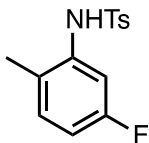
#### 4-(1H-Pyrrol-1-yl)aniline, (**3-3e**)



Following **GP 3-1**: (2 mol % **C3-4**, 140 °C, 20 minutes) the title compound was isolated in 56% yield. Purified by column chromatography (10:1, hexanes/EtOAc) to yield a light brown solid in 76% yield from the corresponding chloride.  $^1\text{H}$  NMR (500 MHz,  $\text{CDCl}_3$ ):  $\delta$  7.23-7.22 (m, 2H), 7.02-7.01 (m, 2H), 6.77-6.75 (m, 2H), 6.35-6.34 (m, 2H), 3.76 (br s, 2H);  $^{13}\text{C}\{^1\text{H}\}$  NMR (125.8 MHz,  $\text{CDCl}_3$ ):  $\delta$  144.7, 133.1, 122.6, 119.9, 115.9, 109.7.

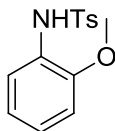
Agrees with data previously reported in the literature.<sup>[46]</sup>

N-(5-Fluoro-2-methylphenyl)-4-methylbenzenesulfonamide (**3-3f**)



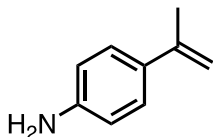
Following **GP 3-1**: (5 mol% **C3-4**, 140 °C, 20 minutes). The crude product was tosylated using a literature procedure<sup>[66]</sup> to yield a white solid in 63% yield. <sup>1</sup>H NMR (300 MHz, CDCl<sub>3</sub>): δ 7.70-7.65 (m, 2H), 7.28-7.25 (m, 2H), 7.19-7.15 (m, 1H), 7.06-7.01 (m, 1H), 6.80-6.73 (m, 1H), 6.57 (br s, 1H), 2.41 (s, 3H), 1.99 (s, 3H); <sup>13</sup>C{<sup>1</sup>H} NMR (75.5 MHz, CDCl<sub>3</sub>): δ 161.3 (*J*<sub>CF</sub> = 244.0 Hz), 144.1, 136.4, 135.6 (*J*<sub>CF</sub> = 10.4 Hz), 129.7, 127.1, 125.2 (*J*<sub>CF</sub> = 3.1 Hz), 112.3 (*J*<sub>CF</sub> = 21.1 Hz), 110.1 (*J*<sub>CF</sub> = 25.3 Hz), 21.5, 16.8; HRMS *m/z* ESI<sup>+</sup> found 302.0621 [M + Na]<sup>+</sup> calculated for C<sub>14</sub>H<sub>14</sub>FNO<sub>2</sub>SNa 302.0627.

2-Anisidine (**3-3g**)



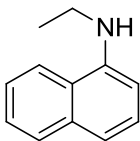
Following **GP 3-1**: (5 mmol ammonium acetate, 5 mol% **C3-4**, 160 °C, 30 minutes) The crude product was tosylated using a literature procedure<sup>[66]</sup> to yield a brown oil in 57% yield. <sup>1</sup>H NMR (300 MHz, CDCl<sub>3</sub>): δ 7.68-7.65 (m, 2H), 7.55-7.52 (m, 1H), 7.22-7.19 (m, 2H), 7.07-7.01 (m, 2H), 6.94-6.88 (m, 1H), 6.76-6.73 (m, 1H), 3.66 (s, 3H), 2.37 (s, 3H); <sup>13</sup>C{<sup>1</sup>H} NMR (75.5 MHz, CDCl<sub>3</sub>): δ 149.4, 143.6, 136.4, 129.3, 127.3, 126.1, 125.2, 121.1, 121.0, 110.6, 55.6, 21.5.

#### 4-Amino- $\alpha$ -methylstyrene (**3-3h**)



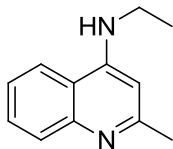
Following **GP 3-1**: (3 mol% **C3-4**, 140 °C, 20 minutes). Purified by column chromatography (0% EtOAc/100% hexanes to 30/70% EtOAc/hexanes gradient) to yield a brown oil in 65% yield from the corresponding chloride.  $^1\text{H}$  NMR (300 MHz,  $\text{CDCl}_3$ ):  $\delta$  7.30-7.36 (m, 2H), 6.63-6.70 (m, 2H), 5.25-5.29 (m, 1H), 4.92-4.97 (m, 1H), 3.68 (br s, 2H), 2.13 (s, 3H);  $^{13}\text{C}\{^1\text{H}\}$  NMR (75.5 MHz,  $\text{CDCl}_3$ ):  $\delta$  145.8, 142.7, 131.6, 126.4, 114.7, 109.3, 21.8. Agrees with data previously reported in the literature.<sup>[47]</sup>

#### N-ethylnaphthalen-1-amine (**3-3i**)



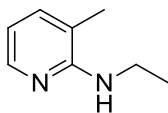
Following **GP 3-1**: (1 mol% **C3-4**, 136.2  $\mu\text{L}$  1-chloronaphthalene, 407.7 mg ethylammonium chloride, 100 °C, 5 minutes), the reaction was stirred at 110 °C for 5 minutes. The title product was isolated as a dark oil (99%).  $^1\text{H}$  NMR (300 MHz,  $\text{CDCl}_3$ ):  $\delta$  7.81-7.88 (m, 2H), 7.37-7.53 (m, 3H), 7.29 (d,  $J = 7.9$  Hz, 1H), 6.67 (d,  $J = 6.9$  Hz, 1H), 4.33 (br s, 1H), 3.36 (q,  $J = 7.1$  Hz, 2H), 1.45 (t,  $J = 7.1$ , 3H);  $^{13}\text{C}\{^1\text{H}\}$  (75.4 MHz,  $\text{CDCl}_3$ ):  $\delta$  143.5, 134.3, 128.6, 126.6, 125.6, 124.6, 123.3, 119.8, 117.2, 104.3, 38.7, 14.8. Agrees with previously reported data.<sup>[47]</sup>

*N*-Ethyl-2-methylquinolin-4-amine (**3-3j**)



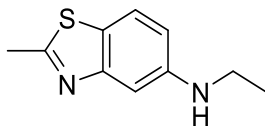
Following **GP 3-1**: (1.0 mmol 4-chloroquinoline, 5.0 mmol ethylammonium chloride, 1 mol% **C3-4**, 140 °C, 5 minutes) the title product was isolated as a white solid in 95% yield. <sup>1</sup>H NMR (300 MHz, DMSO): δ 8.16-8.13 (m, 1H), 7.69-7.66 (m, 1H), 7.50-7.57 (m, 1H), 7.28-7.36 (m, 1H), 6.96-6.93 (m, *J* = 5.1 Hz, 1H), 6.33 (s, 1H), 3.23-3.34 (m, 2H), 2.16 (s, 3H), 1.27 (t, *J* = 7.1 Hz, 3H); <sup>13</sup>C {<sup>1</sup>H} (75.5 MHz, DMSO): δ 158.6, 149.8, 148.0, 128.5, 128.2, 122.8, 121.4, 117.4, 97.9, 36.9, 25.2, 13.7; HRMS *m/z* ESI<sup>+</sup> found 187.1230 [M+H]<sup>+</sup> calculated for C<sub>12</sub>H<sub>15</sub>N<sub>2</sub> 187.1191.

*N*-Ethyl-3-methylpyridin-2-amine (**3-3k**)



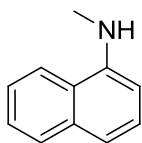
Following **GP 3-1**: (1 mmol 2-chloro-3-methylpyridine, 5 mmol ethylammonium chloride, 5 mol% **C3-4**, 140 °C, 20 minutes) the title product was isolated as a light yellow oil in 73% yield. A 20% ethyl acetate/hexanes eluent system was used for column chromatography on silica gel. <sup>1</sup>H NMR (300 MHz, CDCl<sub>3</sub>): δ 8.06-8.00 (m, 1H), 7.24-7.18 (m, 1H), 6.54-6.48 (m, 1H), 4.05 (br s, 1H) 3.58-3.46 (m, 2H), 2.08 (s, 3H), 1.29 (t, *J* = 7.17, 3H); <sup>13</sup>C {<sup>1</sup>H} NMR (75.5 MHz, CDCl<sub>3</sub>): δ 156.9, 145.5, 136.6, 116.3, 112.3, 36.4, 16.9, 15.2; HRMS *m/z* ESI<sup>+</sup> found 173.1073 [M+H]<sup>+</sup> calculated for C<sub>8</sub>H<sub>13</sub>N<sub>2</sub> 173.1034.

*N*-Ethyl-2-methylbenzo[*d*]thiazol-5-amine (**3-3l**)



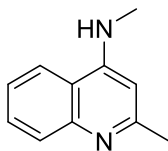
Following **GP 3-1**: (1.0 mmol 5-chloro-2-methylbenzothiazole, 5.0 mmol ethylammonium chloride 2 mol% **C3-4**, 140 °C, 20 minutes) the title product was isolated as a brown solid in 52% yield. <sup>1</sup>H NMR (500 MHz, CDCl<sub>3</sub>): δ 7.58-7.57 (m, 1H), 7.22-7.21 (m, 1H), 6.80-6.75 (m, 1H), 3.25 (q, *J* = 7.1 Hz, 2H), 2.21 (s, 3H), 1.33 (t, *J* = 7.1 Hz, 3H); <sup>13</sup>C{<sup>1</sup>H} (125.8 MHz, CDCl<sub>3</sub>): δ 167.7, 155.1, 147.2, 124.5, 121.6, 113.8, 104.8, 39.3, 20.3, 14.8; HRMS *m/z* ESI<sup>+</sup> found [M+H]<sup>+</sup> calculated for C<sub>10</sub>H<sub>13</sub>N<sub>2</sub>S 193.0755.

*N*-Methylnaphthalen-1-amine (**3-3m**)



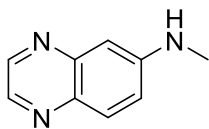
Following **GP 3-1**: (1.0 mmol 1-chloronaphthalene, 5.0 mmol methylammonium chloride, 1 mol% **C3-4**, 110 °C, 5 minutes). The title product was isolated as a brown oil in 99% yield. <sup>1</sup>H NMR (300 MHz, CDCl<sub>3</sub>): δ 7.79-7.88 (m, 2H), 7.40-7.54 (m, 3H), 7.28-7.33 (m, 1H), 6.65 (d, *J* = 7.5 Hz, 1H), 4.48 (br s, 1H), 3.05 (s, 3H); <sup>13</sup>C{<sup>1</sup>H} (75.5 MHz, CDCl<sub>3</sub>): δ 144.5, 134.2, 128.6, 126.7, 125.7, 124.7, 123.4, 119.8, 117.3, 103.8, 31.0. Spectral data are in agreement with the literature.<sup>[47]</sup>

Methyl-(2-methyl-quinolin-4-yl)amine (**3-3n**)



Following **GP 3-1**: (1.0 mmol 4-chloroquinaldine, 5.0 mmol methylammonium chloride, 1 mol% **C3-4**, 140 °C, 5 minutes) the title product was isolated as a white solid in 99% yield. <sup>1</sup>H NMR (500 MHz, CDCl<sub>3</sub>): δ 7.97-7.95 (m, 1H), 7.70-7.68 (m, 1H), 7.65-7.61 (m, 1H), 7.42-7.38 (m, 1H), 6.38 (s, 1H), 5.00 (br s, 1H), 3.09 (d, *J* = 5.0 Hz 3H), 2.67 (s, 3H); <sup>13</sup>C{<sup>1</sup>H} NMR (125.8 MHz, CDCl<sub>3</sub>): δ 159.9, 150.8, 148.4, 129.5, 129.2, 124.1, 119.2, 117.6, 99.0, 30.3, 26.0. Spectral data are in agreement with the literature.<sup>[67]</sup>

Methyl-quinoxalin-6-yl-amine (**3-3o**)



Following **GP 3-1**: (1.0 mmol 6-chloroquinoxaline, 5.0 mmol methylammonium chloride 1 mol% **C3-4**, 140 °C, 15 minutes): The title product was isolated as a bright yellow solid in 99% yield. <sup>1</sup>H NMR (500 MHz, CDCl<sub>3</sub>): δ 8.68 (d, *J* = 2.2 Hz, 1H), 8.54 (d, *J* = 2.0 Hz, 1H), 7.88 (d, *J* = 9.1 Hz, 1H), 7.17-7.15 (m, 1H), 7.00-6.99 (m, 1H), 4.31 (br s, 1H), 3.04 (d, *J* = 5.2 Hz, 3H); <sup>13</sup>C{<sup>1</sup>H} NMR (125.8 MHz, CDCl<sub>3</sub>): δ 145.7, 145.0, 143.4, 140.4, 138.2, 130.1, 122.0, 103.3, 30.5. Spectral data are in agreement with the literature.<sup>[45]</sup>

## Chapter 4 Nickel-Catalyzed Cross-coupling of Secondary Amines/Azoles Using a Wide Bite Angle Ligand

### 4.1 Utility of Wide Bite Angle Ligands in Transition Metal Catalysis

As mentioned previously in this thesis, nickel(0) readily undergoes oxidative addition of aryl halides, thus the reductive elimination step can be rate-limiting for a given cross-coupling reaction. In designing effective nickel cross-coupling catalysts, it therefore makes sense then to design ligands that facilitate reductive elimination, not only to increase catalyst turn over, but to increase selectivity as well. One method of increasing the rate of reductive elimination is to make use of bidentate ligands that have a large bite angle. The bite angle ( $\phi$ ) is defined as the angle formed by the P-M-P bonds of a ligand bound to a metal (**Figure 4-1**).<sup>[68]</sup> These ligands can increase the rate of reductive elimination in two ways. Firstly, by coordinating to the metal at an angle of greater than  $90^\circ$ , the zero-valent metal is electronically favoured over the divalent species; this effect is more pronounced the greater the deviation from the ideal  $90^\circ$  square planar geometry.<sup>[69]</sup> The second effect is steric in origin; as the bite angle of the ancillary ligand becomes larger the reactive ligands are 'pushed' closer together, which also favours the reductive elimination of those ligands. Simply put, the effect on reductive elimination by wide bite angle ligands is from the stabilization or destabilization of the initial, transition state and/or final structure of the complex. It is worthy of consideration, however, that if the ligand bite angle is too large the *trans*-ligated complex can be stabilized over the *cis* complex (**Figure 4-2**), with



reductive elimination being possible only in the *cis* conformation. The bite angle of a bidentate ligand can be determined in two ways: the natural bite angle is determined computationally by binding a ligand to a dummy atom with no angular preferences; the second method is to obtain the angle experimentally from crystallographic data.<sup>[68]</sup> Wide bite angle ligands can have a profound impact on the reactivity of a catalyst, both in terms of activity and selectivity.

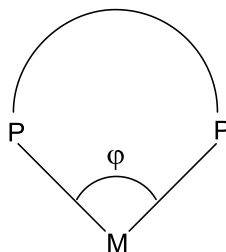


**Figure 4-1:** The bite angle ( $\phi$ ) for a bidentate ligand.

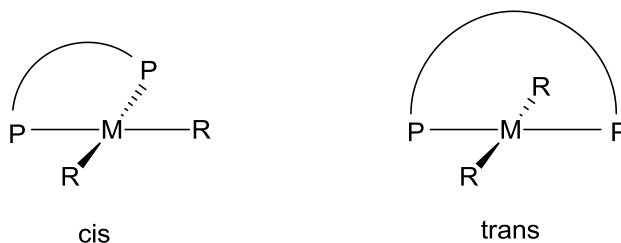


**Figure 4-2:** *Cis* and *trans* geometries in square planar metal complexes

Two of the most successful types of wide bite angle ligands are DPEphos (**L4-1**) and Xantphos (**L4-2**), first synthesized in 1995 (**Figure 4-3**).<sup>[70]</sup> These two classes of ligands are easily tunable to give a large variety of ligands with small variations in their bite angles. The oxygen linker in these ligands is evidently important as other atoms in this position can negatively impact catalytic performance. If the oxygen is replaced by either sulfur or nitrogen, a tridentate pincer ligand is often the result as these atoms are stronger

donors.<sup>[69, 71]</sup> If replaced with carbon, as in **L4-3** (**Figure 4-3**), the result is usually cyclometalation of the C-H bond by the coordinating metal to give a PCP pincer complex.<sup>[69]</sup>

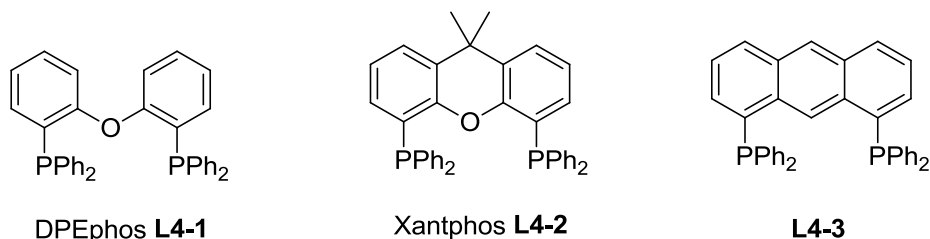
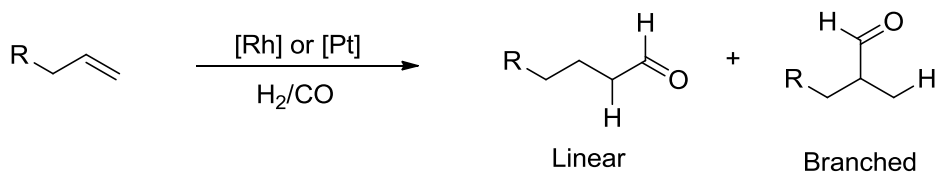


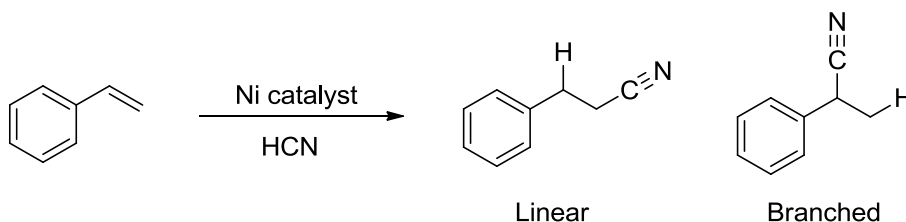
**Figure 4-3:** Examples of wide bite angle ligands.

These ligands **L4-1** and **L4-2** have been successfully employed in many different reaction types, including rhodium and platinum catalyzed hydroformylation reactions (**Scheme 4-1**). One of the challenges in this reaction is the uncontrolled alkene isomerization to give a distribution of products.<sup>[72]</sup> Initial experimental comparisons showed that wide bite angle ligands favoured the formation of linear aldehyde.<sup>[73]</sup> It is thought that wide bite angle ligands enforce an equatorial conformation that leads to the observed selectivity.<sup>[74]</sup> It was shown that the Xantphos ligands gave excellent selectivity, with the variant giving a bite angle of 120° showing the highest selectivity, and a threefold increase in activity, compared to other Xantphos variants.



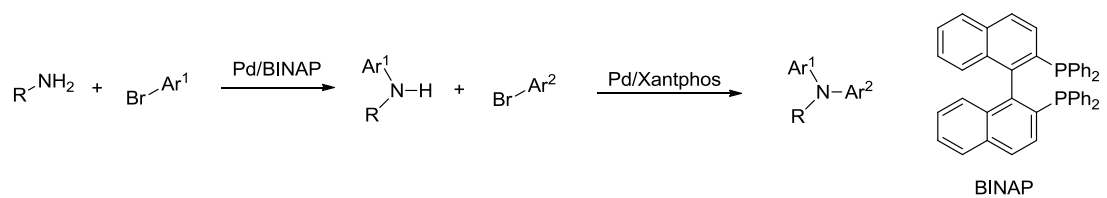
**Scheme 4-1:** General hydroformylation reaction showing linear and branched products.

A dramatic dependence on bite angle was seen in nickel-catalyzed hydrocyanation of styrene (**Scheme 4-2**). Reductive elimination was shown to be the rate limiting step in these reactions, and that rates were enhanced by the use of ligands which afford a bite angle of about  $105^\circ$ .<sup>[75]</sup> In this case, many catalysts were selective for the branched product; however any deviation from a bite angle of  $105^\circ$  was accompanied by a sharp decrease in yield. More conventional ligands featuring a bite angle near  $90^\circ$  provided yields less than 15%.



**Scheme 4-2:** Nickel-catalyzed hydrocyanation showing linear and branched products.

Wide bite angle ligands have also been successfully employed in BHA reactions. In these reactions, a larger bite angle has been correlated with a decrease in  $\beta$ -hydride elimination. In the early development of BHA, Xantphos was used to couple aryl bromides with secondary amines, with low loadings in good yields.<sup>[76]</sup> Xantphos has also been used with BINAP as a two part reaction system in which an alkylamine was coupled with two differing aryl bromides (**Scheme 4-3**).<sup>[77]</sup> This sequential system affords an asymmetric alkyldiarylamine. It has also been suggested that dissociation of one of the P donor atoms leads to a three coordinate palladium species, which aids in reductive elimination.



**Scheme 4-3:** Sequential aminations to give asymmetric aryl amines using Xantphos.

#### 4.1.1 Proposed Application to Nickel-Catalyzed C-N Cross-Coupling

In this context, I became interested in the development of variants of PAd-Dalphos (**L3-17**) ligand based on the Xantphos and DPEphos core structures. The new ligands along with **L4-1** and **L4-2** and derivatives would be used in nickel-catalyzed cross-coupling reactions, such as C-N cross-coupling, in anticipation that they will offer superior performance relative to other catalyst systems including PAd-Dalphos. The synthesis of these ligands would follow the methods previously described in the literature.<sup>[70]</sup> This small library of ligands could be tested alongside PAd-Dalphos, not only in C-N couplings but in other coupling reactions (**Chapter 5**).

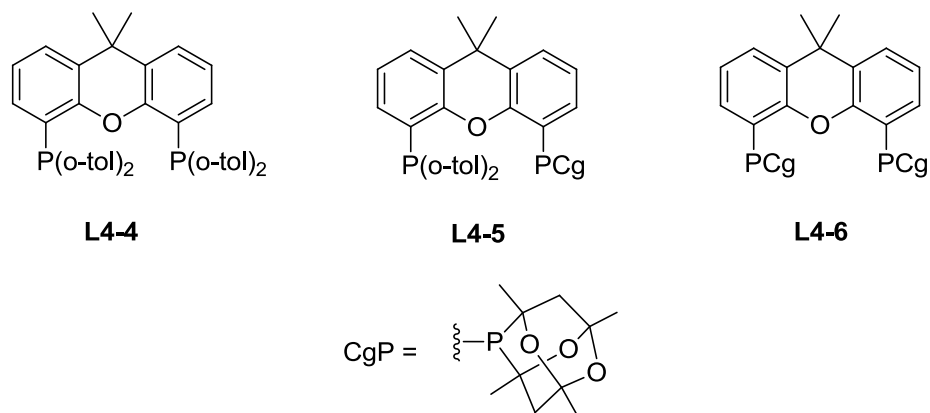
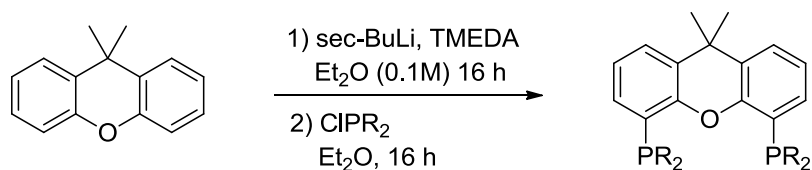


**Figure 4-4:** New Xantphos variants to be synthesized

## 4.2 Results and Discussion

Initial efforts were directed toward the synthesis of both Xantphos as well as DPEphos as shown in **Scheme 4-4**. While **L4-4** could be easily synthesized and purified by this method, other variants proved to be much more challenging. Both variants **L4-5** and **L4-6** require the phosphine halide CgPX, and as such several methods were attempted to prepare this bromide reagent including the use of Br<sub>2</sub>, or NBS (N-bromosuccinimide).<sup>[78]</sup> While the halogenation of **CgPH** was successful, in all cases the only product obtained was the oxide (i.e., **CgP(O)Br**) as evidenced by high resolution mass spectrometry. The use of other several other phosphine chlorides proved to be problematic; for example, the use of chlorobis(3,5-trifluoromethylphenyl)phosphine showed significant side products by <sup>31</sup>P{<sup>1</sup>H} NMR that were unable to be removed by the use of either recrystallization or column chromatography. Despite these setbacks, parent Xantphos, and DPEphos, as well as some commercially available variants (**Figure 4-5**) were screened in nickel-catalyzed C-N cross-coupling (**Table 4-1**).



**Scheme 4-4:** Proposed synthesis of known and new Xantphos ligands, variants of DPEphos to be synthesized in similar fashion.

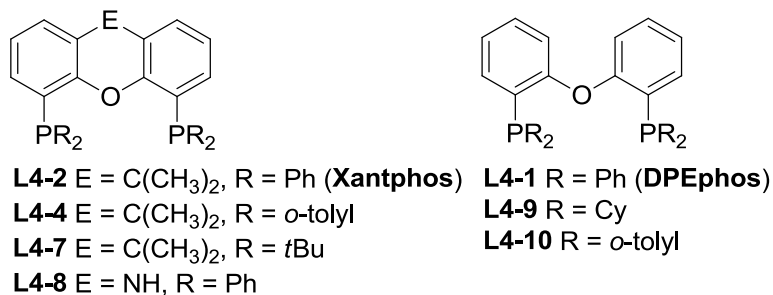


**Figure 4-5:** Wide bite angle ligand variants tested in nickel-catalyzed C-N cross-coupling.

With these ligands in hand precatalyst complexes were sought, similar to **C3-4** as outlined in **Scheme 3-7**, efforts were made to avoid the use of Ni(COD)<sub>2</sub>, due the inhibitory nature of COD. However, practical issues arose in that several of the bulkier bisphosphines (**L4-4**, **L4-7**) were unable to coordinate to NiCl<sub>2</sub>. After filtration, a white insoluble solid was obtained, presumably some nickel species, while the free ligand was found in the mother liquor. Recently a new nickel(II) precursor, (TMEDA)Ni(*o*-tolyl)Cl, was reported.<sup>[79]</sup> This complex, when combined with an appropriate ligand, was shown to be capable of effecting a number of different cross-coupling reactions. As such this complex was employed as the nickel precursor to test Xantphos, DPEphos, and variants in C(sp<sup>2</sup>)-N reactions with several different nucleophiles (**Table 4-1**). From these test reactions, it can be seen that the examined ligands are a poor choice for ammonia, having poor conversions on the basis gas chromatography data. DPEphos (**L4-1**) outperformed the other ligands tested in cross-couplings involving both primary, and secondary

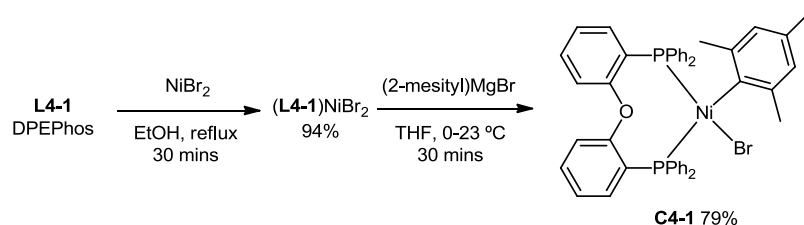
amines/azoles. However, on further analysis reactions involving primary amines significant amounts of undesired diarylation were detected.

Ligand	ammonia <sup>a</sup>	octylamine <sup>b</sup>	morpholine	indole
<b>L4-2</b>	0	50	60	0
<b>L4-4</b>	0	0	0	0
<b>L4-7</b>	0	0	0	0
<b>L4-8</b>	0	0	40	0
<b>L4-1</b>	0	<b>70</b>	<b>90</b>	<b>90</b>
<b>L4-9</b>	0	40	0	0
<b>L4-10</b>	0	0	0	0

**Table 4-1:** Ligand screen for nickel catalyzed C-N cross-coupling. Ammonia from 0.5 M stock solution in 1,4-dioxane. Conversion estimated by gas chromatography. [a] 3 equivalents ammonia. [b] 1-chloronaphthalene was used as the coupling partner with octylamine.

Having identified **L4-1** (i.e., DPEphos) as being a useful ligand in enabling the nickel-catalyzed C(*sp*<sup>2</sup>)-N cross-coupling of secondary amines/azoles with activated (hetero)aryl chlorides. Attention was turned to the synthesis of a well-characterized (**L4-1**)Ni(aryl)X pre-catalyst. Pre-formed Ni(II) complexes of this type, including but not restricted to L<sub>n</sub>Ni(*o*-tolyl)Cl variants,<sup>[80]</sup> are attractive as pre-catalysts in that they are often air-stable and commonly out-perform catalysts generated *in situ* by the addition of a nickel source and ancillary ligand as in **Table 4-1**.<sup>[81]</sup> Efforts to prepare (**L4-1**)Ni(*o*-tolyl)Cl by use of various established literature methods,<sup>[80b, 80c, 80f]</sup> including treatment of (**L4-1**)NiCl<sub>2</sub> with (*o*-tolyl)MgCl, in each case initially afforded a crude orange solid in keeping with other L<sub>n</sub>Ni(*o*-tolyl)Cl complexes; however, in the course of attempting to further

purify/characterize this material, decomposition to a dark, paramagnetic mixture was observed. Encouraged by a report from Jamison and co-workers,<sup>[80b]</sup> whereby the incorporation of a 2-mesityl rather than *o*-tolyl group is shown to increase pre-catalyst stability, The synthesis of (L4-1)Ni(2-mesityl)Br was pursued, as outlined in **Scheme 4-5**. I was gratified to find that the readily prepared intermediate (L4-1)NiBr<sub>2</sub> was efficiently transformed into (L4-1)Ni(2-mesityl)Br (**C4-1**) upon treatment with (2-mesityl)MgBr.



**Scheme 4-5:** Synthesis of the air-stable precatalyst **C4-1**.

Complex **C4-1** proved stable both to isolation and storage as a solid in air and was fully characterized. The solution <sup>31</sup>P{<sup>1</sup>H} NMR spectrum of **C4-1** features two doublets, in keeping with the *cis*-chelated square-planar structure observed in the single-crystal X-ray structure of **C4-1** (P-Ni-P bite angle ~102°; **Figure 4-6**). Whereas this *cis*-geometry mirrors that of several reported L<sub>n</sub>Ni(*o*-tolyl)Cl complexes (L<sub>n</sub>, P-Ni-P bite angles: DPPF,<sup>[80c]</sup> ~102°; CyPF-Cy,<sup>[80e]</sup> ~98°; BINAP, ~93°;<sup>[80b]</sup> PAd-Dalpos,<sup>[80d]</sup> ~87°), *trans*-spanning bisphosphine ligation is observed in analogous DCPF<sup>[80b]</sup> (~144°), DiPPF<sup>[80f]</sup> (~145°), and Xantphos<sup>[80b]</sup> (~156° and featuring κ<sup>3</sup>-POP connectivity) complexes. At first glance, it may be tempting to rationalize the superior catalytic abilities of **L4-1** relative to **L4-2**, especially in the cross-coupling of indole leading to **4-4k** (**Table 4-1**), on the basis of the *cis* versus *trans* bisphosphine ligating behavior of these ligands. However this rationale is inconsistent with the excellent performance of nickel catalysts supported by *trans*-spanning



DiPPF or DCPF in nickel-catalyzed C(*sp*<sup>2</sup>)-N cross-couplings leading to **4k** under similar experimental conditions.<sup>[80f]</sup> It is feasible, however, that the shorter Ni-O distance in (**L4-2**)Ni(*o*-tolyl)Cl (~ 2.54 Å)<sup>[80b]</sup> relative to that in **C4-1** (~ 3.36 Å) contributes to the inferior catalytic performance of the former in our preliminary catalytic screen (**Table 4-1**).

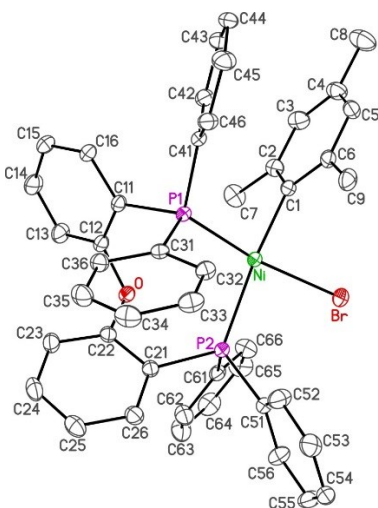


**Figure 4-6:** Single-crystal X-ray structure of **C4-1**, depicted with 30% thermal ellipsoids and with hydrogen atoms omitted for clarity. Selected interatomic distances (Å): Ni-P1 2.1991(7), Ni-P2 2.2998(7), Ni-Br 2.3391(5), Ni-C1 1.935(2).

In an initial effort to test the efficacy of **C4-1** a pre-catalyst, the transformations outlined in **Scheme 2** were examined, under conditions where **L4-1**/(TMEDA)Ni(*o*-tolyl)Cl mixtures were successfully employed. Surprisingly, comparatively poor conversion to the target products was achieved by use of **C4-1**, possibly arising from the increased steric profile of the 2-mesityl group in **C4-1**, relative to *o*-tolyl. This may inhibit catalyst activation that presumably occurs via net transmetalation involving the bulky secondary nitrogen nucleophile (i.e., morpholine or indole). This proposal is consistent with the observation that the addition of a catalytic quantity of PhB(OH)<sub>2</sub> to **C4-1** afforded similar conversions as the test reactions in **Table 4-1**. This activation by the use of PhB(OH)<sub>2</sub>

proceeds via the transmetalation of the boronic acid, and reductive elimination of the resulting biaryl to afford the active Ni(0) species.

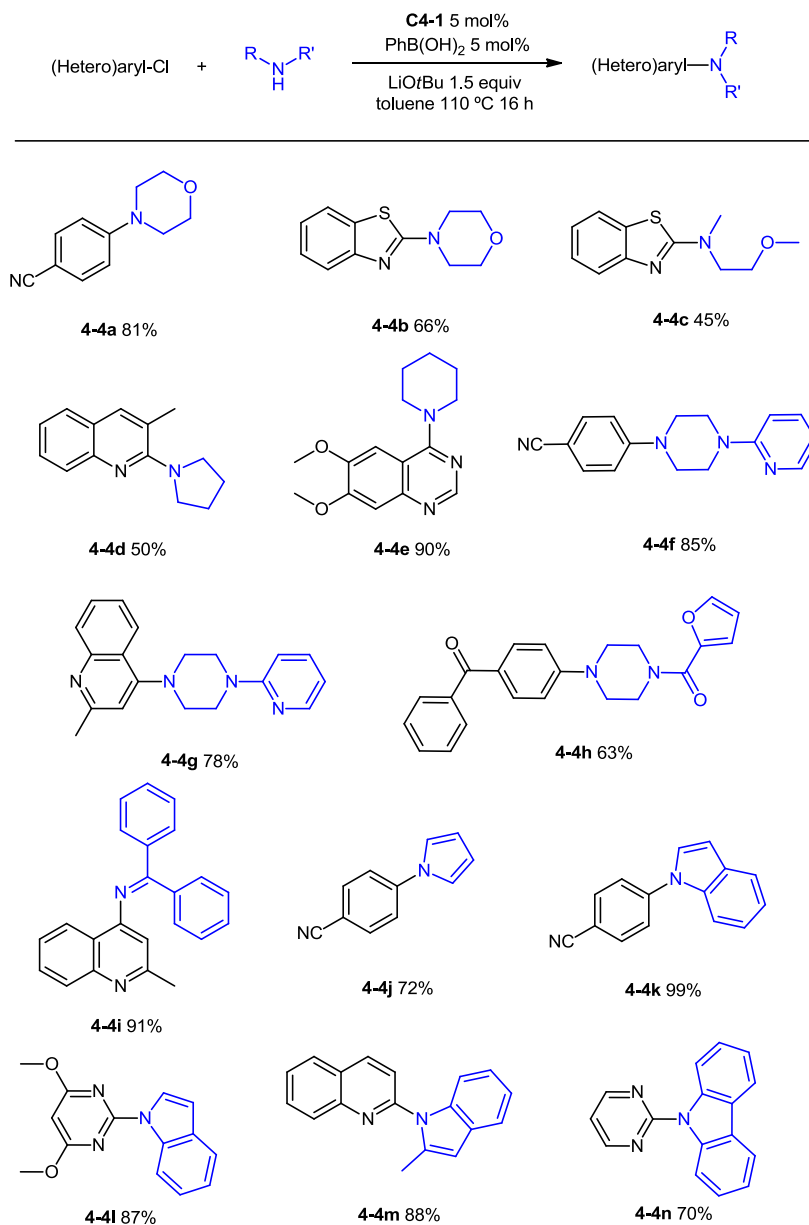


**Table 4-2:** Scope of C(sp<sup>2</sup>)-N cross-coupling using **C4-1**. All reactions were conducted using 1 mmol 1, 1.1 mmol amine, 0.05 mmol **C4-1**, 0.05 mmol phenylboronic acid, 1.5 mmol LiOtBu, in toluene (10 mL), with isolated yields reported.

Having established PhB(OH)<sub>2</sub>-activated **C4-1** as an effective catalyst system for C(sp<sup>2</sup>)-N cross-coupling chemistry, the scope of reactivity with an array of (hetero)aryl chlorides

and secondary amines/azoles (**Table 4-2**) was tested. A diverse set of activated/heteroaryl electrophiles were accommodated in this chemistry, including benzothiazole, quinoline, quinazoline, and pyrimidine derivatives. Conversely, reactions employing electron neutral/rich electrophiles (e.g 1-chloronaphthalene) were unsuccessful. In terms of secondary amine scope, morpholine, (2-methoxyethyl)methylamine, pyrrolidine, piperidine, and *N*-substituted piperazines proved to be compatible substrates, leading to products **4-4a** through **4-4h** (45-90%). The successful cross-coupling of 4-chloroquinoline and benzophenone imine leading to **4-4i** (91%) is the first reported cross-coupling of this nucleophile employing nickel catalysis. Benzophenone imine is an attractive coupling partner in that the corresponding primary aniline can be obtained via hydrolysis; as such, benzophenone imine can be used as an ammonia surrogate where direct ammonia coupling<sup>[82]</sup> is challenging. In further exploring the scope of nucleophile reactivity, *N*-arylated derivatives of pyrrole, indole, and carbazole were each successfully prepared via nickel-catalyzed C(*sp*<sup>2</sup>)-N cross-coupling employing pre-catalyst **C4-1**, affording **4-4j** through **4-4n** in high isolated yield. Across the spectrum of cross-couplings documented herein, *ortho*-substitution, ether, ketone, amide, furan, pyridine, and/or nitrile functionalities were well-tolerated. It is worthy of mention that the performance of **C4-1** in the transformation of (hetero)aryl chlorides is competitive both with DPPF/Ni catalyst systems that are employed widely in the cross-coupling of secondary amines,<sup>[80c, 80e, 80f, 83]</sup> as well as (IPr)Ni(styrene)<sub>2</sub> which represents the most effective nickel-based catalyst reported to date for the *N*-arylation of azoles.<sup>[84]</sup>

### 4.3 Summary

In summary, following a preliminary screen of Xantphos, and DPEphos ligand variants, an air-stable DPEphos-ligated nickel pre-catalyst, **C4-1**, was developed and was shown to be effective for the nickel-catalyzed C(*sp*<sup>2</sup>)-N cross-coupling of secondary amines/azoles and activated (hetero)aryl chlorides, leading to sought-after tertiary (hetero)anilines. The identification of DPEphos (**L4-1**) as being useful in this chemistry serves both to diversify the ligand “toolbox” available to synthetic chemists in nickel-catalyzed C(*sp*<sup>2</sup>)-N cross-coupling chemistry, and to expand our appreciation of the ancillary ligand structures that give rise to efficient catalysts in such applications.

### 4.4 Experimental

#### 4.4.1 General Considerations

All reactions were set up inside a nitrogen atmosphere glovebox (unless stated otherwise) and products were isolated using standard benchtop conditions. Toluene used in the glovebox was purified by sparging with nitrogen followed by passage through a double column purification system equipped with one alumina packed column and one copper-Q5 packed column. THF was purified by distillation over sodium and benzophenone. Solvents used in the glovebox were stored over 4 Å molecular sieves. All other reagents, solvents and materials were used as received from commercial sources (unless stated otherwise).

Product purification was performed by column chromatography or by a Biotage Isolera One automated column using 25 g Snap KP-Sil cartridges. All  $^1\text{H}$  NMR and  $^{13}\text{C}$  NMR spectra were recorded using a Bruker AV-500 or AV-300 spectrometer at 300 K. Chemical shifts are expressed in parts per million (ppm) using the residual solvent peak ( $^1\text{H}$  7.26 ppm,  $^{13}\text{C}$  77.1 ppm for  $\text{CDCl}_3$  and  $^1\text{H}$  5.32 ppm,  $^{13}\text{C}$  53.8 ppm for  $\text{CD}_2\text{Cl}_2$ ) as an internal reference. Coupling constants are ( $J$ ) are reported in Hertz (Hz). Splitting patterns are described as follows: br, broad; s, singlet; d, doublet; t, triplet; q, quartet; m, multiplet. Mass spectra were obtained using ion trap instruments using electrospray ionization, in positive ion mode. GC data was obtained using an instrument equipped with a SGE BP-5, 30 m, 0.25 mm internal diameter column.

#### **4.4.2 General Procedures**

##### **General Ligand Screening Procedure for the Formation of Aryl Amines**

In a nitrogen atmosphere glovebox: (TMEDA)Ni(o-tolyl)Cl (5 mol%, 0.015 mmol, 4.5 mg), ligand (7.5 mol%, 0.0225 mmol), LiOtBu (1.5 equiv, 0.45 mmol, 36 mg), 4-chlorobenzonitrile (1 equiv, 0.3 mmol, 41.3 mg), amine (1.1 equiv, 0.33 mmol) were added to an oven dried 1 dram vial containing a magnetic stir bar. 3 mL of toluene was added, the vial was sealed with a screw cap featuring a PTFE/silicone septum and removed from the glovebox. The reaction was magnetically stirred at 110 °C for 16 hours. The reaction was then cooled to room temperature and a 0.1 mL aliquot was taken, filtered and diluted with MeOH and subjected to GC analysis.

### Preparation of (DPEphos)Ni(mes)Br (C4-1)

Preparation followed a procedure outlined in the literature.<sup>[85]</sup> On the benchtop, NiBr<sub>2</sub> (6 mmol, 1.3 g) was added to an oven dried 100 mL 2 necked round bottom flask equipped with a stir bar and reflux condenser. 60 mL of absolute ethanol was added and sparged with nitrogen for 30 minutes. DPEphos (6 mmol, 3.2 g) was added in one portion under positive pressure of nitrogen. The flask was sealed and refluxed for 30 minutes. The reaction was then cooled to 0 °C in an ice bath and then filtered. The solids were washed 3 times with 10 mL cold absolute ethanol and then 3 times with 10 mL diethyl ether. The solid was then collected by dissolving in dichloromethane, removal of the solvent gave 4.26 g of a dark green solid, which was presumed to be (DPEphos)NiBr<sub>2</sub>, 94% yield.

(DPEphos)NiBr<sub>2</sub> (3.96 mmol, 3.0 g) was added to an oven dried 100 mL round bottom flask equipped with a magnetic stir bar. 40 mL of THF was added and the reaction cooled to 0 °C. 2-mesitylmagnesium bromide (1M in THF, 3.96 mmol, 3.9 mL) was added dropwise with stirring. Once the addition was complete, the reaction was allowed to warm to room temperature and stirred for 30 minutes. Once the reaction was complete, the THF was removed with the aid of a rotary evaporator and ca. 15 mL of cold MeOH was added. The reaction was filtered and the solids were washed 3 times with 15 mL cold MeOH, then 3 times with 15 mL hexanes. The solid was collected by dissolving with dichloromethane, removal of the solvent gave 2.48 g of **C4-1** as a light orange powder (79% yield). <sup>1</sup>H NMR (300 MHz, CD<sub>2</sub>Cl<sub>2</sub>): δ 7.95 (br s, 4H), 7.72-7.63 (m, 1H), 7.57-7.39 (br m, 7H), 7.22-7.12 (br m, 3H), 7.08-6.84 (br m, 5H), 6.71-6.64 (m, 1H), 6.55-6.47 (m, 1H), 6.31-6.07 (br m, 4 H), 5.35-5.34 (m, 4H), 2.54 (br s, 6H), 2.16 (s, 3H); <sup>31</sup>P{<sup>1</sup>H} NMR

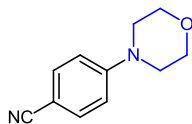
(121.5 MHz, CD<sub>2</sub>Cl<sub>2</sub>)  $\delta$  10.8 (d,  $J = 15$  Hz), 5.5 (d,  $J = 15$  Hz); Despite prolonged acquisition times satisfactory <sup>13</sup>C{<sup>1</sup>H} NMR data could not be obtained for **C4-1**, owing both to hindered rotation that is apparent in the <sup>1</sup>H NMR spectrum, and slow decomposition to paramagnetic by-products upon standing in solution for extended periods. Anal. Calculated for C<sub>45</sub>H<sub>39</sub>O<sub>1</sub>P<sub>2</sub>Ni<sub>1</sub>Br<sub>1</sub> C, 67.85; H, 4.94. Found: C, 67.49; H, 4.81. Crystals suitable for x-ray diffraction were grown by slow evaporation of a dichloromethane solution.

#### **General Catalytic Procedure (GP 4-1)**

Unless otherwise specified, **C4-1** (39.8 mg, 0.05 mmol, 5 mol%), phenylboronic acid (6.1 mg, 0.05 mmol, 5 mol%), aryl chloride (1 mmol), amine (1.1 mmol), LiOtBu (1.5 mmol) were added to an oven dried 4 dram vial containing a magnetic stir bar. The vial was sealed with a screw cap featuring a PTFE/silicone septum and removed from the glove box. The reaction was placed in a temperature controlled aluminum heating block set to 110 °C and magnetically stirred for 16 h (unoptimized). The reaction was then cooled to room temperature, taken up in ca. 30 mL EtOAc and washed 3 times with ca. 50 mL brine. The organic layer was dried over Na<sub>2</sub>SO<sub>4</sub>, filtered and concentrated with the aid of a rotary evaporator.

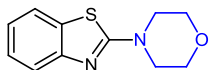
### 4.4.3 Characterization of Isolated Materials

#### 4-morpholinobenzonitrile, **4-4a**



Following **GP 4-1** (aryl halide 137.6 mg, amine 96.2 uL), the title product was obtained via flash chromatography using silica and 30% EtOAc in hexanes. The product was isolated as light yellow solid (81%).  $^1\text{H}$  NMR (500 MHz,  $\text{CDCl}_3$ ):  $\delta$  7.54 (d,  $J = 9.1$  Hz, 2H), 6.89 (d,  $J = 9.1$  Hz, 2H), 3.88 (t,  $J = 4.9$  Hz, 4H), 3.31 (t,  $J = 4.9$  Hz, 4H);  $^{13}\text{C}\{^1\text{H}\}$  NMR (125.8 MHz,  $\text{CDCl}_3$ ):  $\delta$  153.7, 133.7, 120.0, 114.2, 101.2, 66.6, 47.5; This is in agreement with previously reported spectra.<sup>[86]</sup>

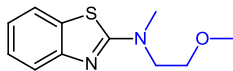
#### 4-(benzo[d]thiazol-2-yl)morpholine, **4-4b**



Following **GP 4-1** (aryl halide 134.6 uL, amine 96.2 uL), the title product was isolated via flash chromatography over  $\text{SiO}_2$  using 20% EtOAc in hexanes. The product was isolated as a beige solid (66%).  $^1\text{H}$  NMR (500 MHz,  $\text{CDCl}_3$ ):  $\delta$  7.65 (d,  $J = 7.8$  Hz, 1H), 7.61 (d,  $J = 8.0$  Hz, 1H), 7.37-7.32 (m, 1H), 7.16-7.14 (m, 1H), 3.87 (t,  $J = 4.7$  Hz, 4H), 3.66 (t,  $J = 5.0$  Hz, 4H);  $^{13}\text{C}\{^1\text{H}\}$  NMR (125.8 MHz,  $\text{CDCl}_3$ ):  $\delta$  169.2, 125.7, 130.8, 126.3, 121.9, 120.9, 119.5, 66.4, 48.7;

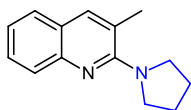


N-(2-methoxyethyl)-N-methylbenzo[d]thiazol-2-amine, **4-4c**



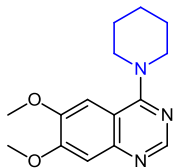
Following **GP 4-1** (aryl halide 130.2 uL, amine 119.6 uL), the title product was isolated via automated column using a 0-20% EtOAc in hexanes gradient. The product was isolated as a yellow oil (45%).  $^1\text{H}$  NMR (500 MHz,  $\text{CDCl}_3$ ):  $\delta$  7.62 (d,  $J = 7.8$  Hz, 1H), 7.58 (d,  $J = 8.0$  Hz, 1H), 7.33-7.28 (m, 1H), 7.10-7.05 (m, 1H), 3.79 (t,  $J = 5.4$  Hz, 2H), 3.71 (t,  $J = 5.2$  Hz, 2H), 3.40 (s, 3H), 3.27 (s, 3H);  $^{13}\text{C}\{^1\text{H}\}$  NMR (125.8 MHz,  $\text{CDCl}_3$ ):  $\delta$  168.4, 153.3, 131.0, 126.1, 121.1, 120.7, 118.9, 70.7, 59.2, 52.9, 39.8;  $m/z$  ESI $^+$  found 245.0719  $[\text{M}+\text{Na}]^+$  calculated for  $\text{C}_{11}\text{H}_{14}\text{N}_2\text{NaOS}$  245.0725.

3-methyl-2-(pyrrolidin-1-yl)quinoline, **4-4d**



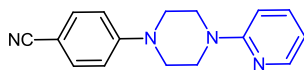
Following **GP 4-1** (aryl halide 177.6 mg, amine 91.8 uL), the title product was isolated via flash chromatography over  $\text{SiO}_2$  using 5% EtOAc in hexanes. The product was isolated as a yellow oil (50%).  $^1\text{H}$  NMR (500 MHz,  $\text{CDCl}_3$ ):  $\delta$  7.75 (d,  $J = 8.4$  Hz, 1H), 7.67 (s, 1H), 7.57 (d,  $J = 7.9$  Hz, 1H), 7.53-7.48 (m, 1H), 7.25-7.20 (m, 1H), 3.76-3.71 (m, 4H), 2.52 (s, 3H), 2.03-1.97 (m, 4H);  $^{13}\text{C}\{^1\text{H}\}$  NMR (125.8 MHz,  $\text{CDCl}_3$ ):  $\delta$  158.7, 146.6, 138.1, 128.5, 126.5, 126.4, 124.3, 122.3, 50.0, 25.9, 21.5;  $m/z$  ESI $^+$  found 213.1386  $[\text{M}+\text{H}]^+$  calculated for  $\text{C}_{14}\text{H}_{17}\text{N}_2$  213.1386.

6,7-dimethoxy-4-(piperidin-1-yl)quinazoline, **4-4e**



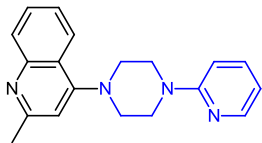
Follow **GP 4-1** (aryl halide 224.6 mg, amine 108.7 uL), the title product was isolated via flash chromatography over SiO<sub>2</sub> using 80-100% EtOAc in hexanes. The product was isolated as a yellow solid (90%). <sup>1</sup>H NMR (500 MHz, CDCl<sub>3</sub>): δ 8.67 (s, 1H), 7.24 (s, 1H), 7.14 (s, 1H), 4.04 (s, 3H), 4.01 (s, 3H), 3.63-3.59 (m, 4H), 1.86-1.75 (m, 6H); <sup>13</sup>C{<sup>1</sup>H} NMR (125.8 MHz, CDCl<sub>3</sub>): δ 164.6, 154.5, 153.4, 149.2, 148.2, 111.8, 107.6, 103.6, 56.3, 56.1, 21.2, 26.1, 24.9; *m/z* ESI<sup>+</sup> found 274.1550 [M+H]<sup>+</sup> calculated for C<sub>15</sub>H<sub>20</sub>N<sub>3</sub>O<sub>2</sub> 274.1556

4-(4-(pyridin-2-yl)piperazin-1-yl)benzonitrile **4-4f**



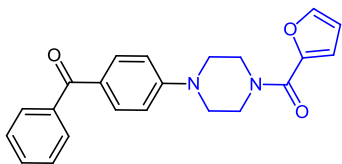
Following **GP 4-1** (aryl halide 137.6 mg, amine 175.5 uL), the title product was obtained via automated column using a 0-20% EtOAc in hexanes gradient. The product was isolated as light yellow solid (85%). <sup>1</sup>H NMR (500 MHz, CDCl<sub>3</sub>): δ 8.26-8.21 (m, 1H), 7.58-7.49 (m, 3H), 6.94-6.87 (m, 2H), 6.73-6.69 (m, 2H), 3.77-3.71 (m, 4H), 3.53-3.47 (m, 4H); <sup>13</sup>C{<sup>1</sup>H} NMR (125.8 MHz, CDCl<sub>3</sub>): δ 159.1, 153.3, 148.2, 137.8, 133.7, 120.1, 114.3, 114.0, 107.2, 100.6, 47.0, 44.8; *m/z* ESI<sup>+</sup> found 265.1448 [M+H]<sup>+</sup> calculated for C<sub>16</sub>H<sub>17</sub>N<sub>4</sub> 265.1454.

2-methyl-4-(4-(pyridin-2-yl)piperazin-1-yl)quinolone, **4-4g**



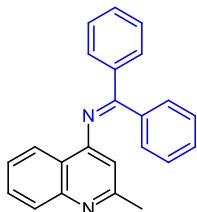
Following **GP 4-1** (aryl halide 201.6 uL, amine 267.5 uL), the title product was obtained via automated column using a 20-50% EtOAc in hexanes gradient. The product was isolated as a light yellow solid (78%).  $^1\text{H}$  NMR (500 MHz,  $\text{CDCl}_3$ ):  $\delta$  8.29-8.24 (m, 1H), 8.08-7.98 (m, 2H), 7.69-7.61 (m, 1H), 7.59-7.51 (m, 1H), 7.50-7.43 (m, 1H), 6.81-6.67 (m, 3H), 3.86-3.80 (m, 4H), 3.38-3.31 (m, 4H), 2.70 (s, 3H);  $^{13}\text{C}\{^1\text{H}\}$  NMR (125.8 MHz,  $\text{CDCl}_3$ ):  $\delta$  159.5, 159.4, 156.7, 149.3, 148.0, 137.6, 129.3, 129.1, 124.6, 123.3, 121.8, 113.8, 109.5, 107.2, 52.0, 45.4, 25.6;  $m/z$   $\text{ESI}^+$  found 305.1761  $[\text{M}+\text{H}]^+$  calculated for  $\text{C}_{19}\text{H}_{21}\text{N}_4$  305.1760.

(4-(4-benzoylphenyl)piperazin-1-yl)(furan-2-yl)methanone, **4-4h**



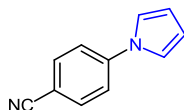
Following **GP 4-1** (aryl halide 217.0 mg, amine 198.2 mg), the title product was isolated via flash chromatography over  $\text{SiO}_2$  using 80% EtOAc in hexanes. The product was isolated as a thick yellow oil (64%).  $^1\text{H}$  NMR (500 MHz,  $\text{CDCl}_3$ ):  $\delta$  7.87-7.82 (m, 2H), 7.79-7.75 (m, 2H), 7.61-7.56 (m, 1H), 7.55-7.54 (m, 1H), 7.51-7.47 (m, 2H), 7.12-7.10 (m, 1H), 6.96-6.92 (m, 2H), 6.56-6.53 (m, 1H), 4.03 (br s, 4H), 3.53-3.47 (m, 4H);  $^{13}\text{C}\{^1\text{H}\}$  NMR (125.8 MHz,  $\text{CDCl}_3$ ):  $\delta$  195.3, 159.3, 153.6, 148.0, 144.1, 138.8, 132.7, 131.7, 129.7, 128.3, 128.1, 117.1, 113.8, 111.6, 47.7, 44.0 (br);  $m/z$   $\text{ESI}^+$  found 383.1366  $[\text{M}+\text{Na}]^+$  calculated for  $\text{C}_{22}\text{H}_{20}\text{N}_2\text{NaO}_3$  383.1372.

N-(diphenylmethylene)-2-methylquinolin-4-amine, **4-4i**



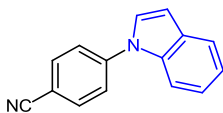
Follow **GP 4-1** (aryl halide 201.6 uL, amine 199.4 mg), the title product was isolated via flash chromatography over SiO<sub>2</sub> using 40% EtOAc in hexanes. The product was isolated as a light yellow solid (91%). <sup>1</sup>H NMR (300 MHz, CDCl<sub>3</sub>, at 340 K): δ 7.93 (t, *J* = 7.9 Hz, 2H), 7.72-7.22 (br m, 12H), 6.32 (s, 1H), 2.52 (s, 3H); <sup>13</sup>C {<sup>1</sup>H} NMR (125.8 MHz, CDCl<sub>3</sub>): δ 169.5, 159.3, 155.9, 148.4, 131.4 (br), 129.6, 129.5 (br), 128.7, 128.3, 125.2, 123.7, 121.3, 109.5, 25.6; *m/z* ESI<sup>+</sup> found 323.1543 [M+H]<sup>+</sup> calculated for C<sub>23</sub>H<sub>19</sub>N<sub>2</sub> 323.1549.

4-(1H-pyrrol-1-yl)benzonitrile, **4-4j**



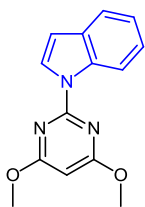
Following **GP 4-1** (aryl halide 137.6 mg, amine 76.3 uL), the title product was obtained via flash chromatography on silica using 10% EtOAc in hexanes. The product was isolated as beige solid (72%). <sup>1</sup>H NMR (500 MHz, CDCl<sub>3</sub>): δ 7.75 (d, *J* = 8.8 Hz, 2H), 7.52 (d, *J* = 8.8 Hz, 2H), 7.17 (t, *J* = 2.2 Hz, 2H), 6.44 (t, *J* = 2.2 Hz, 2H); <sup>13</sup>C {<sup>1</sup>H} NMR (125.8 MHz, CDCl<sub>3</sub>): δ 143.9, 134.0, 120.2, 119.1, 118.6, 112.3, 108.8; *m/z* ESI<sup>+</sup> found 191.0580 [M+Na]<sup>+</sup> calculated for C<sub>11</sub>H<sub>8</sub>N<sub>2</sub>Na 191.0585.

4-(1H-indol-1-yl)benzonitrile, **4-4k**



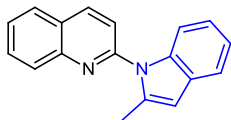
Following **GP 4-1** (aryl halide 137.6 mg, amine 76.3 uL), the title product was obtained via flash chromatography on basic alumina using 5% EtOAc in hexanes. The product was isolated as beige solid (99%).  $^1\text{H}$  NMR (500 MHz,  $\text{CDCl}_3$ ):  $\delta$  7.84 (d,  $J = 8.5$  Hz, 2H), 7.74 (d,  $J = 7.7$  Hz, 1H), 7.69-7.63 (m, 3H), 7.38 (d,  $J = 3.3$  Hz, 1H), 7.30 (t,  $J = 7.3$ , 1H), 7.26 (t,  $J = 7.7$ , 1H) 6.79 (d,  $J = 3.3$  Hz, 1H);  $^{13}\text{C}\{^1\text{H}\}$  NMR (125.8 MHz,  $\text{CDCl}_3$ ):  $\delta$  143.7, 135.4, 133.9, 130.1, 127.2, 124.0, 123.4, 121.8, 121.5, 118.6, 110.5, 109.5, 105.9; This is in agreement with previously reported spectra.<sup>[87]</sup>

1-(4,6-dimethoxypyrimidin-2-yl)-1H-indole, **4-4l**



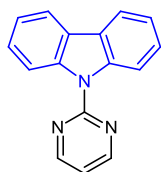
Following **GP 4-1** (aryl halide 174.5 mg, amine 128.7 mg), the title product was isolated via automated column using a 0-20% EtOAc in hexanes gradient. The product was isolated as a white solid (87%).  $^1\text{H}$  NMR (500 MHz,  $\text{CDCl}_3$ ):  $\delta$  8.80 (d,  $J = 8.4$  Hz, 1H), 8.29 (d,  $J = 3.6$  Hz, 1H), 7.66 (d,  $J = 7.7$  Hz, 1H), 7.39-7.34 (m, 1H), 7.30-7.25 (m, 1H), 6.70 (d,  $J = 3.6$  Hz, 1H), 4.11 (s, 6 H);  $^{13}\text{C}\{^1\text{H}\}$  NMR (125.8 MHz,  $\text{CDCl}_3$ ):  $\delta$  172.1, 156.4, 135.5, 131.5, 126.2, 123.7, 122.1, 121.0, 116.2, 106.7, 85.1, 54.5;  $m/z$  ESI<sup>+</sup> found 278.0900 [M+Na]<sup>+</sup> calculated for  $\text{C}_{14}\text{H}_{13}\text{N}_3\text{NaO}_2$  278.0906.

2-(2-methyl-1H-indol-1-yl)quinolone, **4-4m**



Following **GP 4-1** (aryl halide 133.0 uL, amine 144.3 mg), the title product was isolated via flash chromatography on basic alumina using 5% EtOAc in hexanes. The product was isolated as a thick yellow oil (88%).  $^1\text{H}$  NMR (500 MHz,  $\text{CDCl}_3$ ):  $\delta$  8.36 (d,  $J = 8.6$  Hz, 1H), 8.16 (d,  $J = 8.4$  Hz, 1H), 7.94 (d,  $J = 8.0$  Hz, 1H), 7.85-7.79 (m, 1H), 7.66-7.60 (m, 3H), 7.58-7.53 (m, 1H), 7.23-7.16 (m, 2H), 6.52 (s, 1H), 2.61 (s, 3H);  $^{13}\text{C}\{^1\text{H}\}$  NMR (125.8 MHz,  $\text{CDCl}_3$ ):  $\delta$  150.7, 147.8, 138.6, 137.3, 137.2, 130.4, 129.2, 129.1, 127.7, 126.9, 126.8, 121.9, 121.1, 120.0, 119.3, 110.7, 104.1, 14.5; This is in agreement with previously reported spectra.<sup>[88]</sup>

9-(pyrimidin-2-yl)-9H-carbazole, **4-4n**



Following **GP 4-1** (aryl halide 114.5 mg, amine 183.9 mg), the title product was isolated via automated column using a 0-5% EtOAc in hexanes gradient. The product was isolated as a white solid (70%).  $^1\text{H}$  NMR (500 MHz,  $\text{CDCl}_3$ ):  $\delta$  8.92-8.86 (m, 4H), 8.12 (d,  $J = 7.7$  Hz, 2H), 7.57-7.53 (m, 2H), 7.41 (t,  $J = 7.6$  Hz, 2H), 7.15 (t,  $J = 4.7$  Hz, 1H);  $^{13}\text{C}\{^1\text{H}\}$  NMR (125.8 MHz,  $\text{CDCl}_3$ ):  $\delta$  159.4, 158.0, 139.3, 126.8, 126.0, 122.5, 119.7, 116.4, 116.1; This is in agreement with previously reported spectra.<sup>[89]</sup>

## Chapter 5 (DPEphos)Ni(mesityl)Br: An Air-Stable Pre-Catalyst for Suzuki-Miyaura Cross-Couplings Yielding Biheteroaryls

### 5.1 Nickel catalyzed Suzuki-Miyaura Cross-Coupling Reactions

As mentioned in Section 1.2, the palladium-catalyzed Suzuki-Miyaura (SM) C(sp<sup>2</sup>)-C(sp<sup>2</sup>) cross-coupling of (pseudo)aryl halides with aryl boron reagents has become one of the most important cross-coupling reaction in the synthetic chemist's arsenal.<sup>[90],[91]</sup> A recent report states that approximately 25% of all new biologically active molecules reported in the *Journal of Medicinal Chemistry* in 2014 have at least one SM cross-coupling step as part of their synthesis.<sup>[92]</sup> Since the first report by Miyaura and Suzuki, numerous reports have improved on the original catalytic methodology. Over the past couple of decades, many nickel-based catalysts have been developed for SM cross-coupling reactions. Of particular note, catalysts employing the use of PPh<sub>3</sub>, PCy<sub>3</sub>, and N-heterocyclic carbenes as ancillary ligands have proven to be particularly effective in this chemistry.<sup>[93]</sup> While these catalysts are quite effective in the cross-coupling of a diverse set of heteroaryl (pseudo)halides, the use of heteroaryl boron reagents is much less developed. Catalysts that are capable of using these reagents in SM reactions are attractive, given the prevalence of the unsymmetrical biheteroaryl motif in biologically active compounds.<sup>[94]</sup> However, the synthesis of biheteroaryl compounds by use of SM cross-coupling protocols represents a potential challenge, owing in part to the possibility of catalyst inhibition by the substrate

and/or product. Additionally, it has been shown that heteroaryl boronic acids are particularly prone to unwanted proto-deborylation at elevated temperatures.<sup>[95]</sup>

In a landmark publication by Ge and Hartwig,<sup>[96]</sup> air-stable (DPPF)Ni(cinnamyl)Cl (DPPF = 1,1'-bis(diphenylphosphino)ferrocene; 0.5 mol% Ni, 50-80 °C) was employed successfully as a pre-catalyst in the first highly effective nickel-catalyzed SM reactions employing heteroaryl chlorides or bromides and five-membered heteroaryl boronic acids, leading to unsymmetrical biheteroaryls. The lack of reactivity of pyridinyl boronic acids under the conditions employed was encountered as a limitation of this synthetic protocol.<sup>[96]</sup>

The use of single-component, air-stable pre-catalysts such as (DPPF)Ni(cinnamyl)Cl, as demonstrated by Ge, and Hartwig,<sup>[96]</sup> provides practical advantages relative to commonly employed protocols employing air-sensitive Ni(COD)<sub>2</sub> (COD = 1,5-cyclooctadiene) as the nickel source.<sup>[97]</sup> Building on this theme, Hazari and co-workers<sup>[98]</sup> subsequently demonstrated that air-stable (DPPF)Ni(*o*-tolyl)Cl (**C3-1**),<sup>[79b]</sup> initially reported by Buchwald and co-workers,<sup>[44]</sup> can be employed in room temperature cross-couplings of selected heteroaryl chlorides and benzo[*b*]furan-2-yl- or benzo[*b*]thien-2-yl-boronic acid (5 examples, 2.5 mol% Ni). Garg and co-workers<sup>[99]</sup> have reported on the successful application of (PCy<sub>3</sub>)<sub>2</sub>NiCl<sub>2</sub> as a pre-catalyst for SM cross-couplings of heteroaryl chlorides, bromides, mesylates, or sulfamates with 3-furanyl- or 3-thienyl-boronic acid, as well as 2-methoxy-3-pyridinyl-boronic acid (1-10 mol% Ni, ≥ 100 °C). The latter transformations, while limited to a single pyridinyl nucleophile, represent the first and only successful nickel-catalyzed SM cross-couplings of pyridinyl boronic acids leading to unsymmetrical biheteroaryls. More recently, Ando *et al.*<sup>[100]</sup> documented the



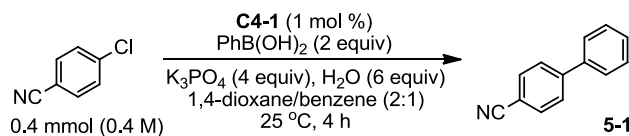
utility of Cp(NHC)NiCl (1 mol%)/PPh<sub>3</sub> (20 mol%) catalytic mixtures in the SM cross-coupling of heteroaryl chlorides or bromides with 3-furanyl- or 3-thienyl-boronic acid (90 °C), thus affording unsymmetrical biheteroaryls. The addition of PPh<sub>3</sub> in this catalyst system, while operationally inconvenient, proved crucial in suppressing homocoupling of the (hetero)aryl boronic acid. Despite this progress, the nickel-catalyzed SM cross-coupling of heteroaryl halides and heteroaryl boronic acids remains relatively unexplored. As such, the identification of alternative nickel catalysts that are effective in providing access to unsymmetrical biheteroaryls with broad scope remains an important challenge.

In Chapter 4, my work on the development of (DPEphos)Ni(mesityl)Br (**C4-1**) for use in the C-N cross-coupling of (hetero)aryl halides and secondary amines or azoles;<sup>[101]</sup> notably, **C4-1** was found to perform competitively versus (DPPF)Ni(*o*-tolyl)Cl<sup>[44]</sup> (**C3-1**) in such transformations. On the basis of this finding, and my observation that the effective use of **C4-1** in C-N cross-couplings required activation with a catalytic amount of PhB(OH)<sub>2</sub>, it seemed feasible that pre-catalyst **C4-1** would be well-suited to nickel-catalyzed SM cross-couplings.

## 5.2 Results and Discussion

In an initial effort to probe the potential utility of **C4-1** in SM chemistry, the room temperature cross-coupling of 4-chlorobenzonitrile and phenylboronic acid using 1 mol % **C4-1** was examined as outlined in **Table 5-1**. It was found that the use of a 1,4-dioxane:benzene (2:1) solvent mixture, in the presence of K<sub>3</sub>PO<sub>4</sub> with added water,

afforded high conversion to desired biaryl product **5-1** after 4 h; the use of alternative solvent media, base, or the exclusion of water afforded inferior results. The beneficial role of added water in this context may arise from the more facile formation of a putative (DPEphos)Ni(aryl)OH species; such  $L_nM(\text{aryl})\text{OH}$  complexes ( $M = \text{Ni}, \text{Pd}$ ) have been shown to be more reactive towards transmetallation compared to analogous  $L_nM(\text{aryl})X$  complexes ( $X = \text{halide}$ ) in SM reactions.<sup>[102]</sup> Under optimized conditions, use of the DPPF pre-catalyst **C3-1** in place of **C4-1** gave only 50% conversion to **5-1**, showcasing the potential utility of **C4-1** in room temperature SM reactions. Pre-catalysts based on PAd-Dalpos (**C3-4**)<sup>[80d]</sup> or Xantphos (**C5-1**)<sup>[103]</sup> afforded no conversion of the substrates. Efforts to employ a reduced amount of base or  $\text{PhB}(\text{OH})_2$  led to inferior results, and the use of related boronic ester or potassium trifluoroborate reagents proved ineffective under these conditions.



Deviation from above	Conversion to <b>5-1</b> (%) <sup>a</sup>
none	>90
1,4-dioxane	10
toluene	70
water, 50 °C	60
no water	80
THF	nd
MeCN, K <sub>2</sub> CO <sub>3</sub>	nd
<b>C3-1</b>	50
<b>C3-4</b>	nd
<b>C5-1</b>	nd
1.1 equiv PhB(OH) <sub>2</sub>	80
2 equiv K <sub>3</sub> PO <sub>4</sub>	40
PhBpin	nd
PhBneopent	nd
PhBF <sub>3</sub> K	nd

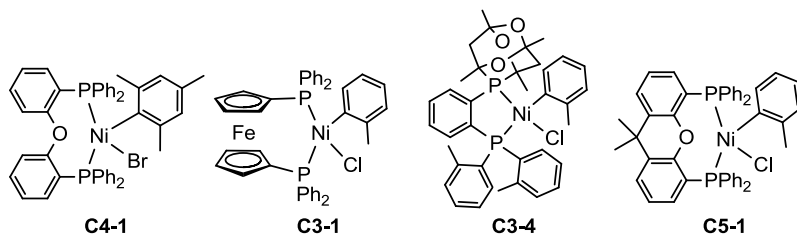


**Table 5-1:** Optimization of Conditions and Pre-Catalyst Screening,<sup>a</sup> and precatalysts tested. <sup>a</sup>Estimated conversion to 1 on the basis of calibrated GC data, nd = not detected.

With optimized conditions in hand, the scope of room temperature SM cross-couplings using **C4-1** was examined, including for the construction of unsymmetrical biheteroaryls (**Table 5-2**). It was found that to facilitate more challenging transformations of this type a higher catalyst loading (2 mol% **C4-1**), and longer reaction times (16 h) were required to ensure optimal conversion. A selection of five-membered heteroaryl boronic acids in combination with (hetero)aryl chlorides, and bromides were employed successfully in this chemistry (**5-2a** through **5-2p**), with isolated yields that are generally comparable to those achieved by use of DPPF-based nickel pre-catalysts.<sup>[96, 98]</sup> In the context of SM reactions employing **C4-1** leading to unsymmetrical biheteroaryls, *N*-Boc pyrrole, (benzo)furan, (benzo)thiophene, and unprotected NH-indole structures proved compatible in the boronic acid substrate, as did pyridine, pyrimidine, (iso)quinoline, quinaldine, quinazoline,

quinoxaline, and unprotected NH-indole frameworks in the heteroaryl electrophile reaction partner. The tolerance of trifluoromethyl, ketone, aldehyde, and ether groups was also demonstrated. Despite the established ability of **C4-1** in C-N cross-coupling chemistry (see Chapter 4),<sup>[101]</sup> under the conditions employed formation of the SM cross-coupling product **5-2p** is favored over *N*-arylation of the primary aniline moiety within the boronic acid substrate.

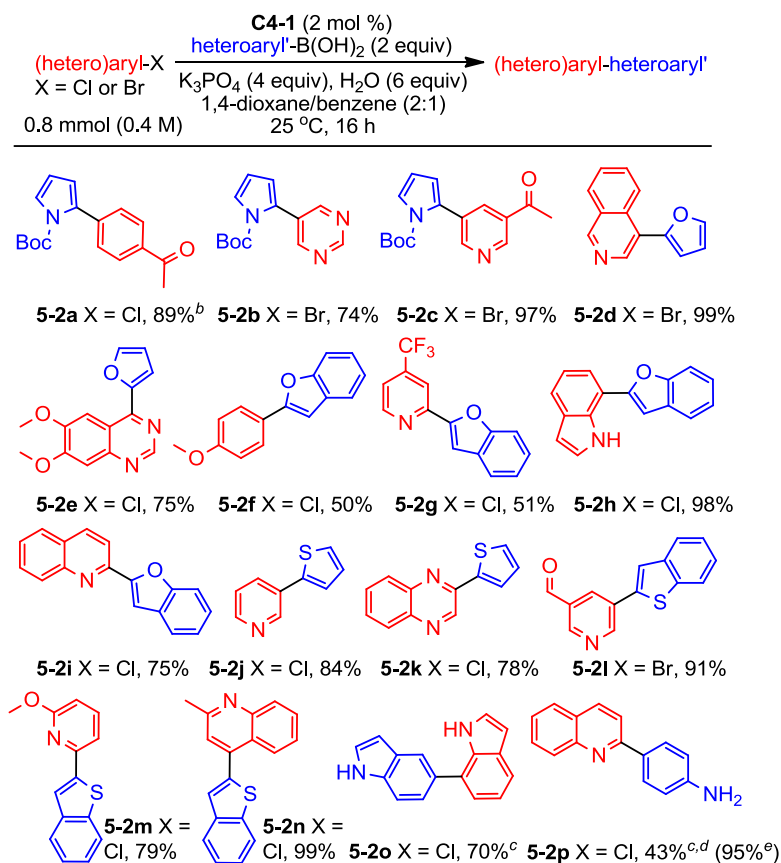
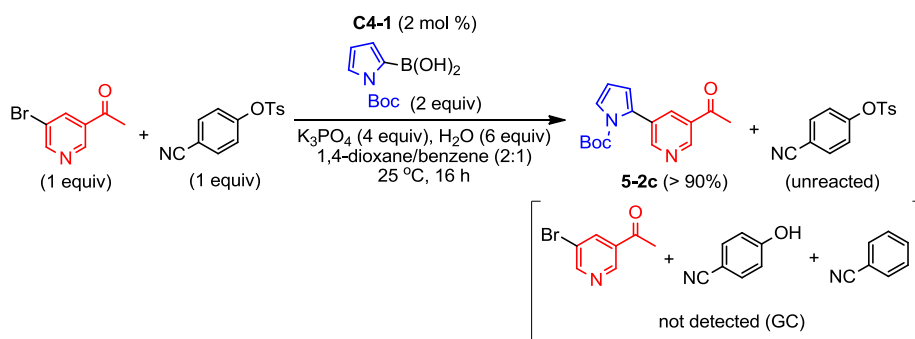


**Table 5-2:** Suzuki-Miyaura Cross-Couplings Using **C4-1**.<sup>a</sup> <sup>a</sup>Unless stated, isolated yields reported. <sup>b</sup>1 mol% **C4-1**. <sup>c</sup>50 °C. <sup>d</sup>**5-2p** was found to decompose partially under the chromatographic conditions employed. <sup>e</sup>NMR yield relative to 1,4-di-tert-butylbenzene.

Some limitations were encountered in this chemistry. Application of **C4-1** as a pre-catalyst for SM cross-couplings with sterically hindered electrophiles such as 2-chloro-*m*-xylene proved problematic, with negligible turnover observed. As well, electron-rich aryl

chlorides presented a challenge, as evidenced by the moderate yield (50%) obtained for **5-2f**. While (hetero)aryl chlorides and bromides were found to be effective in these SM cross-couplings using **C4-1** (Table 5-2), sulfonate electrophiles (e.g., mesylates, tosylates, and triflates) failed to react. Intrigued by this observation, I sought to assess whether sulfonate electrophiles were inert or gave rise to catalyst deactivation in this reaction setting, by examining the progress of the otherwise successful SM cross-coupling leading to the unsymmetrical biheteroaryl **5-2c** by use of **C4-1**, in the presence of an added aryl tosylate (Scheme 5-1). Gas chromatographic analysis of the reaction mixture revealed the clean formation of **5-2c**, with the aryl tosylate remaining unconsumed; neither the derived phenol, nor aryl tosylate reduction by-products were detected.



**Scheme 5-1:** Electrophile Selectivity in Suzuki-Miyaura Cross-couplings Using **C4-1**.

The nickel-catalyzed SM cross-coupling of pyridinyl boronic acids and (hetero)aryl halides leading to unsymmetrical biheteroaryls is limited to a report by Garg and co-workers,<sup>[99]</sup> whereby the cross-coupling of 2-methoxy-3-pyridinyl-boronic acid with 3-chloropyridine or 5-bromopyrimidine by use of  $(\text{PCy}_3)_2\text{NiCl}_2$  as a pre-catalyst is described. Initial efforts to employ pyridinyl boronic acids as cross-coupling partners with **C4-1** under the conditions outlined in **Scheme 5-2** were unsuccessful, as no conversion of the starting

materials was observed on the basis of gas chromatographic analysis. However, in employing modified conditions described by Watson and co-workers<sup>[104]</sup> for the nickel-catalyzed  $sp^3$ - $sp^2$  cross-coupling of pyridinyl boronic acids and alkylpyridinium electrophiles, the successful cross-coupling of 4-chloro-2-fluorotoluene and 3-pyridinylboronic acid by use of **C4-1** was achieved (**Table 5-3**). While high conversion of the test substrates was noted under these conditions, the isolated yield of the target product **5-3a** was found to be 61%, with 2-fluorotoluene being the major by-product. Increasing the reaction temperature from 60 °C to 110 °C resulted in high substrate conversion, but only the formation of hydrodehalogenation was detected under these conditions; whereas no substrate conversion was achieved at 25 °C. Diminished conversion and yield of **5-3a** occurred when using lower loadings of **C4-1**. No substrate conversion was achieved under our otherwise optimal conditions when ethanol was excluded, underscoring the importance of this additive in the successful formation of **5-3a**. The addition of 18-crown-6 was tested, given that a large amount of insoluble material, potentially including potassium borate species, was observed in these cross-coupling reactions; however, this addition had no effect on the outcome of the reaction.

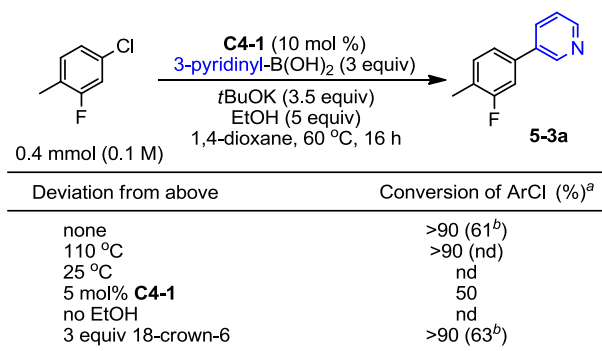


**Table 5-3.** Optimization of Conditions for Pyridinyl Boronic Acids Using **C4-1**. <sup>a</sup>Estimated conversion of aryl chloride on the basis of calibrated GC data, nd = not detected. <sup>b</sup>Isolated yield of **5-3a**.

Having identified suitable conditions for SM cross-couplings of pyridinyl boronic acids and (hetero)aryl halides employing **C4-1**, (**Table 5-3**), the reaction scope with respect to pyridinyl-boronic acids was explored (**Table 5-4**). Several successful cross-couplings of this type were achieved by use of either 3-pyridinyl-boronic acid or *ortho*-substituted variants, affording the target products (**3a-3f**) in synthetically useful isolated yields (54-88%); in all cases, no (hetero)aryl halide remained at the end of the reaction, in keeping with competing side reactivity including electrophile hydrodehalogenation. The success of the cross-coupling was found to be sensitive to the structure of the pyridine nucleophile, with 2-methyl-4-pyridinyl-boronic acid and an electron-poor 3-pyridinyl-boronic acid failing to react (**5-3g** through **5-3i**) under conditions whereby other 3-pyridinyl-boronic acids worked well. Notwithstanding these limitations, the successful cross-couplings leading to the new compounds **5-3a** through **5-3f** represent the most diverse collection of such nickel-catalyzed transformations reported thus far in the literature, thereby underscoring the utility of pre-catalyst **C4-1**.

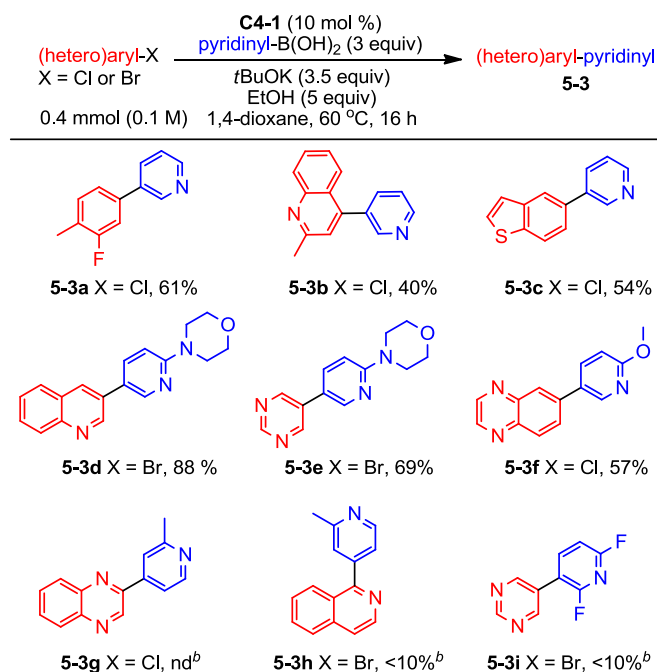


**Table 5-4:** Suzuki-Miyaura Cross-couplings of Pyridinyl Boronic Acids Using **C4-1**.<sup>a</sup>  
<sup>a</sup>Unless stated, isolated yields reported. <sup>b</sup>Estimated conversion to 3 on the basis of calibrated GC data, nd = not detected.

### 5.3 Summary

In summary, the air-stable (DPEphos)Ni(mesityl)Br (**C4-1**) has been shown to be an effective pre-catalyst for Suzuki-Miyaura cross-couplings of (hetero)aryl chlorides or bromides, and (hetero)aryl boronic acids, including rather challenging transformations leading to unsymmetrical biheteroaryls for which few competent nickel-based catalysts are known. A diverse collection of reaction partners were accommodated in this chemistry, in many cases at room temperature (2 mol% **C4-1**). In keeping with previous literature reports, SM cross-couplings involving pyridinyl boronic acids and heteroaryl electrophiles proved difficult, and required more forcing reaction conditions (10 mol% **C4-1**, 60 °C).



Nonetheless, the modest established substrate scope achieved by use of **C4-1** exceeds that previously reported for nickel-catalyzed SM cross-couplings leading to unsymmetrical biheteroaryls.

## 5.4 Experimental

### 5.4.1 General Considerations

All reactions were set up inside a nitrogen atmosphere glovebox (unless stated otherwise) and products were isolated using standard benchtop conditions. Toluene and benzene that were used in the glovebox were purified by sparging with nitrogen followed by passage through a double column purification system equipped with one alumina packed column and one copper-Q5 packed column. THF and 1,4-dioxane were purified by distillation over sodium/benzophenone. Solvents used in the glovebox were stored over 4 Å molecular sieves. Degassed water refers to water that has been sparged with nitrogen gas, and sealed under a nitrogen atmosphere. Tribasic potassium phosphate (Sigma-Aldrich) was ground to a fine powder, but was otherwise used as received. Pre-catalysts **C4-1**,<sup>[101]</sup> **C3-1**,<sup>[44]</sup> **C3-4**,<sup>[80d]</sup> and **C5-1**<sup>[103]</sup> were prepared by using literature procedures. All other reagents, solvents and materials were used as received from commercial sources. Product purification was performed by use of column chromatography on silica, as indicated. All <sup>1</sup>H NMR and <sup>13</sup>C{<sup>1</sup>H} NMR spectra were recorded using a Bruker AV-500 or AV-300 spectrometer at 300 K. Chemical shifts are expressed in parts per million (ppm) using the

residual NMR solvent peak as an internal reference. Coupling constants ( $J$ ) are reported in Hertz (Hz). Splitting patterns are described as follows: br, broad; s, singlet; d, doublet; t, triplet; q, quartet; m, multiplet. Mass spectra were obtained using ion trap instruments employing electrospray ionization, in positive ion mode. GC data were obtained using an instrument equipped with a SGE BP-5, 30 m, 0.25 mm internal diameter column.

#### 5.4.2 General Procedures

**General Procedure for Cross-coupling (GP 5-1).** Unless otherwise specified, **C4-1** (12.7 mg, 0.016 mmol, 2 mol %), aryl halide (0.8 mmol), boronic acid (1.6 mmol), and K<sub>3</sub>PO<sub>4</sub> (679 mg, 3.2 mmol), were added to a oven dried 4 dram vial containing a magnetic stir bar. 1,4-Dioxane (1.3 mL) and benzene (700  $\mu$ L) were added, the vial was sealed with a screwcap featuring a PTFE/silicone septum and was removed from the glovebox. Degassed water (86  $\mu$ L) was added via a gas-tight syringe. The reaction mixture was magnetically stirred for 16 hours at room temperature. Note: On several occasions, the base became clumpy and stuck to the bottom of the reaction vial; in these cases it was noted that reactions were more successful if efficient stirring was maintained. After 16 h, the reaction mixture was taken up in EtOAc (ca. 10 mL) and extracted with distilled water (3 x 10 mL). The organic layer was dried over anhydrous Na<sub>2</sub>SO<sub>4</sub>, filtered, and concentrated with the aid of a rotary evaporator.

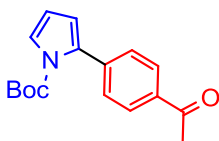
#### **General Procedure for Cross-coupling Using Pyridinyl Boronic Acids (GP 5-2).**

Unless otherwise specified, **C4-1** (31.9 mg, 0.04 mmol, 10 mol %), aryl halide (0.4 mmol),

boronic acid (1.2 mmol), and KOtBu (157.1 mg, 1.4 mmol), were added to a oven dried 4 dram vial containing a magnetic stir bar. 1,4-Dioxane (4 mL) and EtOH (101.7  $\mu$ L) were added. The vial was sealed with a screwcap featuring a PTFE/silicone septum and was removed from the glovebox. The reaction mixture was magnetically stirred for 16 hours in a temperature-controlled aluminum heating block set to 60  $^{\circ}$ C. After 16 h, the reaction mixture was cooled to room temperature, taken up in EtOAc (ca. 10 mL) and extracted with distilled water (3 x 10 mL). The organic layer was dried over anhydrous Na<sub>2</sub>SO<sub>4</sub>, filtered, and concentrated with the aid of a rotary evaporator.

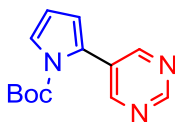
### 5.4.3 Characterization of isolated products

tert-Butyl 2-(4-acetylphenyl)-1H-pyrrole-1-carboxylate, **5-2a**.



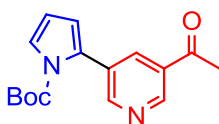
Following **GP 5-1** (1 mol% **C4-1**, aryl halide 103.6  $\mu$ L, boronic acid 337.6 mg), the title product was obtained via flash chromatography using silica and 10% EtOAc in hexanes. The product was isolated as light yellow oil (89%). <sup>1</sup>H NMR (500.1 MHz, CDCl<sub>3</sub>):  $\delta$  7.98-7.97 (m, 2H), 7.49-7.47 (m, 2H), 7.41-7.40 (m, 1H), 6.30-6.29 (m, 1H), 6.29-6.27 (m, 1H), 2.65 (s, 3H), 1.43 (s, 9H); <sup>13</sup>C{<sup>1</sup>H} NMR (125.8 MHz, CDCl<sub>3</sub>):  $\delta$  197.6, 149.0, 138.9, 135.5, 133.9, 129.0 (two signals), 128.9, 127.6, 123.5, 115.5, 110.8, 84.0, 27.6, 26.5; this is in agreement with previously reported spectra.<sup>[105]</sup>

tert-Butyl 2-(pyrimidin-5-yl)-1H-pyrrole-1-carboxylate, **5-2b**.



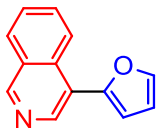
Following **GP 5-1** (aryl halide 127.2 ng, boronic acid 337.6 mg), the title product was obtained via flash chromatography using silica and 30% EtOAc in hexanes. The product was isolated as white solid (74%).  $^1\text{H}$  NMR (500.1 MHz,  $\text{CDCl}_3$ ):  $\delta$  9.15 (s, 1H), 8.76 (s, 2H), 7.49-7.48 (m, 1H), 6.36-6.32 (m, 2H), 1.46 (s, 9H);  $^{13}\text{C}\{^1\text{H}\}$  NMR (125.8 MHz,  $\text{CDCl}_3$ ):  $\delta$  156.9, 156.3, 148.7, 128.6, 127.5, 124.1, 116.5, 111.2, 84.7, 27.7;  $m/z$  ESI $^+$  found 268.1067  $[\text{M}+\text{Na}]^+$  calculated for  $\text{C}_{13}\text{H}_{15}\text{N}_3\text{NaO}_2$  268.1056.

tert-Butyl 2-(5-acetylpyridin-3-yl)-1H-pyrrole-1-carboxylate, **5-2c**.



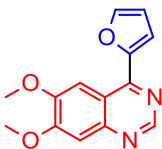
Following **GP 5-1** (aryl halide 160.0 mg, boronic acid 337.6 mg), the title product was obtained via flash chromatography using silica and 40% EtOAc in hexanes. The product was isolated as white solid (97%).  $^1\text{H}$  NMR (500.1 MHz,  $\text{CDCl}_3$ ):  $\delta$  9.10 (d,  $J = 1.7$  Hz, 1H), 8.80 (d,  $J = 1.8$  Hz, 1H), 8.24 (t,  $J = 2.1$  Hz, 1H), 7.46-7.45 (m, 1H), 6.34-6.33 (m, 1H), 6.31 (t,  $J = 3.4$  Hz, 1H), 2.68 (s, 3H) 1.43 (s, 9H);  $^{13}\text{C}\{^1\text{H}\}$  NMR (125.8 MHz,  $\text{CDCl}_3$ ):  $\delta$  196.7, 153.4, 149.1, 148.1, 135.9, 131.5, 130.7, 130.3, 124.0, 116.4, 111.3, 84.7, 27.9, 27.0;  $m/z$  ESI $^+$  found 309.1213  $[\text{M}+\text{Na}]^+$  calculated for  $\text{C}_{16}\text{H}_{18}\text{N}_2\text{NaO}_3$  309.1210.

4-(Furan-2-yl)isoquinoline, **5-2d**.



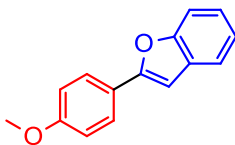
Following **GP 5-1** (aryl halide 166.5 mg, boronic acid 179.1 mg), the title product was obtained via flash chromatography using silica and 30% EtOAc in hexanes. The product was isolated as yellow oil (99%).  $^1\text{H}$  NMR (500.1 MHz,  $\text{CDCl}_3$ ):  $\delta$  9.23 (s, 1H), 8.80 (s, 1H), 8.45 (d,  $J = 8.6$  Hz, 1H), 8.04 (d,  $J = 8.2$  Hz, 1H), 7.80-7.77 (m, 1H), 7.71-7.66 (m, 2H), 6.84 (d,  $J = 3.3$  Hz, 1H), 6.65-6.64 (m, 1H);  $^{13}\text{C}\{^1\text{H}\}$  NMR (125.8 MHz,  $\text{CDCl}_3$ ):  $\delta$  152.3, 151.1, 143.2, 142.1, 132.6, 130.9, 128.4, 128.0, 127.3, 124.6, 122.2, 111.5, 109.9; this is in agreement with previously reported spectra.<sup>[106]</sup>

4-(Furan-2-yl)-6,7-dimethoxyquinazoline, **5-2e**.



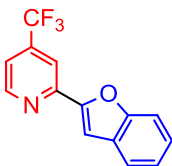
Following **GP 5-1** (aryl halide 179.7 mg, boronic acid 179.1 mg), the title product was obtained via flash chromatography using silica and 100% EtOAc. The product was isolated as light yellow solid (75%).  $^1\text{H}$  NMR (500.1 MHz,  $\text{CDCl}_3$ ):  $\delta$  9.13 (s, 1H), 8.19 (s, 1H), 7.81 (s, 1H), 7.54 (d,  $J = 3.2$  Hz, 1H), 7.37 (s, 1H), 6.72-6.71 (m, 1H), 4.11 (s, 3H), 4.10 (s, 3H);  $^{13}\text{C}\{^1\text{H}\}$  NMR (125.8 MHz,  $\text{CDCl}_3$ ):  $\delta$  155.9, 153.9, 153.5, 152.3, 150.8, 150.1, 145.5, 116.8, 115.4, 112.6, 107.1, 104.1, 56.5, 56.3;  $m/z$  ESI<sup>+</sup> found 257.1946  $[\text{M}+\text{H}]^+$  calculated for  $\text{C}_{14}\text{H}_{13}\text{N}_2\text{O}_3$  257.0921.

2-(4-Methoxyphenyl)benzofuran, **5-2f**.



Following **GP 5-1** (aryl halide 98.0  $\mu\text{L}$ , boronic acid 258.6 mg), the title product was obtained via flash chromatography using silica and 10% EtOAc in hexanes. The product was isolated as yellow oil (50%).  $^1\text{H}$  NMR (500.1 MHz,  $\text{CDCl}_3$ ):  $\delta$  7.85-7.82 (m, 2H), 7.59-7.58 (m, 1H), 7.53 (d,  $J = 7.6$  Hz, 1H), 7.30-7.27 (m, 1H), 7.26-7.23 (m, 1H), 7.03-7.00 (m, 2H), 6.92 (s, 1H), 3.90 (s, 3H);  $^{13}\text{C}\{^1\text{H}\}$  NMR (125.8 MHz,  $\text{CDCl}_3$ ):  $\delta$  159.9, 156.0, 154.7, 129.4, 126.4, 123.7, 123.3, 122.8, 120.5, 114.2, 110.9, 99.6, 55.3; this is in agreement with previously reported spectra.<sup>[107]</sup>

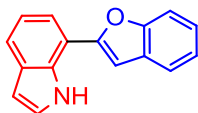
2-(Benzofuran-2-yl)-4-(trifluoromethyl)pyridine, **5-2g**.



Following **GP 5-1** (aryl halide 102.9  $\mu\text{L}$ , boronic acid 258.6 mg), the title product was obtained via flash chromatography using silica and 5% EtOAc in hexanes. The product was isolated as a white solid (51%).  $^1\text{H}$  NMR (300.1 MHz,  $\text{CDCl}_3$ ):  $\delta$  8.86 (d,  $J = 5.0$ , 1H), 8.12 (s, 1H), 7.69 (d,  $J = 7.7$ , 1H), 7.61 (d,  $J = 8.2$ , 1H), 7.56 (s, 1H), 7.46 (d,  $J = 5.1$ , 1H), 7.40 (t,  $J = 7.23$ , 1H), 7.32 (d,  $J = 7.5$ , 1H);  $^{19}\text{F}\{^1\text{H}\}$  NMR (282.3 MHz,  $\text{CDCl}_3$ ):  $\delta$  -65.0;  $^{13}\text{C}\{^1\text{H}\}$  NMR (125.8 MHz,  $\text{CDCl}_3$ ):  $\delta$  155.4, 153.7, 150.8, 150.5, 139.2 (q,  $^2J_{\text{CF}} = 34.3$  Hz), 128.5, 125.8, 123.4, 122.7 (q,  $^1J_{\text{CF}} = 273.4$  Hz), 122.0, 118.0 (q,  $^3J_{\text{CF}} = 3.5$  Hz), 115.2

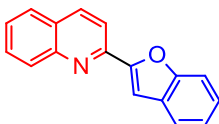
(q,  $^3J_{CF} = 3.5$  Hz), 111.6, 106.3;  $m/z$  ESI<sup>+</sup> found 286.0451 [M+Na]<sup>+</sup> calculated for C<sub>14</sub>H<sub>8</sub>F<sub>3</sub>NNaO 286.0450.

7-(Benzofuran-2-yl)-1H-indole, **5-2h**.



Following **GP 5-1** (aryl halide 122.3 mg, boronic acid 258.6 mg), the title product was obtained via flash chromatography using silica and 10% EtOAc in hexanes. The product was isolated as a white solid (98%). <sup>1</sup>H NMR (500.1 MHz, CDCl<sub>3</sub>): δ 9.54 (br s, 1H), 7.75 (d,  $J = 7.8$  Hz, 1H), 7.71-7.64 (m, 3H), 7.42 (t,  $J = 2.8$  Hz, 1H), 7.39-7.32 (m, 2H), 7.26 (t,  $J = 7.6$  Hz, 1H), 7.17 (s, 1H), 6.70-6.69 (m, 1H); <sup>13</sup>C{<sup>1</sup>H} NMR (125.8 MHz, CDCl<sub>3</sub>): δ 156.5, 154.7, 132.3, 129.4, 129.0, 125.1, 124.2, 123.4, 121.8, 121.0, 120.1, 119.4, 114.2, 111.1, 102.8, 101.6;  $m/z$  ESI<sup>+</sup> found 256.0742 [M+Na]<sup>+</sup> calculated for C<sub>16</sub>H<sub>11</sub>NNaO 256.0733.

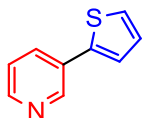
2-(Benzofuran-2-yl)quinoline, **5-2i**.



Following **GP 5-1** (aryl halide 130.8 mg, boronic acid 258.6 mg), the title product was obtained via flash chromatography using silica and 20% EtOAc in hexanes. The product was isolated as a white solid (75%). <sup>1</sup>H NMR (500.1 MHz, CDCl<sub>3</sub>): δ 8.29 (d,  $J = 8.6$ , 1H), 8.26 (br s, 1H), 8.07 (d,  $J = 8.6$  Hz, 1H), 7.87-7.85 (m, 1H), 7.80-7.77 (m, 1H), 7.74-7.72 (m, 1H), 7.70 (br s, 1H), 7.68-7.67 (m, 1H), 7.60-7.57 (m, 1H), 7.43-7.39 (m, 1H), 7.34-

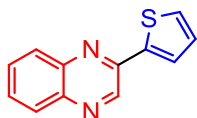
7.31 (m, 1H);  $^{13}\text{C}\{^1\text{H}\}$  NMR (125.8 MHz,  $\text{CDCl}_3$ ):  $\delta$  155.6, 155.2, 149.0, 148.2, 136.7, 129.9, 129.6, 128.7, 127.6, 126.6, 125.5, 123.2, 121.7, 118.1, 111.8, 106.9;  $m/z$  ESI<sup>+</sup> found 246.0909 [M+H]<sup>+</sup> calculated for  $\text{C}_{17}\text{H}_{12}\text{NO}$  246.0913.

3-(Thiophen-2-yl)pyridine, **5-2j**.



Following **GP 5-1** (aryl halide 76.1  $\mu\text{L}$ , boronic acid 204.7 mg), the title product was obtained via flash chromatography using silica and 30% EtOAc in hexanes. The product was isolated as a white solid (84%).  $^1\text{H}$  NMR (300.1 MHz,  $\text{CDCl}_3$ ):  $\delta$  8.90 (br s, 1H), 8.53 (br s, 1H), 7.90-7.87 (m, 1H), 7.38-7.30 (m, 3H), 7.14 (t,  $J = 4.2$  Hz, 1H);  $^{13}\text{C}\{^1\text{H}\}$  NMR (75.4 MHz,  $\text{CDCl}_3$ ):  $\delta$  148.3, 146.9, 140.3, 133.0, 130.4, 128.2, 126.0, 124.2, 123.6; this is in agreement with previously reported spectra.<sup>[108]</sup>

2-(Thiophen-2-yl)quinoxaline, **5-2k**.

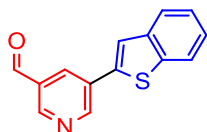


Following **GP 5-1** (aryl halide 131.7 mg, boronic acid 204.7 mg), the title product was obtained via flash chromatography using silica and 15% EtOAc in hexanes. The product was isolated as a white solid (78%).  $^1\text{H}$  NMR (500.1 MHz,  $\text{CDCl}_3$ ):  $\delta$  9.27 (s, 1H), 8.11-8.09 (m, 2H), 7.90-7.89 (m, 1H), 7.79-7.76 (m, 1H), 7.74-7.71 (m, 1H), 7.58-7.57 (m, 1H), 7.25-7.23 (m, 1H);  $^{13}\text{C}\{^1\text{H}\}$  NMR (125.8 MHz,  $\text{CDCl}_3$ ):  $\delta$  147.3, 142.2, 142.1, 142.0,



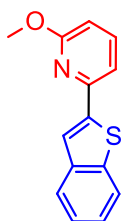
141.3, 130.4, 129.7, 129.1, 129.1, 128.4, 126.9; this is in agreement with previously reported spectra.<sup>[109]</sup>

5-(Benzo[b]thiophen-2-yl)nicotinaldehyde, **5-2l**.



Following **GP 5-1** (aryl halide 148.8 mg, boronic acid 284.8 mg), the title product was obtained via flash chromatography using silica and 30% EtOAc in hexanes. The product was isolated as a white solid (91%). <sup>1</sup>H NMR (500.1 MHz, CDCl<sub>3</sub>): δ 10.2 (s, 1H), 9.22 (br s, 1H), 9.04 (br, 1H), 8.44-8.43 (m, 1H), 7.91-7.84 (m, 2H), 7.73 (s, 1H), 7.46-7.37 (m, 2H); <sup>13</sup>C{<sup>1</sup>H} NMR (125.8 MHz, CDCl<sub>3</sub>): δ 190.3, 152.0, 150.9, 140.1, 139.9, 138.5, 132.5, 131.3, 131.1, 125.4, 125.0, 124.1, 122.4, 121.9; this is in agreement with previously reported spectra.<sup>[96]</sup>

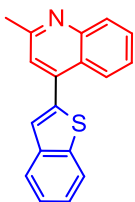
2-(Benzo[b]thiophen-2-yl)-6-methoxypyridine, **5-2m**.



Following **GP 5-1** (aryl halide 95.1 μL, boronic acid 284.8 mg), the title product was obtained via flash chromatography using silica and 1% EtOAc in hexanes. The product was isolated as a white solid (79%). <sup>1</sup>H NMR (300.1 MHz, CDCl<sub>3</sub>): δ 7.88-7.80 (m, 3H), 7.62 (t, *J* = 7.5 Hz, 1H), 7.39-7.35 (m, 3H), 6.70 (d, *J* = 8.1 Hz, 1H), 4.07 (s, 3H); <sup>13</sup>C{<sup>1</sup>H} NMR (75.4 MHz, CDCl<sub>3</sub>): δ 163.6, 149.9, 144.9, 140.5, 140.5, 139.0, 124.8, 124.4, 124.0.

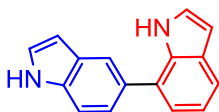
122.4, 120.8, 112.2, 109.8, 53.4;  $m/z$  ESI<sup>+</sup> found 242.0630 [M+H]<sup>+</sup> calculated for C<sub>14</sub>H<sub>12</sub>NOS 242.0634.

4-(Benzo[b]thiophen-2-yl)-2-methylquinoline, **5-2n**.



Following **GP 5-1** (aryl halide 161.3  $\mu$ L, boronic acid 284.8 mg), the title product was obtained via flash chromatography using silica and 25% EtOAc in hexanes. The product was isolated as a white solid (99%). <sup>1</sup>H NMR (500.1 MHz, CDCl<sub>3</sub>):  $\delta$  8.31 (d,  $J$  = 8.4 Hz, 1H), 8.1 (d,  $J$  = 8.4 Hz, 1H), 7.95 (d,  $J$  = 7.6, 1H), 7.91 (d,  $J$  = 7.5 Hz, 1H), 7.76 (t,  $J$  = 7.2 Hz, 1H), 7.61 (s, 1H), 7.55 (t,  $J$  = 7.3 Hz, 1H), 7.49-7.43 (m, 3H), 2.83 (s, 3H); <sup>13</sup>C {<sup>1</sup>H} NMR (125.8 MHz, CDCl<sub>3</sub>):  $\delta$  158.4, 148.6, 140.9, 140.3, 139.9, 139.1, 129.6, 129.2, 126.2, 125.3, 125.2, 124.9, 124.8, 124.7, 124.0, 123.0, 122.2, 25.3;  $m/z$  ESI<sup>+</sup> found 276.0840 [M+H]<sup>+</sup> calculated for C<sub>18</sub>H<sub>14</sub>NS 276.0841.

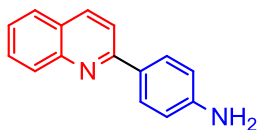
1H,1'H-5,7'-Biindole, **5-2o**.



Following **GP 5-1** (aryl halide 121.3 mg, boronic acid 257.6 mg), except the reaction was stirred in a temperature controlled aluminum block hot plate set to 50 °C for 16 hours. The title product was obtained via flash chromatography using silica and 30% EtOAc in hexanes. The product was isolated as a white solid (70%). <sup>1</sup>H NMR (500.1 MHz, CDCl<sub>3</sub>):

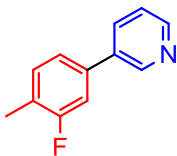
$\delta$  8.51 (br s, 1H), 8.22 (br s, 1H), 7.95 (s, 1H), 7.68 (d,  $J = 7.7$  Hz, 1H), 7.55-7.50 (m, 2H), 7.33-7.24 (m, 4H), 6.68-6.67 (m, 2H);  $^{13}\text{C}\{^1\text{H}\}$  NMR (125.8 MHz,  $\text{CDCl}_3$ ):  $\delta$  135.4, 134.4, 131.2, 128.6, 128.3, 127.1, 125.2, 124.3, 123.0, 122.2, 120.5, 120.3, 119.4, 111.8, 103.2, 103.1;  $m/z$  ESI<sup>+</sup> found 255.0902  $[\text{M}+\text{Na}]^+$  calculated for  $\text{C}_{16}\text{H}_{12}\text{N}_2\text{Na}$  255.0893.

4-(Quinolin-2-yl)aniline, **5-2p**.



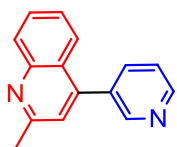
Following **GP 5-1** (aryl halide 130.9 mg, HCl salt of the aniline boronic acid 277.5 mg), except the reaction was stirred in a temperature controlled aluminum block hot plate set to 50 °C for 16 hours. The title product was obtained via flash chromatography using silica and 40% EtOAc in hexanes. The product was isolated as a yellow solid (43%).  $^1\text{H}$  NMR (300.1 MHz,  $\text{CDCl}_3$ ):  $\delta$  8.17-8.12 (m, 2H), 8.05 (d,  $J = 8.4$  Hz, 2H), 7.81 (t,  $J = 8.6$  Hz, 2H), 7.70 (t,  $J = 7.29$ , 1H), 7.48 (t,  $J = 7.2$  Hz, 1H), 6.82 (d,  $J = 8.4$  Hz, 2H), 3.89 (br s, 2H);  $^{13}\text{C}\{^1\text{H}\}$  NMR (125.8 MHz,  $\text{CDCl}_3$ ):  $\delta$  157.2, 148.3, 147.7, 136.3, 129.9, 129.4, 129.3, 128.7, 127.3, 126.7, 125.5, 118.3, 115.1;  $m/z$  ESI<sup>+</sup> found 221.1073  $[\text{M}+\text{H}]^+$  calculated for  $\text{C}_{15}\text{H}_{13}\text{N}$  221.1077. The reaction was repeated following **GP5-1**, and the crude residue was analyzed by using 1,4-di-*tert*-butylbenzene (19.0 mg 0.1 mmol) as an integration standard. Integration of the product against the standard indicated a 95% yield of **5-2p**.

3-(3-Fluoro-4-methylphenyl)pyridine, **5-3a**.



Following **GP 5-2** (aryl halide 48.8  $\mu\text{L}$ , boronic acid 147.5 mg), the title product was obtained via flash chromatography using silica and 30% EtOAc in hexanes. The product was isolated as a yellow oil (61%).  $^1\text{H}$  NMR (300.1 MHz,  $\text{CDCl}_3$ ):  $\delta$  8.85 (s, 1H), 8.62 (d,  $J = 3.4$  Hz, 1H), 7.86 (d,  $J = 7.8$ , 1H), 7.40-7.37 (m, 1H), 7.33-7.22 (m, 3H), 2.36 (d,  $^4J_{\text{CF}} = 1.7$  Hz, 3H);  $^{19}\text{F}\{^1\text{H}\}$  NMR (470.5 MHz,  $\text{CDCl}_3$ ):  $\delta$  -116.6;  $^{13}\text{C}\{^1\text{H}\}$  NMR (125.8 MHz,  $\text{CDCl}_3$ ):  $\delta$  161.6 (d,  $^1J_{\text{CF}} = 245.5$  Hz), 148.6, 148.0, 137.3 (d,  $^3J_{\text{CF}} = 7.8$  Hz), 135.4, 134.0, 132.0 (d,  $^3J_{\text{CF}} = 5.7$  Hz), 124.7 (d,  $^2J_{\text{CF}} = 17.3$  Hz), 123.5, 122.3 (d,  $^4J_{\text{CF}} = 2.9$  Hz), 133.5 (d,  $^2J_{\text{CF}} = 23.3$  Hz), 14.2 (d,  $^3J_{\text{CF}} = 3.4$  Hz);  $m/z$  ESI $^+$  found 188.0863  $[\text{M}+\text{H}]^+$  calculated for  $\text{C}_{12}\text{H}_{11}\text{FN}$  188.0870.

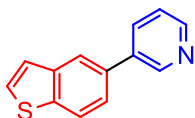
2-Methyl-4-(pyridin-3-yl)quinoline, **5-3b**.



Following **GP 5-2** (aryl halide 80.6  $\mu\text{L}$ , boronic acid 147.5 mg), the title product was obtained via flash chromatography using silica and 50% EtOAc in hexanes. The product was isolated as a waxy yellow solid (40%).  $^1\text{H}$  NMR (300.1 MHz,  $\text{CDCl}_3$ ):  $\delta$  8.78 (d,  $J = 1.8$  Hz, 1H), 8.76 (dd,  $J = 4.9$  Hz,  $J = 1.5$  Hz, 1H), 8.13 (d, 8.4 Hz, 1H), 7.86-7.84 (m, 1H), 7.78 (d,  $J = 8.3$  Hz, 1H), 7.75-7.72 (m, 1H), 7.50-7.47 (m, 1H), 7.26 (s, 1H), 2.81 (s, 3H);  $^{13}\text{C}\{^1\text{H}\}$  NMR (125.8 MHz,  $\text{CDCl}_3$ ):  $\delta$  158.5, 149.9, 149.6, 148.3, 144.6, 136.8, 133.9,

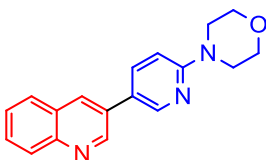
129.6, 129.2, 126.2, 124.8, 124.7, 123.2, 122.4, 25.3;  $m/z$  ESI<sup>+</sup> found 221.1070[M+H]<sup>+</sup> calculated for C<sub>15</sub>H<sub>13</sub>N<sub>2</sub> 221.1073.

3-(Benzo[b]thiophen-5-yl)pyridine, **5-3c**.



Following **GP 5-2** (aryl halide 67.5 mg, boronic acid 147.5 mg), the title product was obtained via flash chromatography using silica and 30% EtOAc in hexanes. The product was isolated as a waxy yellow solid (54%). <sup>1</sup>H NMR (300.1 MHz, CDCl<sub>3</sub>): δ 8.96 (d,  $J$  = 1.8 Hz, 1H), 8.65-8.64 (m, 1H), 8.05 (m, 1H), 8.01 (d,  $J$  = 8.4 Hz, 1H), 7.98-7.96 (m, 1H), 7.59 (dd,  $J$  = 8.3 Hz,  $J$  = 1.6 Hz, 1H), 7.55 (d,  $J$  = 5.4 Hz, 1H), 7.45-7.41 (m, 2H); <sup>13</sup>C {<sup>1</sup>H} NMR (125.8 MHz, CDCl<sub>3</sub>): δ 148.5, 148.3, 140.2, 139.5, 136.8, 134.5, 134.2, 127.5, 123.9, 123.5, 123.5, 123.1, 122.1;  $m/z$  ESI<sup>+</sup> found 212.0533 [M+H]<sup>+</sup> calculated for C<sub>13</sub>H<sub>10</sub>NS 212.0528.

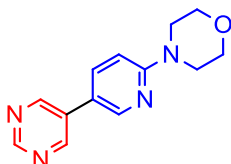
4-(5-(Quinolin-3-yl)pyridin-2-yl)morpholine, **5-3d**.



Following **GP 5-2** (aryl halide 54.4 mg, boronic acid 249.6 mg), the title product was obtained via flash chromatography using silica and 70% EtOAc in hexanes. The product was isolated as a white solid (88%). <sup>1</sup>H NMR (300.1 MHz, CDCl<sub>3</sub>): δ 9.16 (d,  $J$  = 2.2 Hz, 1H), 8.61 (d,  $J$  = 2.4 Hz, 1H), 8.25 (d,  $J$  = 2.1 Hz, 1H), 8.15 (d,  $J$  = 8.4 Hz, 1H), 7.91-7.89 (m, 2H), 7.75-7.72 (m, 1H), 7.62-7.59 (m, 1H), 6.81 (d,  $J$  = 8.8 Hz, 1H), 3.89 (t,  $J$  = 4.7

Hz, 4H), 3.64 (t,  $J = 5.0$  Hz, 4H);  $^{13}\text{C}\{^1\text{H}\}$  NMR (125.8 MHz,  $\text{CDCl}_3$ ):  $\delta$  159.0, 149.2, 147.1, 146.5, 136.2, 131.7, 131.1, 129.2, 129.1, 128.1, 127.7, 127.0, 123.3, 106.8, 66.7, 45.5;  $m/z$  ESI<sup>+</sup> found 292.1443 [M+H]<sup>+</sup> calculated for  $\text{C}_{18}\text{H}_{18}\text{N}_3\text{O}$  292.1444.

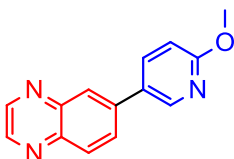
4-(5-(Pyrimidin-5-yl)pyridin-2-yl)morpholine, **5-3e**.



Following **GP 5-2** (aryl halide 63.6 mg, boronic acid 249.6 mg), the title product was obtained via flash chromatography using silica and 100% EtOAc. The product was isolated as a white solid (69%).  $^1\text{H}$  NMR (300.1 MHz,  $\text{CD}_2\text{Cl}_2$ ):  $\delta$  9.14 (s, 1H), 8.93 (s, 1H), 8.47 (d,  $J = 2.3$  Hz, 1H), 7.79 (dd,  $J = 8.8$  Hz,  $J = 2.5$  Hz, 1H), 6.81 (d,  $J = 8.8$  Hz, 1H), 3.84 (t,  $J = 4.7$  Hz, 4H), 3.61 (t,  $J = 5.1$  Hz, 4H);  $^{13}\text{C}\{^1\text{H}\}$  CO<sub>n</sub>

NMR (125.8 MHz,  $\text{CD}_2\text{Cl}_2$ ):  $\delta$  159.4, 156.9, 153.8, 146.1, 135.7, 131.8, 119.4, 106.8, 66.6, 45.3;  $m/z$  ESI<sup>+</sup> found 243.1234 [M+H]<sup>+</sup> calculated for  $\text{C}_{13}\text{H}_{15}\text{N}_4\text{O}$  243.1240.

6-(6-Methoxypyridin-3-yl)quinoxaline, **5-3f**.



Following **GP 5-2** (aryl halide 65.8 mg, boronic acid 183.5 mg), the title product was obtained via flash chromatography using silica and 50% EtOAc in hexanes. The product was isolated as a light yellow solid (57%).  $^1\text{H}$  NMR (300.1 MHz,  $\text{CDCl}_3$ ):  $\delta$  8.91-8.88 (m, 2H), 8.29 (d,  $J = 1.9$  Hz, 1H), 8.22 (d,  $J = 8.7$  Hz, 1H), 8.03-7.98 (m, 2H), 6.94 (d,  $J = 8.6$

Hz, 1H), 4.05 (s, 3H);  $^{13}\text{C}\{^1\text{H}\}$  NMR (125.8 MHz,  $\text{CDCl}_3$ ):  $\delta$  164.5, 145.8, 145.7, 145.0, 143.5, 142.5, 139.9, 137.8, 130.4, 129.3, 128.7, 126.5, 111.5, 53.9;  $m/z$  ESI $^+$  found 260.0799  $[\text{M}+\text{Na}]^+$  calculated for  $\text{C}_{14}\text{H}_{11}\text{NaN}_3\text{O}$  260.0794.

## Chapter 6 Conclusions and Future Work

### 6.1 Chapter 2: Palladium Catalyzed C-O Cross-Coupling

Chapter 2 of this document detailed my ancillary ligand survey of several state-of-the-art catalyst systems in palladium-catalyzed C-O cross-coupling. While my initial goal of establishing Mor-Dalphos (**L2-5**) as a superior ligand in these reactions was not met, I was able to establish trends of reactivity at both room temperature, as well as at elevated temperatures (90 °C).

While these trends in reactivity were established, several challenges presented themselves. Firstly, reactions involving five-membered heterocyclic electrophiles performed poorly, even at elevated temperatures and long reactions times. Secondly, bulky secondary and tertiary aliphatic alcohols also gave diminished yields, potentially due to the increased steric bulk of the nucleophiles. Further research could address these issues through the identification of additional ligands that are capable of accommodating these challenging reaction partners. In a similar vein to Chapter 3, it could also be possible to address these challenges through the development of a new first row metal catalyst. While several nickel catalysts have been developed for C-N cross-coupling, C-O cross-coupling has not received as much attention. Therefore, the development of nickel catalysts could potentially solve many of the outstanding challenges in palladium chemistry.



## 6.2 Chapter 3: Microwave Assisted Monoarylation of Ammonium Salts

Chapter 3 outlined my work utilizing microwave heating for nickel catalyzed C-N cross-coupling of ammonium salts, using a new ligand complex designed for nickel catalysis. This system was capable of effectively performing cross-coupling reactions utilizing ammonium acetate, methylammonium chloride, ethylammonium chloride as coupling partners with a diverse set of (hetero)aryl electrophiles. While these transformations were effective, several outstanding challenges remain: polyarylation products were often detected in reactions involving activated heteroaryl halides with ammonium acetate, and electron rich electrophiles were stubbornly unreactive, with significant amounts of starting material detected. It may be tempting, in the first case, to simply increase the equivalents of ammonia to statistically favour the monoarylated product. However, the subsequent increase of required base to generate free ammonia makes this solution less attractive. To address both of these challenges, further ligand design may be the more appropriate solution. While this may seem like the obvious choice, this method is more challenging than it may first appear, due to that the trends in the effects of ancillary ligands on nickel-catalyzed reactions are not as understood compared to those of the more studied precious metal catalysts.

### 6.3 Chapter 4: Wide Bite Angle Ligands in Nickel-Catalyzed C-N Cross-Coupling

Chapter 4 detailed my work in the development of (DPEphos)Ni(mesityl)Br (**C4-1**) for use in C-N cross-coupling reactions of secondary amines, and azoles. While this catalyst compared favourably to other state-of-the-art catalysts for these reactions the observation that only activated (hetero)aryl electrophiles were compatible leaves room for improvement. Further tuning of the DPEphos core may be able to address this issue.

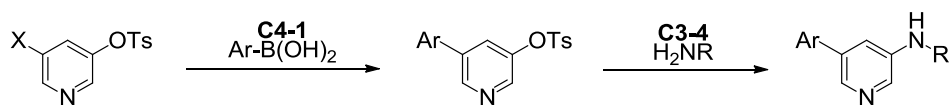
An additional avenue of potential research is the further comparison of **C4-1** of other reactions in which DPPF is successful, similar to the work outlined in Chapter 5. For example, DPPF has been employed in a mixed ligand system for the borylation of aryl (pseudo)halide electrophiles.<sup>[29, 110]</sup> Given the work described in Chapter 5, should **C4-1** be capable in these reactions, the potential for a one pot borylation-Suzuki cross-coupling would be an attractive method for biaryl synthesis.

### 6.4 Chapter 5: Suzuki-Miyaura Cross-Coupling using (DPEphos)Ni(mesityl)Br

Chapter 5 discusses the use of **C4-1** for using in Suzuki-Miyaura cross-coupling reactions to afford unsymmetrical biheteroaryl products. The cross-coupling of challenging 5-membered heterocyclic boronic acids with a variety of heteroaryl halides was accomplished at room temperature in high yields. Despite excellent reactivity with heteroaryl halides, phenol derived electrophiles failed to react; the observation that these

substrates are inert under these reactions conditions allows for the opportunity to perform SM reactions in the presence of these electrophiles followed by an additional cross-coupling to yield more highly functionalized biheteroaryls.

Additionally, **C4-1** was also able to utilize pyridyl boronic acids as coupling partners. While these reactions were limited to 3-pyridyl boronic acids, and the observation of significant amounts of hydrodehalogenation byproducts, this protocol represents a step forward as only a handful of examples exist using these substrates in nickel catalysis. Future avenues of research will be to identify conditions to attenuate the formation of deleterious hydrodehalogenation, as well to expand the scope beyond 3-pyridyl boronic acids.



**Scheme 6-1:** Example of potential two-step cross-coupling enabled by selective Suzuki-Miyaura cross-coupling with **C4-1**.

## References

- [1] J. F. Hartwig, in *Organotransition Metal Chemistry: from Bonding to Catalysis*, University Science Books, **2010**, pp. 539-542.
- [2] M. A. Fox, J. K. Whitesell, *Organic Chemistry 3rd ed.*, Jones and Bartlett, Mississauga, On, **2004**, pp. 953-958.
- [3] a) W. S. Knowles, *Angew. Chem. Int. Ed.* **2002**, *41*, 1998-2007; b) R. Noyori, *Angew. Chem. Int. Ed.* **2002**, *41*, 2008-2022; c) K. B. Sharpless, *Angew. Chem. Int. Ed.* **2002**, *41*, 2024-2032.
- [4] a) Y. Chauvin, *Angew. Chem. Int. Ed.* **2006**, *45*, 3740-3747; b) R. H. Grubbs, *Angew. Chem. Int. Ed.* **2006**, *45*, 3760-3765; c) R. R. Schrock, *Angew. Chem. Int. Ed.* **2006**, *45*, 3748-3759.
- [5] N. Miyaura, A. Suzuki, *J. Chem. Soc., Chem. Commun.* **1979**, 866-867.
- [6] S. Baba, E. Negishi, *J. Am. Chem. Soc.* **1976**, *98*, 6729-6731.
- [7] R. F. Heck, J. P. Nolley, *J. Org. Chem* **1972**, *37*, 2320-2322.
- [8] K. Tamao, K. Sumitani, M. Kumada, *J. Am. Chem. Soc.* **1972**, *94*, 4374-4376.
- [9] A. M. Echavarren, J. K. Stille, *J. Am. Chem. Soc.* **1987**, *109*, 5478-5486.
- [10] K. Sonogashira, Y. Tohda, N. Hagihara, *Tetrahedron Lett.* **1975**, *16*, 4467-4470.
- [11] R. F. Heck, *Acc. Chem. Res.* **1979**, *12*, 146-151.
- [12] R. J. Lundgren, M. Stradiotto, *Chem. Eur. J.* **2012**, *18*, 9758-9769.
- [13] F. Damkaci, C. Sigindere, T. Sobiech, E. Vik, J. Malone, *Tetrahedron Lett.* **2017**, *58*, 3559-3564.
- [14] J. S. Marcum, K. A. McGarry, C. J. Ferber, T. B. Clark, *J. Org. Chem* **2016**, *81*, 7963-7969.
- [15] a) H. Lu, C. Li, *Org. Lett.* **2006**, *8*, 5365-5367; b) Y. Zhang, X. Yang, Q. Yao, D. Ma, *Org. Lett.* **2012**, *14*, 3056-3059.
- [16] a) J. Niu, P. Guo, J. Kang, Z. Li, J. Xu, S. Hu, *J. Org. Chem* **2009**, *74*, 5075-5078; b) R. E. Shade, A. M. Hyde, J.-C. Olsen, C. A. Merlic, *J. Am. Chem. Soc.* **2010**, *132*, 1202-1203.

- [17] K. E. Torraca, X. Huang, C. A. Parrish, S. L. Buchwald, *J. Am. Chem. Soc.* **2001**, *123*, 10770-10771.
- [18] A. V. Vorogushin, X. Huang, S. L. Buchwald, *J. Am. Chem. Soc.* **2005**, *127*, 8146-8149.
- [19] S. Gowrisankar, A. G. Sergeev, P. Anbarasan, A. Spannenberg, H. Neumann, M. Beller, *J. Am. Chem. Soc.* **2010**, *132*, 11592-11598.
- [20] a) Q. Shelby, N. Kataoka, G. Mann, J. Hartwig, *J. Am. Chem. Soc.* **2000**, *122*, 10718-10719; b) C. A. Parrish, S. L. Buchwald, *J. Org. Chem.* **2001**, *66*, 2498-2500.
- [21] T. Hu, T. Schulz, C. Torborg, X. Chen, J. Wang, M. Beller, J. Huang, *Chem. Commun.* **2009**, 7330-7332.
- [22] X. Wu, B. P. Fors, S. L. Buchwald, *Angew. Chem. Int. Ed.* **2011**, *50*, 9943-9947.
- [23] P. E. Maligres, J. Li, S. W. Krska, J. D. Schreier, I. T. Raheem, *Angew. Chem. Int. Ed.* **2012**, *51*, 9071-9074.
- [24] S. Enthaler, A. Company, *Chem. Soc. Rev.* **2011**, *40*, 4912-4924.
- [25] Y. Xiong, T. Huang, X. Ji, J. Wu, S. Cao, *Org. Biomol. Chem.* **2015**, *13*, 7389-7392.
- [26] a) R. J. Lundgren, B. D. Peters, P. G. Alsabeh, M. Stradiotto, *Angew. Chem. Int. Ed.* **2010**, *49*, 4071-4074; b) R. J. Lundgren, M. Stradiotto, *Angew. Chem. Int. Ed.* **2010**, *49*, 8686-8690.
- [27] C. W. Cheung, S. L. Buchwald, *Org. Lett.* **2013**, *15*, 3998-4001.
- [28] S. C. Baker, D. P. Kelly, J. C. Murrell, *Nature* **1991**, *350*, 627-628.
- [29] D. A. Wilson, C. J. Wilson, C. Moldoveanu, A.-M. Resmerita, P. Corcoran, L. M. Hoang, B. M. Rosen, V. Percec, *J. Am. Chem. Soc.* **2010**, *132*, 1800-1801.
- [30] B. Schlummer, U. Scholz, *Adv. Synth. Catal.* **2004**, *346*, 1599-1626.
- [31] M. K. Masanori Kosugi, Toshihiko Migita, *Chem. Lett.* **1983**, *12*, 927-928.
- [32] a) A. S. Guram, R. A. Rennels, S. L. Buchwald, *Angew. Chem. Int. Ed.* **1995**, *34*, 1348-1350; b) J. Louie, J. F. Hartwig, *Tetrahedron Lett.* **1995**, *36*, 3609-3612.

- [33] a) M. G. Organ, M. Abdel-Hadi, S. Avola, I. Dubovyk, N. Hadei, E. A. B. Kantchev, C. J. O'Brien, M. Sayah, C. Valente, *Chem. Eur. J.* **2008**, *14*, 2443-2452; b) I. P. Beletskaya, A. V. Cheprakov, *Organometallics* **2012**, *31*, 7753-7808; c) M.-L. Louillat, F. W. Patureau, *Chem. Soc. Rev.* **2014**, *43*, 901-910.
- [34] D. S. Surry, S. L. Buchwald, *Chem. Sci.* **2011**, *2*, 27-50.
- [35] T. Ogata, J. F. Hartwig, *J. Am. Chem. Soc.* **2008**, *130*, 13848-13849.
- [36] G. J. Withbroe, R. A. Singer, J. E. Sieser, *Org. Process Res. Dev.* **2008**, *12*, 480-489.
- [37] A. Tewari, M. Hein, A. Zapf, M. Beller, *Tetrahedron* **2005**, *61*, 9705-9709.
- [38] J. Kim, H. J. Kim, S. Chang, *Eur. J. Org. Chem.* **2013**, *2013*, 3201-3213.
- [39] Q. Shen, J. F. Hartwig, *J. Am. Chem. Soc.* **2006**, *128*, 10028-10029.
- [40] S. Z. Tasker, E. A. Standley, T. F. Jamison, *Nature* **2014**, *509*, 299-309.
- [41] M. R. Friedfeld, M. Shevlin, J. M. Hoyt, S. W. Krska, M. T. Tudge, P. J. Chirik, *Science* **2013**, *342*, 1076-1080.
- [42] Y. Yang, S.-L. Shi, D. Niu, P. Liu, S. L. Buchwald, *Science* **2015**, *349*, 62-66.
- [43] J. P. Wolfe, S. L. Buchwald, *J. Am. Chem. Soc.* **1997**, *119*, 6054-6058.
- [44] N. H. Park, G. Teverovskiy, S. L. Buchwald, *Org. Lett.* **2014**, *16*, 220-223.
- [45] R. A. Green, J. F. Hartwig, *Org. Lett.* **2014**, *16*, 4388-4391.
- [46] A. Borzenko, N. L. Rotta-Loria, P. M. MacQueen, C. M. Lavoie, R. McDonald, M. Stradiotto, *Angew. Chem. Int. Ed.* **2015**, *54*, 3773-3777.
- [47] R. A. Green, J. F. Hartwig, *Angew. Chem. Int. Ed.* **2015**, *54*, 3768-3772.
- [48] a) R. Gedye, F. Smith, K. Westaway, H. Ali, L. Baldisera, L. Laberge, J. Rousell, *Tetrahedron Lett.* **1986**, *27*, 279-282; b) R. J. Giguere, T. L. Bray, S. M. Duncan, G. Majetich, *Tetrahedron Lett.* **1986**, *27*, 4945-4948.
- [49] D. V. Stass, J. R. Woodward, C. R. Timmel, P. J. Hore, K. A. McLauchlan, *Chem. Phys. Lett.* **2000**, *329*, 15-22.
- [50] M. Larhed, C. Moberg, A. Hallberg, *Acc. Chem. Res.* **2002**, *35*, 717-727.

- [51] M. Koley, N. Dastbaravardeh, M. Schnürch, M. D. Mihovilovic, *ChemCatChem* **2012**, *4*, 1345-1352.
- [52] B. U. W. Maes, K. T. J. Loones, G. L. F. Lemièrè, R. A. Dommissè, *Synlett* **2003**, *2003*, 1822-1825.
- [53] M. Larhed, A. Hallberg, *J. Org. Chem* **1996**, *61*, 9582-9584.
- [54] C. Strauss, R. Trainor, *Aust. J. Chem.* **1995**, *48*, 1665-1692.
- [55] D. M. P. Mingos, D. R. Baghurst, *Chem. Soc. Rev.* **1991**, *20*, 1-47.
- [56] M. Lukasiewicz, D. Bogdal, J. Pielichowski, *Adv. Synth. Catal.* **2003**, *345*, 1269-1272.
- [57] L. Perreux, A. Loupy, *Tetrahedron* **2001**, *57*, 9199-9223.
- [58] a) L. An, Y.-L. Xiao, Q.-Q. Min, X. Zhang, *Angew. Chem. Int. Ed.* **2015**, n/a-n/a; b) T. Kurahashi, S. Matsubara, *Acc. Chem. Res.* **2015**, *48*, 1703-1716.
- [59] a) M. Hidai, T. Kashiwagi, T. Ikeuchi, Y. Uchida, *J. Organomet. Chem.* **1971**, *30*, 279-282; b) E. L. Muetterties, D. H. Gerlach, A. R. Kane, G. W. Parshall, J. P. Jesson, *J. Am. Chem. Soc.* **1971**, *93*, 3543-3544; c) V. V. Grushin, H. Alper, *Chem. Rev.* **1994**, *94*, 1047-1062.
- [60] V. P. Ananikov, *ACS Catalysis* **2015**, *5*, 1964-1971.
- [61] S. Ge, R. A. Green, J. F. Hartwig, *J. Am. Chem. Soc.* **2014**, *136*, 1617-1627.
- [62] M. Epstein, S. A. Buckler, *J. Am. Chem. Soc.* **1961**, *83*, 3279-3282.
- [63] G. Adjabeng, T. Brenstrum, J. Wilson, C. Frampton, A. Robertson, J. Hillhouse, J. McNulty, A. Capretta, *Org. Lett.* **2003**, *5*, 953-955.
- [64] P. G. Pringle, M. B. Smith, *Phosphorus(III) Ligands in Homogeneous Catalysis: Design and Synthesis* John Wiley & Sons Ltd, Chichester, UK, **2012**, pp. 391-404.
- [65] N. Iranpoor, F. Panahi, *Adv. Synth. Catal.* **2014**, *356*, 3067-3073.
- [66] A. Borzenko, N. L. Rotta-Loria, P. M. MacQueen, C. M. Lavoie, R. McDonald, M. Stradiotto, *Angew. Chem. Int. Ed.* **2015**, *54*, 3773-3777.
- [67] S. C. Teguh, N. Klonis, S. Duffy, L. Lucantoni, V. M. Avery, C. A. Hutton, J. B. Baell, L. Tilley, *J. Med. Chem.* **2013**, *56*, 6200-6215.

- [68] M.-N. Birkholz, Z. Freixa, P. W. N. M. van Leeuwen, *Chem. Soc. Rev.* **2009**, *38*, 1099-1118.
- [69] P. C. J. Kamer, P. W. N. M. van Leeuwen, J. N. H. Reek, *Acc. Chem. Res.* **2001**, *34*, 895-904.
- [70] M. Kranenburg, Y. E. M. van der Burgt, P. C. J. Kamer, P. W. N. M. van Leeuwen, K. Goubitz, J. Fraanje, *Organometallics* **1995**, *14*, 3081-3089.
- [71] a) S. Hillebrand, B. Bartkowska, J. Bruckmann, C. Krüger, M. W. Haenel, *Tetrahedron Lett.* **1998**, *39*, 813-816; b) Y. Guari, G. P. F. van Strijdonck, M. D. K. Boele, J. N. H. Reek, P. C. J. Kamer, P. W. N. M. van Leeuwen, *Chem. Eur. J.* **2001**, *7*, 475-482.
- [72] F. Agbossou, J.-F. Carpentier, A. Mortreux, *Chem. Rev.* **1995**, *95*, 2485-2506.
- [73] C. P. Casey, G. T. Whiteker, M. G. Melville, L. M. Petrovich, J. A. Gavney, D. R. Powell, *J. Am. Chem. Soc.* **1992**, *114*, 5535-5543.
- [74] J. M. Brown, A. G. Kent, *J. Chem. Soc.* **1987**, 1597-1607.
- [75] a) M. Kranenburg, P. C. J. Kamer, P. W. N. M. van Leeuwen, D. Vogt, W. Keim, *J. Chem. Soc., Chem. Commun.* **1995**, 2177-2178; b) J. E. Marcone, K. G. Moloy, *J. Am. Chem. Soc.* **1998**, *120*, 8527-8528.
- [76] Y. Guari, D. S. van Es, J. N. H. Reek, P. C. J. Kamer, P. W. N. M. van Leeuwen, *Tetrahedron Lett.* **1999**, *40*, 3789-3790.
- [77] M. C. Harris, O. Geis, S. L. Buchwald, *J. Org. Chem.* **1999**, *64*, 6019-6022.
- [78] J. H. Downing, J. Floure, K. Heslop, M. F. Haddow, J. Hopewell, M. Lusi, H. Phetmung, A. G. Orpen, P. G. Pringle, R. I. Pugh, D. Zambrano-Williams, *Organometallics* **2008**, *27*, 3216-3224.
- [79] a) J. Magano, S. Monfette, *ACS Catalysis* **2015**, *5*, 3120-3123; b) J. D. Shields, E. E. Gray, A. G. Doyle, *Org. Lett.* **2015**, *17*, 2166-2169.
- [80] a) M. Marín, R. J. Rama, M. C. Nicasio, *Chem. Rec.* **2016**, *16*, 1819-1832; b) E. A. Standley, S. J. Smith, P. Muller, T. F. Jamison, *Organometallics* **2014**, *33*, 2012-2018; c) N. H. Park, G. Teverovskiy, S. L. Buchwald, *Org. Lett.* **2014**, *16*, 220-223; d) C. M. Lavoie, P. M. MacQueen, N. L. Rotta-Loria, R. S. Sawatzky, A. Borzenko, A. J. Chisholm, B. K. V. Hargreaves, R. McDonald, M. J. Ferguson, M. Stradiotto, *Nat. Commun.* **2016**, *7*, 11073; e) J. S. K. Clark, C. M. Lavoie, P. M. MacQueen, M. J. Ferguson, M. Stradiotto, *Organometallics* **2016**, *35*, 3248-3254; f) J. S. K. Clark, C. N. Voth, M. J. Ferguson, M. Stradiotto, *Organometallics* **2017**, *36*, 679-686.



- [81] N. Hazari, P. R. Melvin, M. M. Beromi, *Nat. Chem. Rev.* **2017**, *1*, 25.
- [82] M. Stradiotto, in *New Trends in Cross-Coupling: Theory and Application* (Ed.: T. J. Colacot), Royal Society of Chemistry, Cambridge, UK, **2014**, pp. 228-253.
- [83] a) B. H. Lipshutz, H. Ueda, *Angew. Chem. Int. Ed.* **2000**, *39*, 4492-4494; b) S. Tasler, B. H. Lipshutz, *J. Org. Chem.* **2003**, *68*, 1190-1199; c) L. Ackermann, W. F. Song, R. Sandmann, *J. Organomet. Chem.* **2011**, *696*, 195-201; d) L. Ackermann, R. Sandmann, W. F. Song, *Org. Lett.* **2011**, *13*, 1784-1786; e) N. Iranpoor, F. Panahi, *Adv. Synth. Catal.* **2014**, *356*, 3067-3073; f) S. S. Kampmann, A. N. Sobolev, G. A. Koutsantonis, S. G. Stewart, *Adv. Synth. Catal.* **2014**, *356*, 1967-1973; g) J. D. Shields, E. E. Gray, A. G. Doyle, *Org. Lett.* **2015**, *17*, 2166-2169; h) P. S. Hanley, T. P. Clark, A. L. Krasovskiy, M. S. Ober, J. P. O'Brien, T. S. Staton, *ACS Catal.* **2016**, *6*, 3515-3519.
- [84] S. G. Rull, J. F. Blandez, M. R. Fructos, T. R. Belderrain, M. C. Nicasio, *Adv. Synth. Catal.* **2015**, *357*, 907-911.
- [85] E. A. Standley, S. J. Smith, P. Müller, T. F. Jamison, *Organometallics* **2014**, *33*, 2012-2018.
- [86] F. Rataboul, A. Zapf, R. Jackstell, S. Harkal, T. Riermeier, A. Monsees, U. Dingerdissen, M. Beller, *Chem. Eur. J.* **2004**, *10*, 2983-2990.
- [87] E. Colacino, L. Villebrun, J. Martinez, F. Lamaty, *Tetrahedron* **2010**, *66*, 3730-3735.
- [88] S. G. Rull, J. F. Blandez, M. R. Fructos, T. R. Belderrain, M. C. Nicasio, *Adv. Synth. Catal.* **2015**, *357*, 907-911.
- [89] J. K. Kwon, J. H. Cho, Y.-S. Ryu, S. H. Oh, E. K. Yum, *Tetrahedron* **2011**, *67*, 4820-4825.
- [90] a) N. Miyaura, A. Suzuki, *Chem. Rev.* **1995**, *95*, 2457-2483; b) N. T. S. Phan, M. Van Der Sluys, C. W. Jones, *Adv. Synth. Catal.* **2006**, *348*, 609-679; c) R. Martin, S. L. Buchwald, *Acc. Chem. Res.* **2008**, *41*, 1461-1473; d) C. Torborg, M. Beller, *Adv. Synth. Catal.* **2009**, *351*, 3027-3043; e) G. A. Molander, B. Canturk, *Angew. Chem. Int. Ed.* **2009**, *48*, 9240-9261; f) V. F. Slagt, A. H. M. de Vries, J. G. de Vries, R. M. Kellogg, *Org. Process Res. Dev.* **2010**, *14*, 30-47; g) S. D. Roughley, A. M. Jordan, *J. Med. Chem.* **2011**, *54*, 3451-3479; h) C. C. C. J. Seechurn, M. O. Kitching, T. J. Colacot, V. Snieckus, *Angew. Chem. Int. Ed.* **2012**, *51*, 5062-5085; i) C. Valente, S. Çalimsiz, K. H. Hoi, D. Mallik, M. Sayah, M. G. Organ, *Angew. Chem. Int. Ed.* **2012**, *51*, 3314-3332; j) A. J. J. Lennox, G. C. Lloyd-Jones, *Chem. Soc. Rev.* **2014**, *43*, 412-443; k) A. S. Guram, *Org. Process Res. Dev.* **2016**, *20*, 1754-1764.

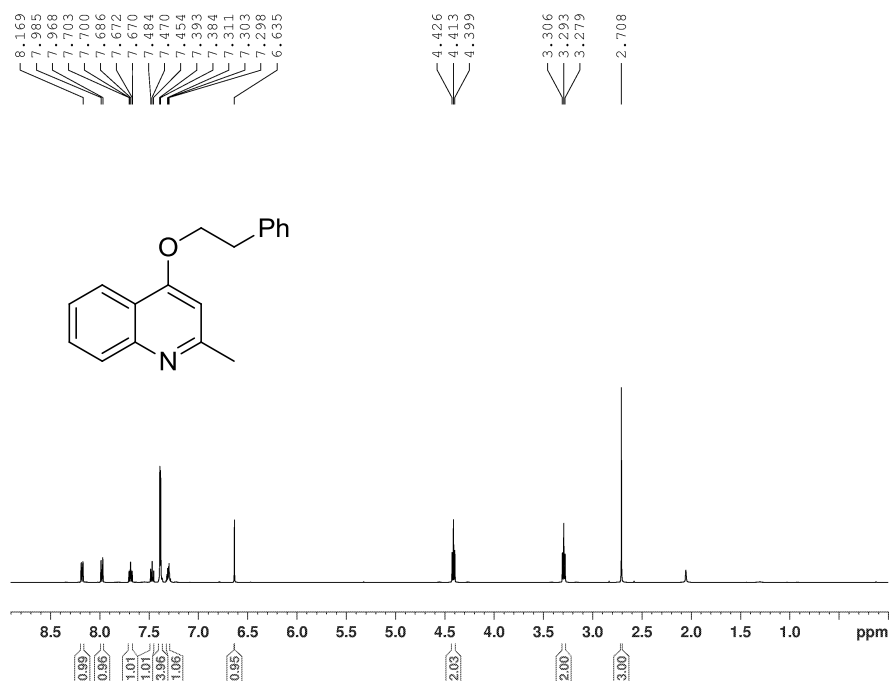
- [91] A. Suzuki, *Angew. Chem. Int. Ed.* **2011**, *50*, 6722-6737.
- [92] D. G. Brown, J. Boström, *J. Med. Chem.* **2016**, *59*, 4443-4458.
- [93] a) B.-T. Guan, Y. Wang, B.-J. Li, D.-G. Yu, Z.-J. Shi, *J. Am. Chem. Soc.* **2008**, *130*, 14468-14470; b) K. W. Quasdorf, X. Tian, N. K. Garg, *J. Am. Chem. Soc.* **2008**, *130*, 14422-14423; c) D.-G. Yu, M. Yu, B.-T. Guan, B.-J. Li, Y. Zheng, Z.-H. Wu, Z.-J. Shi, *Org. Lett.* **2009**, *11*, 3374-3377; d) K. W. Quasdorf, M. Rienner, K. V. Petrova, N. K. Garg, *J. Am. Chem. Soc.* **2009**, *131*, 17748-17749; e) K. W. Quasdorf, A. Antoft-Finch, P. Liu, A. L. Silberstein, A. Komaromi, T. Blackburn, S. D. Ramgren, K. N. Houk, V. Snieckus, N. K. Garg, *J. Am. Chem. Soc.* **2011**, *133*, 6352-6363; f) P. Leowanawat, N. Zhang, V. Percec, *J. Org. Chem.* **2012**, *77*, 1018-1025; g) P. Leowanawat, N. Zhang, M. Safi, D. J. Hoffman, M. C. Fryberger, A. George, V. Percec, *J. Org. Chem.* **2012**, *77*, 2885-2892; h) Q. Chen, X.-H. Fan, L.-P. Zhang, L.-M. Yang, *RSC Advances* **2014**, *4*, 53885-53890; i) X. Chen, H. Ke, G. Zou, *ACS Catalysis* **2014**, *4*, 379-385; j) S. Handa, E. D. Slack, B. H. Lipshutz, *Angew. Chem. Int. Ed.* **2015**, *54*, 11994-11998; k) L. Guo, X. Liu, C. Baumann, M. Rueping, *Angew. Chem. Int. Ed.* **2016**, *55*, 15415-15419; l) J. Malineni, R. L. Jezorek, N. Zhang, V. Percec, *Synthesis* **2016**, *48*, 2795-2807; m) N. A. Weires, E. L. Baker, N. K. Garg, *Nat. Chem.* **2016**, *8*, 75-79.
- [94] P. L. Beaulieu, M. Bos, M. G. Cordingley, C. Chabot, G. Fazal, M. Garneau, J. R. Gillard, E. Jolicoeur, S. LaPlante, G. McKercher, M. Poirier, M. A. Poupart, Y. S. Tsantrizos, J. M. Duan, G. Kukolj, *J. Med. Chem.* **2012**, *55*, 7650-7666.
- [95] P. A. Cox, A. G. Leach, A. D. Campbell, G. C. Lloyd-Jones, *J. Am. Chem. Soc.* **2016**, *138*, 9145-9157.
- [96] S. Ge, J. F. Hartwig, *Angew. Chem. Int. Ed.* **2012**, *51*, 12837-12841.
- [97] N. Hazari, P. R. Melvin, M. M. Beromi, *Nat. Rev. Chem.* **2017**, *1*, 0025.
- [98] L. M. Guard, M. Mohadjer Beromi, G. W. Brudvig, N. Hazari, D. J. Vinyard, *Angew. Chem. Int. Ed.* **2015**, *54*, 13352-13356.
- [99] S. D. Ramgren, L. Hie, Y. Ye, N. K. Garg, *Org. Lett.* **2013**, *15*, 3950-3953.
- [100] S. Ando, H. Matsunaga, T. Ishizuka, *J. Org. Chem.* **2017**, *82*, 1266-1272.
- [101] R. S. Sawatzky, M. J. Ferguson, M. Stradiotto, *Synlett* **2017**, *28*, 1586-1591.
- [102] a) B. P. Carrow, J. F. Hartwig, *J. Am. Chem. Soc.* **2011**, *133*, 2116-2119; b) A. H. Christian, P. Müller, S. Monfette, *Organometallics* **2014**, *33*, 2134-2137.
- [103] E. A. Standley, S. J. Smith, P. Muller, T. F. Jamison, *Organometallics* **2014**, *33*, 2012-2018.

- [104] C. H. Basch, J. Liao, J. Xu, J. J. Piane, M. P. Watson, *J. Am. Chem. Soc.* **2017**, *139*, 5313-5316.
- [105] S. Lou, G. C. Fu, *Adv. Synth. Catal.* **2010**, *352*, 2081-2084.
- [106] Y. Yang, N. J. Oldenhuis, S. L. Buchwald, *Angew. Chem. Int. Ed.* **2013**, *52*, 615-619.
- [107] M. Jacubert, O. Provot, J. F. Peyrat, A. Hamze, J. D. Brion, M. Alami, *Tetrahedron* **2010**, *66*, 3775-3787.
- [108] S. H. Kim, R. D. Rieke, *Tetrahedron* **2010**, *66*, 3135-3146.
- [109] D. M. Knapp, E. P. Gillis, M. D. Burke, *J. Am. Chem. Soc.* **2009**, *131*, 6961-6963.
- [110] P. Leowanawat, A.-M. Resmerita, C. Moldoveanu, C. Liu, N. Zhang, D. A. Wilson, L. M. Hoang, B. M. Rosen, V. Percec, *J. Org. Chem* **2010**, *75*, 7822-7828.

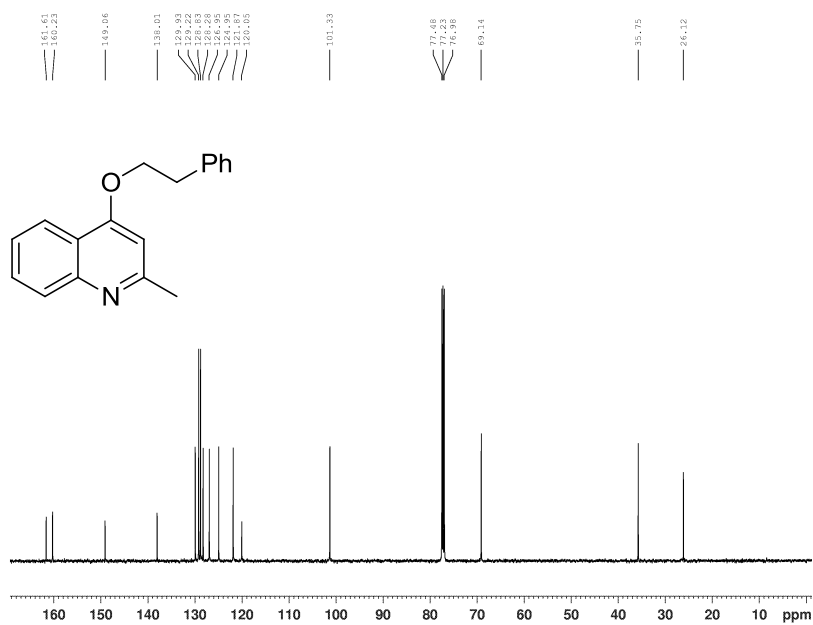
# Appendix

## Chapter 2 Characterization Data

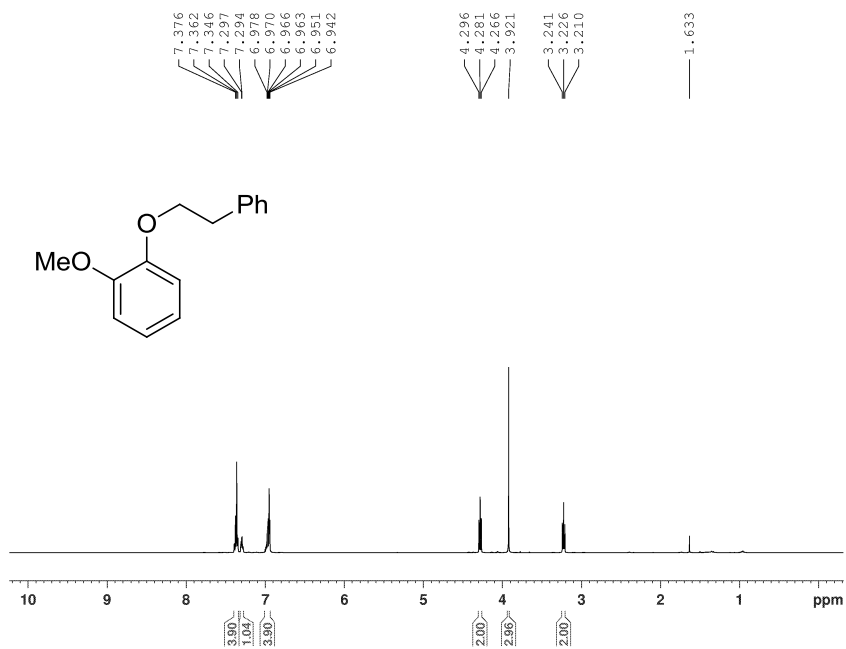
$^1\text{H}$  NMR of **2-2a**, ( $\text{CDCl}_3$ , 500.1 MHz)



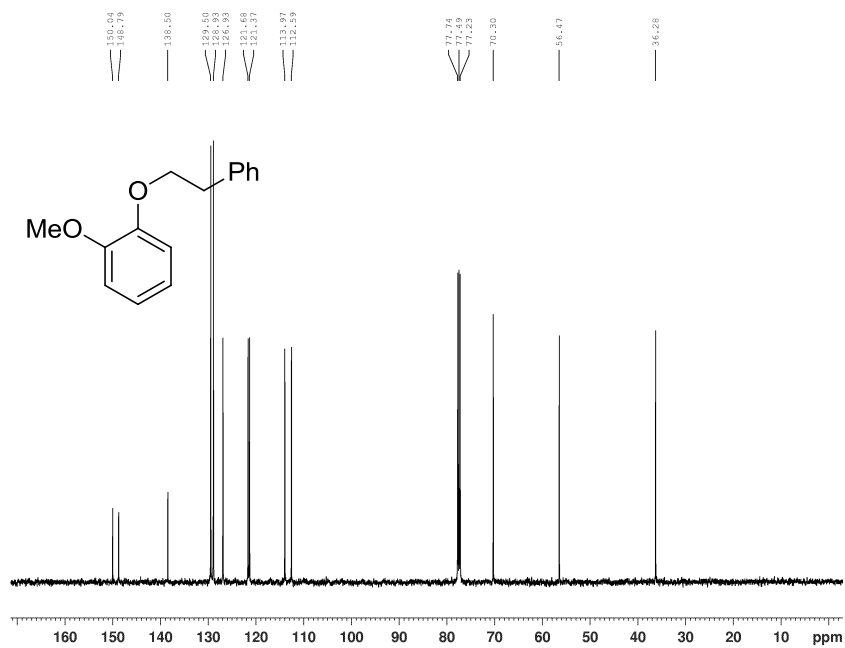
$^{13}\text{C}\{^1\text{H}\}$  NMR of **2-2a**, ( $\text{CDCl}_3$ , 125.8 MHz)



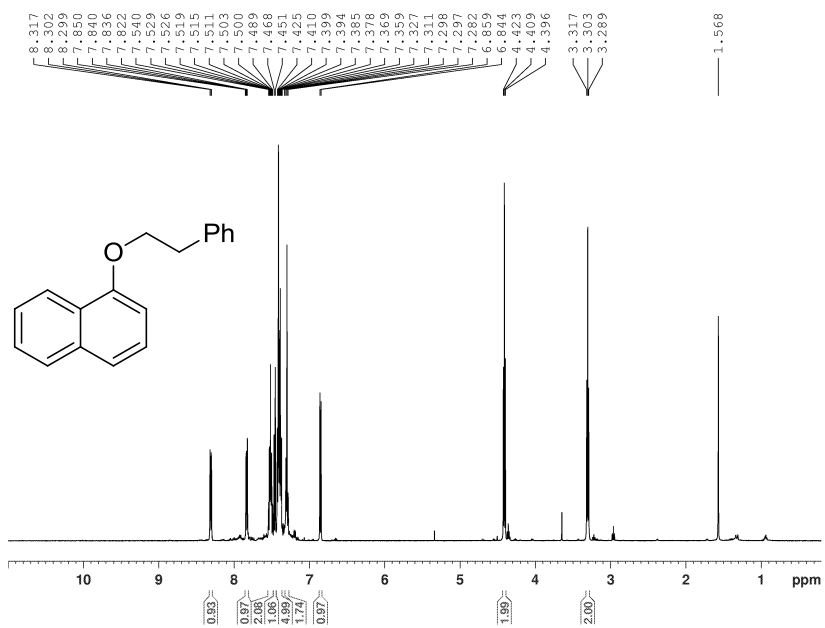
$^1\text{H}$  NMR of **2-2b**, ( $\text{CDCl}_3$ , 500.1 MHz)



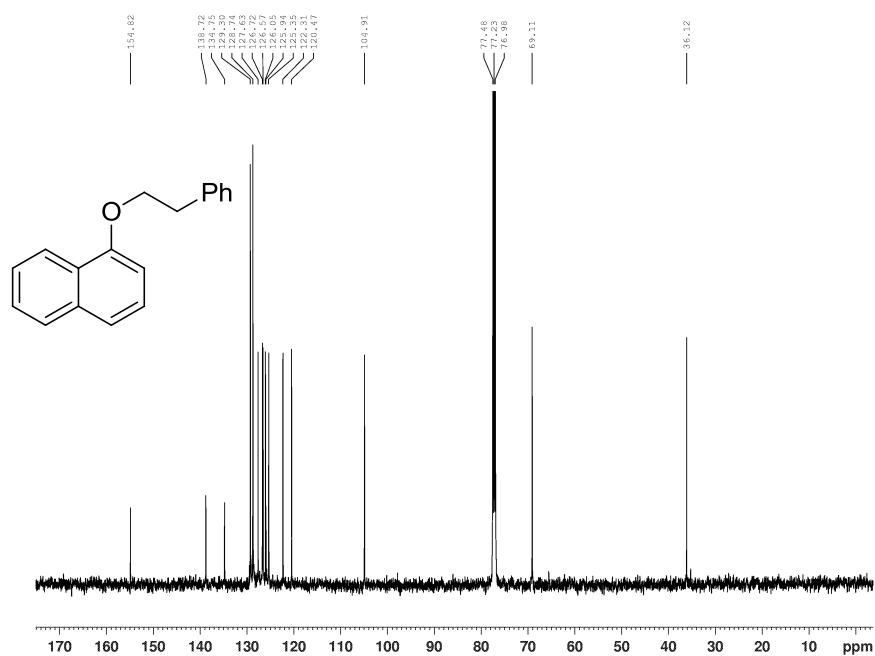
$^{13}\text{C}\{^1\text{H}\}$  NMR of **2-2b**, ( $\text{CDCl}_3$ , 125.8 MHz)



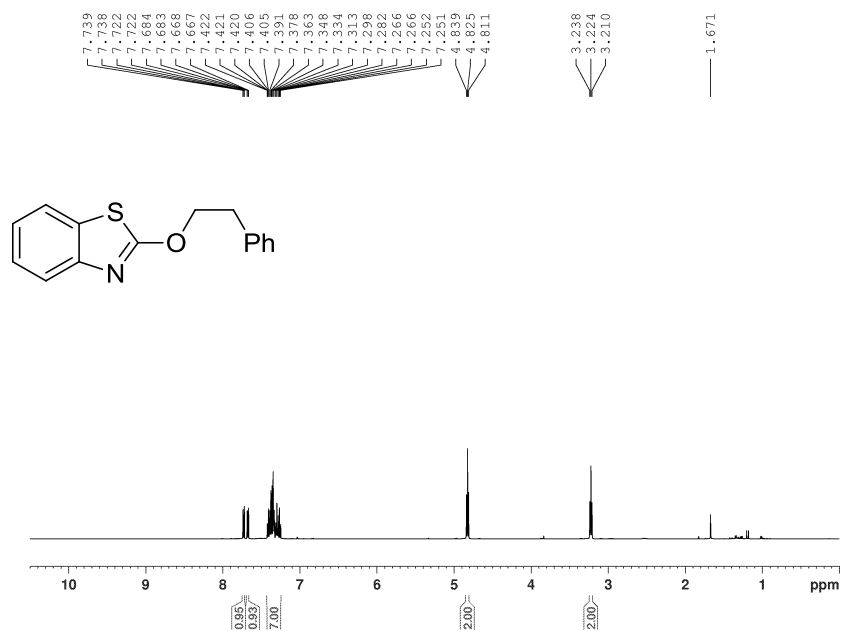
$^1\text{H}$  NMR of **2-2c**, ( $\text{CDCl}_3$ , 500.1 MHz)



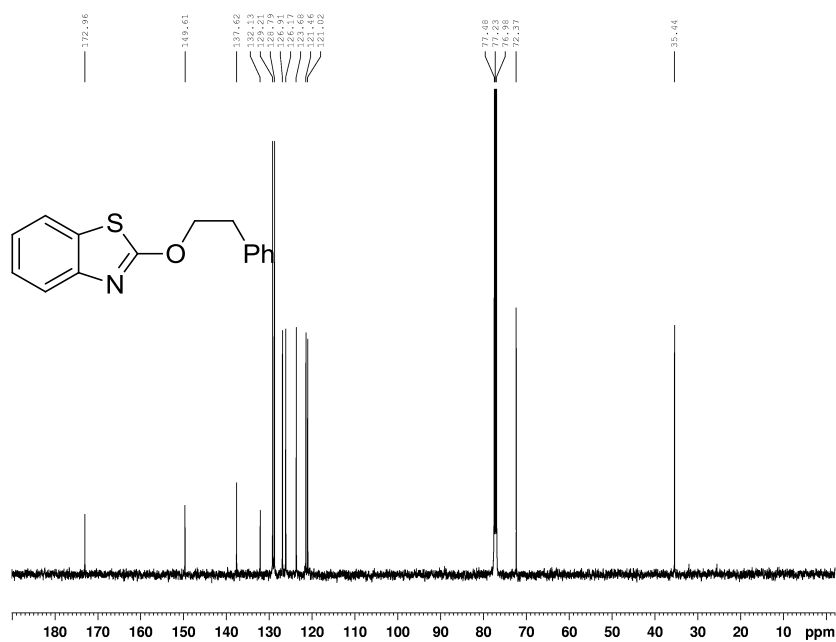
$^{13}\text{C}\{^1\text{H}\}$  NMR of **2-2c**, ( $\text{CDCl}_3$ , 125.8 MHz)



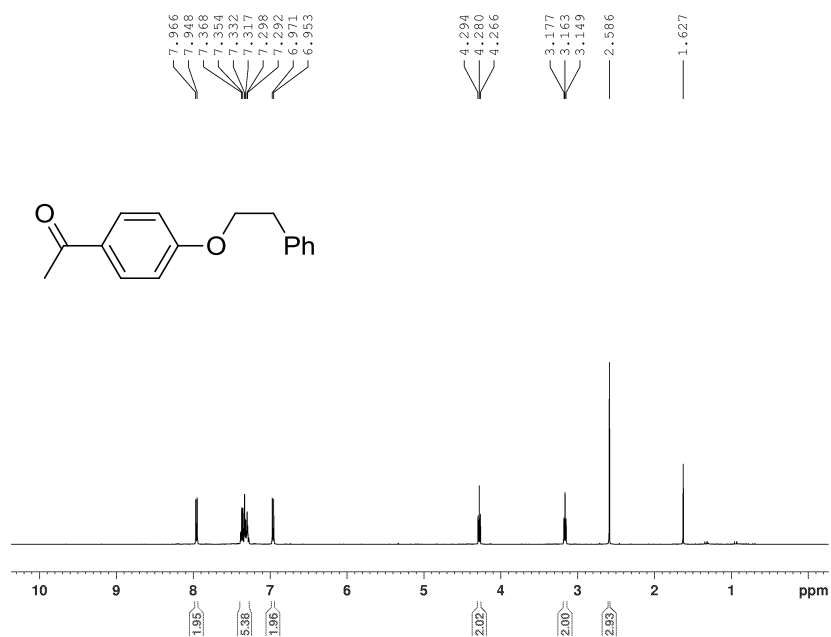
$^1\text{H}$  NMR of **2-2j**, ( $\text{CDCl}_3$ , 500.1 MHz)



$^{13}\text{C}\{^1\text{H}\}$  NMR of **2-2j**, ( $\text{CDCl}_3$ , 125.8 MHz)

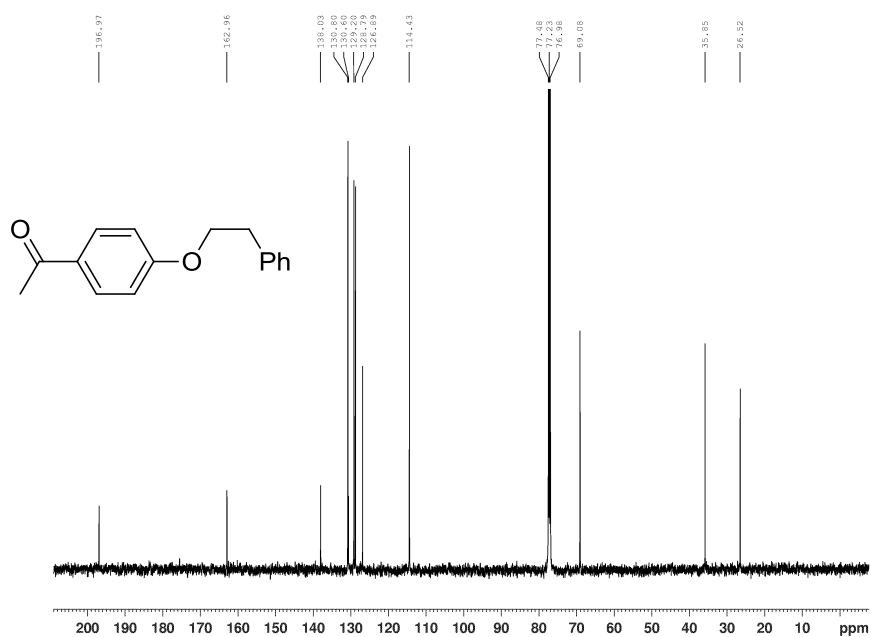


$^1\text{H}$  NMR of **2-2j**, ( $\text{CDCl}_3$ , 500.1 MHz)

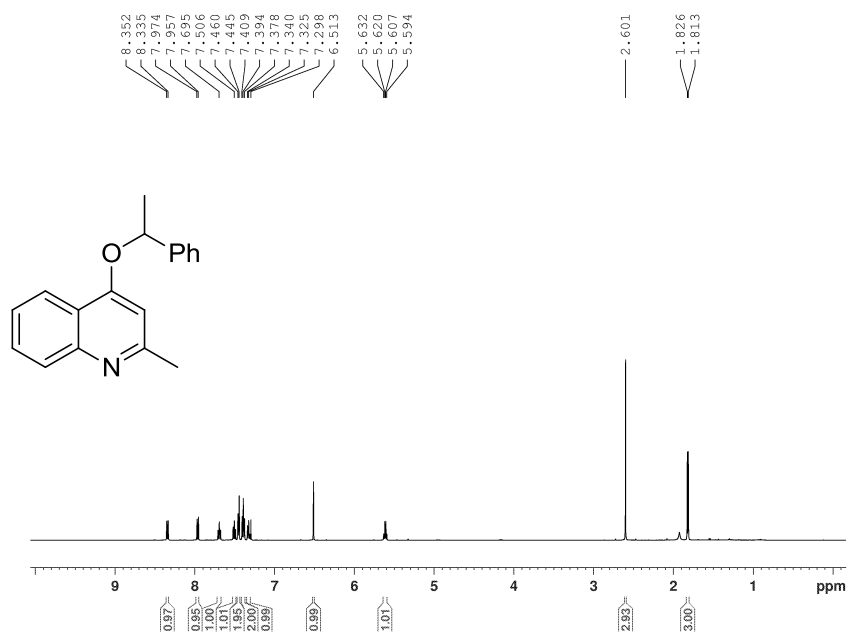




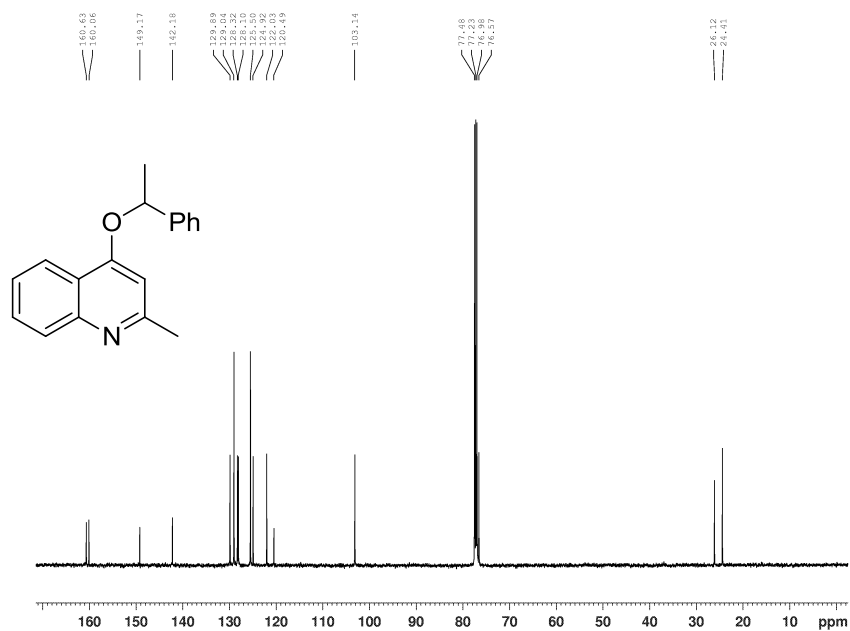
$^{13}\text{C}\{^1\text{H}\}$  NMR of **2-2j**, ( $\text{CDCl}_3$ , 125.8 MHz)



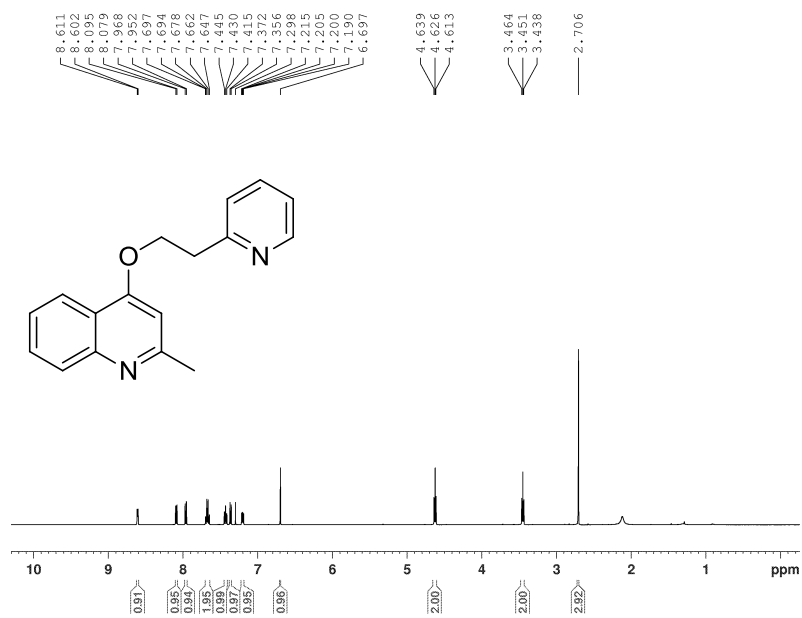
$^1\text{H}$  NMR of **2-2s**, ( $\text{CDCl}_3$ , 500.1 MHz)



$^{13}\text{C}\{^1\text{H}\}$  NMR of **2-2s**, ( $\text{CDCl}_3$ , 125.8 MHz)



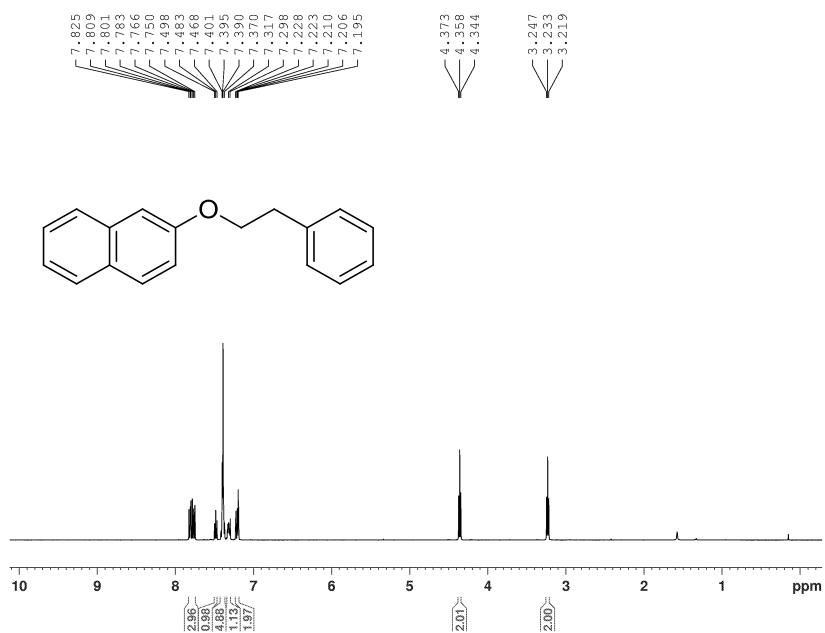
$^1\text{H}$  NMR of **2-2x**, ( $\text{CDCl}_3$ , 500.1 MHz)



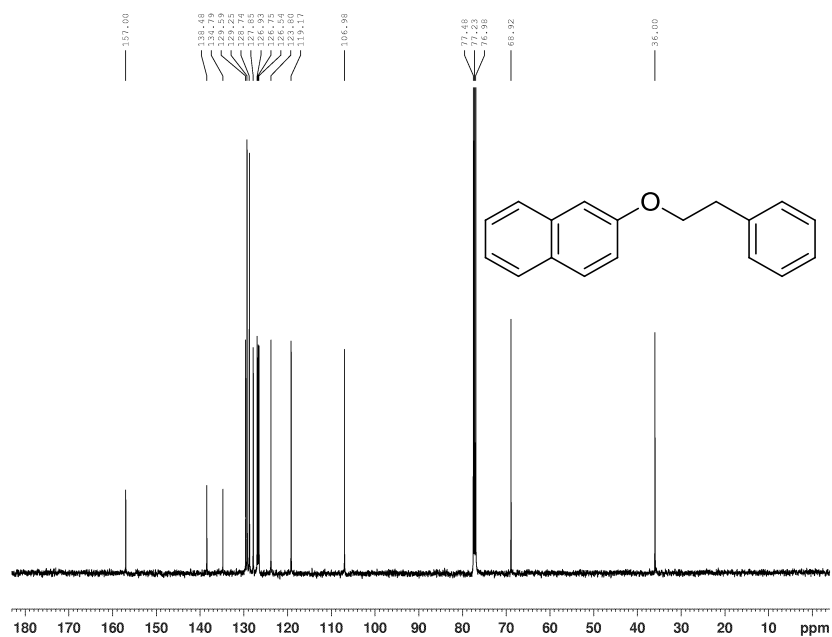
$^{13}\text{C}\{^1\text{H}\}$  NMR of **2-2x**, ( $\text{CDCl}_3$ , 125.8 MHz)



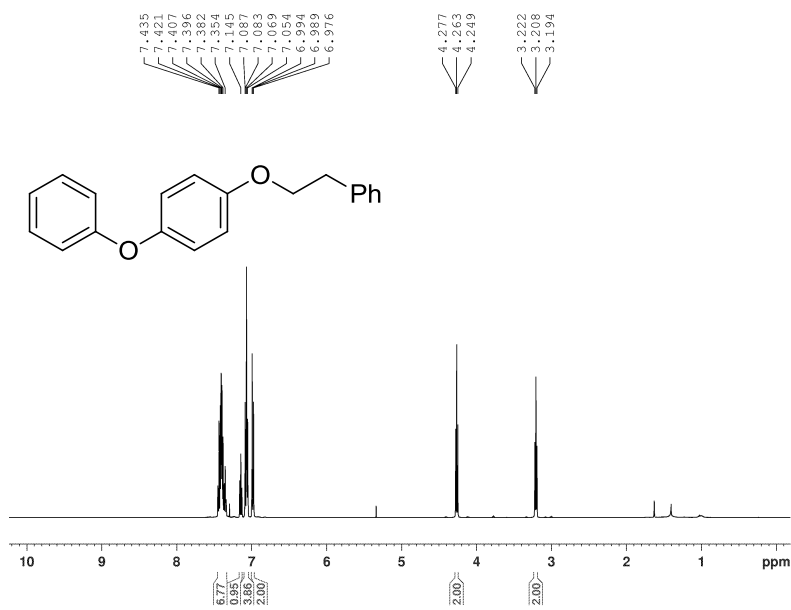
$^1\text{H}$  NMR of **2-2aa**, ( $\text{CDCl}_3$ , 500.1 MHz)



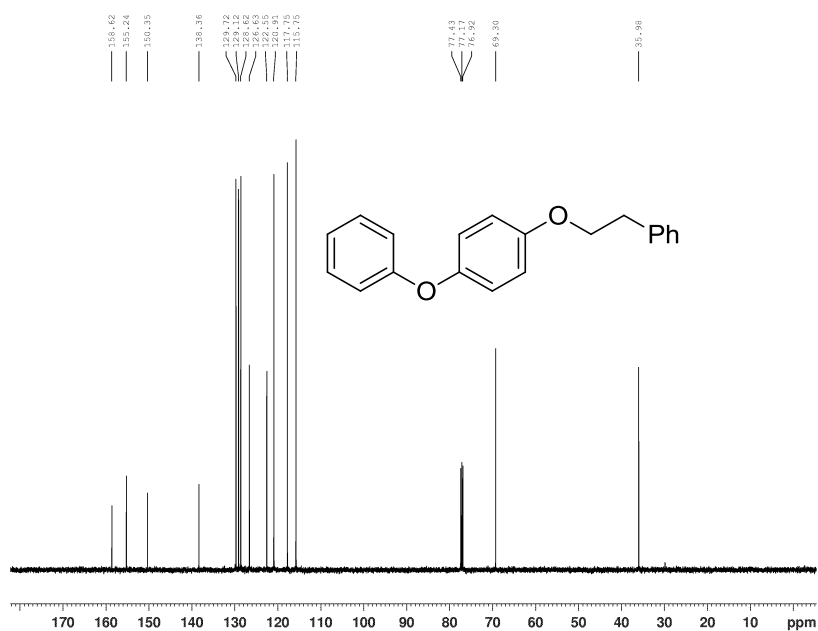
$^{13}\text{C}\{^1\text{H}\}$  NMR of **2-2a**, ( $\text{CDCl}_3$ , 125.8 MHz)



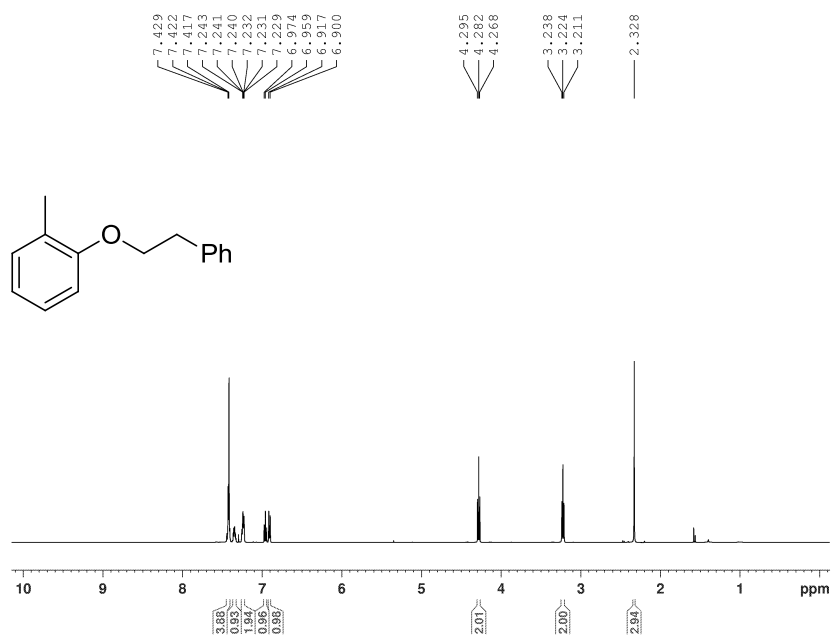
$^1\text{H}$  NMR of **2-2ab**, ( $\text{CDCl}_3$ , 500.1 MHz)



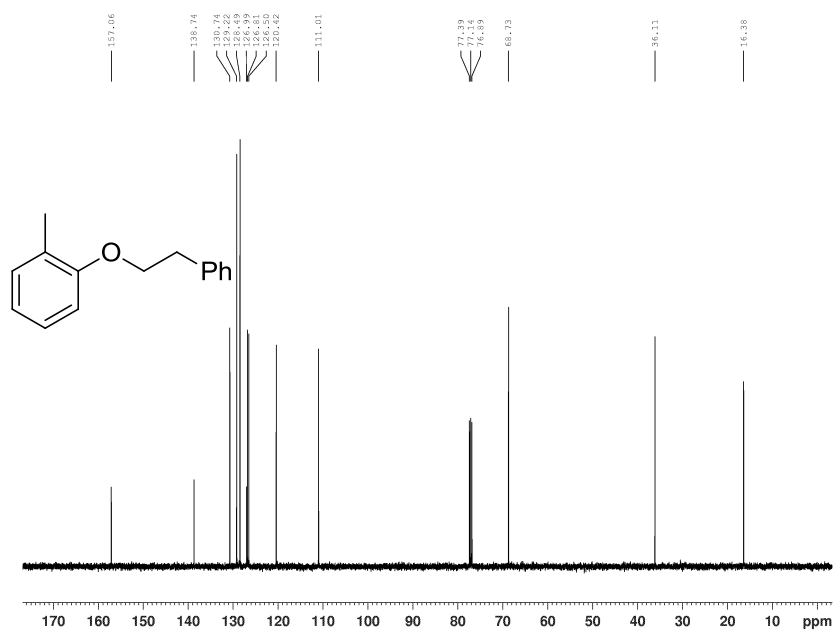
$^{13}\text{C}\{^1\text{H}\}$  NMR of **2-2b**, ( $\text{CDCl}_3$ , 125.8 MHz)



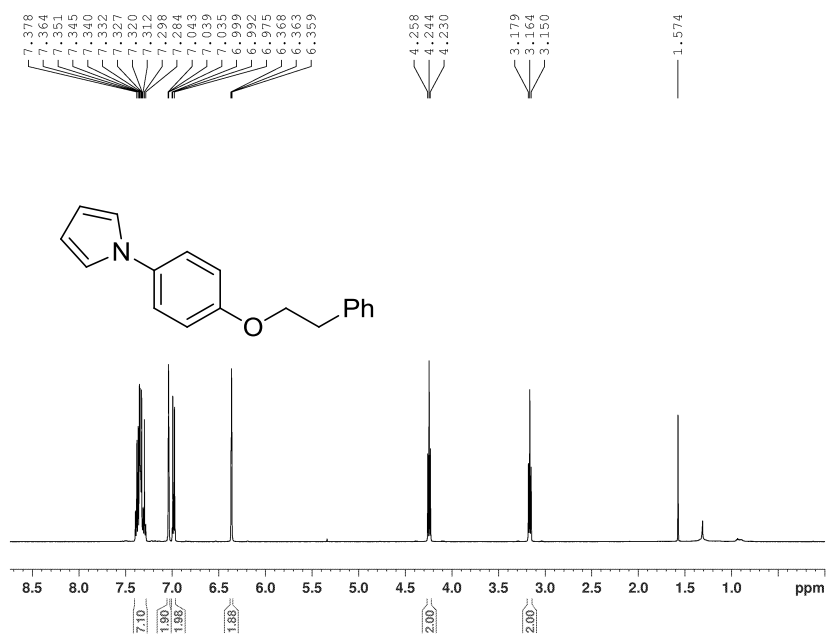
$^1\text{H}$  NMR of **2-2ac**, ( $\text{CDCl}_3$ , 500.1 MHz)



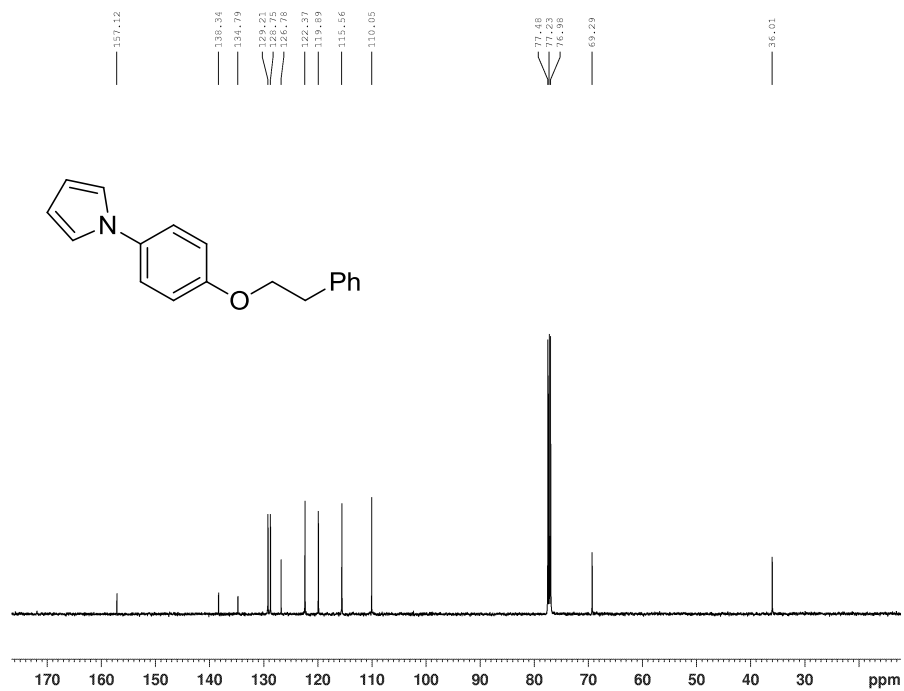
$^{13}\text{C}\{^1\text{H}\}$  NMR of **2-2c**, ( $\text{CDCl}_3$ , 125.8 MHz)



$^1\text{H}$  NMR of **2-2ad**, ( $\text{CDCl}_3$ , 500.1 MHz)

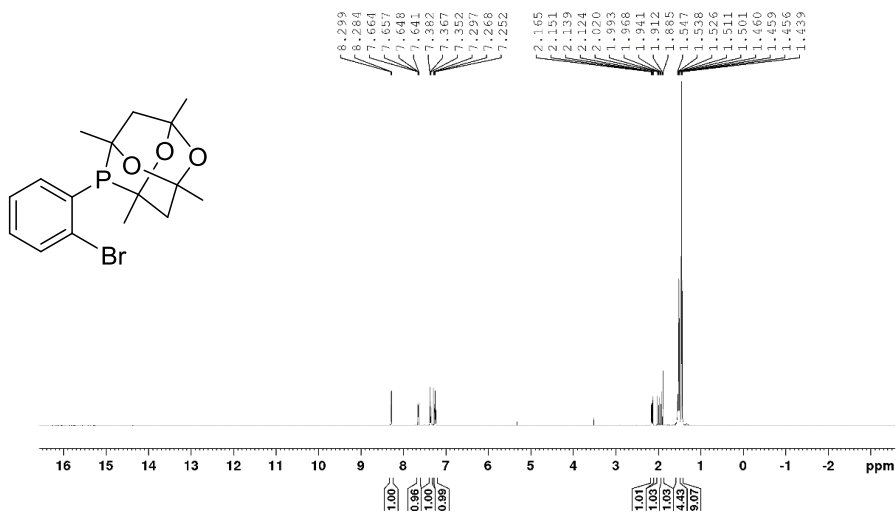


$^{13}\text{C}\{^1\text{H}\}$  NMR of **2-2d**, ( $\text{CDCl}_3$ , 125.8 MHz)

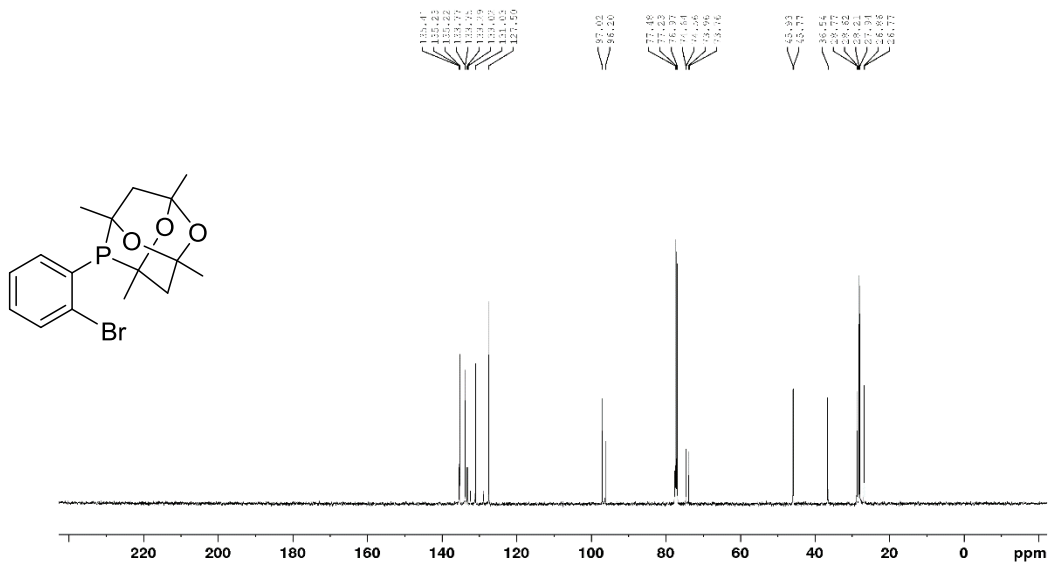


## Chapter 3 Characterization Data

### $^1\text{H}$ NMR Spectrum of **A**, ( $\text{CDCl}_3$ , 500.1 MHz)

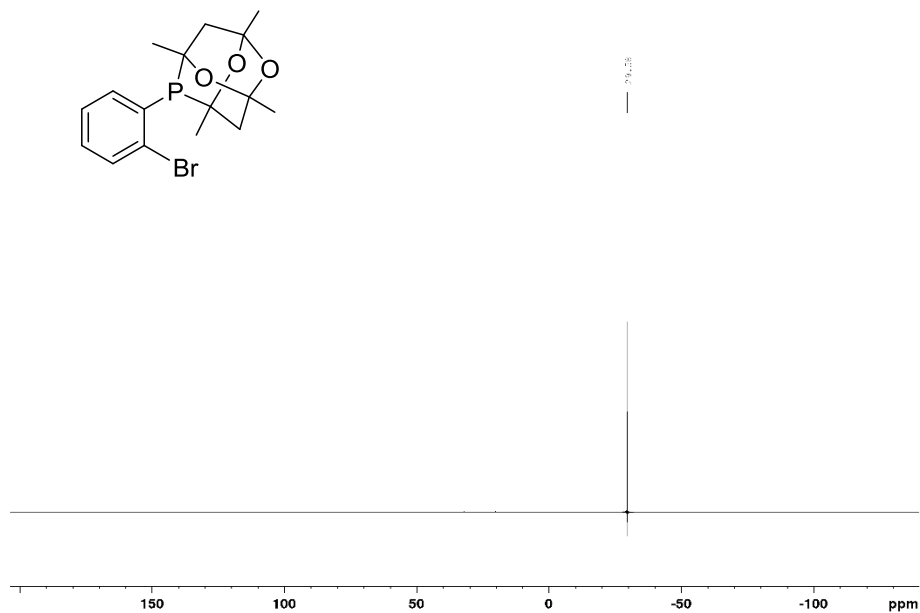


### $^{13}\text{C}\{^1\text{H}\}$ NMR Spectrum of **A**, ( $\text{CDCl}_3$ , 125.8 MHz)

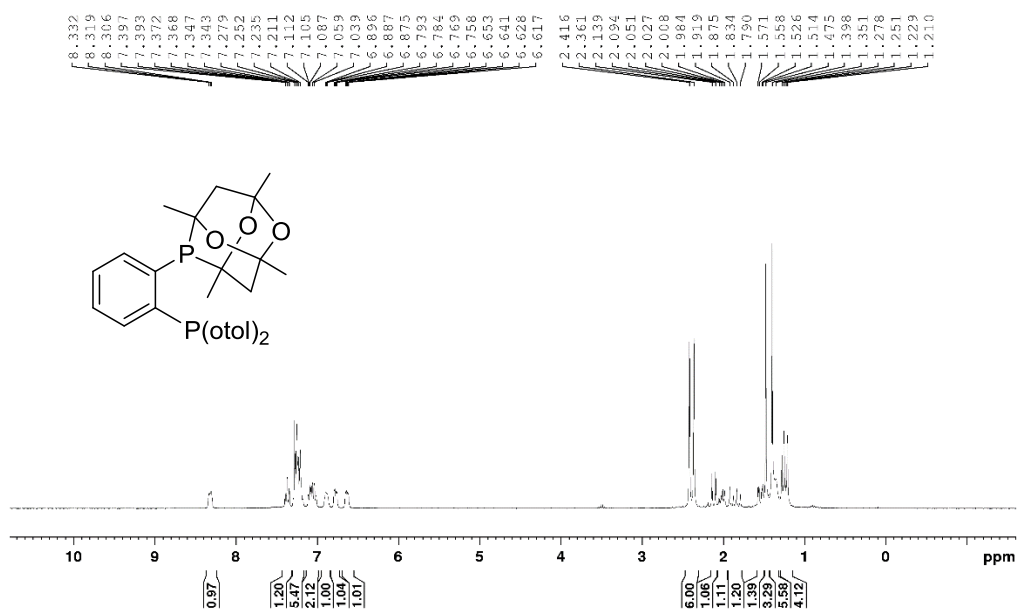




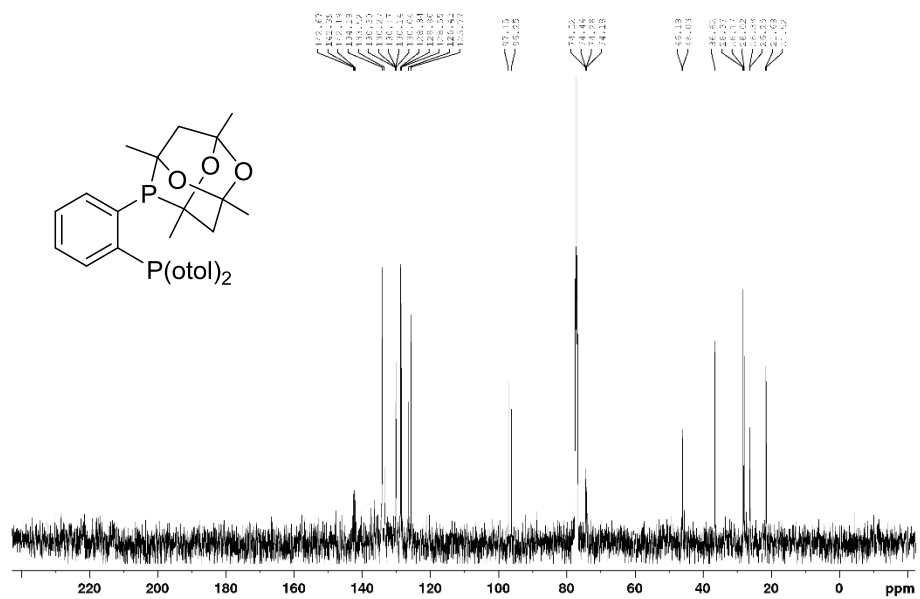
$^{31}\text{P}\{^1\text{H}\}$  NMR Spectrum of **A**, ( $\text{CDCl}_3$ , 202.5 MHz)



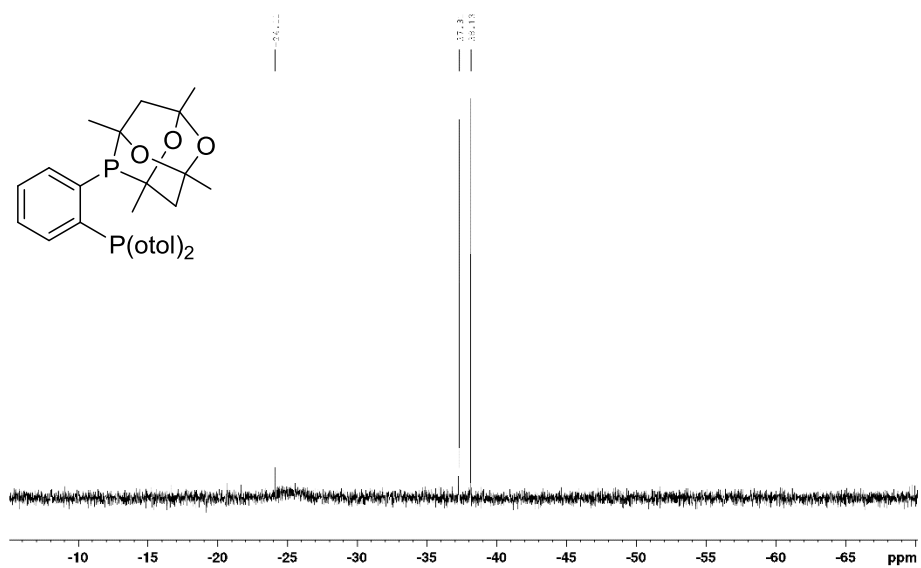
$^1\text{H}$  NMR Spectrum of **L3-17**, ( $\text{CDCl}_3$ , 300.1 MHz)



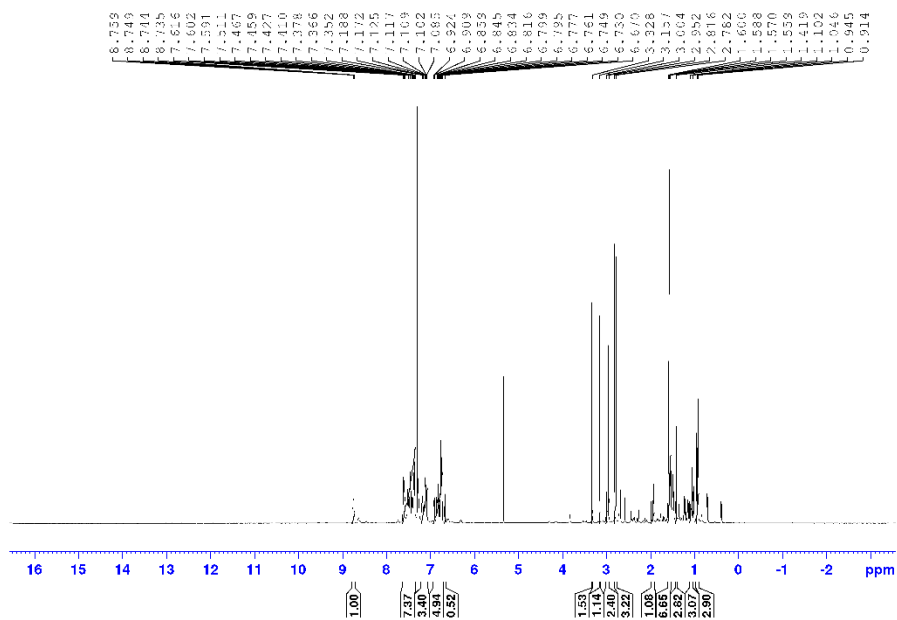
$^{13}\text{C}\{^1\text{H}\}$  NMR Spectrum of **L3-17**, ( $\text{CDCl}_3$ , 125.8 MHz)



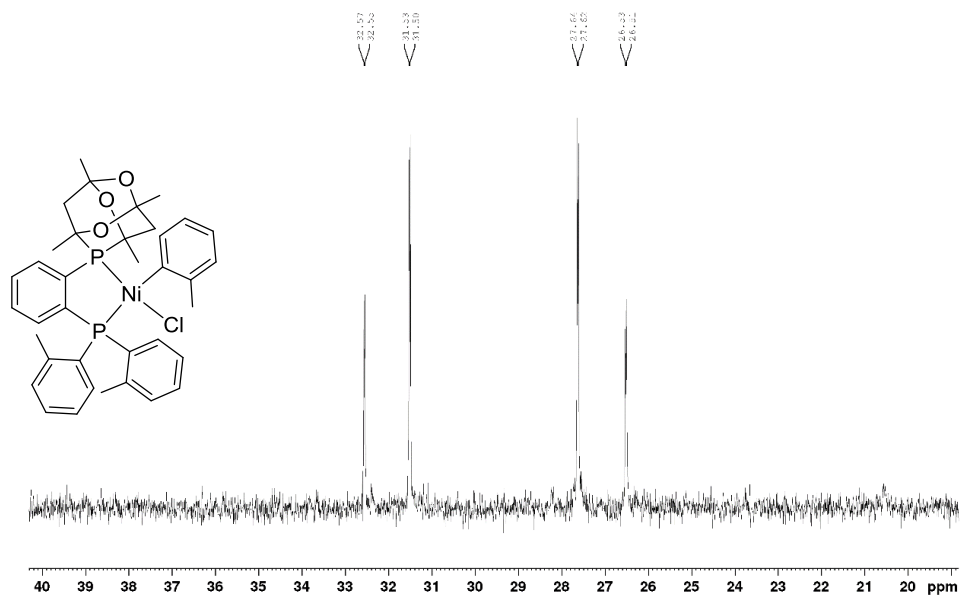
$^{31}\text{P}\{^1\text{H}\}$  NMR Spectrum of **L3-17**, ( $\text{CDCl}_3$ , 202.5 MHz)



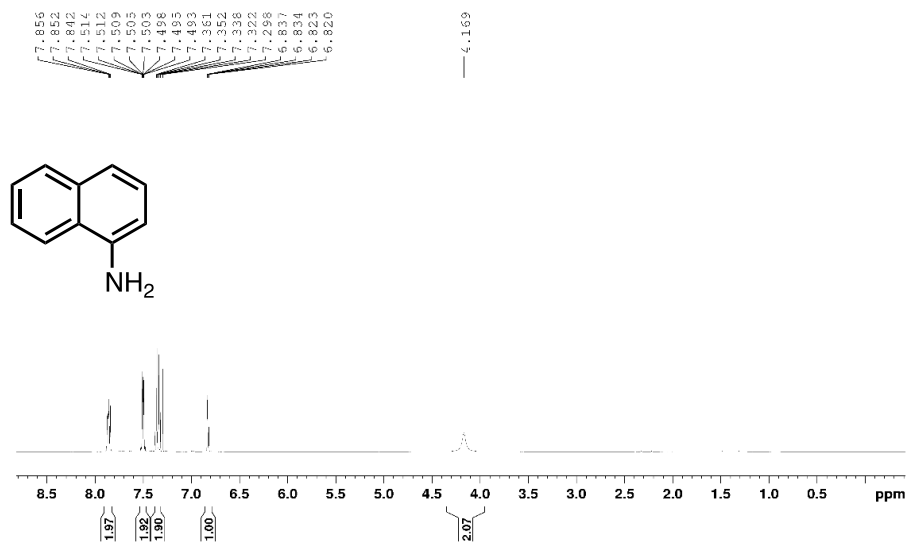
$^1\text{H}$  NMR Spectrum of **C3-4**, ( $\text{CDCl}_3$ , 500.1 MHz)



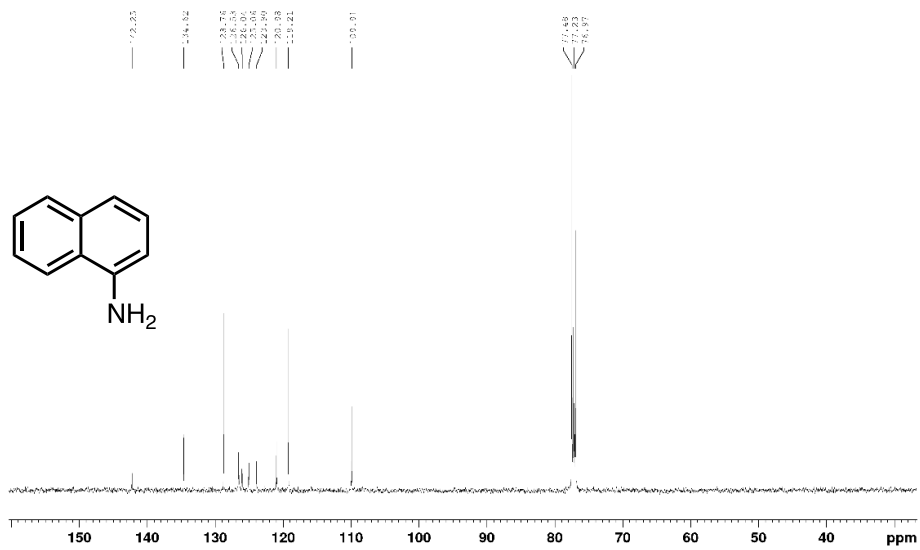
$^{31}\text{P}\{^1\text{H}\}$  NMR Spectrum of **C3-4**, ( $\text{CDCl}_3$ , 202.5 MHz)



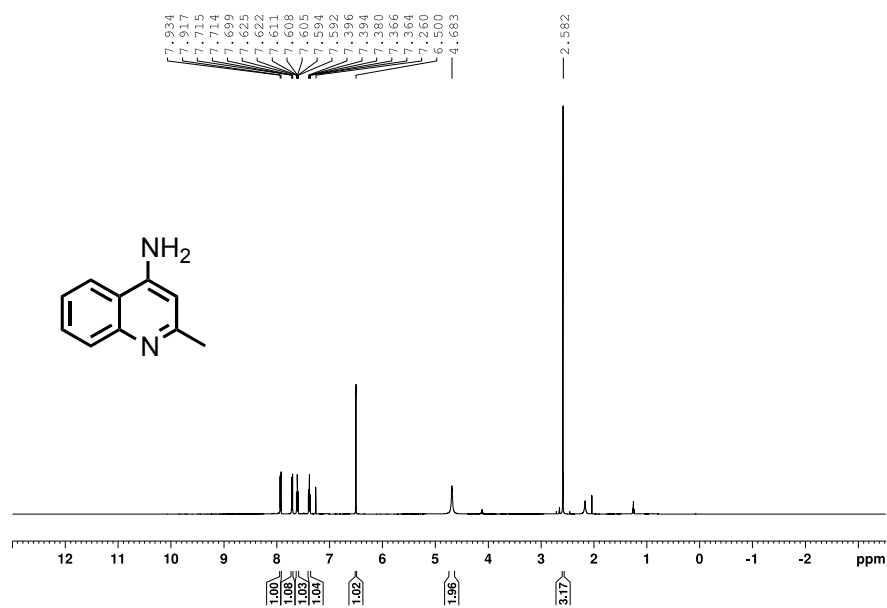
$^1\text{H}$  NMR Spectrum of Naphthalen-1-amine, **3-3a** ( $\text{CDCl}_3$ , 500.1 MHz)



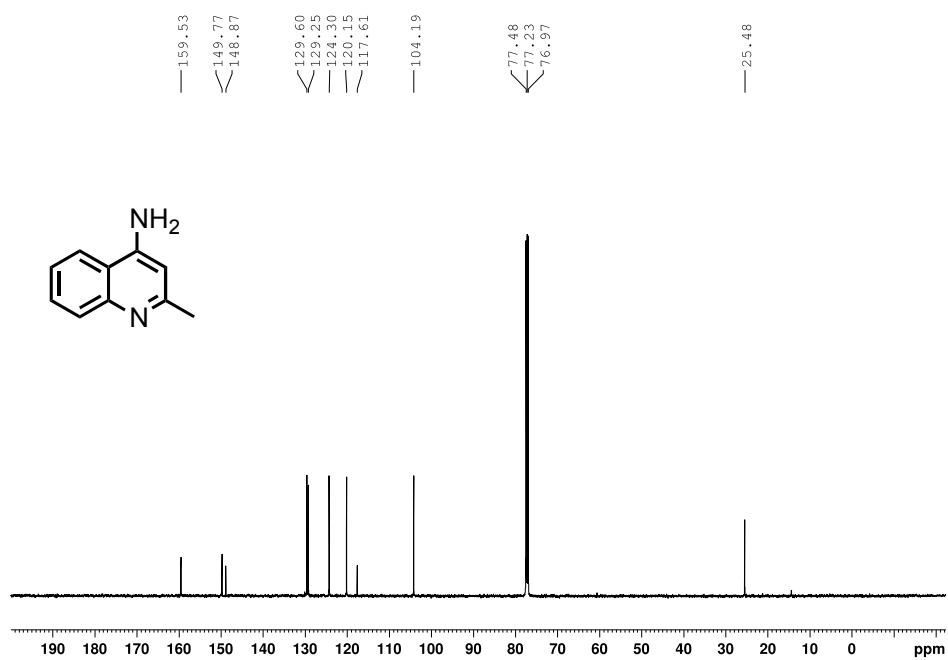
$^{13}\text{C}\{^1\text{H}\}$  NMR Spectrum of Naphthalen-1-amine, **3-3a** ( $\text{CDCl}_3$ , 500 MHz)



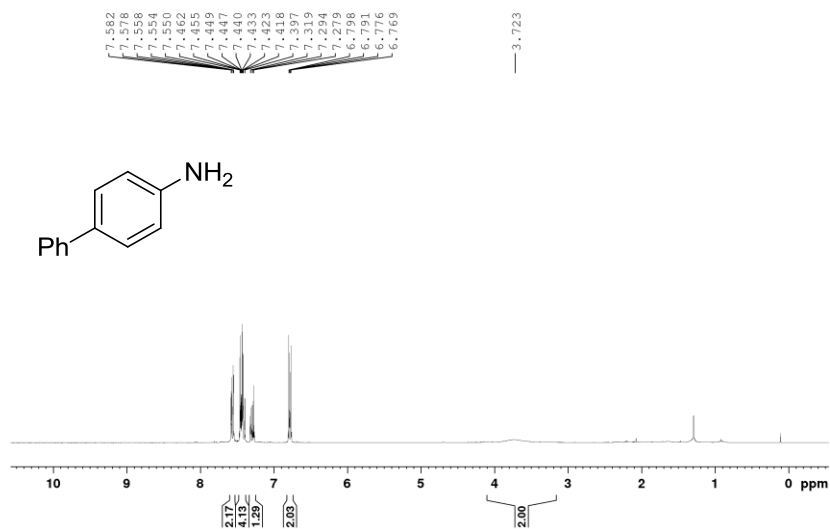
$^1\text{H}$  NMR Spectrum of 4-aminoquinaldine, **3-3b** ( $\text{CDCl}_3$ , 500.1 MHz)



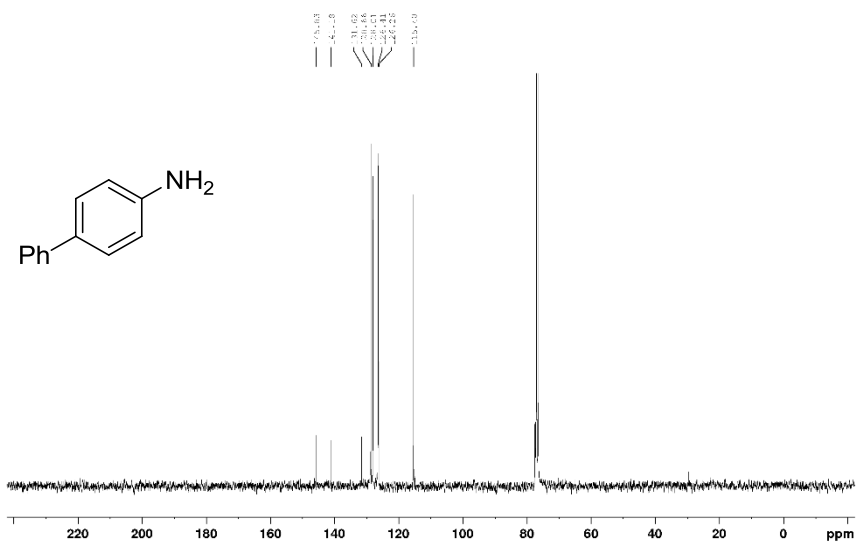
$^{13}\text{C}\{^1\text{H}\}$  NMR Spectrum of 4-aminoquinaldine, **3-3b** ( $\text{CDCl}_3$ , 125.8 MHz)



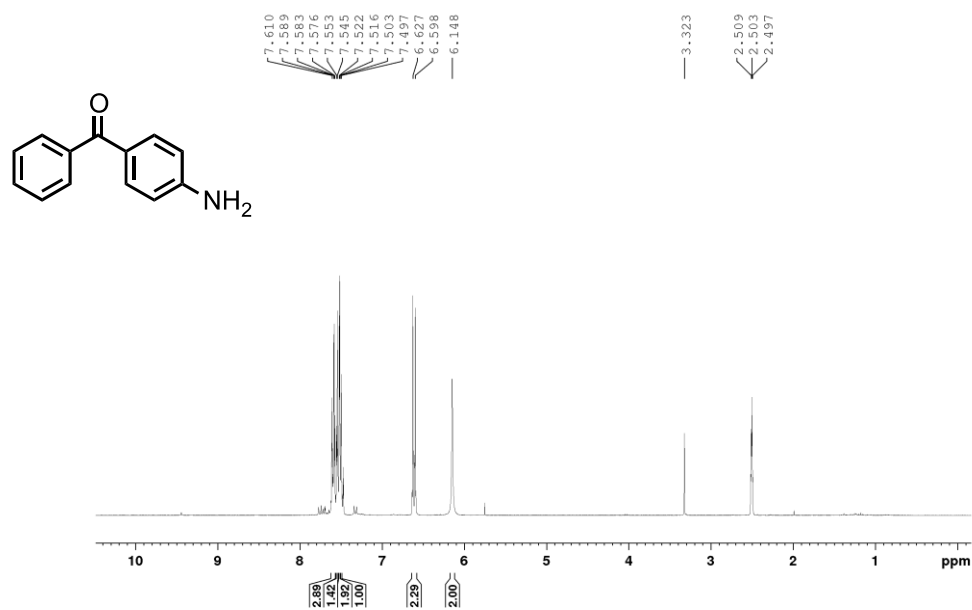
<sup>1</sup>H NMR Spectrum of 4-phenylaniline, **3-3c** (CDCl<sub>3</sub>, 300.1 MHz)



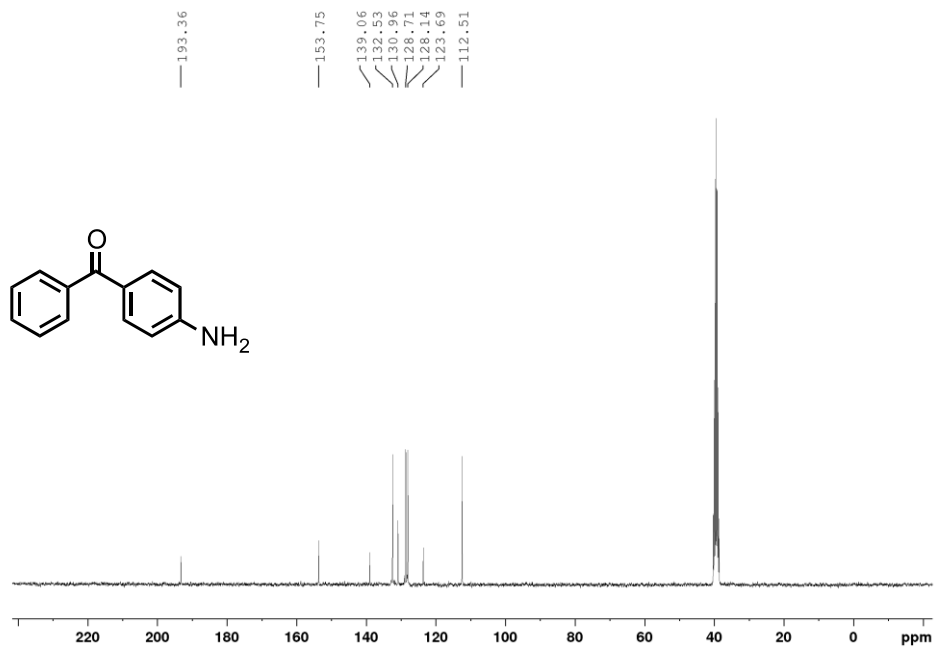
<sup>13</sup>C NMR Spectrum of 4-phenylaniline, **3-3c** (CDCl<sub>3</sub>, 75.5 MHz)



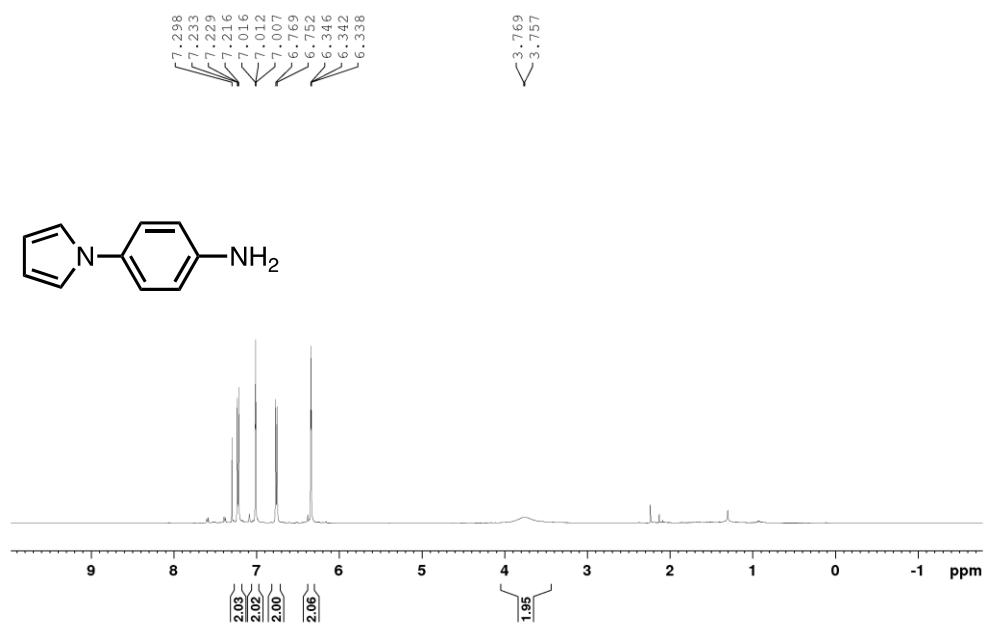
$^1\text{H}$  NMR Spectrum of 4-aminobenzophenone, **3-3d** ( $\text{CDCl}_3$ , 300.1 MHz)



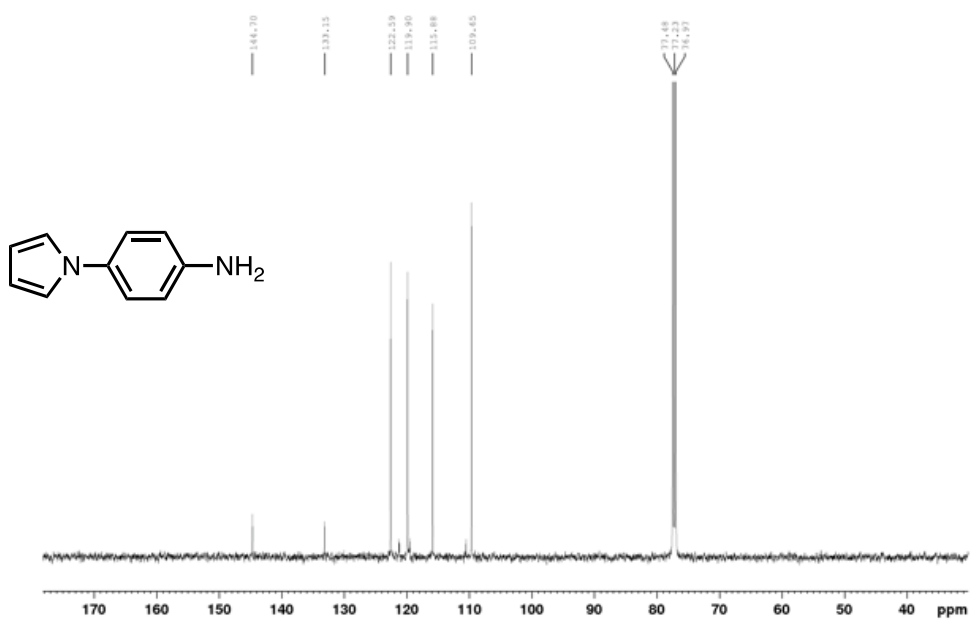
$^{13}\text{C}\{^1\text{H}\}$  NMR Spectrum of 4-aminobenzophenone, **3-3d** ( $\text{CDCl}_3$ , 75.4 MHz)



<sup>1</sup>H NMR Spectrum of 4-(1H-pyrrol-1-yl)aniline, **3-3e** (CDCl<sub>3</sub>, 500.1 MHz)

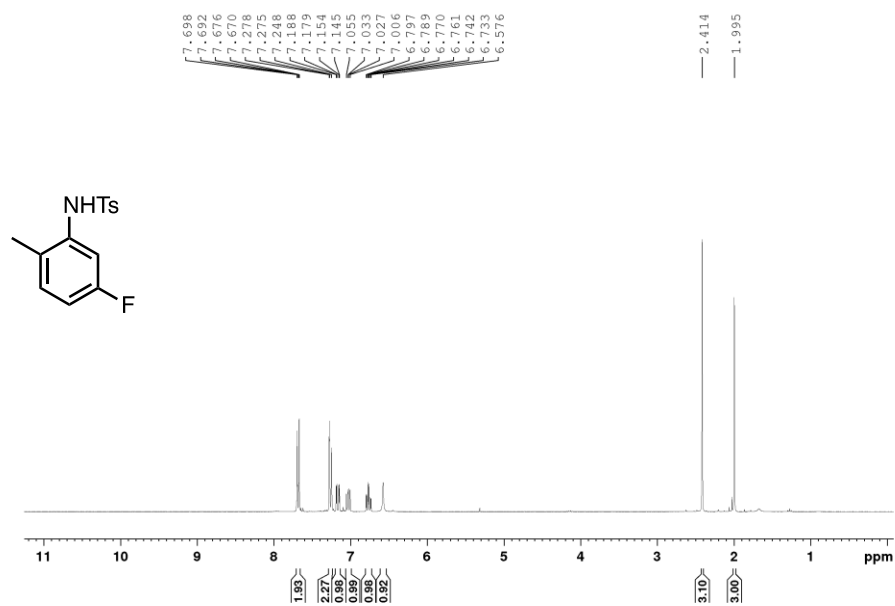


<sup>13</sup>C NMR Spectrum of 4-(1H-pyrrol-1-yl)aniline, **3-3e** (CDCl<sub>3</sub>, 125.8 MHz)

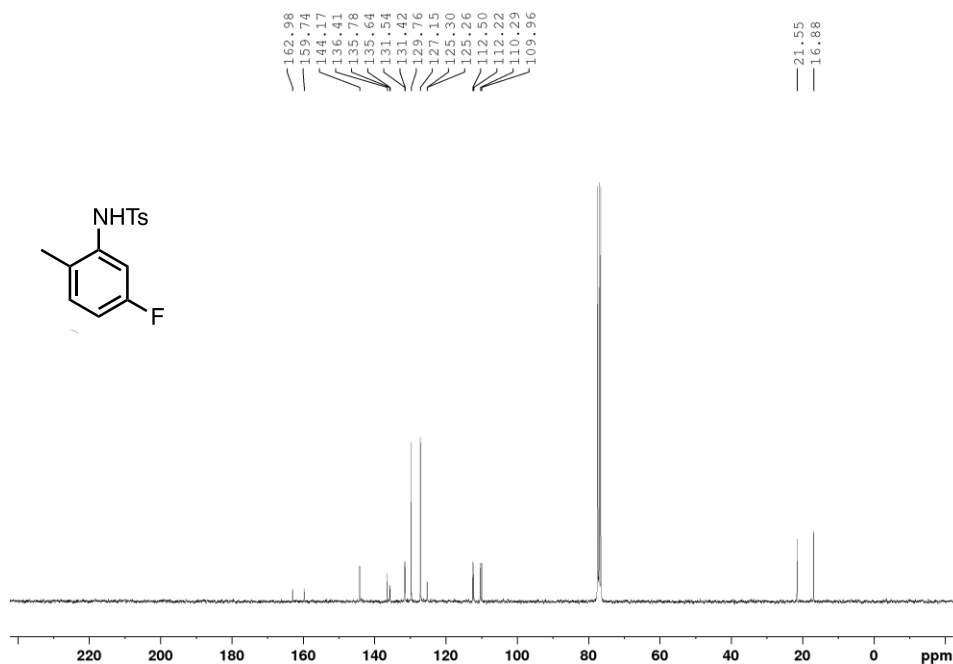




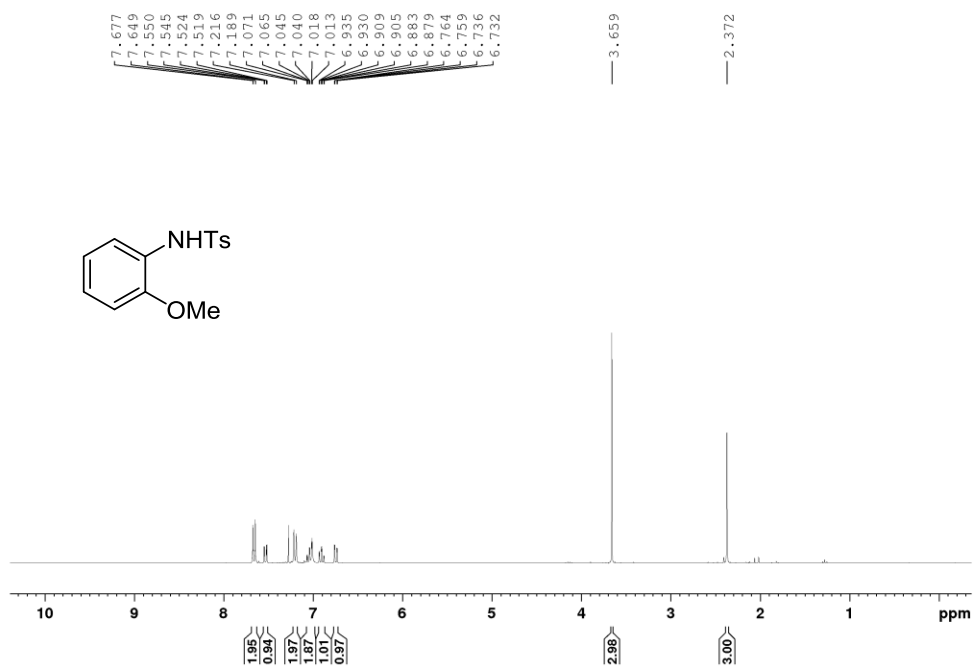
<sup>1</sup>H NMR Spectrum of N-(5-fluoro-2-methylphenyl)-4-methylbenzenesulfonamide, **3-3f**  
(CDCl<sub>3</sub>, 300.1 MHz)



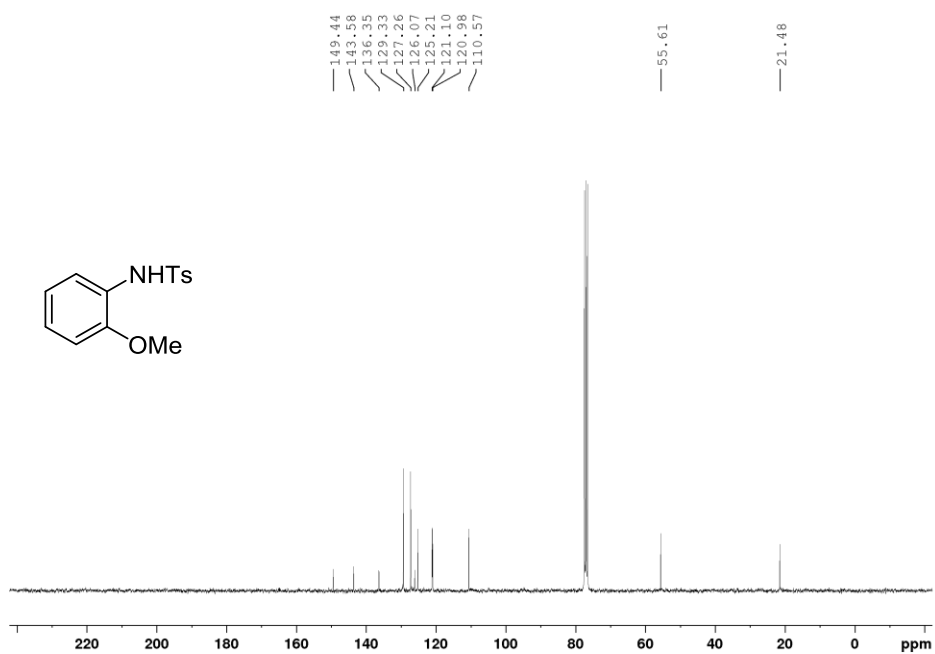
<sup>13</sup>C{<sup>1</sup>H} NMR Spectrum of N-(5-fluoro-2-methylphenyl)-4-methylbenzenesulfonamide, **3-3f**  
(CDCl<sub>3</sub>, 75.5 MHz)



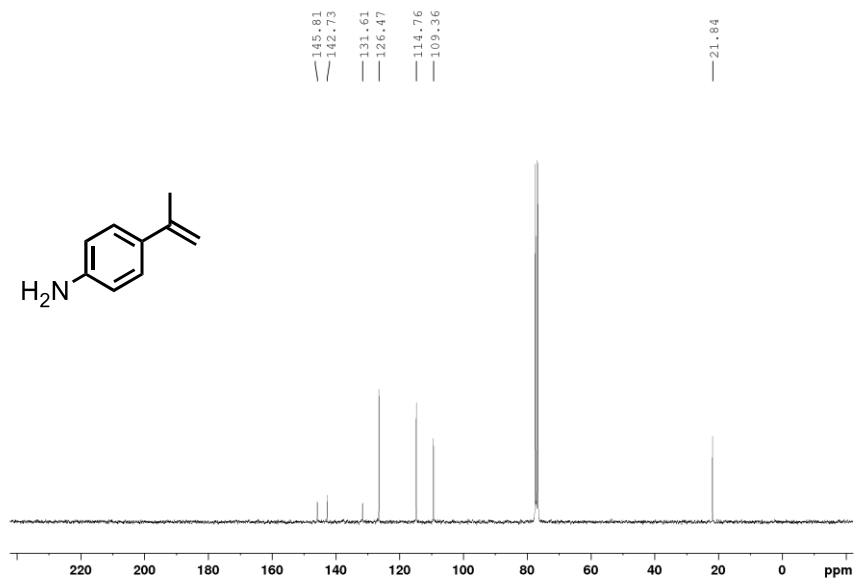
$^1\text{H}$  NMR Spectrum of N-(2-methoxyphenyl)-4-methylbenzenesulfonamide, **3-3g** ( $\text{CDCl}_3$ , 300.1 MHz)



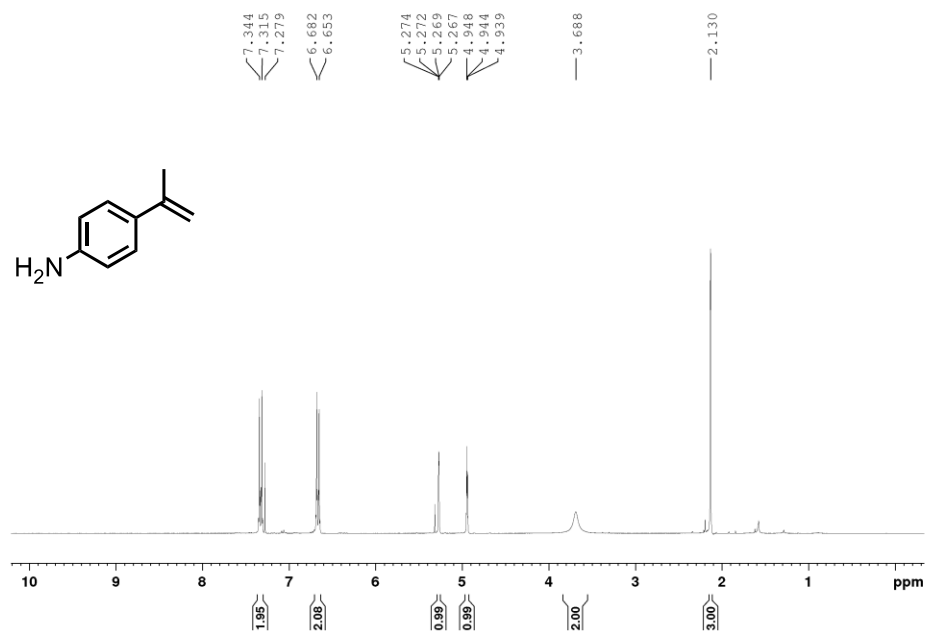
$^{13}\text{C}\{^1\text{H}\}$  NMR Spectrum of N-(2-methoxyphenyl)-4-methylbenzenesulfonamide, **3-3g** ( $\text{CDCl}_3$ , 75.5 MHz)



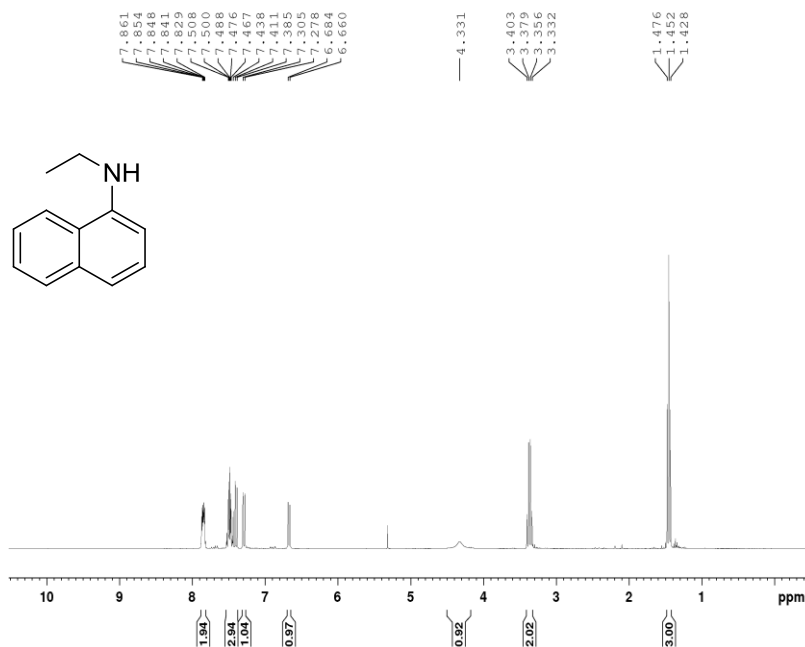
$^1\text{H}$  NMR Spectrum of 4-amino- $\alpha$ -methylstyrene, **3-3h** ( $\text{CDCl}_3$ , 300.1 MHz)



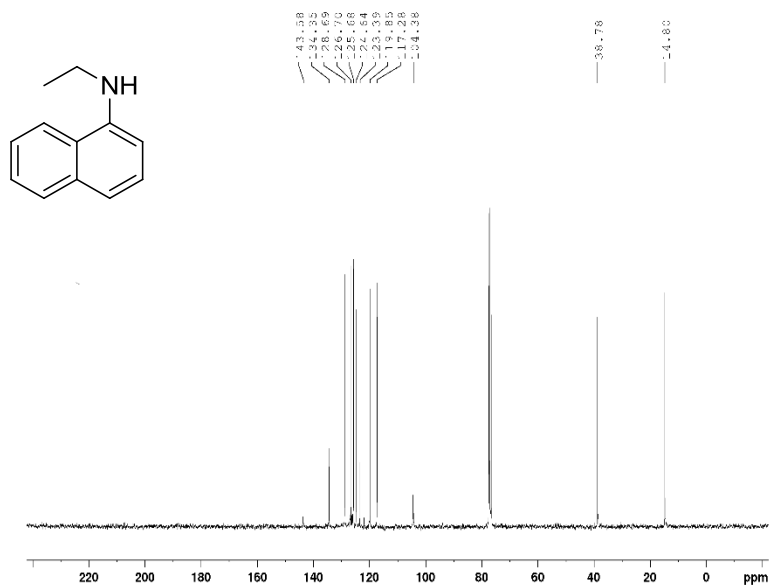
$^{13}\text{C}\{^1\text{H}\}$  NMR Spectrum of 4-amino- $\alpha$ -methylstyrene, **3-3h** ( $\text{CDCl}_3$ , 75.4 MHz)



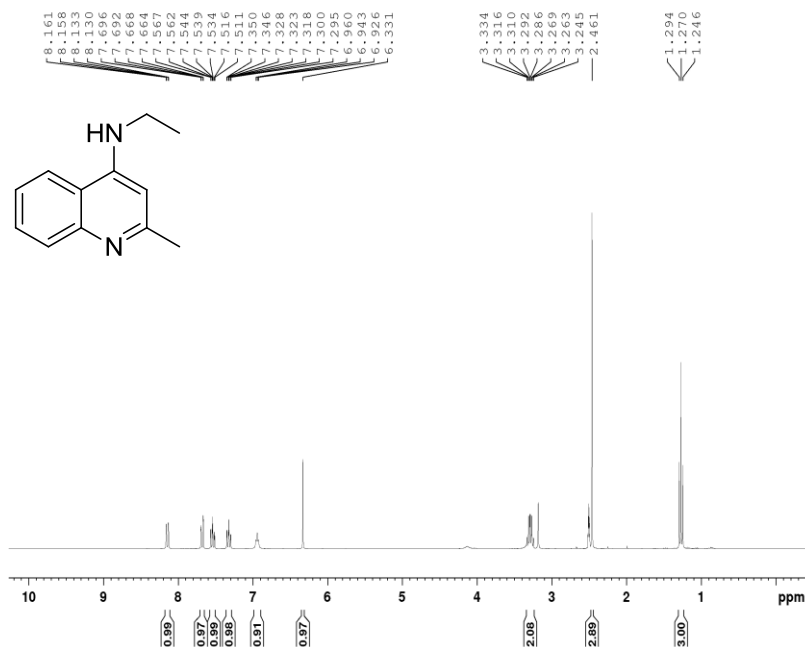
$^1\text{H}$  NMR Spectrum of *N*-ethylnaphthalen-1-amine, **3-3i** ( $\text{CDCl}_3$ , 300 MHz)



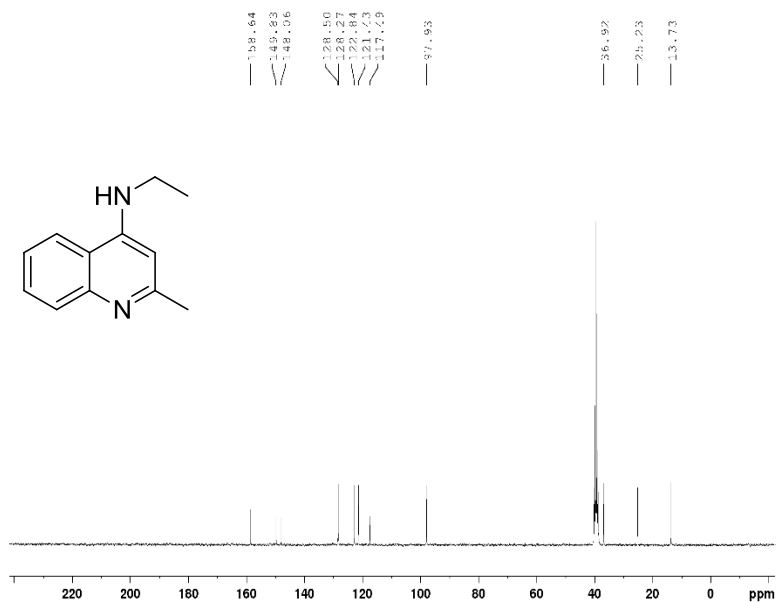
$^{13}\text{C}\{^1\text{H}\}$  NMR Spectrum of *N*-ethylnaphthalen-1-amine, **3-3i** ( $\text{CDCl}_3$ , 75.4 MHz)



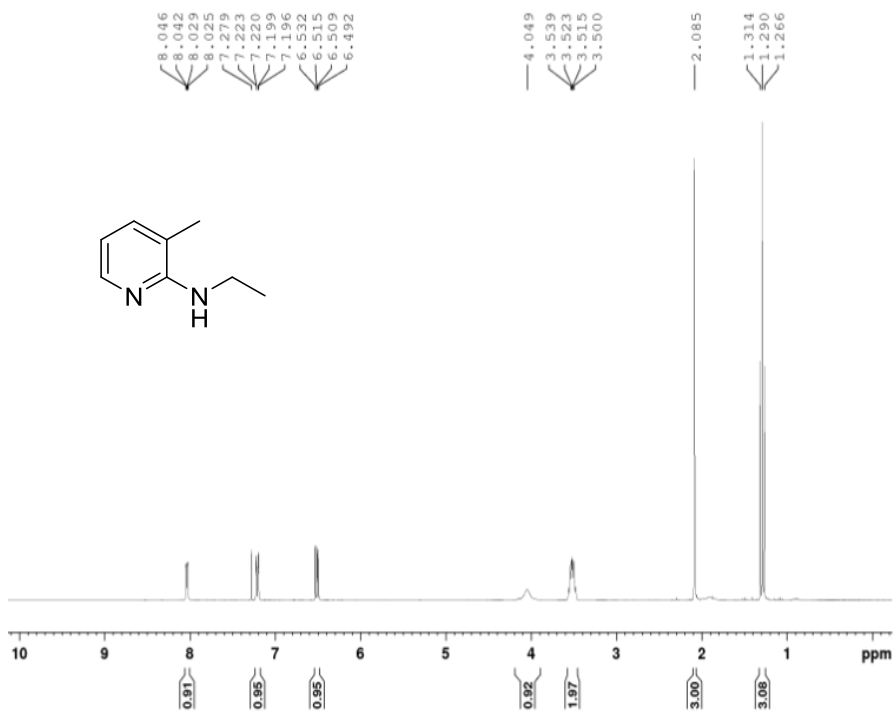
$^1\text{H}$  NMR Spectrum of *N*-ethyl-2-methylquinolin-4-amine, **3-3j** (DMSO, 300 MHz)



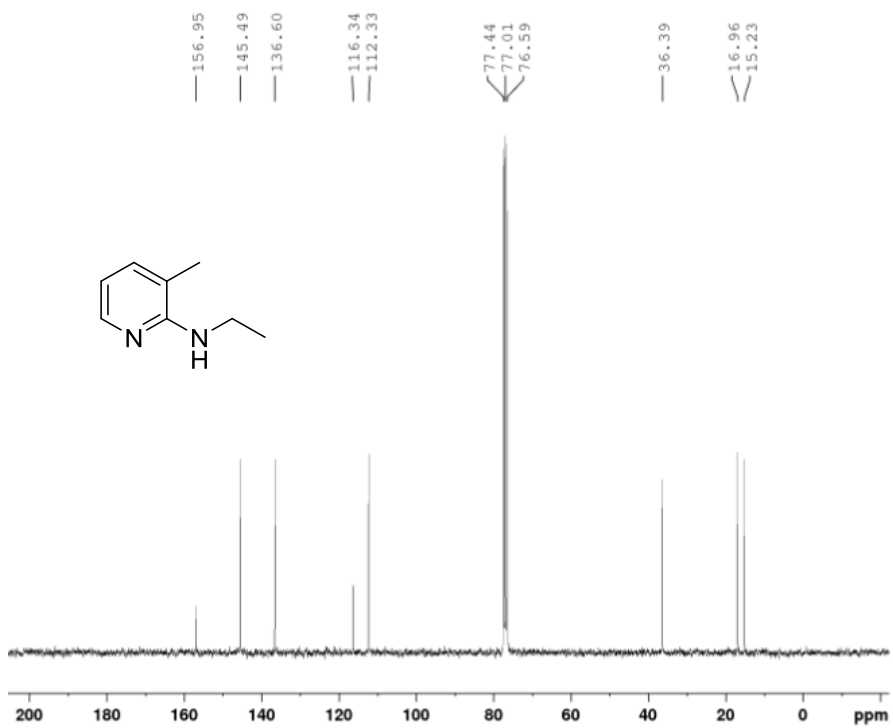
$^{13}\text{C}\{^1\text{H}\}$  NMR Spectrum of *N*-ethyl-2-methylquinolin-4-amine, **3-3j** (DMSO, 75.5 MHz)



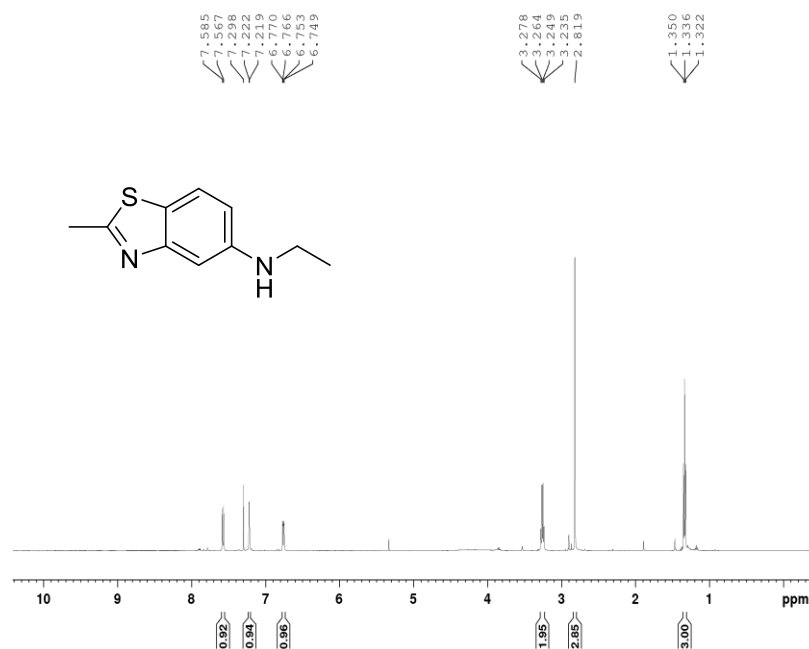
$^1\text{H}$  NMR Spectrum of *N*-ethyl-3-methylpyridin-2-amine, **3-3k** ( $\text{CDCl}_3$ , 300.1 MHz)



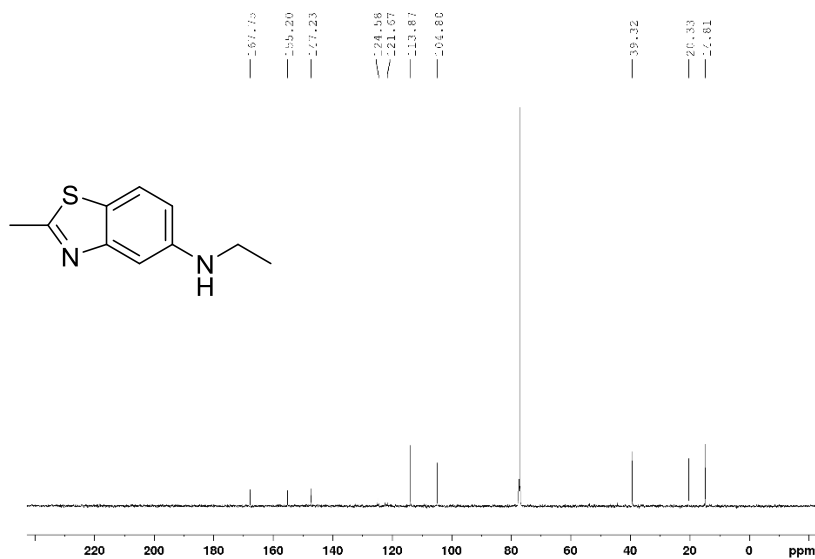
$^{13}\text{C}\{^1\text{H}\}$  NMR Spectrum of *N*-ethyl-3-methylpyridin-2-amine, **3-3k** ( $\text{CDCl}_3$ , 75.5 MHz)



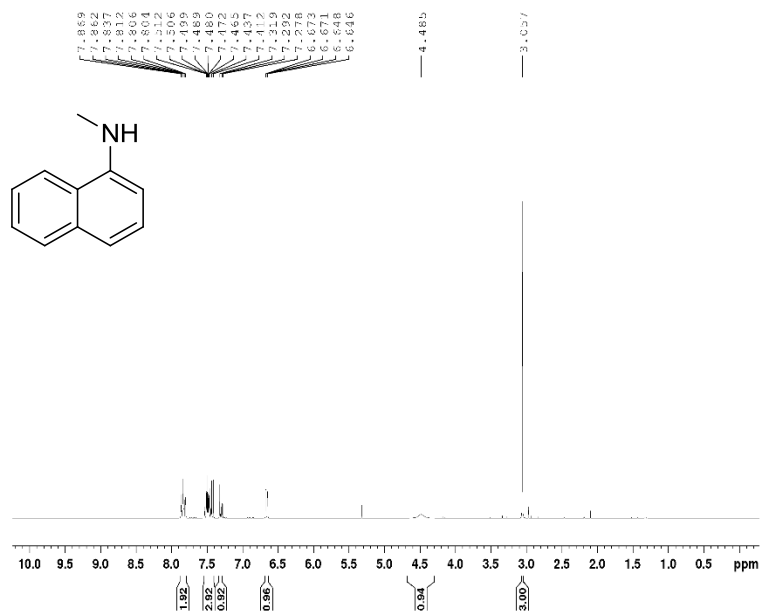
$^1\text{H}$  NMR Spectrum of *N*-ethyl-2-methylbenzo[*d*]thiazol-5-amine, **3-31** ( $\text{CDCl}_3$ , 500.1 MHz)



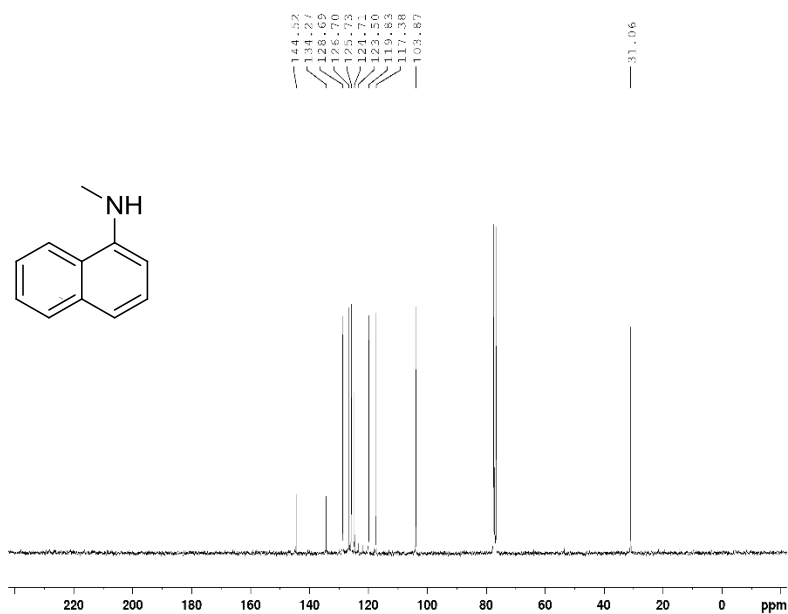
$^{13}\text{C}\{^1\text{H}\}$  NMR Spectrum of *N*-ethyl-2-methylbenzo[*d*]thiazol-5-amine, **3-31** ( $\text{CDCl}_3$ , 125.8 MHz)



$^1\text{H}$  NMR Spectrum of *N*-methylnaphthalen-1-amine, **3-3m** ( $\text{CDCl}_3$ , 300 MHz)

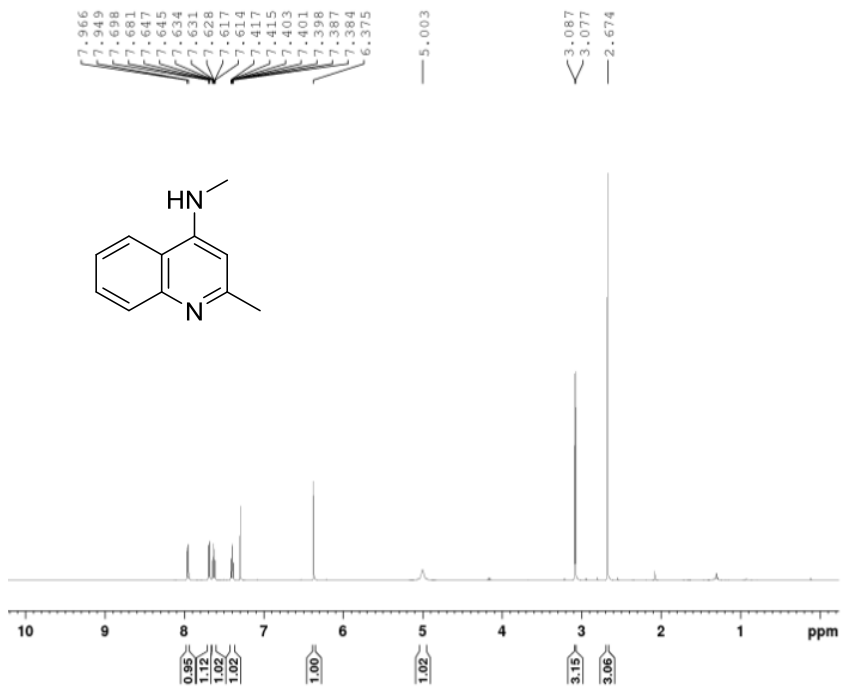


$^{13}\text{C}\{^1\text{H}\}$  NMR Spectrum of *N*-methylnaphthalen-1-amine, **3-3m** ( $\text{CDCl}_3$ , 75.5 MHz)

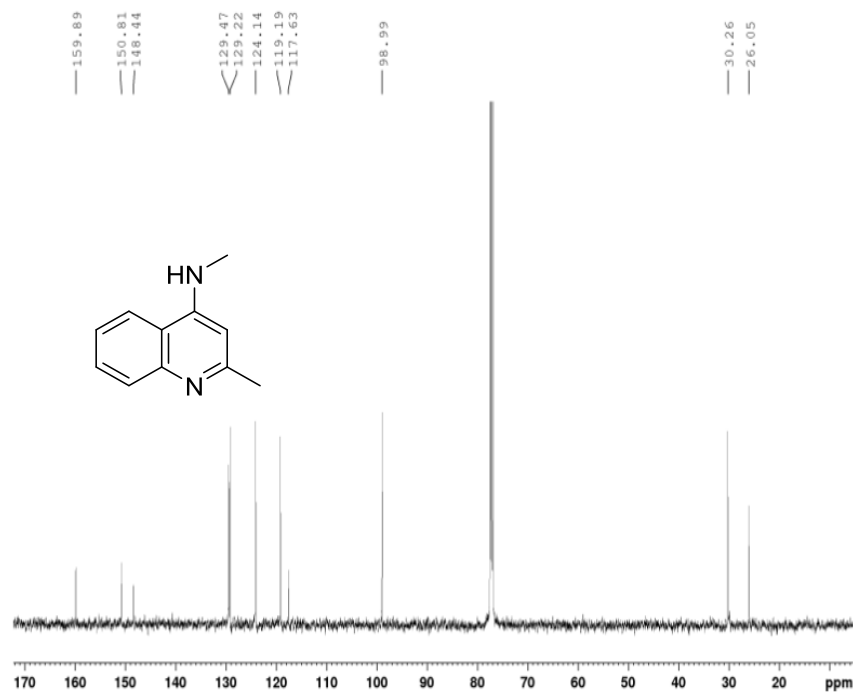




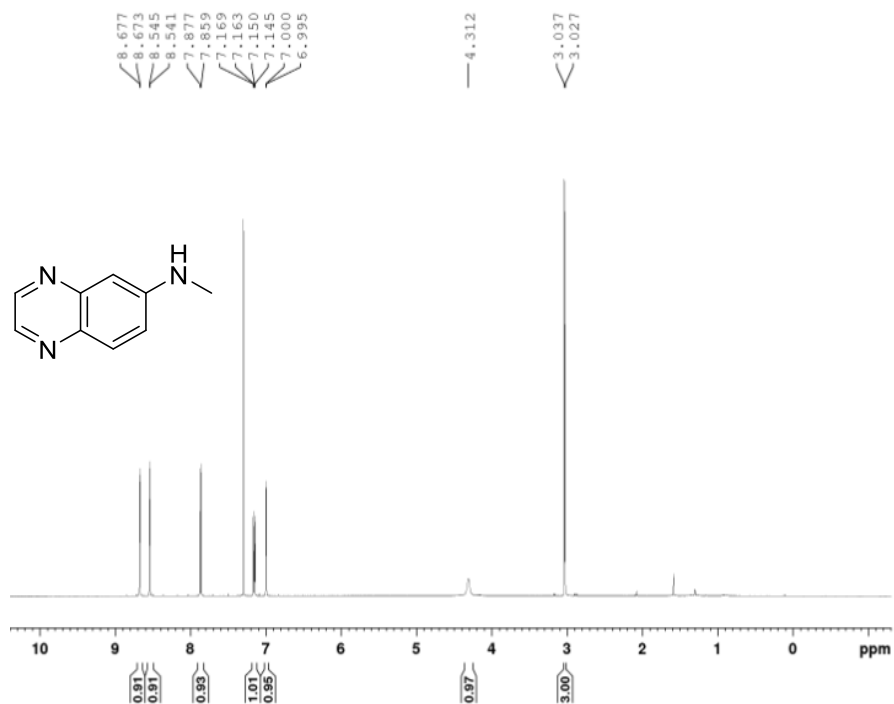
$^1\text{H}$  NMR Spectrum of Methyl-(2-methyl-quinolin-4-yl)amine, **3-3n** ( $\text{CDCl}_3$ , 500.1 MHz)



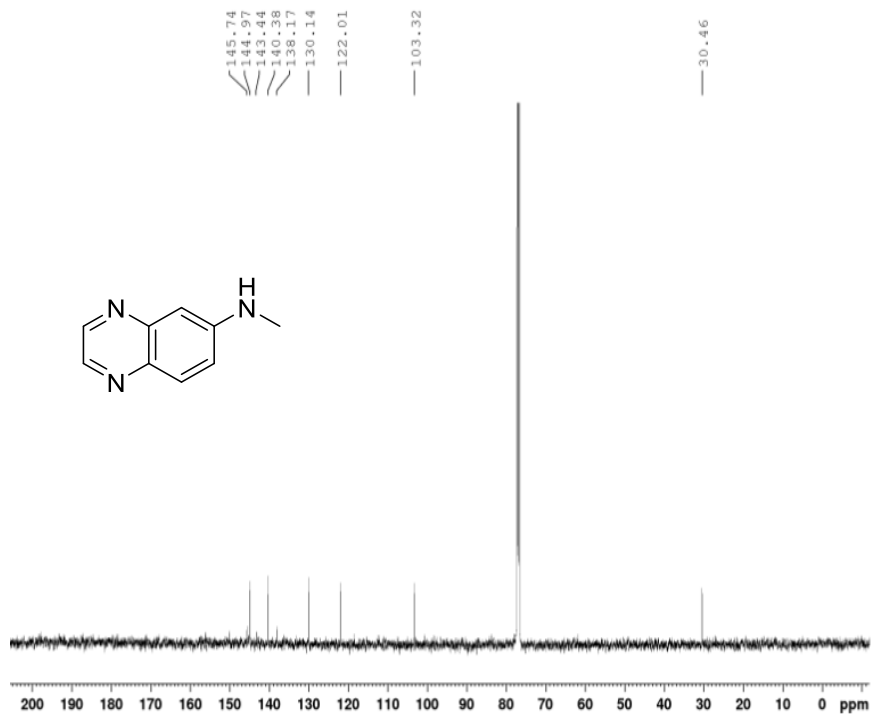
$^{13}\text{C}\{^1\text{H}\}$  NMR Spectrum of Methyl-(2-methyl-quinolin-4-yl)amine, **3-3n** ( $\text{CDCl}_3$ , 125.8 MHz)



$^1\text{H}$  NMR Spectrum of Methyl-quinoxalin-6-yl-amine, **3-3o** ( $\text{CDCl}_3$ , 500.1 MHz)

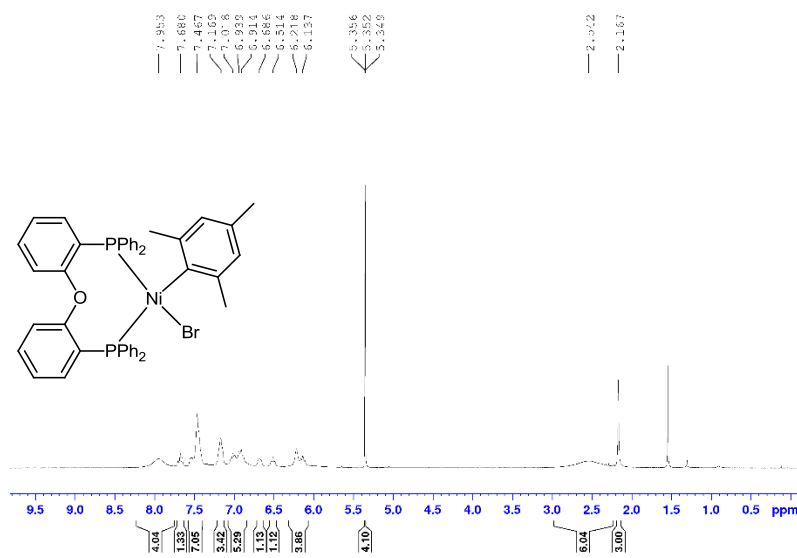


$^{13}\text{C}\{^1\text{H}\}$  NMR Spectrum of Methyl-quinoxalin-6-yl-amine, **3-3o** ( $\text{CDCl}_3$ , 125.8 MHz)

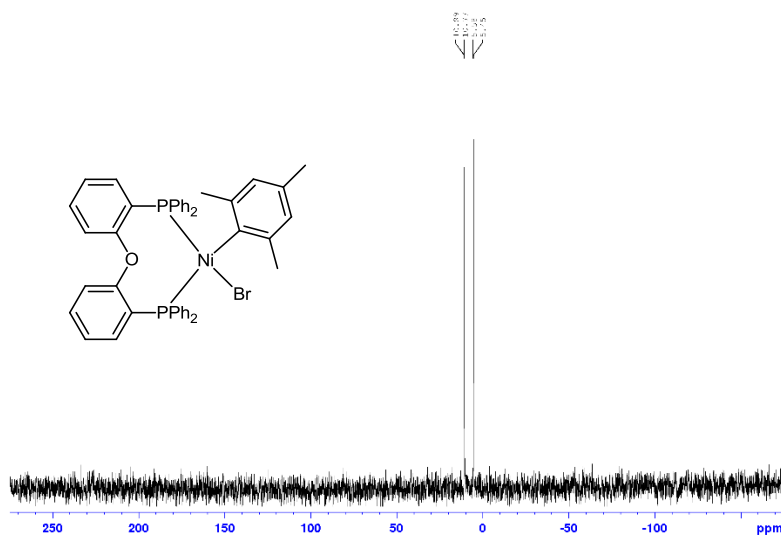


## Chapter 4 Characterization Data

$^1\text{H}$  NMR of **C4-1**, ( $\text{CDCl}_3$ , 500.1 MHz)



$^{31}\text{P}\{^1\text{H}\}$  NMR Spectrum of **C4-1**, ( $\text{CDCl}_3$ , 202.5 MHz)



## X-ray Crystallographic Data for **C3-1**.

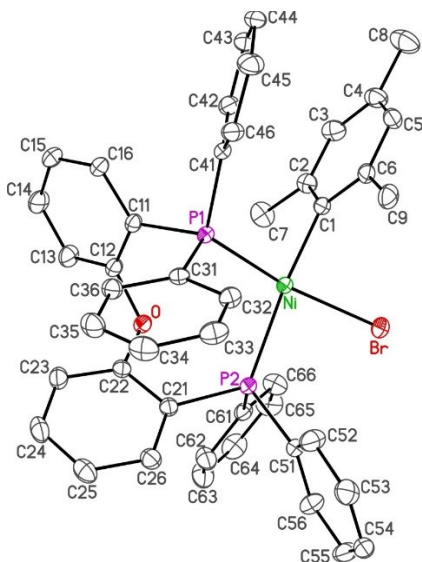


**Table 1.** Crystallographic Experimental Details

### *A. Crystal Data*

formula	C <sub>45</sub> H <sub>39</sub> BrNiOP <sub>2</sub>
formula weight	796.32
crystal dimensions (mm)	0.20 × 0.13 × 0.03
crystal system	monoclinic
space group	<i>P</i> 2 <sub>1</sub> / <i>n</i> (an alternate setting of <i>P</i> 2 <sub>1</sub> / <i>c</i> [No. 14])
unit cell parameters <sup>a</sup>	
<i>a</i> (Å)	13.0003 (2)
<i>b</i> (Å)	13.4838 (2)
<i>c</i> (Å)	21.3588 (4)
∠ (deg)	105.6812 (10)
<i>V</i> (Å <sup>3</sup> )	3604.70 (10)
<i>Z</i>	4
∠ calcd (g cm <sup>-3</sup> )	1.467
<i>μ</i> (mm <sup>-1</sup> )	3.184

### B. Data Collection and Refinement Conditions

diffractometer	Bruker D8/APEX II CCD <sup>b</sup>
radiation ( $\lambda$ [Å])	Cu K $\alpha$ (1.54178) (microfocus source)
temperature (°C)	-100
scan type	$\omega$ and $\phi$ scans (1.0°) (5 s exposures)
data collection $2\theta$ limit (deg)	148.34
total data collected	25392 ( $-16 \leq h \leq 16$ , $-16 \leq k \leq 16$ , $-26 \leq l \leq 26$ )
independent reflections	7123 ( $R_{\text{int}} = 0.0325$ )
number of observed reflections (NO)	6608 [ $F_o^2 \geq 2\sigma(F_o^2)$ ]
structure solution method	intrinsic phasing (SHELXT-2014 <sup>c</sup> )
refinement method	full-matrix least-squares on $F^2$ (SHELXL-2014 <sup>d</sup> )
absorption correction method	Gaussian integration (face-indexed)
range of transmission factors	0.9768–0.5945
data/restraints/parameters	7123 / 0 / 454
goodness-of-fit (S) <sup>e</sup> [all data]	1.034
final R indices <sup>f</sup>	
	$R_1$ [ $F_o^2 \geq 2\sigma(F_o^2)$ ] 0.0391
	$wR_2$ [all data] 0.1156
largest difference peak and hole	0.684 and -1.116 e Å <sup>-3</sup>

<sup>a</sup>Obtained from least-squares refinement of 9924 reflections with  $6.56^\circ < 2\theta < 146.80^\circ$ .

<sup>b</sup>Programs for diffractometer operation, data collection, data reduction and absorption correction were those supplied by Bruker.

(continued)

**Table 1.** Crystallographic Experimental Details (continued)

<sup>c</sup>Sheldrick, G. M. *Acta Crystallogr.* **2015**, *A71*, 3–8. (*SHELXT-2014*)

<sup>d</sup>Sheldrick, G. M. *Acta Crystallogr.* **2015**, *C71*, 3–8. (*SHELXL-2014*)

$eS = [\sum w(F_o^2 - F_c^2)^2 / (n - p)]^{1/2}$  ( $n$  = number of data;  $p$  = number of parameters varied;  
 $w = [\sum^2(F_o^2) + (0.0592P)^2 + 4.5607P]^{-1}$  where  $P = [\text{Max}(F_o^2, 0) + 2F_c^2]/3$ ).

$fR_1 = \sum ||F_o| - |F_c|| / \sum |F_o|$ ;  $wR_2 = [\sum w(F_o^2 - F_c^2)^2 / \sum w(F_o^4)]^{1/2}$ .

**Table 2.** Atomic Coordinates and Equivalent Isotropic Displacement Parameters

Atom	<i>x</i>	<i>y</i>	<i>z</i>	$U_{\text{eq}}, \text{\AA}^2$
Br	0.68336(2)	0.56950(2)	0.74446(2)	0.04000(11)*
Ni	0.60076(3)	0.67778(3)	0.66032(2)	0.02285(11)*
P1	0.55577(4)	0.80573(4)	0.59477(3)	0.02105(13)*
P2	0.44895(5)	0.65321(4)	0.69399(3)	0.02382(13)*
O	0.35150(14)	0.67995(13)	0.56087(8)	0.0286(4)*
C1	0.72769(19)	0.66175(17)	0.63051(12)	0.0257(5)*
C2	0.7197(2)	0.59558(19)	0.57878(14)	0.0326(5)*
C3	0.8104(3)	0.5756(2)	0.55676(16)	0.0409(7)*
C4	0.9081(2)	0.6202(2)	0.58573(17)	0.0430(7)*
C5	0.9139(2)	0.6851(2)	0.63659(15)	0.0369(6)*
C6	0.8259(2)	0.70669(19)	0.65999(13)	0.0300(5)*
C7	0.6146(3)	0.5484(2)	0.54529(17)	0.0453(7)*
C8	1.0055(3)	0.5978(3)	0.5623(2)	0.0630(10)*
C9	0.8400(2)	0.7772(2)	0.71613(14)	0.0387(6)*
C11	0.45718(19)	0.79047(18)	0.51520(11)	0.0251(5)*
C12	0.3710(2)	0.72583(18)	0.50686(12)	0.0277(5)*
C13	0.3043(2)	0.7030(2)	0.44597(14)	0.0392(6)*
C14	0.3199(2)	0.7492(3)	0.39159(14)	0.0430(7)*
C15	0.4006(2)	0.8182(2)	0.39843(13)	0.0377(6)*
C16	0.4684(2)	0.83777(19)	0.45892(13)	0.0307(5)*
C21	0.33018(19)	0.72981(18)	0.66204(12)	0.0268(5)*
C22	0.29464(19)	0.73672(18)	0.59452(13)	0.0277(5)*
C23	0.2069(2)	0.7936(2)	0.56381(15)	0.0362(6)*
C24	0.1512(2)	0.8427(2)	0.60180(17)	0.0415(7)*
C25	0.1833(2)	0.8359(2)	0.66844(17)	0.0408(6)*
C26	0.2730(2)	0.7800(2)	0.69877(14)	0.0334(5)*
C31	0.50296(19)	0.90523(17)	0.63553(12)	0.0242(5)*
C32	0.5593(2)	0.92722(18)	0.69970(13)	0.0298(5)*
C33	0.5249(2)	1.0030(2)	0.73391(14)	0.0379(6)*
C34	0.4323(3)	1.0541(2)	0.70518(16)	0.0403(6)*
C35	0.3758(2)	1.0327(2)	0.64131(16)	0.0397(6)*
C36	0.4113(2)	0.95918(18)	0.60604(13)	0.0295(5)*
C41	0.66577(18)	0.86671(18)	0.57070(11)	0.0246(5)*
C42	0.7094(2)	0.81907(19)	0.52540(13)	0.0313(5)*
C43	0.7961(2)	0.8607(2)	0.50888(14)	0.0383(6)*
C44	0.8393(2)	0.9483(2)	0.53578(13)	0.0361(6)*
C45	0.7976(2)	0.9957(2)	0.58122(15)	0.0418(7)*
C46	0.7095(2)	0.9545(2)	0.59784(13)	0.0311(5)*

C51	0.46484(19)	0.66584(19)	0.78147(12)	0.0279(5)*
C52	0.5140(2)	0.7505(2)	0.81209(14)	0.0427(7)*

**Table 2.** Atomic Coordinates and Displacement Parameters (continued)

Atom	<i>x</i>	<i>y</i>	<i>z</i>	$U_{eq}, \text{\AA}^2$
C53	0.5211(2)	0.7686(3)	0.87794(15)	0.0449(7)*
C54	0.4826(2)	0.7007(3)	0.91225(14)	0.0426(7)*
C55	0.4341(3)	0.6159(2)	0.88265(15)	0.0444(7)*
C56	0.4243(3)	0.5982(2)	0.81790(14)	0.0383(6)*
C61	0.3893(2)	0.52945(19)	0.67341(12)	0.0290(5)*
C62	0.2819(2)	0.5133(2)	0.67029(16)	0.0414(7)*
C63	0.2355(3)	0.4212(2)	0.65419(19)	0.0531(9)*
C64	0.2952(3)	0.3430(2)	0.64012(18)	0.0523(8)*
C65	0.4001(3)	0.3577(2)	0.64348(19)	0.0551(9)*
C66	0.4482(3)	0.4505(2)	0.65994(17)	0.0431(7)*

Anisotropically-refined atoms are marked with an asterisk (\*). The form of the anisotropic displacement parameter is:  $\exp[-2\pi^2(h^2a^{*2}U_{11} + k^2b^{*2}U_{22} + l^2c^{*2}U_{33} + 2klb^{*c^*}U_{23} + 2hla^{*c^*}U_{13} + 2hka^{*b^*}U_{12})]$ .



**Table 3.** Selected Interatomic Distances (Å)

Atom1	Atom2	Distance	Atom1	Atom2	Distance
Br	Ni	2.3391(5)	C22	C23	1.384(4)
Ni	P1	2.1991(7)	C23	C24	1.393(4)
Ni	P2	2.2998(7)	C24	C25	1.374(5)
Ni	C1	1.935(2)	C25	C26	1.392(4)
P1	C11	1.843(2)	C31	C32	1.400(4)
P1	C31	1.831(2)	C31	C36	1.393(3)
P1	C41	1.839(2)	C32	C33	1.398(4)
P2	C21	1.829(2)	C33	C34	1.379(4)
P2	C51	1.831(3)	C34	C35	1.394(5)
P2	C61	1.842(3)	C35	C36	1.397(4)
O	C12	1.391(3)	C41	C42	1.403(3)
O	C22	1.391(3)	C41	C46	1.372(4)
C1	C2	1.402(4)	C42	C43	1.388(4)
C1	C6	1.400(3)	C43	C44	1.366(4)
C2	C3	1.409(4)	C44	C45	1.389(4)
C2	C7	1.502(4)	C45	C46	1.401(4)
C3	C4	1.390(5)	C51	C52	1.383(4)
C4	C5	1.381(5)	C51	C56	1.392(4)
C4	C8	1.514(4)	C52	C53	1.406(4)
C5	C6	1.397(4)	C53	C54	1.350(5)
C6	C9	1.502(4)	C54	C55	1.374(5)
C11	C12	1.393(3)	C55	C56	1.375(4)
C11	C16	1.403(3)	C61	C62	1.398(4)
C12	C13	1.388(4)	C61	C66	1.386(4)
C13	C14	1.380(4)	C62	C63	1.383(4)
C14	C15	1.381(4)	C63	C64	1.390(5)
C15	C16	1.378(4)	C64	C65	1.360(5)
C21	C22	1.393(4)	C65	C66	1.401(4)
C21	C26	1.393(4)			

**Table 4.** Selected Interatomic Angles (deg)

Atom1	Atom2	Atom3	Angle	Atom1	Atom2	Atom3	Angle
Br	Ni	P1	165.18(3)	C11	C12	C13	122.4(2)
Br	Ni	P2	85.67(2)	C12	C13	C14	119.5(3)
Br	Ni	C1	85.86(7)	C13	C14	C15	119.7(3)
P1	Ni	P2	102.07(3)	C14	C15	C16	120.2(3)
P1	Ni	C1	88.96(7)	C11	C16	C15	121.9(2)
P2	Ni	C1	165.27(7)	P2	C21	C22	115.73(18)
Ni	P1	C11	119.91(8)	P2	C21	C26	126.1(2)
Ni	P1	C31	109.96(8)	C22	C21	C26	118.2(2)
Ni	P1	C41	115.83(8)	O	C22	C21	115.1(2)
C11	P1	C31	105.29(11)	O	C22	C23	123.0(2)
C11	P1	C41	101.05(11)	C21	C22	C23	121.9(2)
C31	P1	C41	103.01(11)	C22	C23	C24	118.7(3)
Ni	P2	C21	120.74(8)	C23	C24	C25	120.7(3)
Ni	P2	C51	115.84(8)	C24	C25	C26	120.0(3)
Ni	P2	C61	113.40(8)	C21	C26	C25	120.5(3)
C21	P2	C51	100.32(11)	P1	C31	C32	117.16(18)
C21	P2	C61	99.45(11)	P1	C31	C36	123.54(19)
C51	P2	C61	104.58(11)	C32	C31	C36	119.3(2)
C12	O	C22	115.14(18)	C31	C32	C33	120.7(3)
Ni	C1	C2	116.26(18)	C32	C33	C34	119.8(3)
Ni	C1	C6	124.00(19)	C33	C34	C35	119.8(2)
C2	C1	C6	119.6(2)	C34	C35	C36	120.8(3)
C1	C2	C3	119.6(3)	C31	C36	C35	119.6(3)
C1	C2	C7	120.6(2)	P1	C41	C42	118.56(19)
C3	C2	C7	119.7(3)	P1	C41	C46	122.18(18)
C2	C3	C4	121.0(3)	C42	C41	C46	119.2(2)
C3	C4	C5	118.3(3)	C41	C42	C43	119.9(3)
C3	C4	C8	120.8(3)	C42	C43	C44	120.8(3)
C5	C4	C8	120.9(3)	C43	C44	C45	119.9(2)
C4	C5	C6	122.5(3)	C44	C45	C46	119.6(3)
C1	C6	C5	119.0(3)	C41	C46	C45	120.6(2)
C1	C6	C9	122.2(2)	P2	C51	C52	118.0(2)
C5	C6	C9	118.9(2)	P2	C51	C56	123.6(2)
P1	C11	C12	121.52(18)	C52	C51	C56	118.2(2)
P1	C11	C16	122.15(19)	C51	C52	C53	120.9(3)
C12	C11	C16	116.2(2)	C52	C53	C54	119.5(3)
O	C12	C11	119.5(2)	C53	C54	C55	120.4(3)
O	C12	C13	118.1(2)	C54	C55	C56	120.9(3)

C51	C56	C55	120.1(3)
P2	C61	C62	120.2(2)
P2	C61	C66	121.7(2)
C62	C61	C66	118.2(3)

**Table 4.** Selected Interatomic Angles (continued)

Atom1	Atom2	Atom3	Angle	Atom1	Atom2	Atom3	Angle
C61	C62	C63	121.0(3)	C64	C65	C66	121.1(3)
C62	C63	C64	120.3(3)	C61	C66	C65	120.2(3)
C63	C64	C65	119.3(3)				

**Table 5.** Torsional Angles (deg)

Atom1	Atom2	Atom3	Atom4	Angle	Atom1	Atom2	Atom3	Atom4	Angle
Br	Ni	P1	C11	168.44(12)	C11	P1	C41	C42	-57.1(2)
Br	Ni	P1	C31	-69.38(13)	C11	P1	C41	C46	126.1(2)
Br	Ni	P1	C41	46.84(14)	C31	P1	C41	C42	-165.8(2)
P2	Ni	P1	C11	-71.16(9)	C31	P1	C41	C46	17.4(2)
P2	Ni	P1	C31	51.02(9)	Ni	P2	C21	C22	51.4(2)
P2	Ni	P1	C41	167.23(9)	Ni	P2	C21	C26	-129.2(2)
C1	Ni	P1	C11	99.00(12)	C51	P2	C21	C22	-179.96(19)
C1	Ni	P1	C31	-138.82(11)	C51	P2	C21	C26	-0.6(2)
C1	Ni	P1	C41	-22.60(12)	C61	P2	C21	C22	-73.1(2)
Br	Ni	P2	C21	169.81(10)	C61	P2	C21	C26	106.3(2)
Br	Ni	P2	C51	48.50(9)	Ni	P2	C51	C52	50.8(2)
Br	Ni	P2	C61	-72.45(9)	Ni	P2	C51	C56	-133.4(2)
P1	Ni	P2	C21	2.60(10)	C21	P2	C51	C52	-80.9(2)
P1	Ni	P2	C51	-118.71(9)	C21	P2	C51	C56	94.9(2)
P1	Ni	P2	C61	120.33(9)	C61	P2	C51	C52	176.4(2)
C1	Ni	P2	C21	-135.2(3)	C61	P2	C51	C56	-7.8(3)
C1	Ni	P2	C51	103.5(3)	Ni	P2	C61	C62	-158.7(2)
C1	Ni	P2	C61	-17.4(3)	Ni	P2	C61	C66	20.6(3)
Br	Ni	C1	C2	100.37(19)	C21	P2	C61	C62	-29.2(2)
Br	Ni	C1	C6	-75.4(2)	C21	P2	C61	C66	150.1(2)
P1	Ni	C1	C2	-93.52(19)	C51	P2	C61	C62	74.2(2)
P1	Ni	C1	C6	90.7(2)	C51	P2	C61	C66	-106.6(2)
P2	Ni	C1	C2	45.4(4)	C22	O	C12	C11	82.8(3)
P2	Ni	C1	C6	-130.4(3)	C22	O	C12	C13	-98.8(3)
Ni	P1	C11	C12	35.2(2)	C12	O	C22	C21	-139.6(2)
Ni	P1	C11	C16	-140.42(18)	C12	O	C22	C23	42.5(3)
C31	P1	C11	C12	-89.3(2)	Ni	C1	C2	C3	-176.4(2)
C31	P1	C11	C16	95.1(2)	Ni	C1	C2	C7	5.6(3)
C41	P1	C11	C12	163.8(2)	C6	C1	C2	C3	-0.4(4)
C41	P1	C11	C16	-11.8(2)	C6	C1	C2	C7	-178.5(3)
Ni	P1	C31	C32	44.95(19)	Ni	C1	C6	C5	176.22(19)
Ni	P1	C31	C36	-135.30(18)	Ni	C1	C6	C9	-3.6(3)
C11	P1	C31	C32	175.44(18)	C2	C1	C6	C5	0.6(4)
C11	P1	C31	C36	-4.8(2)	C2	C1	C6	C9	-179.2(2)
C41	P1	C31	C32	-79.1(2)	C1	C2	C3	C4	0.2(4)
C41	P1	C31	C36	100.7(2)	C7	C2	C3	C4	178.3(3)
Ni	P1	C41	C42	74.1(2)	C2	C3	C4	C5	-0.2(4)
Ni	P1	C41	C46	-102.7(2)	C2	C3	C4	C8	179.5(3)

C3	C4	C5	C6	0.4(4)
C8	C4	C5	C6	-179.3(3)
C4	C5	C6	C1	-0.6(4)
C4	C5	C6	C9	179.2(3)

**Table 5.** Torsional Angles (continued)

Atom1	Atom2	Atom3	Atom4	Angle	Atom1	Atom2	Atom3	Atom4	Angle
P1	C11	C12	O	7.3(3)	C32	C33	C34	C35	-2.5(4)
P1	C11	C12	C13	-171.0(2)	C33	C34	C35	C36	0.6(4)
C16	C11	C12	O	-176.8(2)	C34	C35	C36	C31	1.4(4)
C16	C11	C12	C13	4.9(4)	P1	C41	C42	C43	-176.6(2)
P1	C11	C16	C15	173.2(2)	C46	C41	C42	C43	0.3(4)
C12	C11	C16	C15	-2.7(4)	P1	C41	C46	C45	176.1(2)
O	C12	C13	C14	178.3(3)	C42	C41	C46	C45	-0.7(4)
C11	C12	C13	C14	-3.3(4)	C41	C42	C43	C44	-0.6(4)
C12	C13	C14	C15	-0.7(5)	C42	C43	C44	C45	1.3(5)
C13	C14	C15	C16	2.8(5)	C43	C44	C45	C46	-1.7(5)
C14	C15	C16	C11	-1.1(4)	C44	C45	C46	C41	1.5(4)
P2	C21	C22	O	3.2(3)	P2	C51	C52	C53	174.9(2)
P2	C21	C22	C23	-178.8(2)	C56	C51	C52	C53	-1.2(4)
C26	C21	C22	O	-176.2(2)	P2	C51	C56	C55	-176.1(2)
C26	C21	C22	C23	1.7(4)	C52	C51	C56	C55	-0.4(4)
P2	C21	C26	C25	-179.8(2)	C51	C52	C53	C54	2.3(5)
C22	C21	C26	C25	-0.4(4)	C52	C53	C54	C55	-1.9(5)
O	C22	C23	C24	175.9(2)	C53	C54	C55	C56	0.3(5)
C21	C22	C23	C24	-1.9(4)	C54	C55	C56	C51	0.8(5)
C22	C23	C24	C25	0.7(4)	P2	C61	C62	C63	179.3(3)
C23	C24	C25	C26	0.5(4)	C66	C61	C62	C63	0.0(5)
C24	C25	C26	C21	-0.7(4)	P2	C61	C66	C65	-179.0(3)
P1	C31	C32	C33	179.2(2)	C62	C61	C66	C65	0.2(5)
C36	C31	C32	C33	-0.6(4)	C61	C62	C63	C64	-0.7(5)
P1	C31	C36	C35	178.8(2)	C62	C63	C64	C65	1.1(6)
C32	C31	C36	C35	-1.4(4)	C63	C64	C65	C66	-0.9(6)
C31	C32	C33	C34	2.5(4)	C64	C65	C66	C61	0.3(6)

**Table 6.** Anisotropic Displacement Parameters ( $U_{ij}$ , Å<sup>2</sup>)

Atom	$U_{11}$	$U_{22}$	$U_{33}$	$U_{23}$	$U_{13}$	
	$U_{12}$					
Br	0.03368(16) 0.00926(11)	0.04659(18)	0.03918(18)	0.02044(12)	0.00894(13)	
Ni	0.0226(2) 0.00140(14)	0.0235(2)	0.0225(2)	0.00415(15)	0.00618(17)	
P1	0.0231(3) 0.0007(2)	0.0209(3)	0.0192(3)	0.00129(19)	0.0057(2)	-
P2	0.0238(3)	0.0251(3)	0.0228(3)	0.0043(2)	0.0066(2)	0.0005(2)
O	0.0286(8) 0.0010(7)	0.0311(9)	0.0254(9)	0.0044(7)	0.0064(7)	-
C1	0.0246(11) 0.0020(9)	0.0254(11)	0.0272(12)	0.0047(9)	0.0070(10)	
C2	0.0340(13) 0.0013(10)	0.0285(12)	0.0363(14)	-0.0004(10)	0.0112(11)	
C3	0.0482(16) 0.0057(12)	0.0335(14)	0.0469(17)	-0.0011(12)	0.0233(14)	
C4	0.0381(15) 0.0088(12)	0.0403(15)	0.0570(19)	0.0115(13)	0.0235(14)	
C5	0.0253(12) 0.0006(10)	0.0385(14)	0.0451(16)	0.0114(12)	0.0067(12)	
C6	0.0265(11) 0.0005(9)	0.0303(12)	0.0307(13)	0.0081(10)	0.0034(10)	
C7	0.0449(16) 0.0078(12)	0.0366(15)	0.0514(18)	-0.0148(13)	0.0077(14)	-
C8	0.0480(19)	0.058(2)	0.094(3)	0.004(2)	0.038(2)	0.0069(16)
C9	0.0369(14) 0.0072(11)	0.0420(15)	0.0310(14)	0.0007(11)	-0.0016(12)	-
C11	0.0276(11)	0.0268(11)	0.0196(11)	0.0004(8)	0.0043(9)	0.0023(9)
C12	0.0287(11) 0.0004(9)	0.0311(12)	0.0217(12)	0.0025(9)	0.0043(10)	
C13	0.0355(14) 0.0094(12)	0.0457(16)	0.0307(14)	0.0016(11)	-0.0010(12)	-
C14	0.0423(15) 0.0050(13)	0.0588(19)	0.0224(13)	-0.0002(12)	-0.0007(12)	-
C15	0.0417(15) 0.0028(12)	0.0489(16)	0.0225(13)	0.0062(11)	0.0087(12)	
C16	0.0319(12)	0.0346(13)	0.0248(12)	0.0056(10)	0.0064(10)	



	0.0002(10)					
C21	0.0247(11)	0.0253(11)	0.0302(13)	0.0031(9)	0.0072(10)	-
	0.0013(9)					
C22	0.0228(11)	0.0281(11)	0.0320(13)	0.0055(9)	0.0073(10)	-
	0.0033(9)					
C23	0.0281(12)	0.0393(14)	0.0377(15)	0.0083(11)	0.0030(11)	
	0.0002(10)					
C24	0.0292(13)	0.0366(14)	0.0546(19)	0.0082(13)	0.0043(13)	
	0.0076(11)					
C25	0.0341(14)	0.0348(14)	0.0556(19)	-0.0025(12)	0.0157(14)	
	0.0056(11)					
C26	0.0311(12)	0.0336(13)	0.0363(14)	0.0008(11)	0.0108(11)	
	0.0019(10)					
C31	0.0268(11)	0.0222(10)	0.0258(12)	0.0011(9)	0.0110(10)	-
	0.0033(9)					
C32	0.0331(12)	0.0291(12)	0.0275(13)	-0.0027(9)	0.0089(11)	-
	0.0019(9)					
C33	0.0502(16)	0.0349(14)	0.0324(14)	-0.0080(11)	0.0174(13)	-
	0.0064(12)					
C34	0.0481(16)	0.0301(13)	0.0493(17)	-0.0088(12)	0.0243(14)	
	0.0010(11)					
C35	0.0387(14)	0.0337(14)	0.0499(17)	0.0013(12)	0.0175(13)	
	0.0090(11)					
C36	0.0296(12)	0.0273(11)	0.0326(13)	0.0018(10)	0.0103(11)	
	0.0017(9)					
C41	0.0233(10)	0.0283(11)	0.0224(11)	0.0067(9)	0.0064(9)	0.0009(9)
C42	0.0340(13)	0.0317(12)	0.0301(13)	0.0036(10)	0.0117(11)	
	0.0021(10)					
C43	0.0333(13)	0.0521(17)	0.0340(14)	0.0065(12)	0.0171(12)	
	0.0057(12)					
C44	0.0264(12)	0.0530(16)	0.0305(14)	0.0060(11)	0.0104(11)	-
	0.0062(11)					
C45	0.0374(14)	0.0457(16)	0.0425(16)	-0.0015(13)	0.0115(13)	-
	0.0150(12)					
C46	0.0318(12)	0.0339(13)	0.0299(13)	0.0013(10)	0.0122(11)	-
	0.0032(10)					
C51	0.0250(11)	0.0343(13)	0.0246(12)	0.0058(9)	0.0073(10)	
	0.0034(9)					
C52	0.0450(16)	0.0520(17)	0.0314(15)	-0.0018(12)	0.0108(13)	-
	0.0168(13)					

**Table 6.** Anisotropic Displacement Parameters (continued)

Atom	$U_{11}$	$U_{22}$	$U_{33}$	$U_{23}$	$U_{13}$	
	$U_{12}$					
C53	0.0347(14) 0.0100(13)	0.0602(19)	0.0363(16)	-0.0119(14)	0.0035(13)	-
C54	0.0309(13) 0.0081(13)	0.073(2)	0.0241(13)	-0.0016(13)	0.0074(11)	
C55	0.0523(17) 0.0048(14)	0.0503(17)	0.0373(16)	0.0112(13)	0.0236(14)	
C56	0.0520(16) 0.0013(12)	0.0329(13)	0.0325(14)	0.0042(11)	0.0158(13)	-
C61	0.0318(12) 0.0030(10)	0.0286(12)	0.0260(12)	0.0043(9)	0.0071(10)	-
C62	0.0334(14) 0.0019(11)	0.0343(14)	0.0551(18)	0.0085(13)	0.0096(13)	-
C63	0.0392(16) 0.0131(13)	0.0450(18)	0.068(2)	0.0125(15)	0.0029(16)	-
C64	0.064(2) 0.0189(15)	0.0368(16)	0.051(2)	-0.0036(14)	0.0079(17)	-
C65	0.068(2) 0.0037(15)	0.0359(16)	0.064(2)	-0.0140(15)	0.0221(19)	-
C66	0.0432(16) 0.0031(12)	0.0343(14)	0.0553(19)	-0.0046(13)	0.0195(14)	-

The form of the anisotropic displacement parameter is:

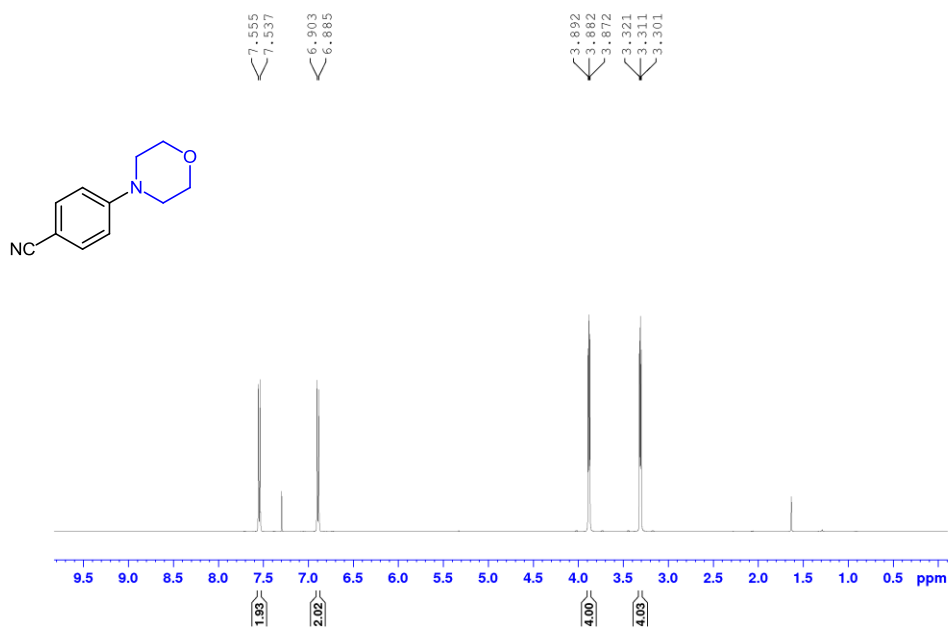
$$\exp[-2\pi^2(h^2a^2U_{11} + k^2b^2U_{22} + l^2c^2U_{33} + 2klb^*c^*U_{23} + 2hla^*c^*U_{13} + 2hka^*b^*U_{12})]$$

**Table 7.** Derived Atomic Coordinates and Displacement Parameters for Hydrogen Atoms

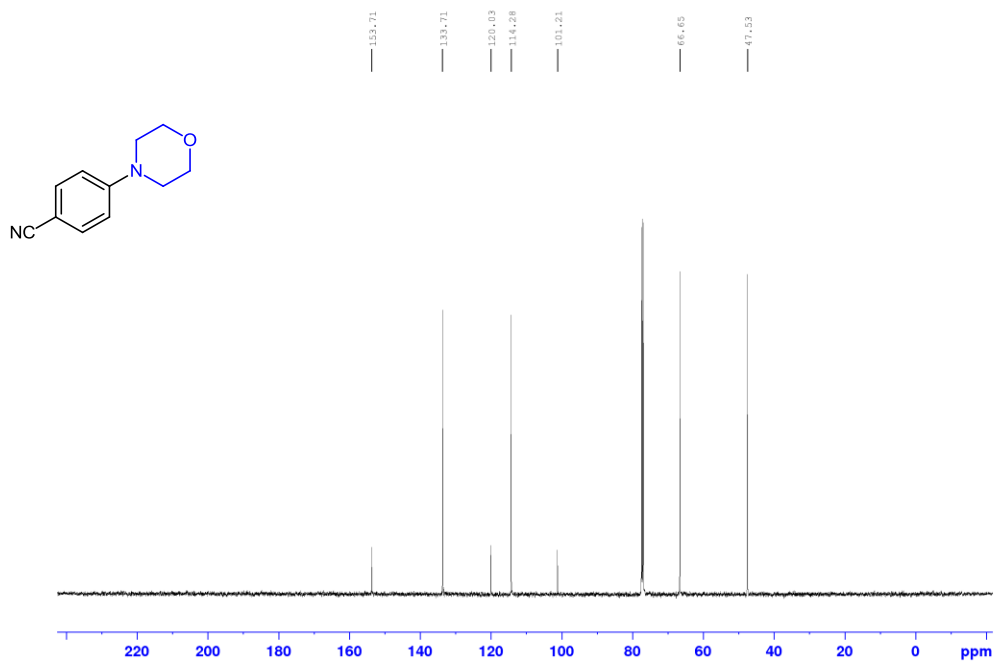
Atom	<i>x</i>	<i>y</i>	<i>z</i>	$U_{\text{eq}}, \text{\AA}^2$
H3	0.8048	0.5309	0.5216	0.049
H5	0.9803	0.7162	0.6564	0.044
H7A	0.5575	0.5977	0.5396	0.054
H7B	0.6006	0.4933	0.5718	0.054
H7C	0.6172	0.5233	0.5027	0.054
H8A	1.0667	0.6357	0.5881	0.076
H8B	0.9915	0.6165	0.5164	0.076
H8C	1.0216	0.5268	0.5671	0.076
H9A	0.7835	0.8275	0.7056	0.046
H9B	0.9099	0.8096	0.7244	0.046
H9C	0.8357	0.7405	0.7550	0.046
H13	0.2485	0.6560	0.4418	0.047
H14	0.2752	0.7337	0.3497	0.052
H15	0.4096	0.8523	0.3613	0.045
H16	0.5243	0.8846	0.4626	0.037
H23	0.1851	0.7989	0.5178	0.043
H24	0.0903	0.8814	0.5814	0.050
H25	0.1443	0.8692	0.6938	0.049
H26	0.2954	0.7761	0.7449	0.040
H32	0.6215	0.8903	0.7202	0.036
H33	0.5652	1.0192	0.7768	0.046
H34	0.4071	1.1038	0.7289	0.048
H35	0.3124	1.0685	0.6215	0.048
H36	0.3732	0.9461	0.5622	0.035
H42	0.6797	0.7584	0.5061	0.038
H43	0.8259	0.8279	0.4785	0.046
H44	0.8977	0.9768	0.5234	0.043
H45	0.8286	1.0557	0.6009	0.050
H46	0.6799	0.9876	0.6282	0.037
H52	0.5434	0.7970	0.7883	0.051
H53	0.5527	0.8280	0.8981	0.054
H54	0.4891	0.7117	0.9571	0.051
H55	0.4070	0.5689	0.9073	0.053
H56	0.3897	0.5396	0.7980	0.046
H62	0.2400	0.5664	0.6794	0.050
H63	0.1625	0.4113	0.6527	0.064
H64	0.2632	0.2800	0.6283	0.063
H65	0.4414	0.3041	0.6345	0.066

H66	0.5215	0.4594	0.6619	0.052
-----	--------	--------	--------	-------

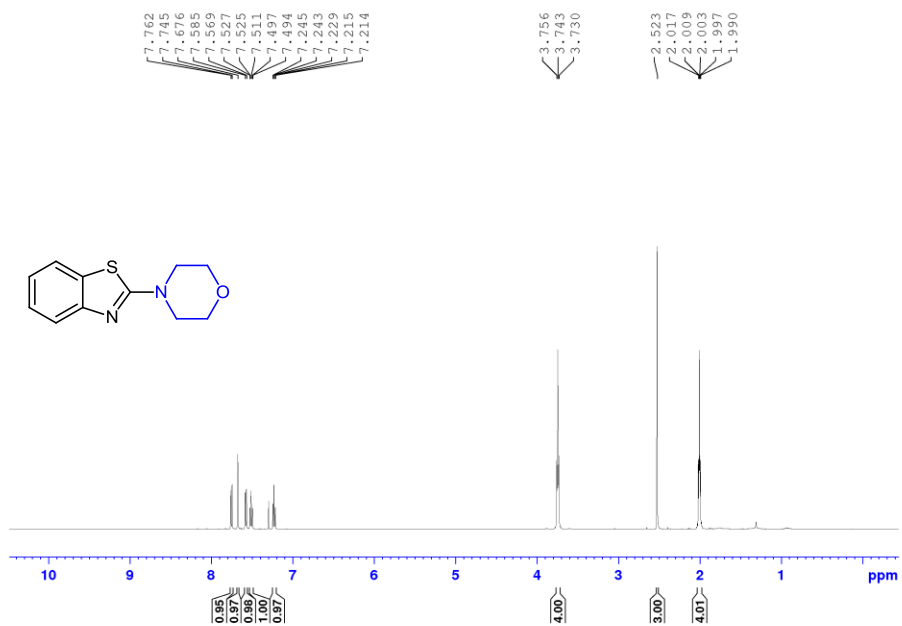
$^1\text{H}$  NMR of **C4-4a**, ( $\text{CDCl}_3$ , 500.1 MHz)



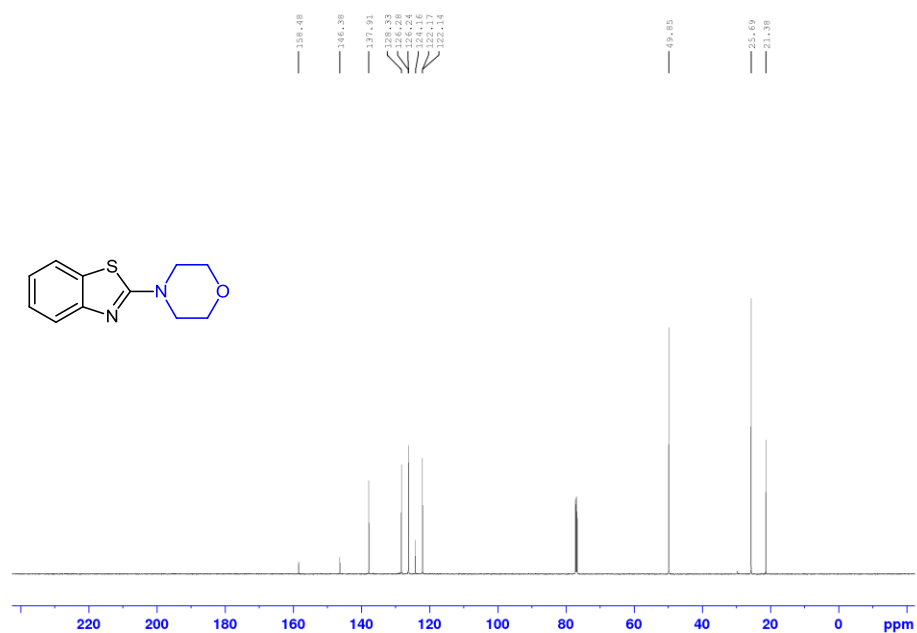
$^{13}\text{C}\{^1\text{H}\}$  NMR of **C4-4a**, ( $\text{CDCl}_3$ , 125.8 MHz)



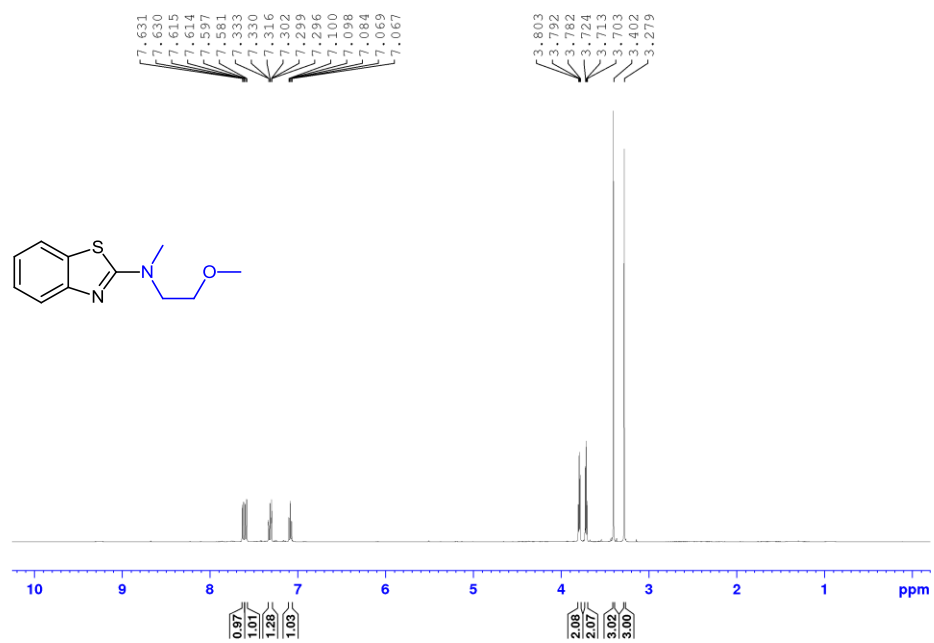
$^1\text{H}$  NMR of **C4-4b**, ( $\text{CDCl}_3$ , 500.1 MHz)



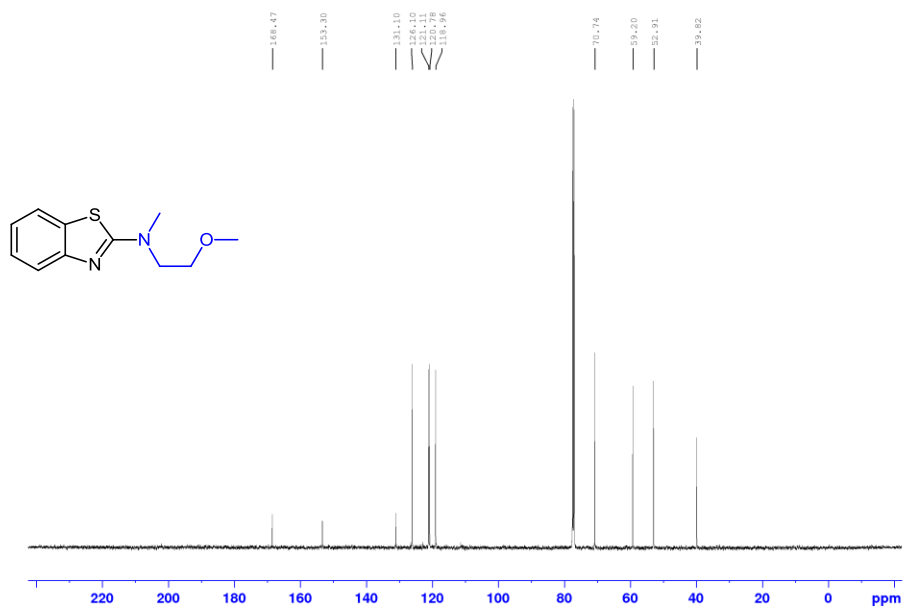
$^{13}\text{C}\{^1\text{H}\}$  NMR of **C4-4b**, ( $\text{CDCl}_3$ , 125.8 MHz)



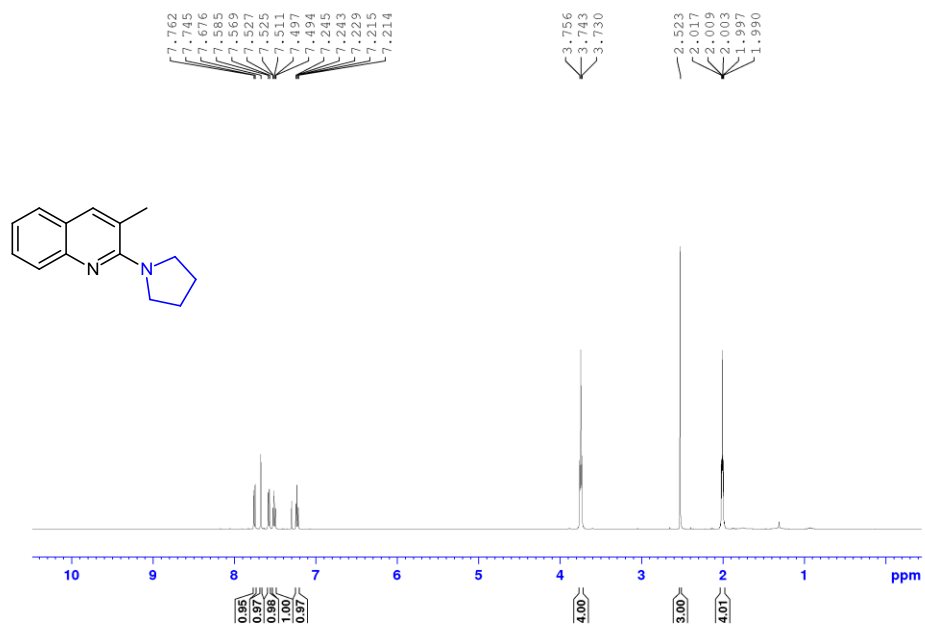
$^1\text{H}$  NMR of **C4-4c**, ( $\text{CDCl}_3$ , 500.1 MHz)



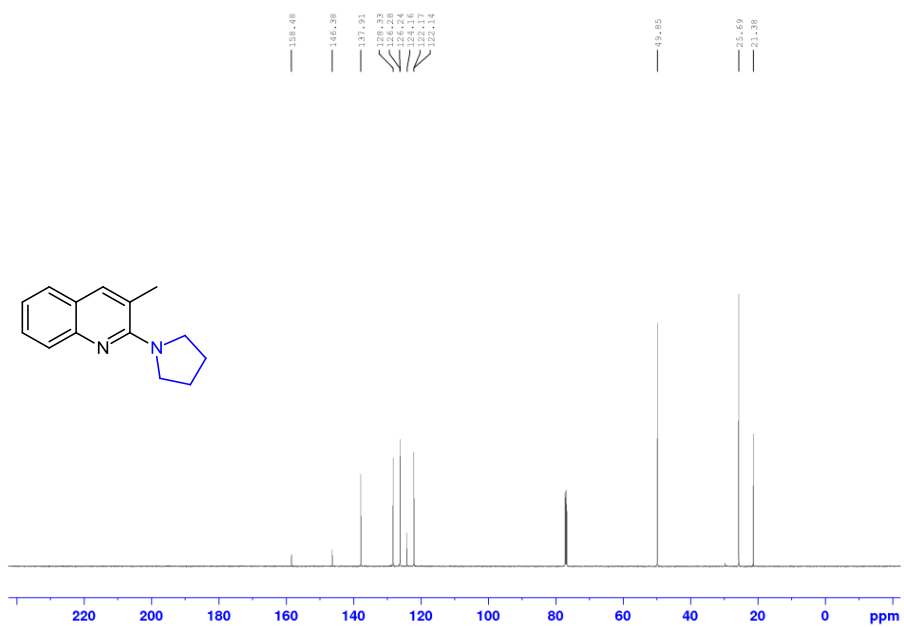
$^{13}\text{C}\{^1\text{H}\}$  NMR of **C4-4c**, ( $\text{CDCl}_3$ , 125.8 MHz)



$^1\text{H}$  NMR of **C4-4d**, ( $\text{CDCl}_3$ , 500.1 MHz)

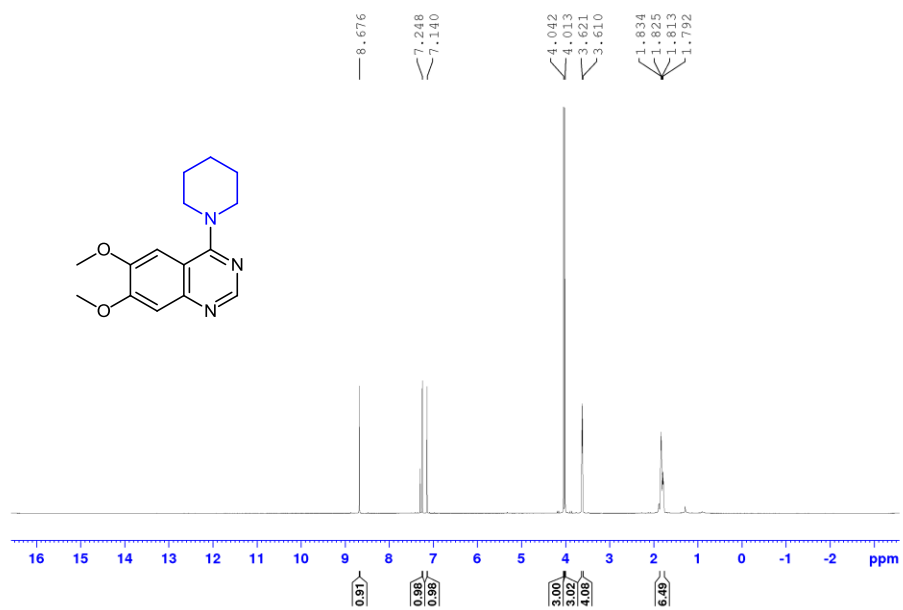


$^{13}\text{C}\{^1\text{H}\}$  NMR of **C4-4d**, ( $\text{CDCl}_3$ , 125.8 MHz)

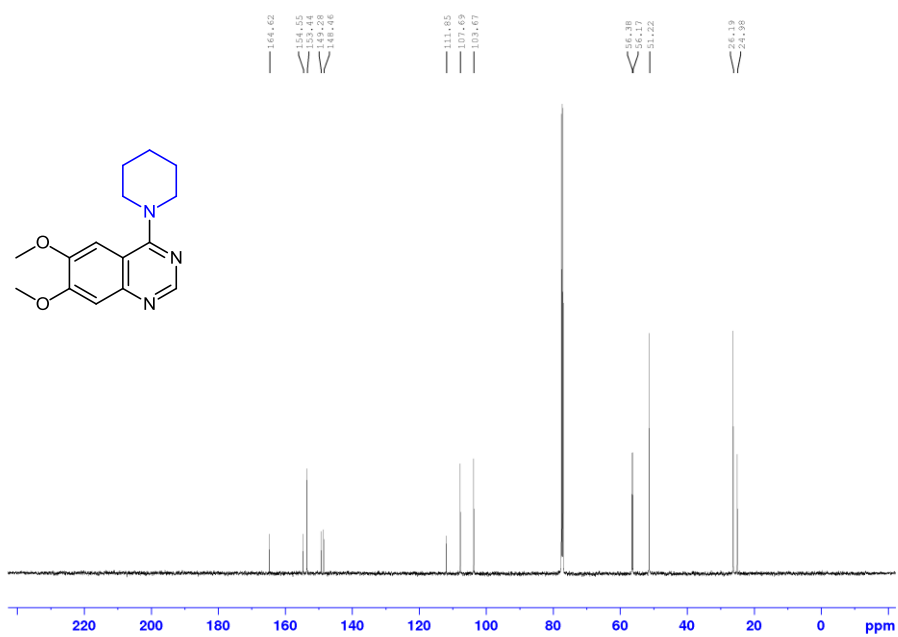




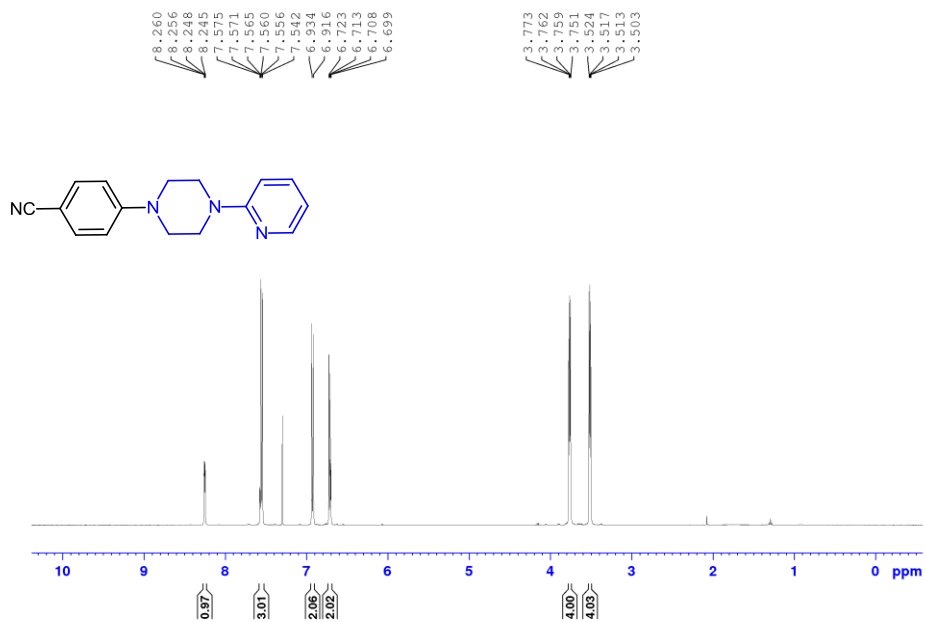
$^1\text{H}$  NMR of **C4-4e**, ( $\text{CDCl}_3$ , 500.1 MHz)



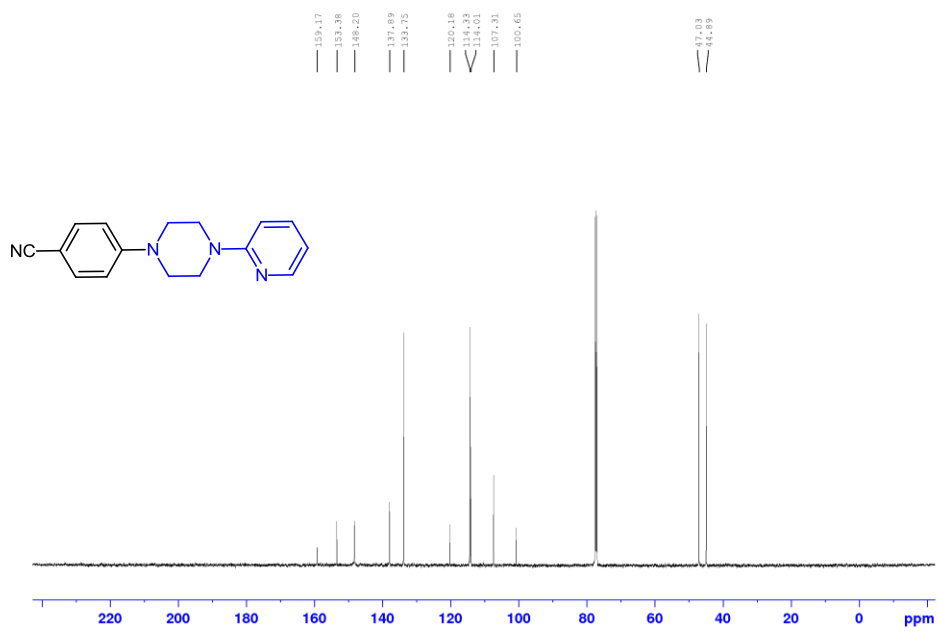
$^{13}\text{C}\{^1\text{H}\}$  NMR of **C4-4e**, ( $\text{CDCl}_3$ , 125.8 MHz)



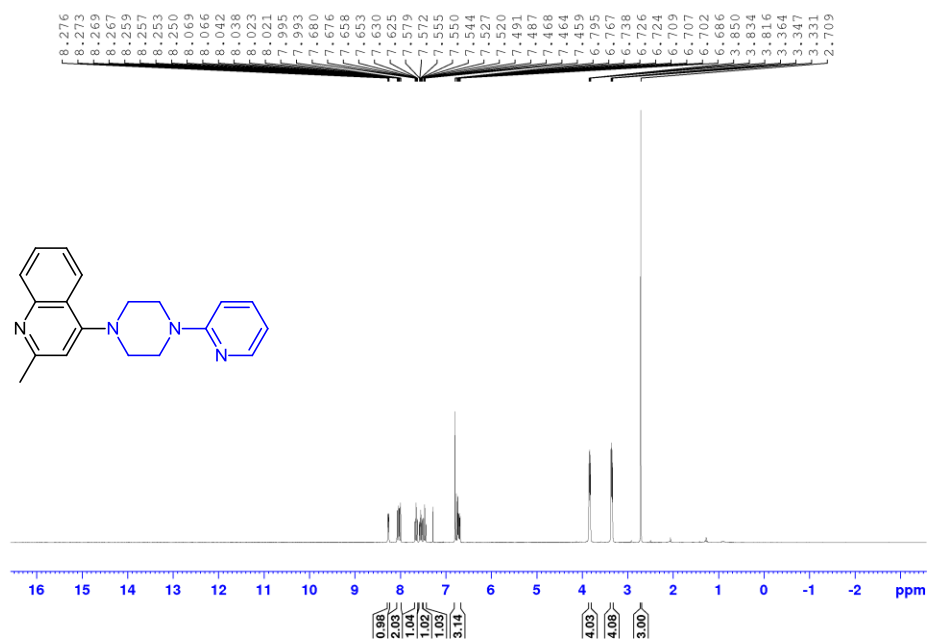
$^1\text{H}$  NMR of **C4-4f**, ( $\text{CDCl}_3$ , 500.1 MHz)



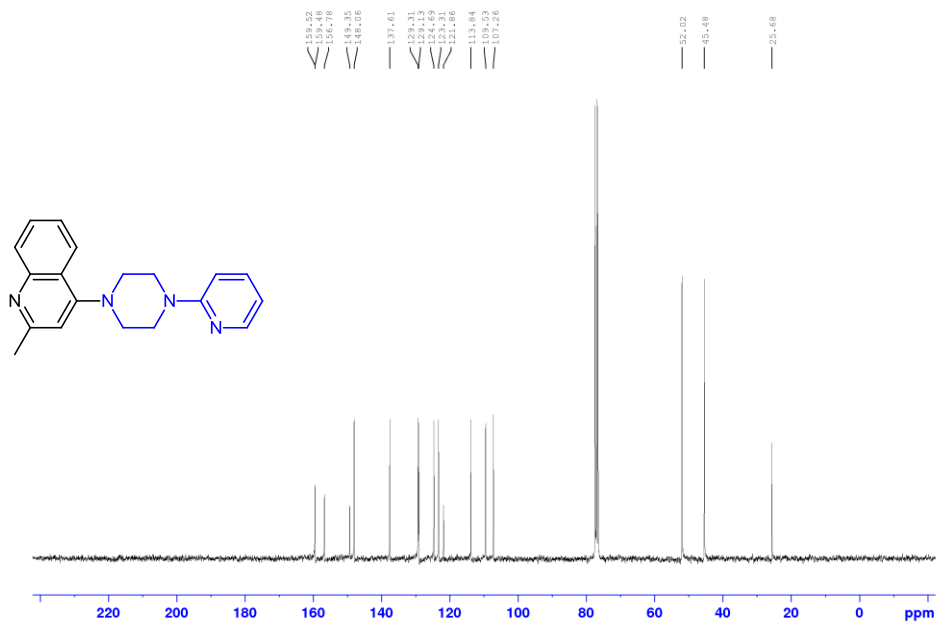
$^{13}\text{C}\{^1\text{H}\}$  NMR of **C4-4f**, ( $\text{CDCl}_3$ , 125.8 MHz)



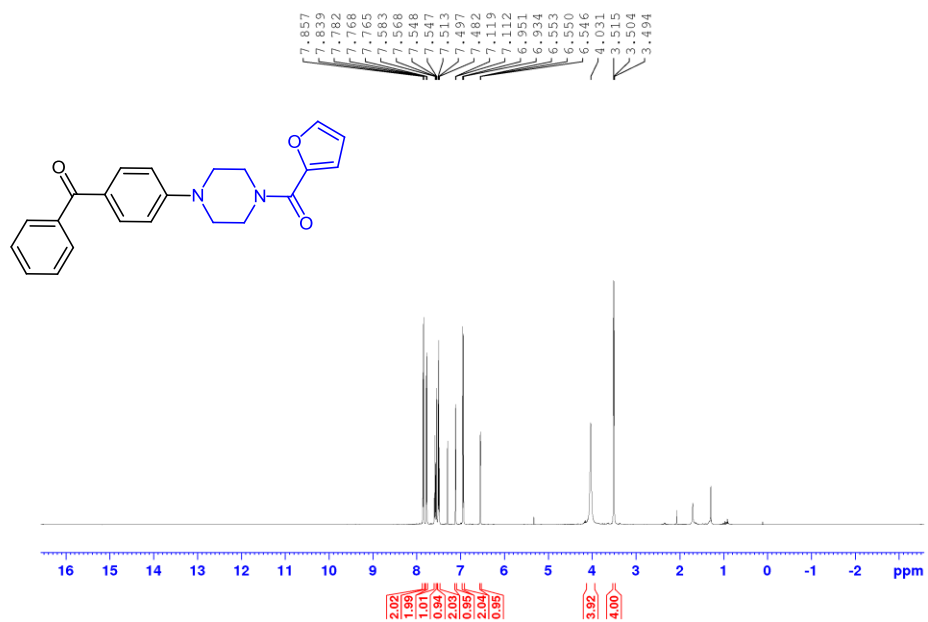
$^1\text{H}$  NMR of **C4-4g**, ( $\text{CDCl}_3$ , 500.1 MHz)



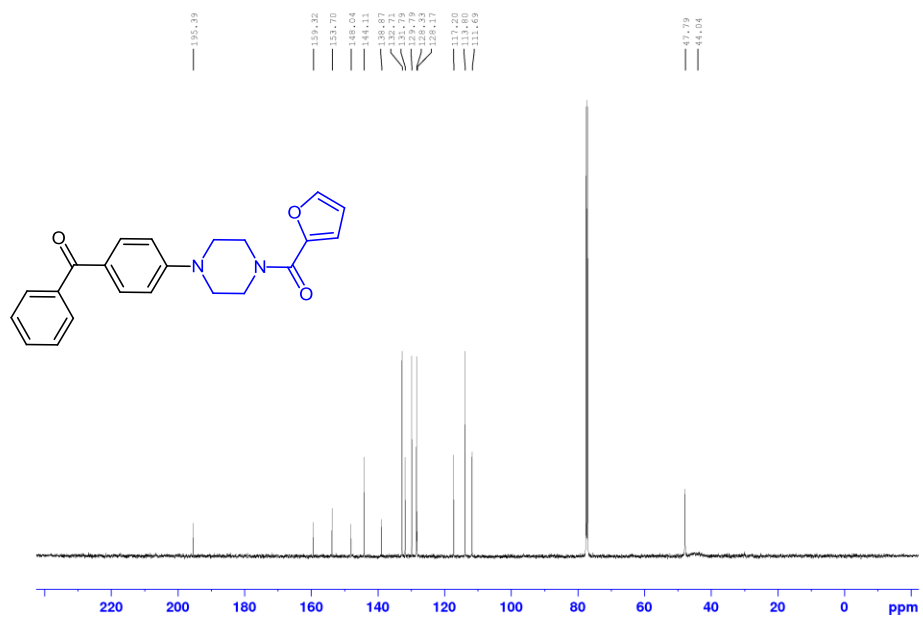
$^{13}\text{C}\{^1\text{H}\}$  NMR of **C4-4g**, ( $\text{CDCl}_3$ , 125.8 MHz)



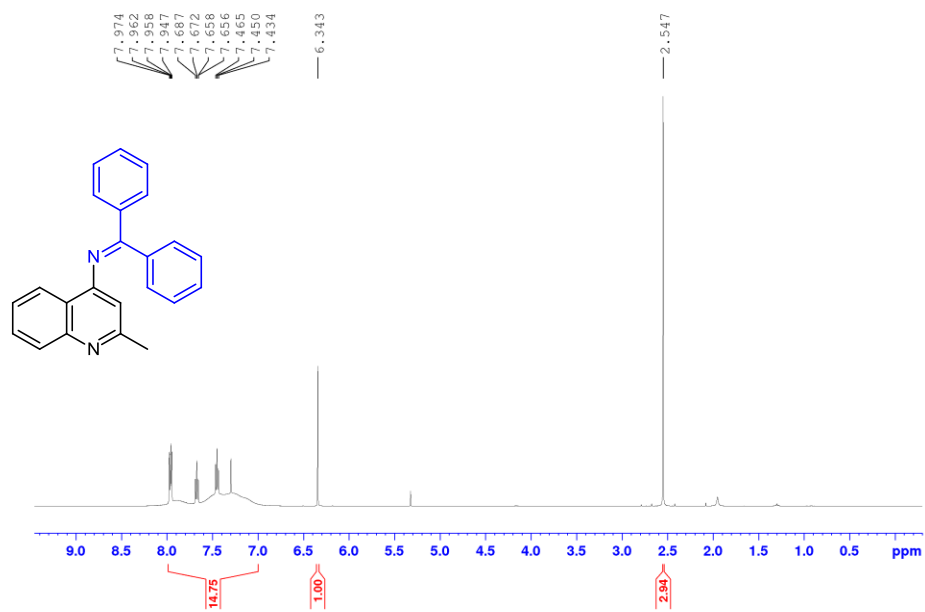
$^1\text{H}$  NMR of **C4-4h**, ( $\text{CDCl}_3$ , 500.1 MHz)



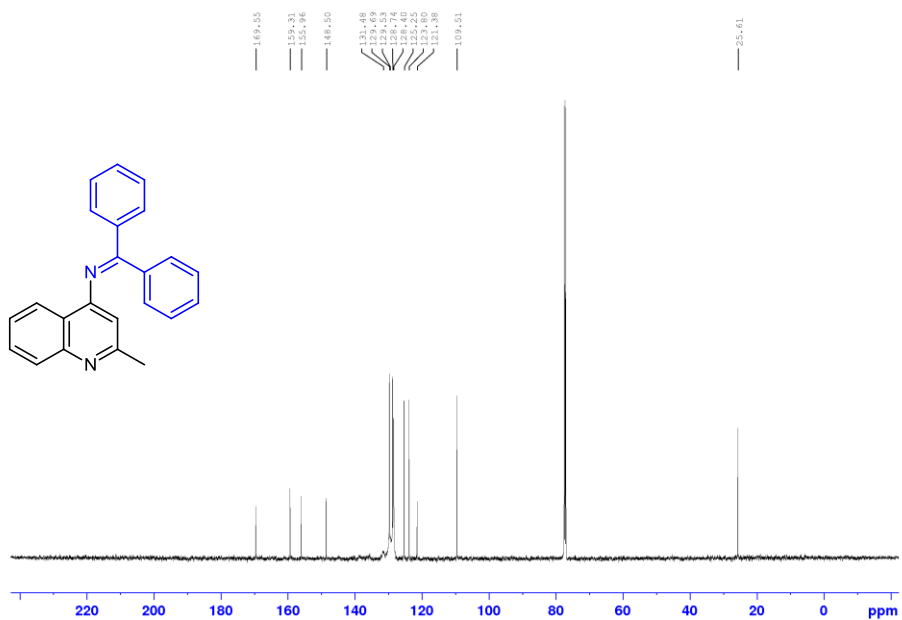
$^{13}\text{C}\{^1\text{H}\}$  NMR of **C4-4h**, ( $\text{CDCl}_3$ , 125.8 MHz)



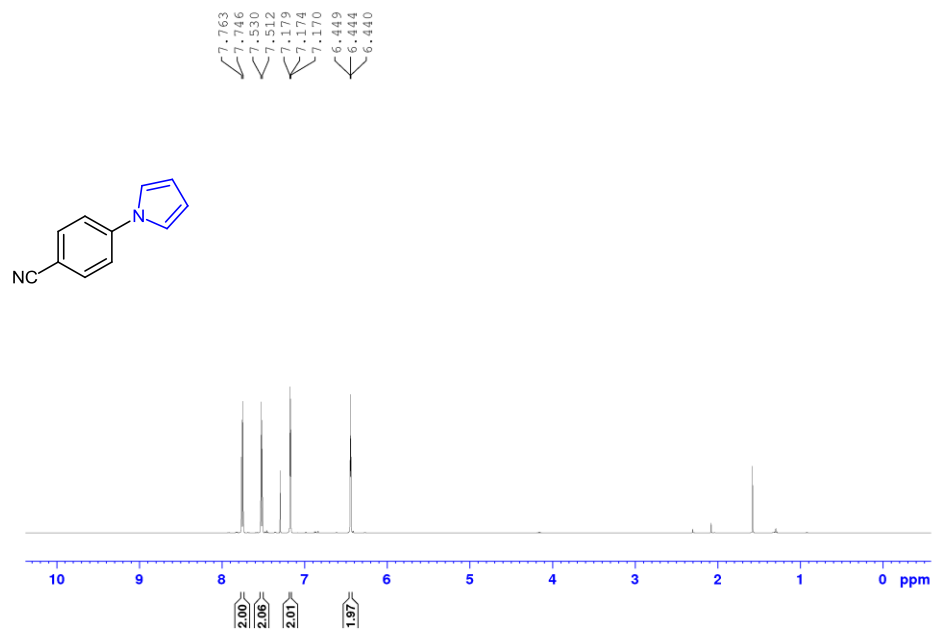
$^1\text{H}$  NMR of **C4-4i**, ( $\text{CDCl}_3$ , 500.1 MHz)



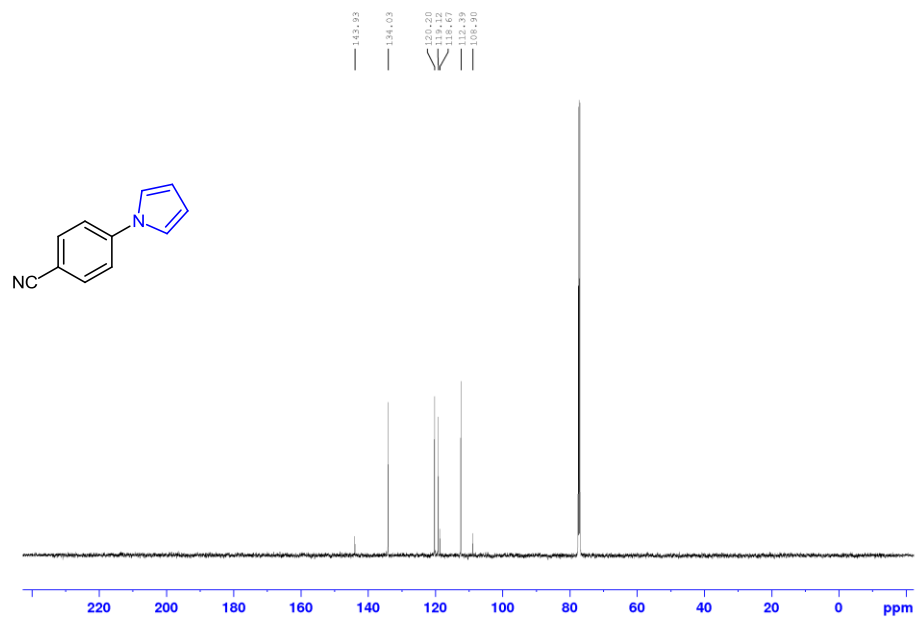
$^{13}\text{C}\{^1\text{H}\}$  NMR of **C4-4i**, ( $\text{CDCl}_3$ , 125.8 MHz)



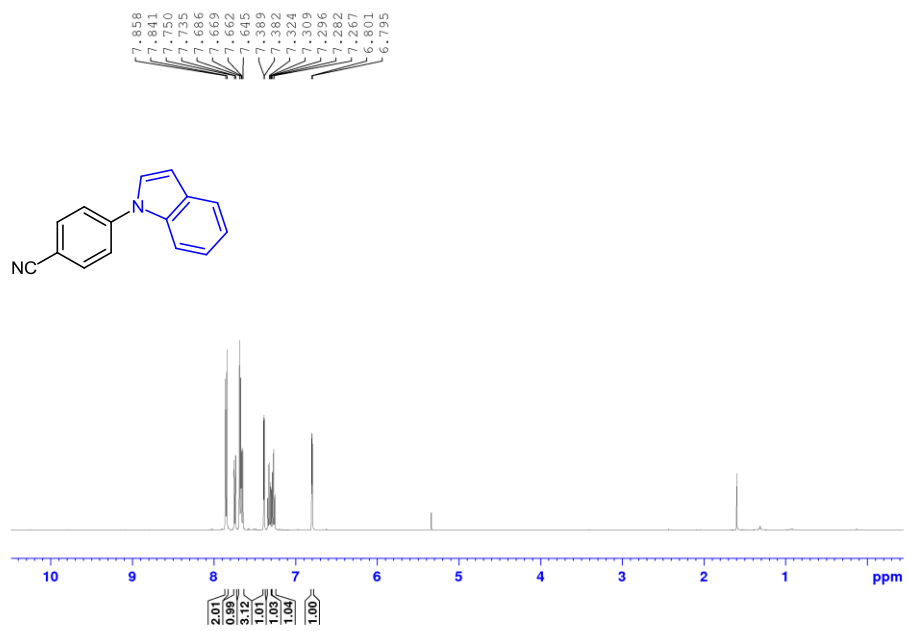
$^1\text{H}$  NMR of **C4-4j**, ( $\text{CDCl}_3$ , 500.1 MHz)



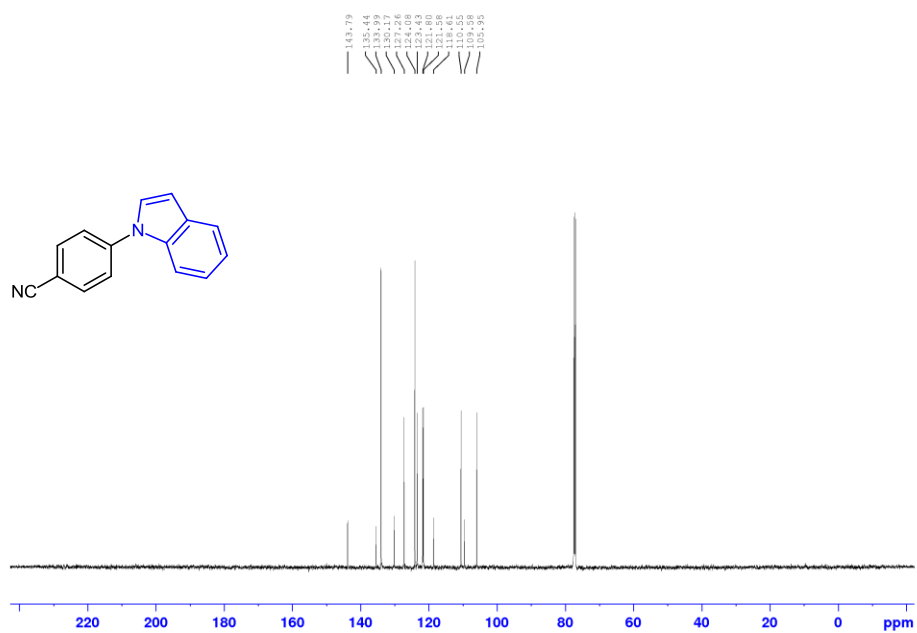
$^{13}\text{C}\{^1\text{H}\}$  NMR of **C4-4j**, ( $\text{CDCl}_3$ , 125.8 MHz)



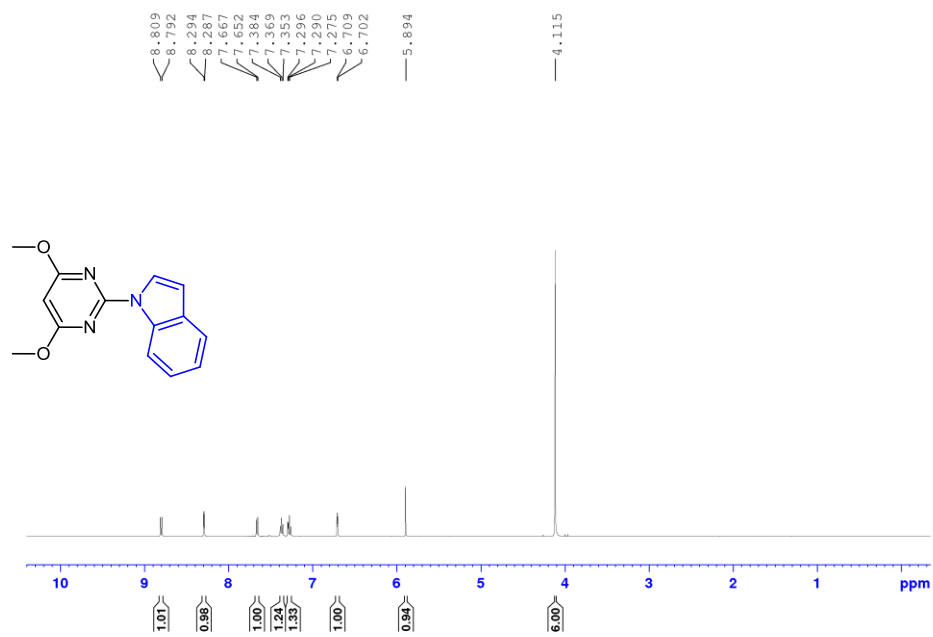
$^1\text{H}$  NMR of **C4-4k**, ( $\text{CDCl}_3$ , 500.1 MHz)



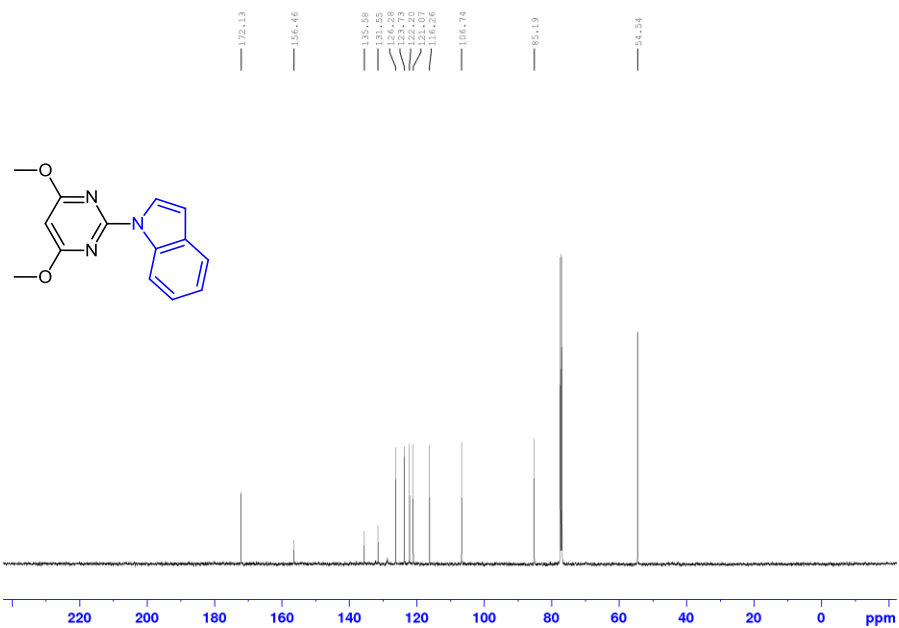
$^{13}\text{C}\{^1\text{H}\}$  NMR of **C4-4k**, ( $\text{CDCl}_3$ , 125.8 MHz)



$^1\text{H}$  NMR of **C4-4I**, ( $\text{CDCl}_3$ , 500.1 MHz)

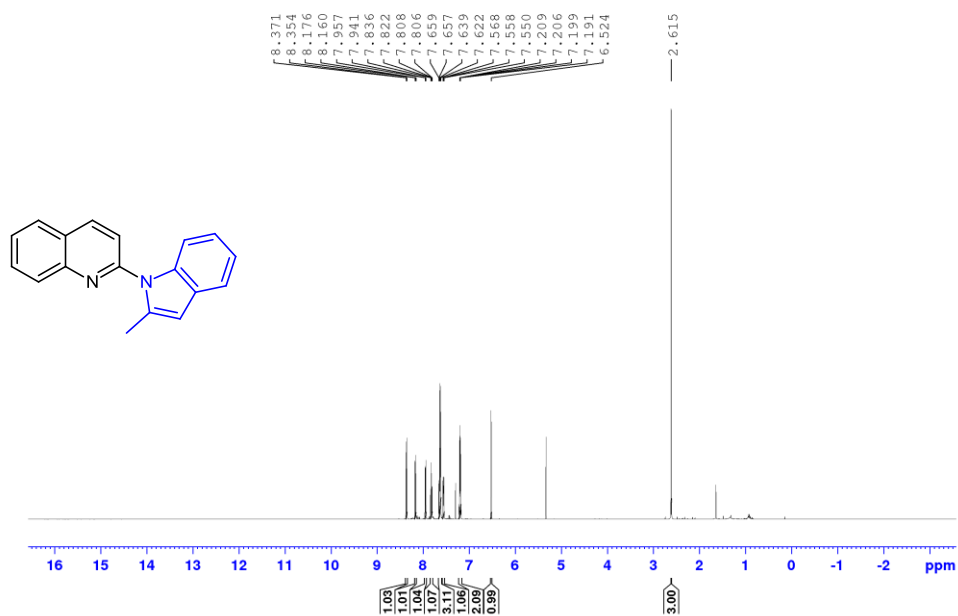


$^{13}\text{C}\{^1\text{H}\}$  NMR of **C4-4I**, ( $\text{CDCl}_3$ , 125.8 MHz)

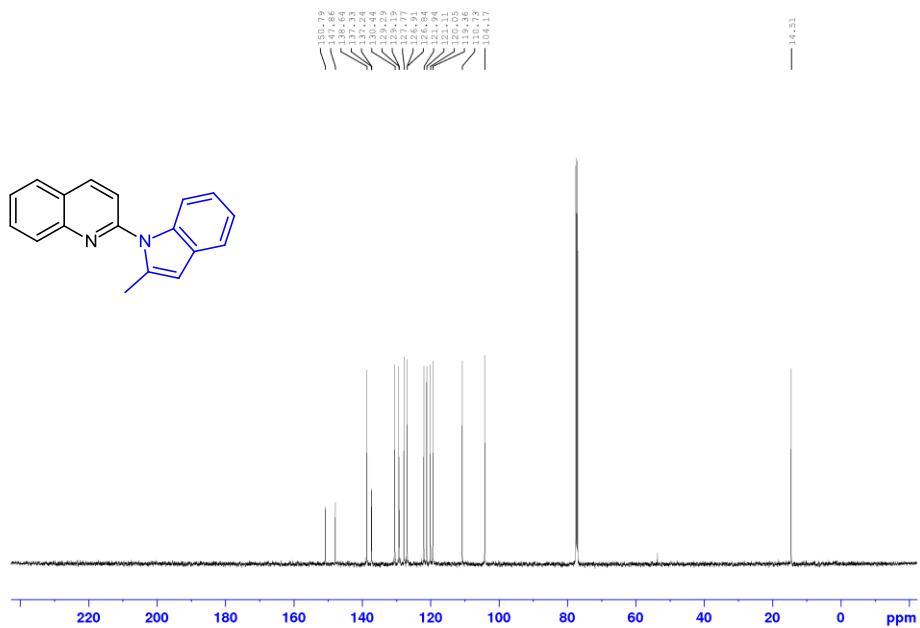




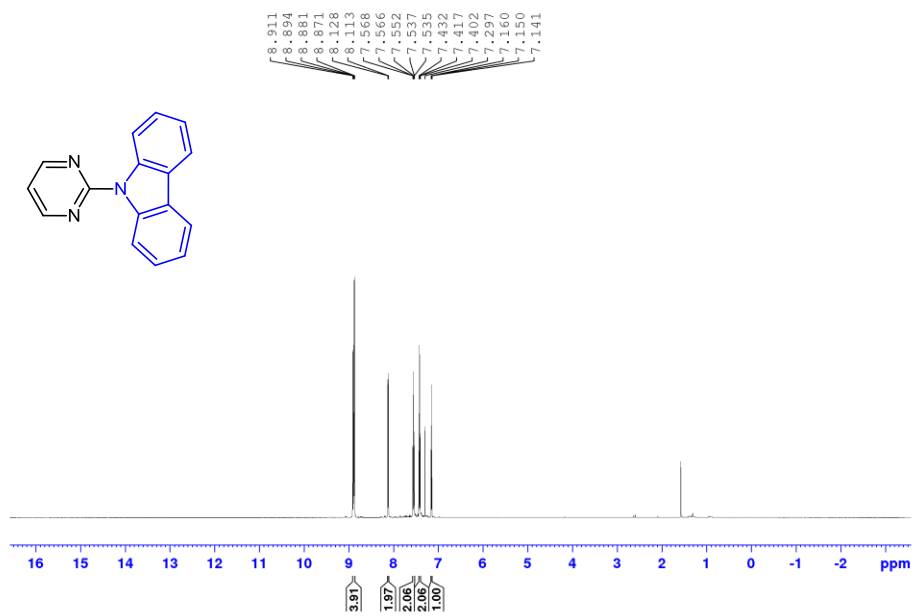
$^1\text{H}$  NMR of **C4-4m**, ( $\text{CDCl}_3$ , 500.1 MHz)



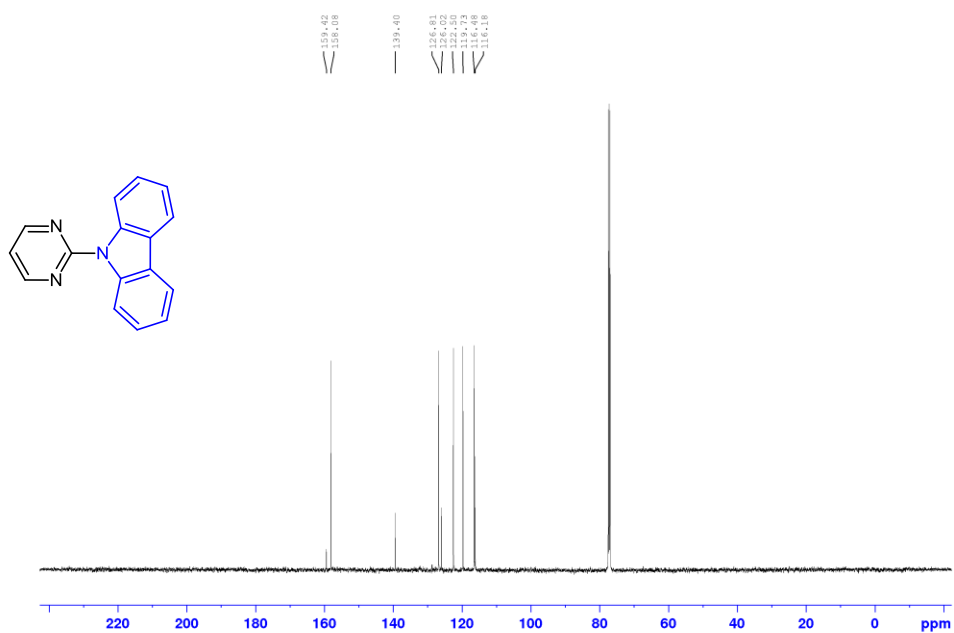
$^{13}\text{C}\{^1\text{H}\}$  NMR of **C4-4m**, ( $\text{CDCl}_3$ , 125.8 MHz)



$^1\text{H}$  NMR of **C4-4n**, ( $\text{CDCl}_3$ , 500.1 MHz)

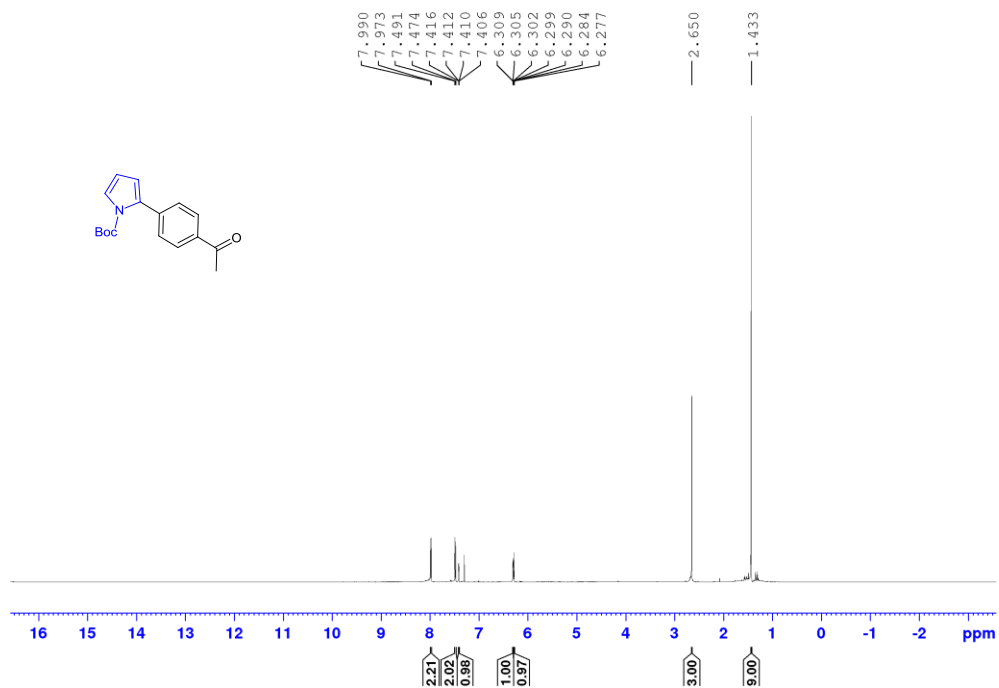


$^{13}\text{C}\{^1\text{H}\}$  NMR of **C4-4n**, ( $\text{CDCl}_3$ , 125.8 MHz)



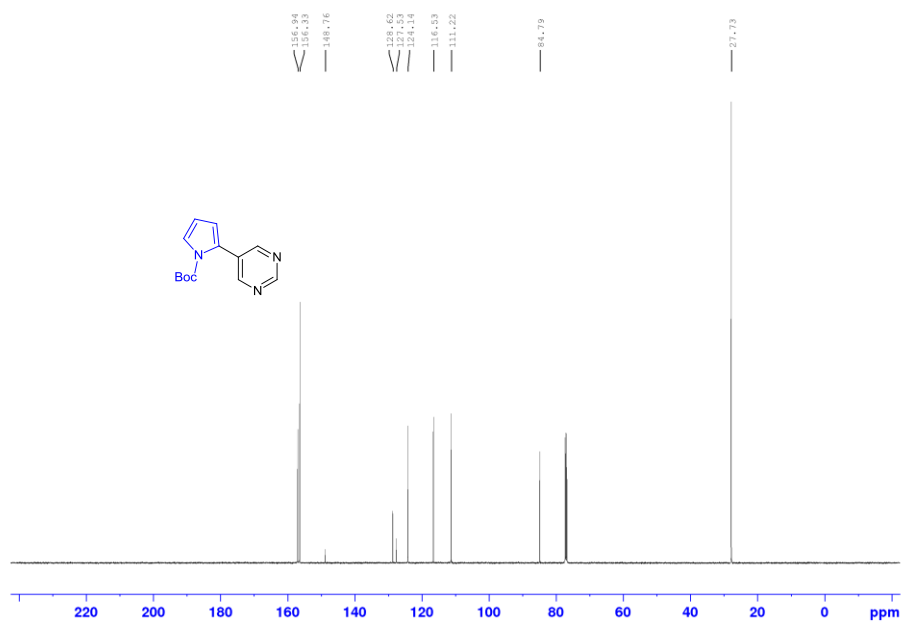
## Chapter 5 Characterization Data

$^1\text{H}$  NMR of **5-2a**, ( $\text{CDCl}_3$ , 500.1 MHz)

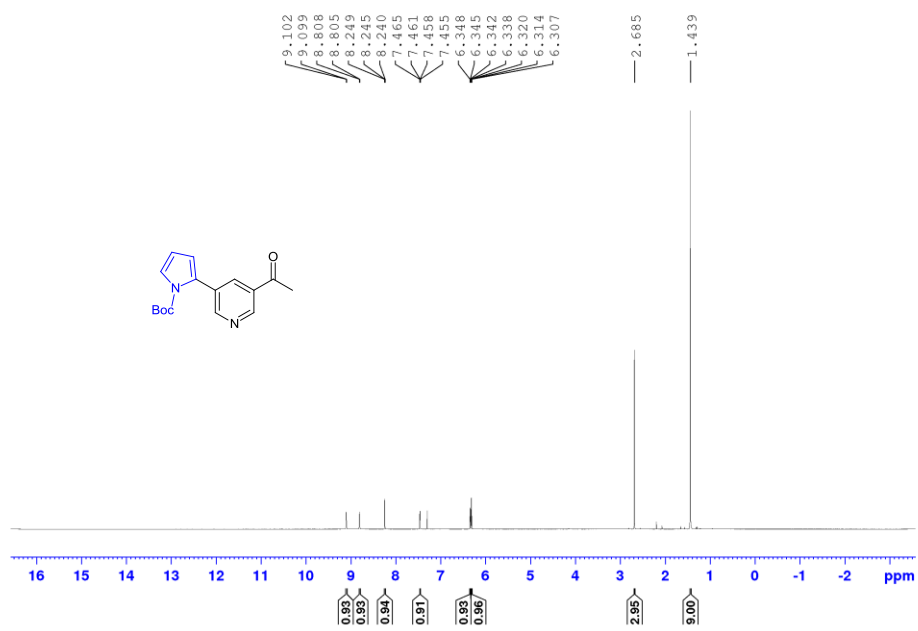




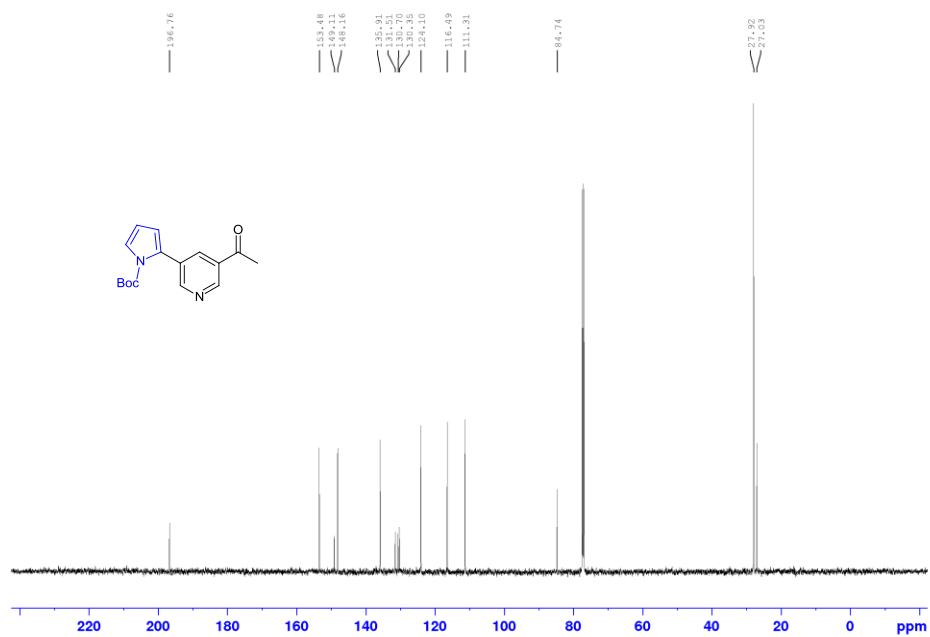
$^{13}\text{C}\{^1\text{H}\}$  NMR of **5-2b**, ( $\text{CDCl}_3$ , 125.8 MHz)



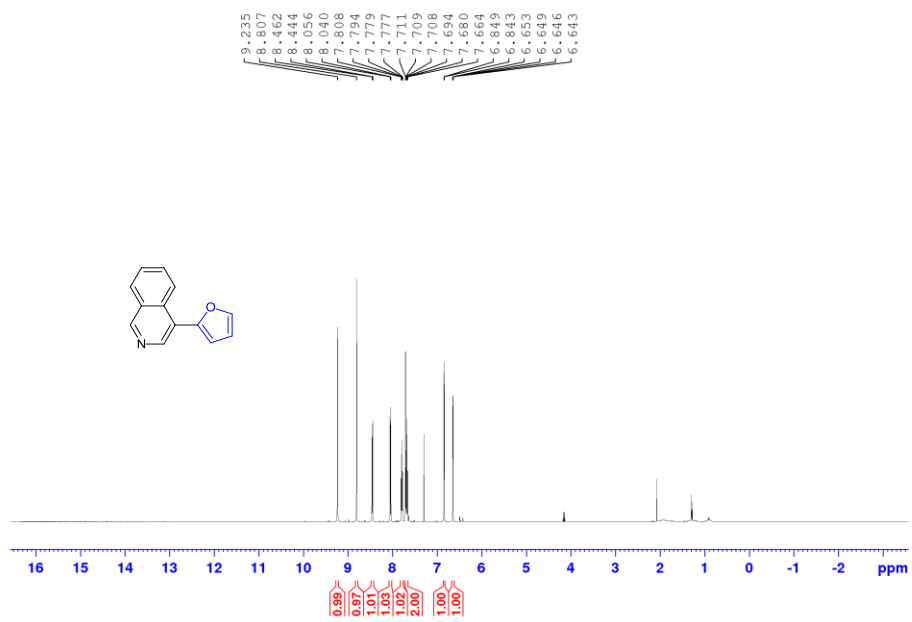
$^1\text{H}$  NMR of **5-2c**, ( $\text{CDCl}_3$ , 500.1 MHz)



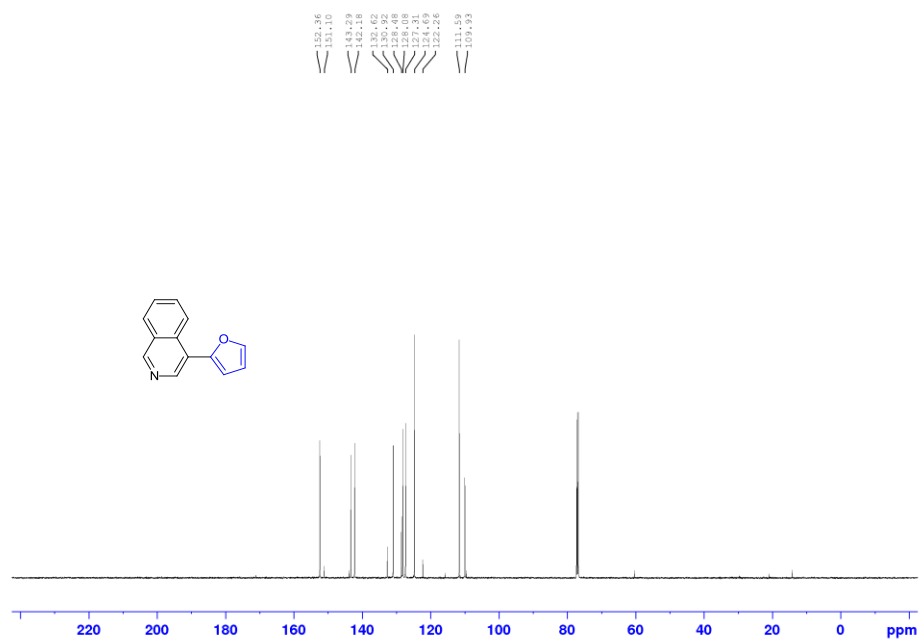
$^{13}\text{C}\{^1\text{H}\}$  NMR of **5-2c**, ( $\text{CDCl}_3$ , 125.8 MHz)



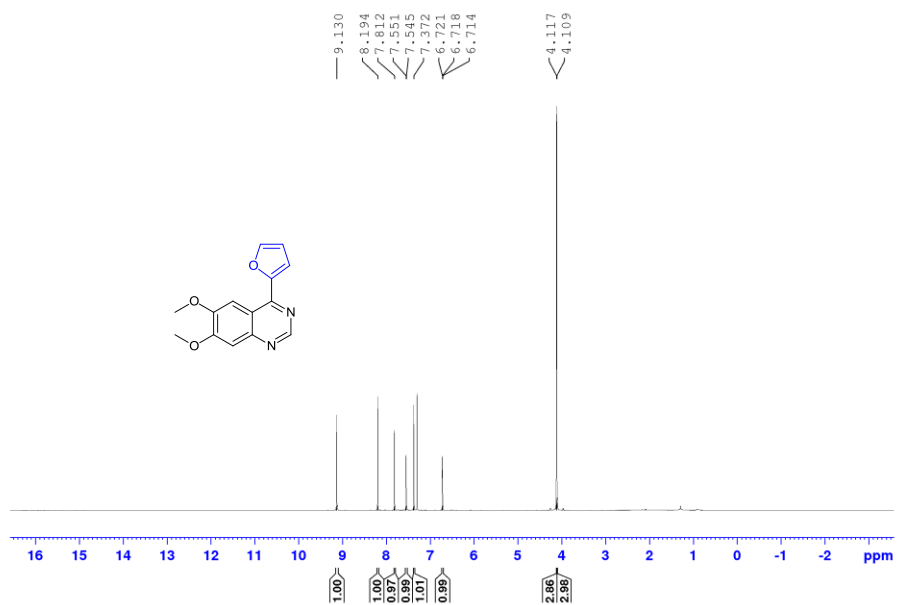
$^1\text{H}$  NMR of **5-2d**, ( $\text{CDCl}_3$ , 500.1 MHz)



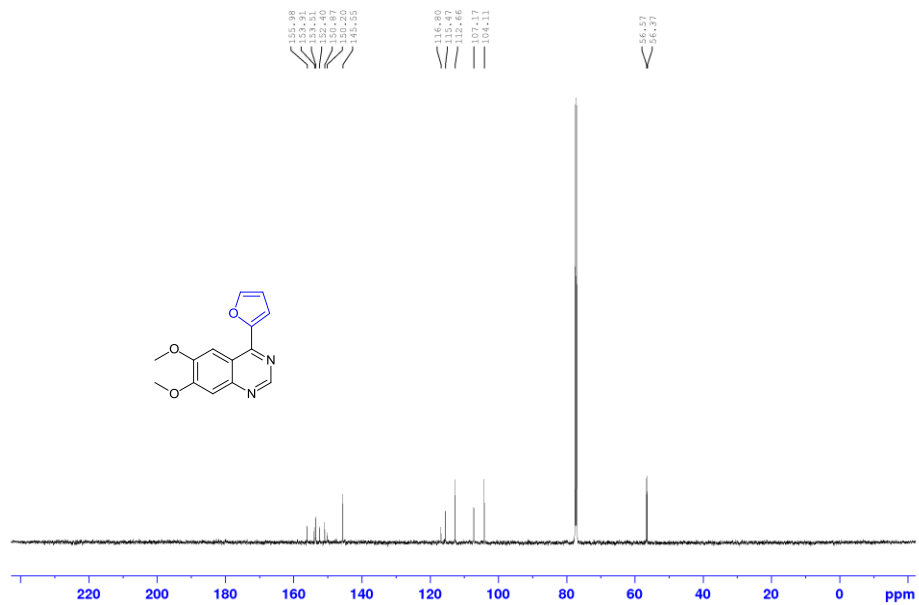
$^{13}\text{C}\{^1\text{H}\}$  NMR of **5-2d**, ( $\text{CDCl}_3$ , 125.8 MHz)



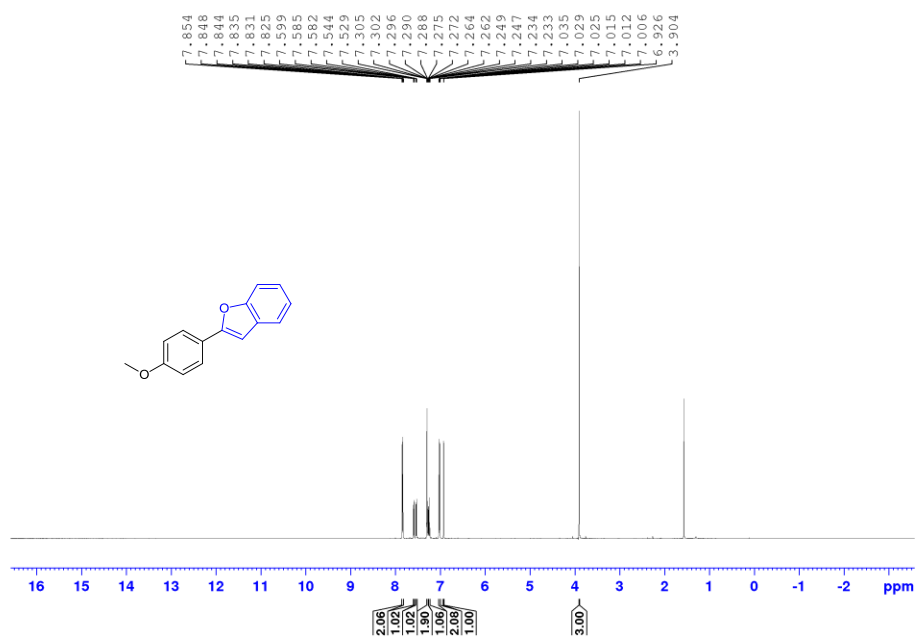
$^1\text{H}$  NMR of **5-2e**, ( $\text{CDCl}_3$ , 500.1 MHz)



$^{13}\text{C}\{^1\text{H}\}$  NMR of **5-2e**, ( $\text{CDCl}_3$ , 125.8 MHz)

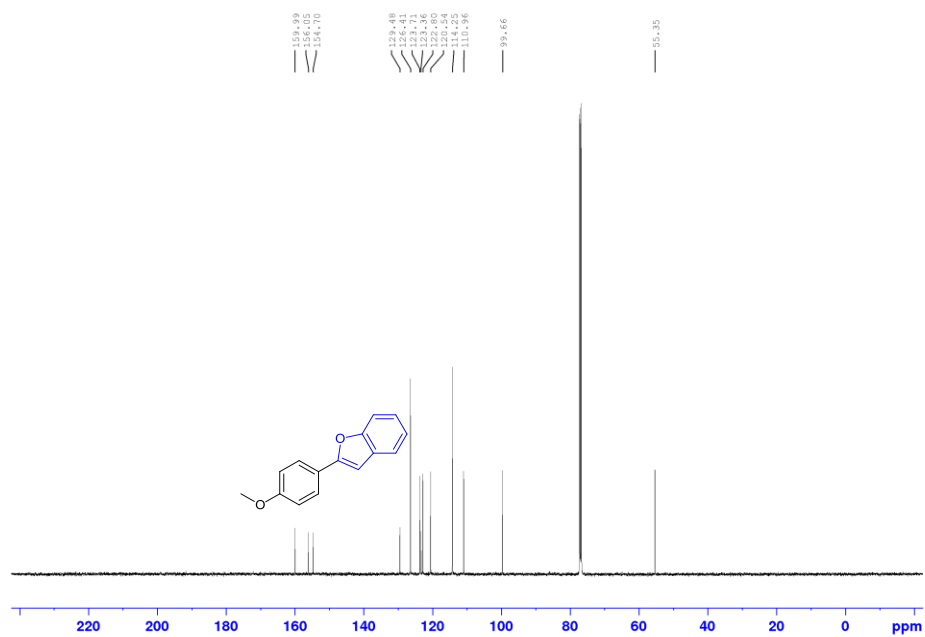


$^1\text{H}$  NMR of **5-2f**, ( $\text{CDCl}_3$ , 500.1 MHz)

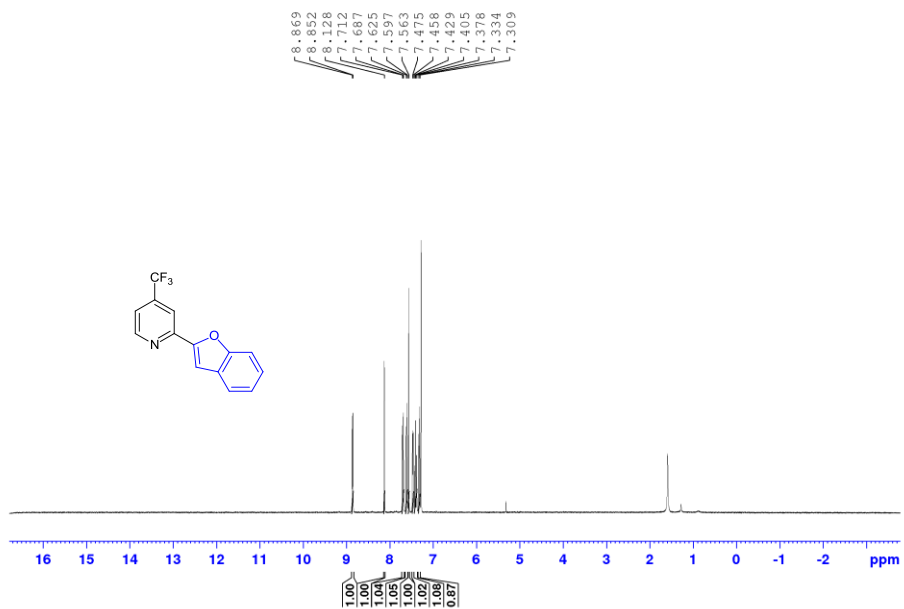




$^{13}\text{C}\{^1\text{H}\}$  NMR of **5-2f**, ( $\text{CDCl}_3$ , 125.8 MHz)



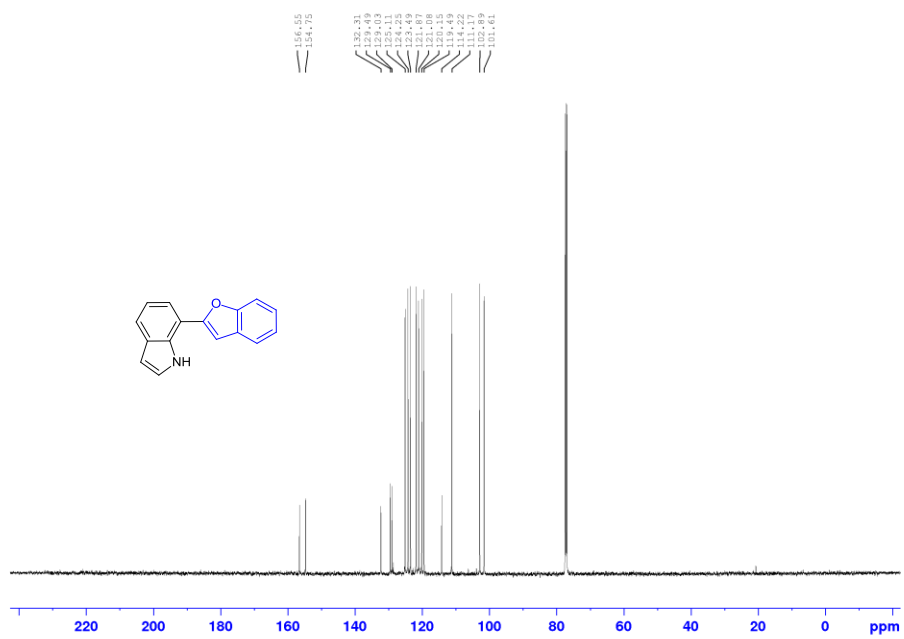
$^1\text{H}$  NMR of **5-2g**, ( $\text{CDCl}_3$ , 300.1 MHz)



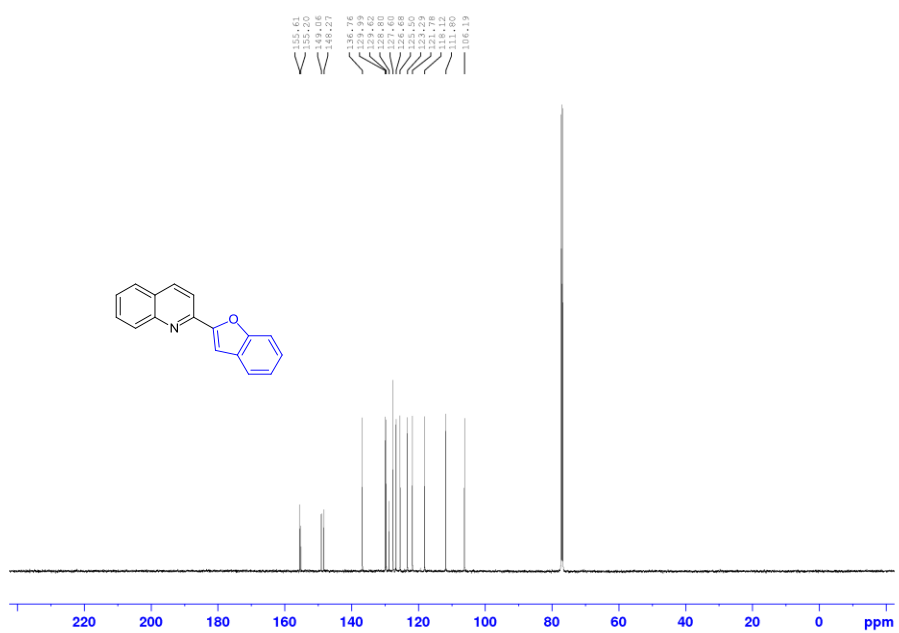




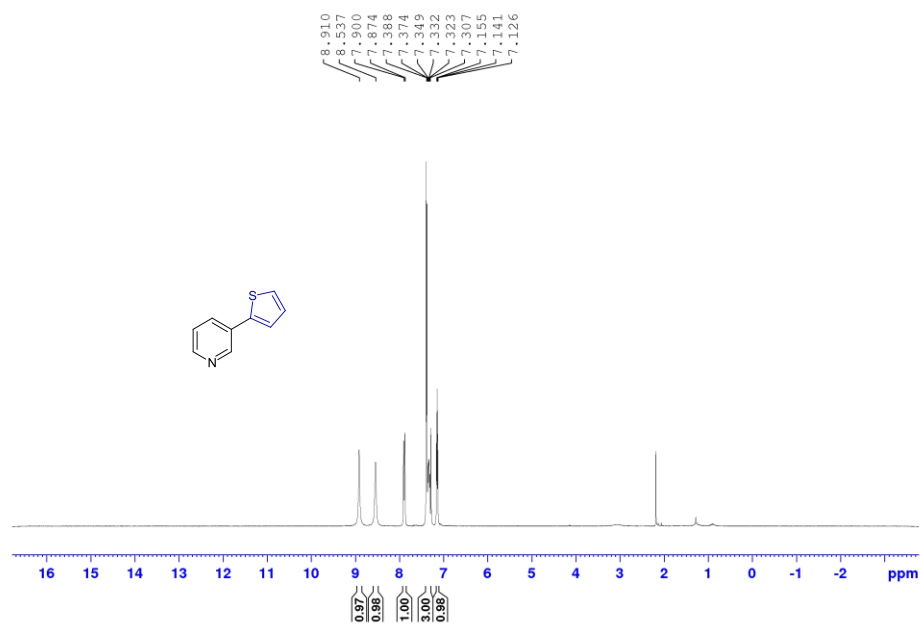
$^{13}\text{C}\{^1\text{H}\}$  NMR of **5-2h**, ( $\text{CDCl}_3$ , 125.8 MHz)



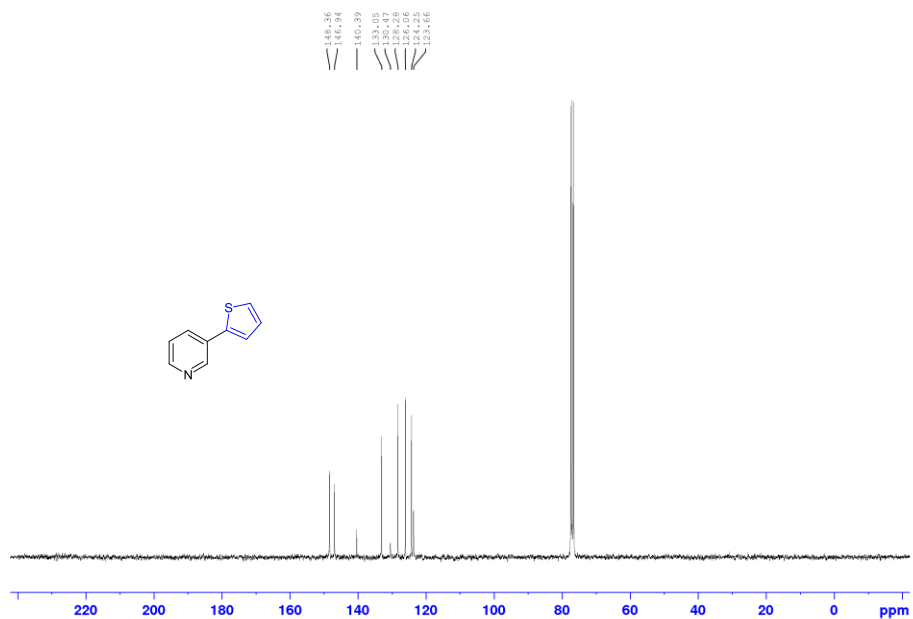
$^{13}\text{C}\{^1\text{H}\}$  NMR of **5-2i**, ( $\text{CDCl}_3$ , 125.8 MHz)



$^1\text{H}$  NMR of **5-2j**, ( $\text{CDCl}_3$ , 500.1 MHz)

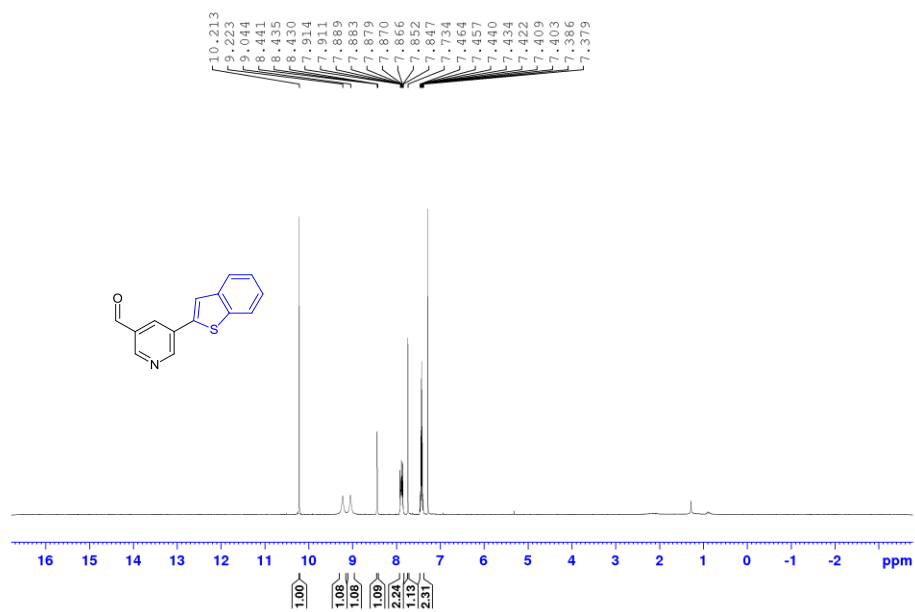


$^{13}\text{C}\{^1\text{H}\}$  NMR of **5-2j** ( $\text{CDCl}_3$ , 75.4 MHz)

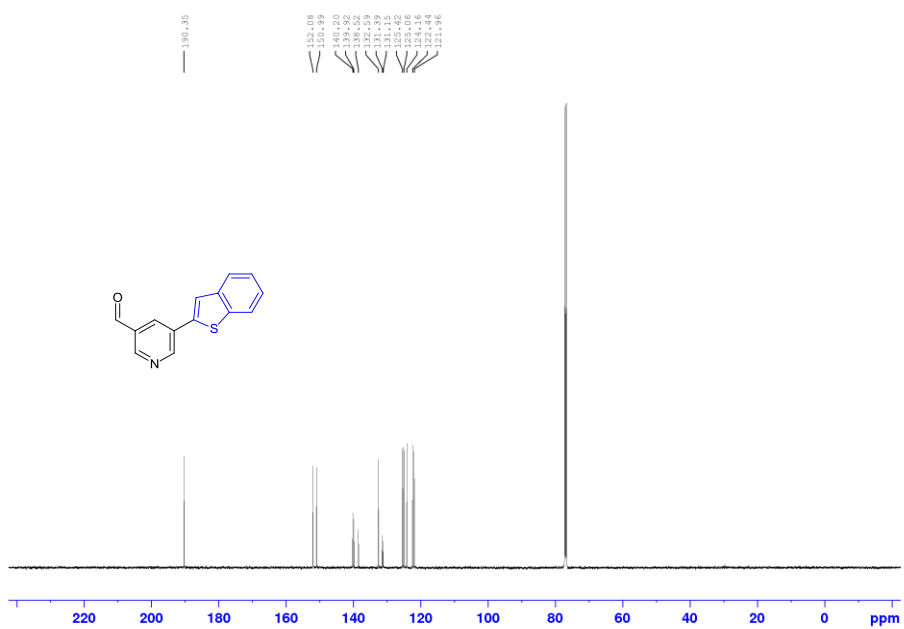




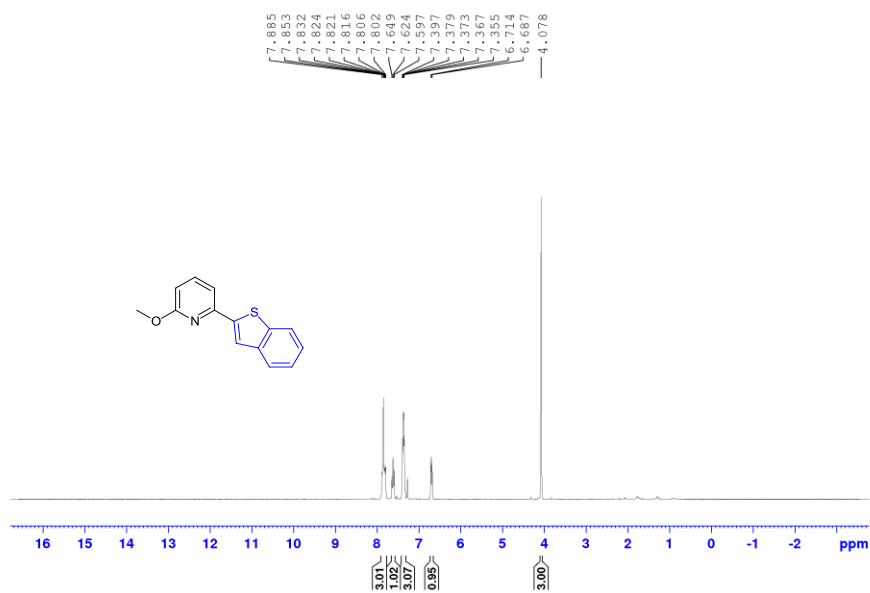
$^1\text{H}$  NMR of **5-21**, ( $\text{CDCl}_3$ , 300.1 MHz)



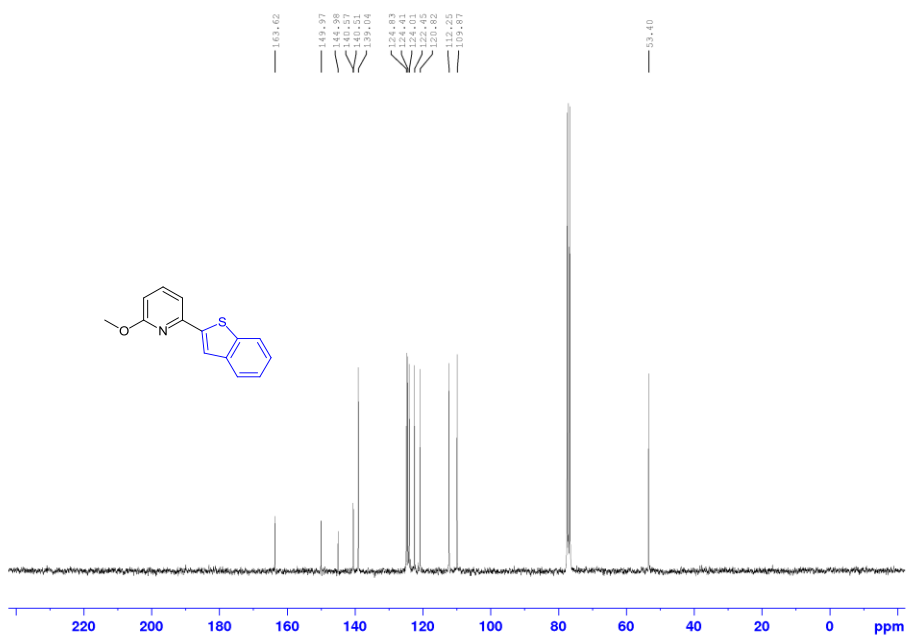
$^{13}\text{C}\{^1\text{H}\}$  NMR of **5-21** ( $\text{CDCl}_3$ , 125.8 MHz)



$^1\text{H}$  NMR of **5-2m**, ( $\text{CDCl}_3$ , 300.1 MHz)

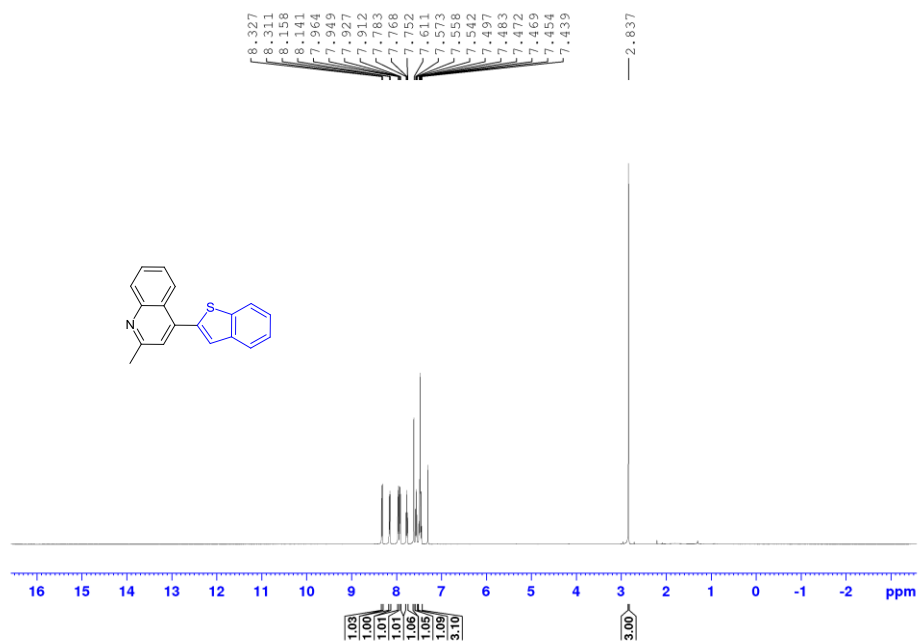


$^{13}\text{C}\{^1\text{H}\}$  NMR of **5-2m** ( $\text{CDCl}_3$ , 75.4 MHz)

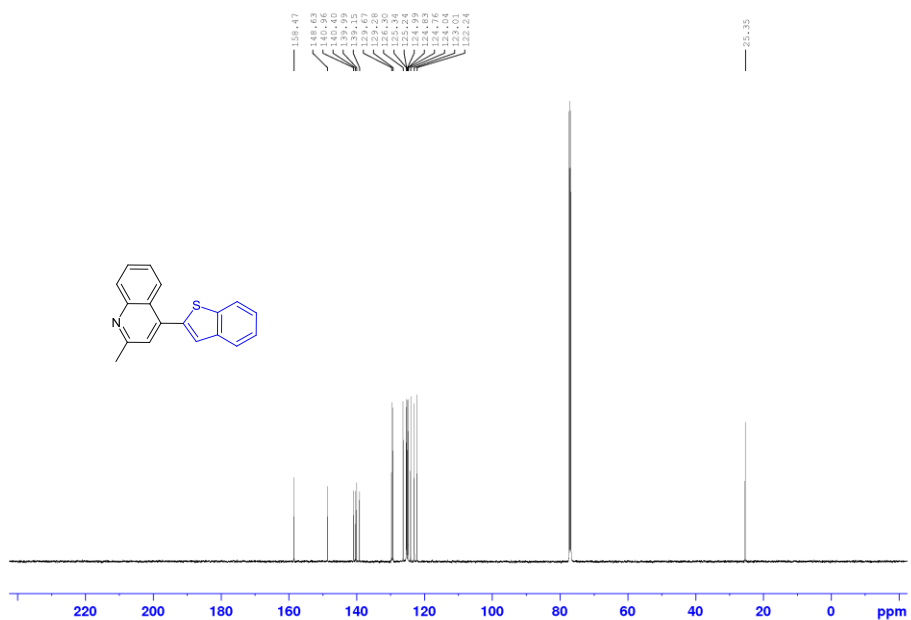




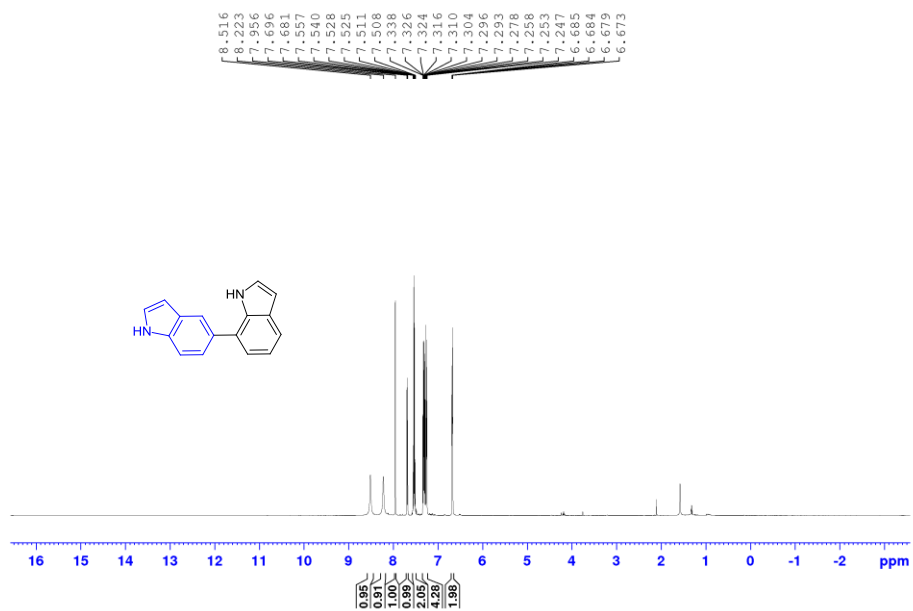
$^1\text{H}$  NMR of **5-2n**, ( $\text{CDCl}_3$ , 500.1 MHz)



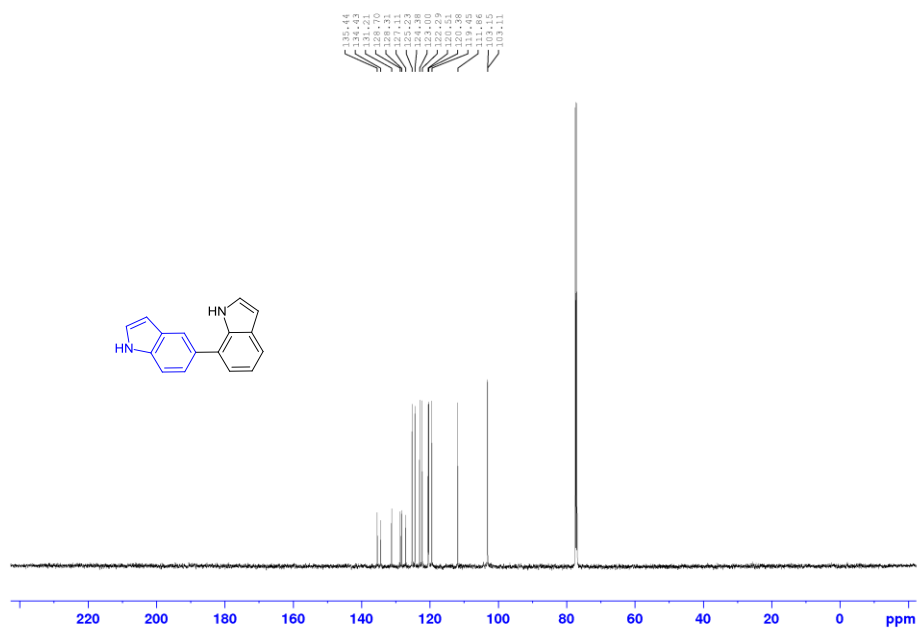
$^{13}\text{C}\{^1\text{H}\}$  NMR of **5-2n** ( $\text{CDCl}_3$ , 125.8 MHz)



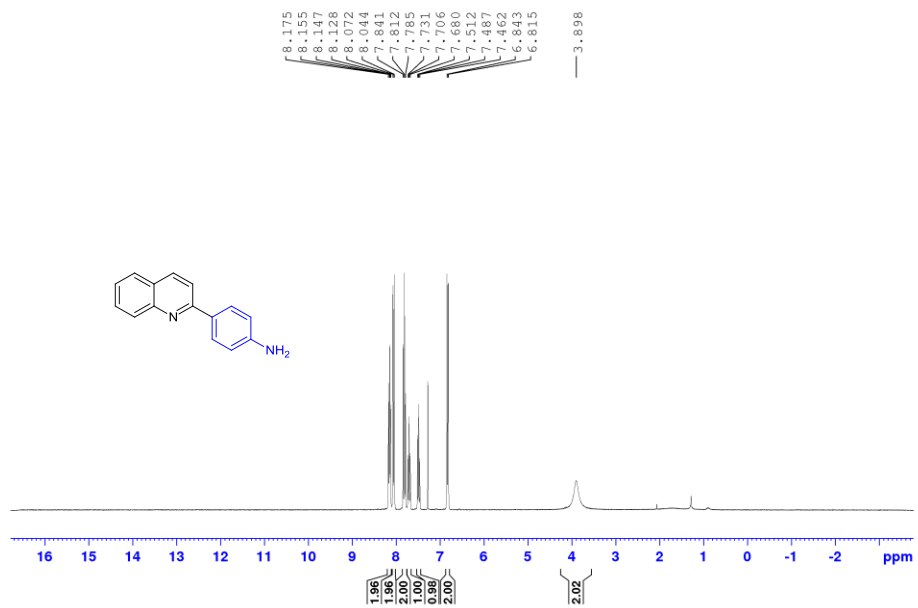
$^1\text{H}$  NMR of **5-2o**, ( $\text{CDCl}_3$ , 500.1 MHz)



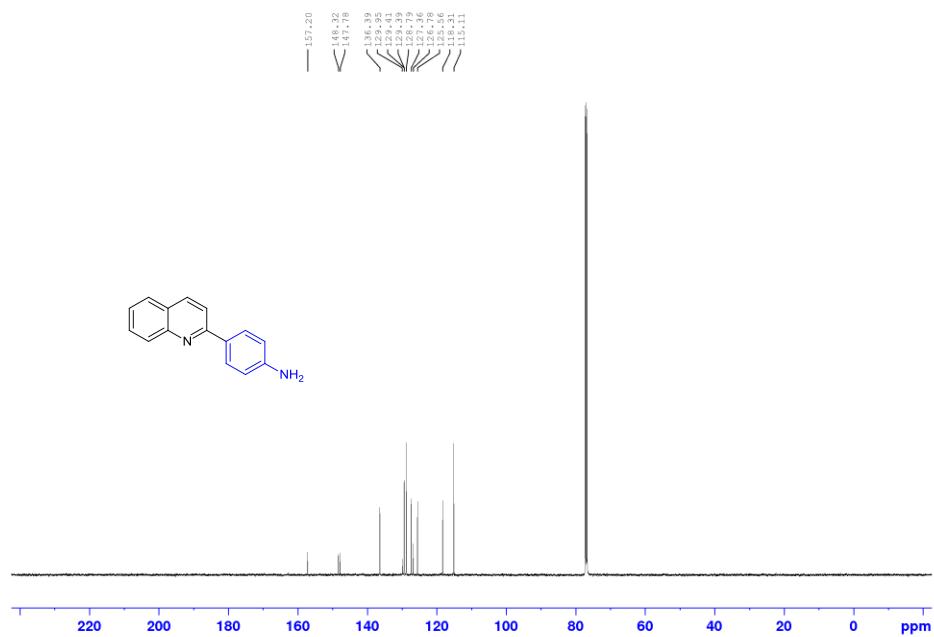
$^{13}\text{C}\{^1\text{H}\}$  NMR of **5-2o** ( $\text{CDCl}_3$ , 125.8 MHz)



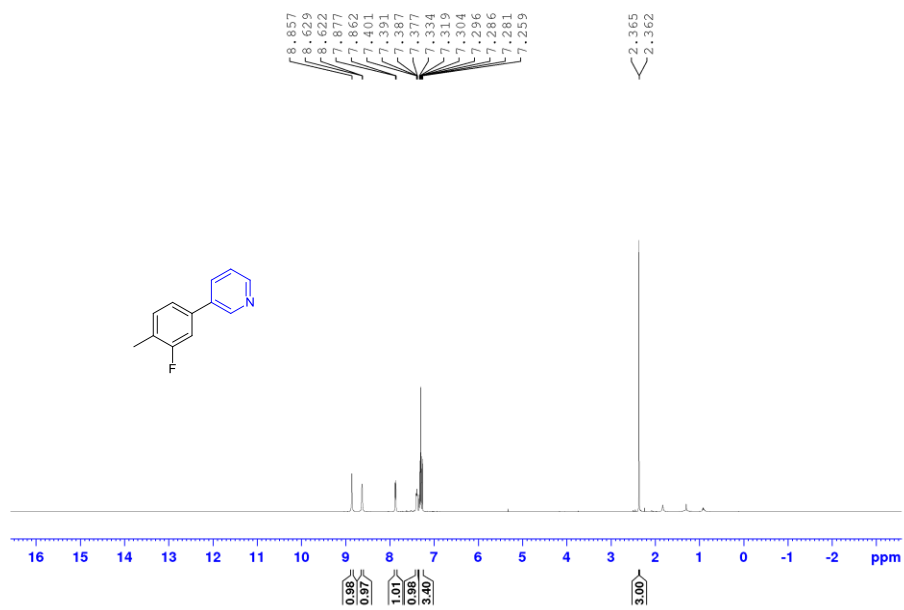
$^1\text{H}$  NMR of **5-2p**, ( $\text{CDCl}_3$ , 300.1 MHz)



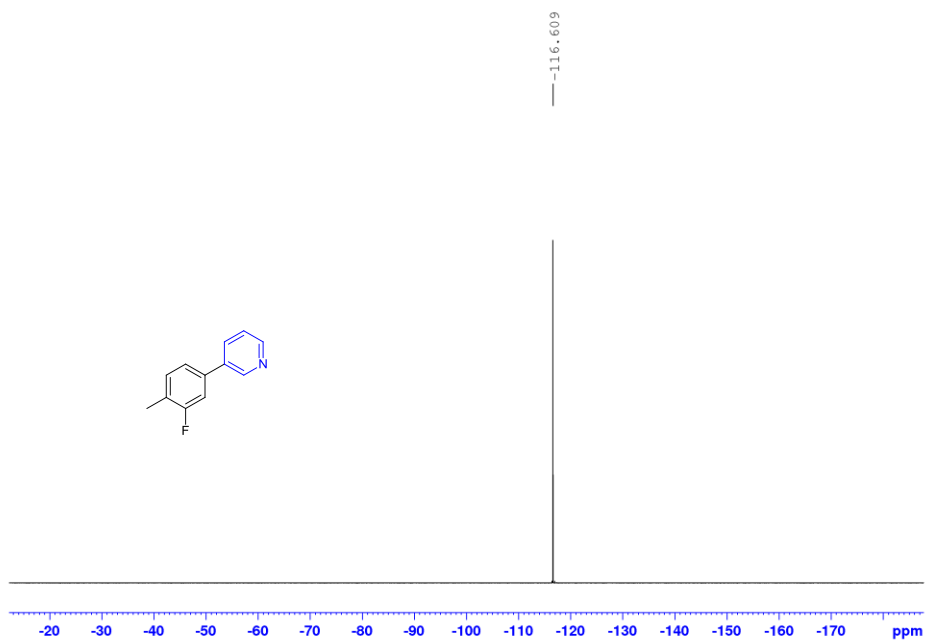
$^{13}\text{C}\{^1\text{H}\}$  NMR of **5-2p** ( $\text{CDCl}_3$ , 125.8 MHz)



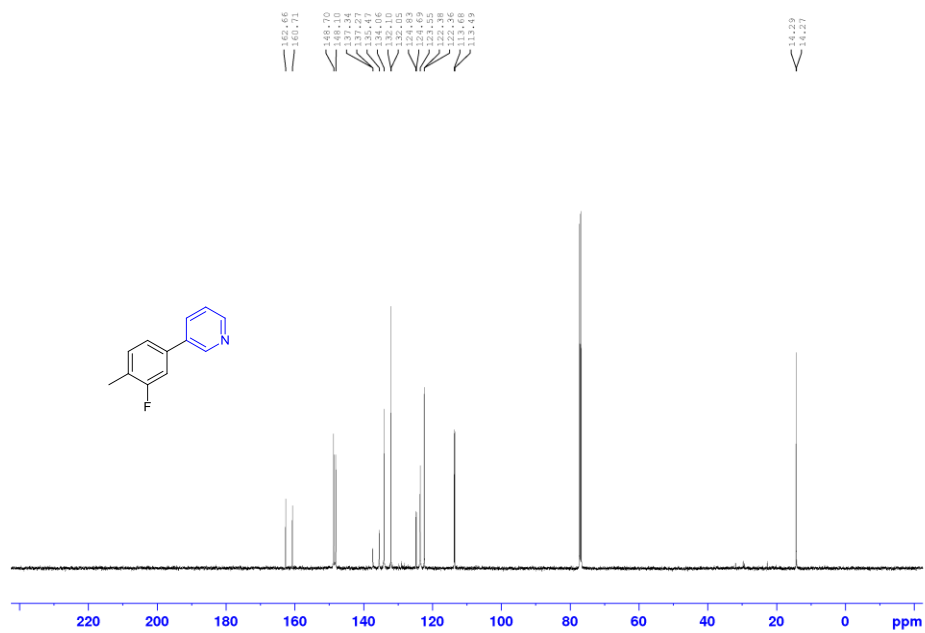
$^1\text{H}$  NMR of **5-3a**, ( $\text{CDCl}_3$ , 500.1 MHz)



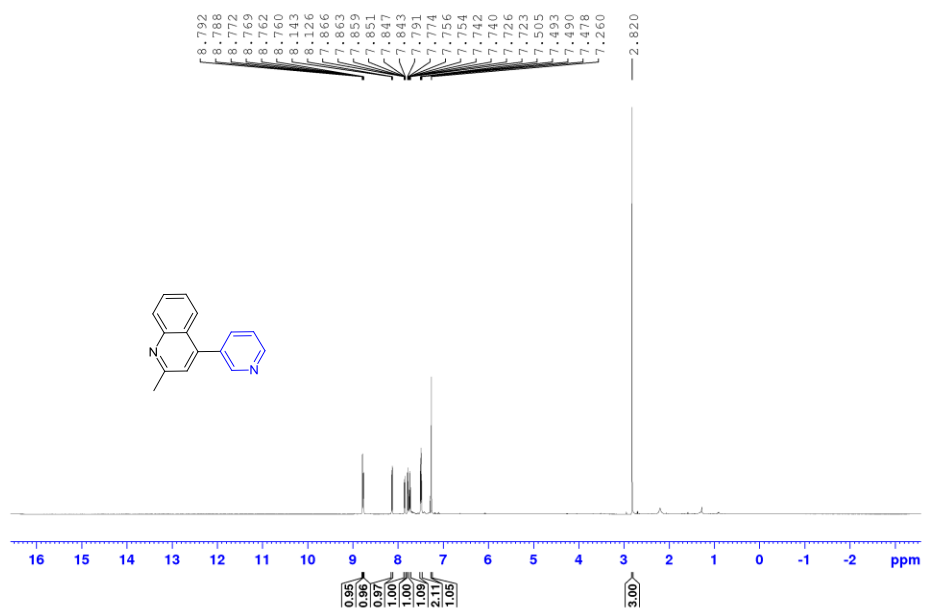
$^{19}\text{F}\{^1\text{H}\}$  NMR of **5-3a**, ( $\text{CDCl}_3$ , 470.5 MHz)



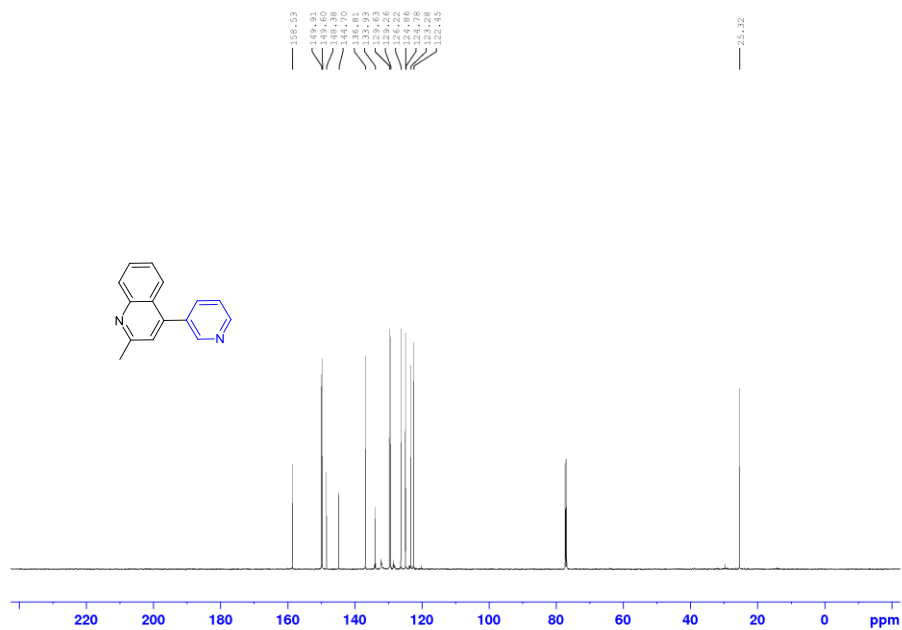
$^{13}\text{C}\{^1\text{H}\}$  NMR of **5-3a** ( $\text{CDCl}_3$ , 125.8 MHz)



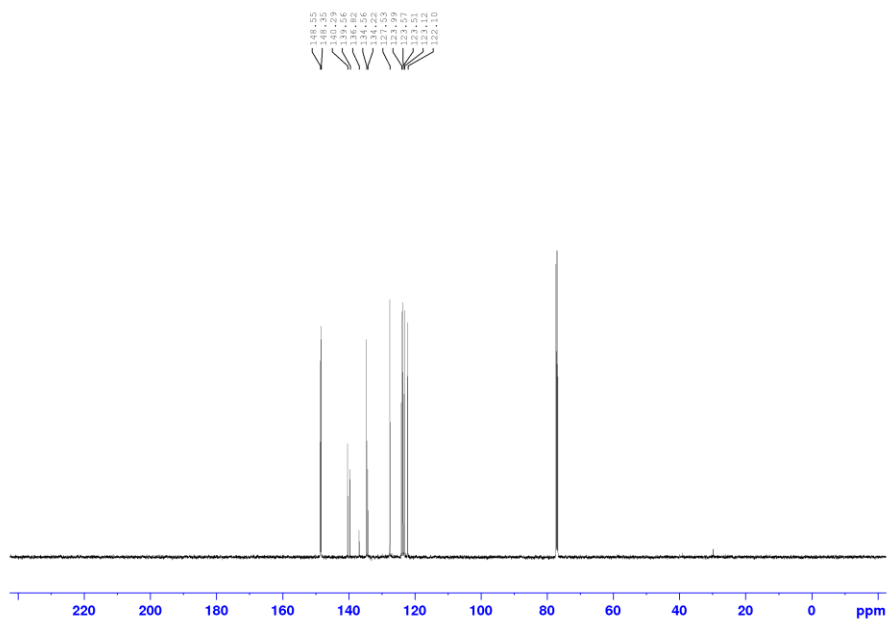
$^1\text{H}$  NMR of **5-3b**, ( $\text{CDCl}_3$ , 500.1 MHz)



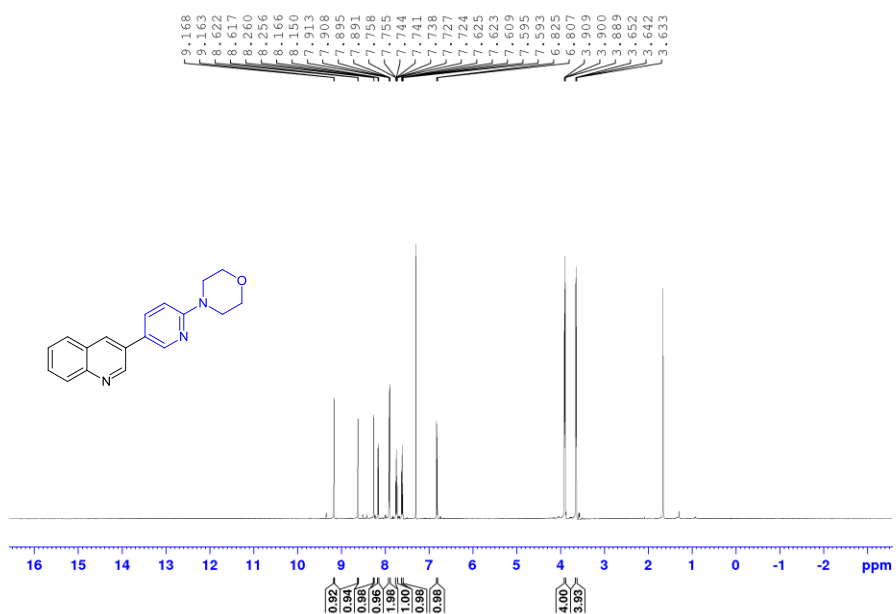
$^{13}\text{C}\{^1\text{H}\}$  NMR of **5-3b** ( $\text{CDCl}_3$ , 125.8 MHz)



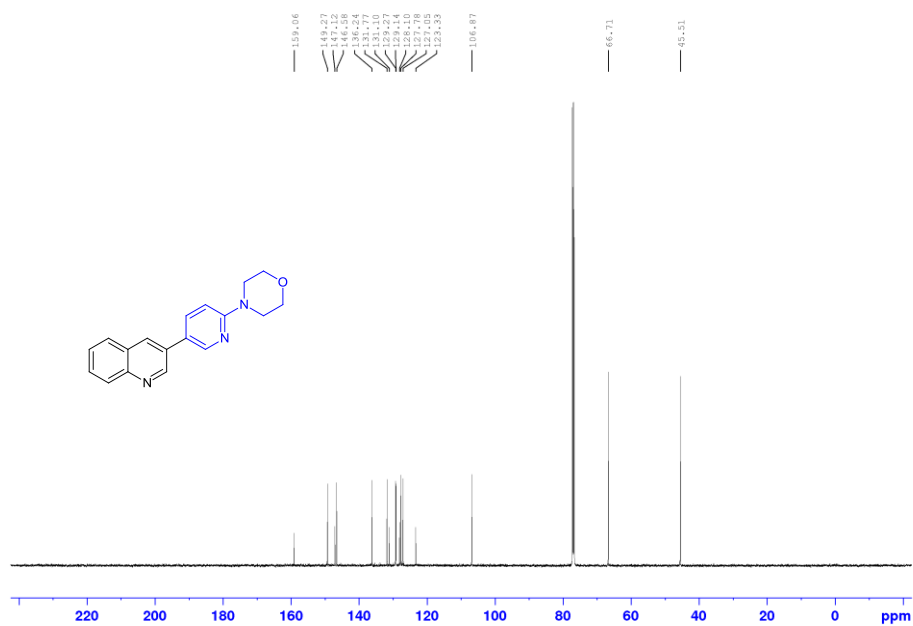
$^{13}\text{C}\{^1\text{H}\}$  NMR of **5-3c** ( $\text{CDCl}_3$ , 125.8 MHz)



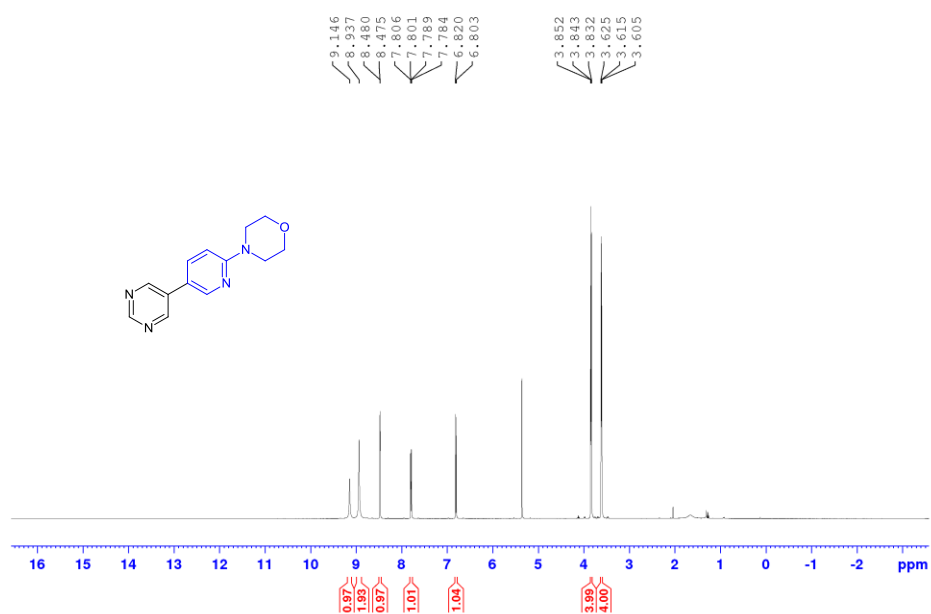
$^1\text{H}$  NMR of **5-3d**, ( $\text{CDCl}_3$ , 500.1 MHz)



$^{13}\text{C}\{^1\text{H}\}$  NMR of **5-3d** ( $\text{CDCl}_3$ , 125.8 MHz)

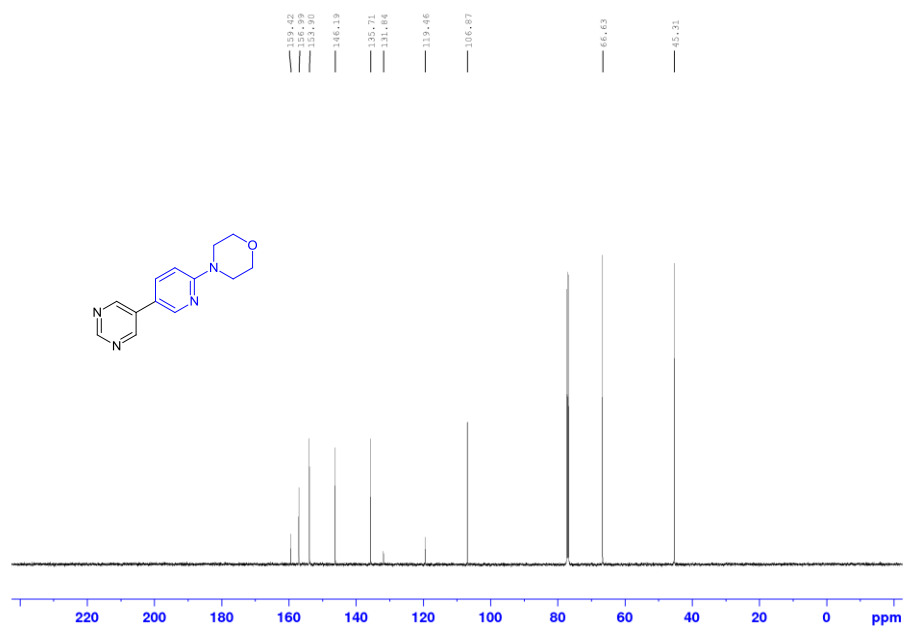


$^1\text{H}$  NMR of **5-3e**, ( $\text{CD}_2\text{Cl}_2$ , 500.1 MHz)

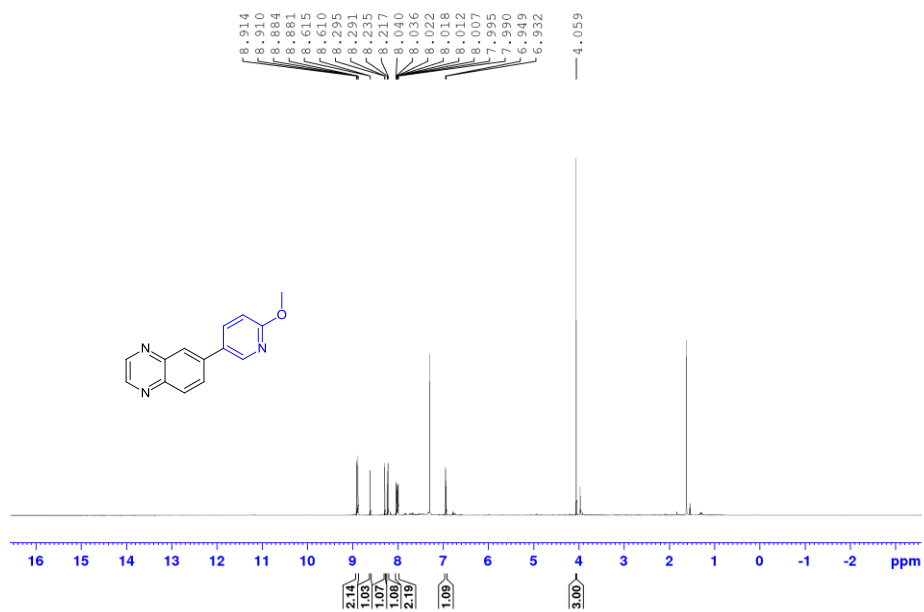




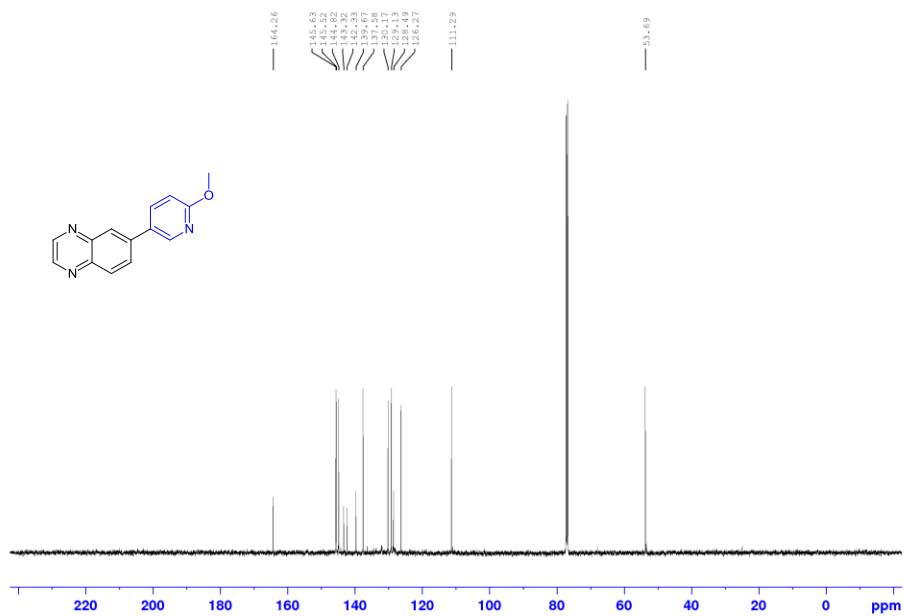
$^{13}\text{C}\{^1\text{H}\}$  NMR of **5-3e** ( $\text{CD}_2\text{Cl}_2$ , 125.8 MHz)



$^1\text{H}$  NMR of **5-3f**, ( $\text{CDCl}_3$ , 500.1 MHz)



$^{13}\text{C}\{^1\text{H}\}$  NMR of **5-3f** ( $\text{CDCl}_3$ , 125.8 MHz)



2 October, 2017

John Wiley & Sons, Inc.  
90 Eglinton Ave East, Suite 300  
Toronto, Ontario, Canada, M4P-2Y3

I am preparing my Ph.D. thesis for submission to the Faculty of Graduate Studies at Dalhousie University, Halifax, Nova Scotia, Canada. I am seeking your permission to include a manuscript version of the following paper(s) as a chapter in the thesis:

A Comparative Ancillary Ligand Survey in Palladium-Catalyzed C–O Cross-Coupling of Primary and Secondary Aliphatic Alcohols, Ryan S. Sawatzky, Breanna K. V. Hargreaves, Mark Stradiotto, *European Journal of Organic Chemistry*, 14, 2444-2449, 2016

Canadian graduate theses are reproduced by the Library and Archives of Canada (formerly National Library of Canada) through a non-exclusive, world-wide license to reproduce, loan, distribute, or sell theses. I am also seeking your permission for the material described above to be reproduced and distributed by the LAC(NLC). Further details about the LAC(NLC) thesis program are available on the LAC(NLC) website ([www.nlc-bnc.ca](http://www.nlc-bnc.ca)).

Full publication details and a copy of this permission letter will be included in the thesis.

Yours sincerely,

Ryan S. Sawatzky

---

Permission is granted for:

- a) the inclusion of the material described above in your thesis.
- b) for the material described above to be included in the copy of your thesis that is sent to the Library and Archives of Canada (formerly National Library of Canada) for reproduction and distribution.

Name: Bettina Loycke Title: Senior Rights Manager  
Signature: \_\_\_\_\_ Date: Oct 13, 2017

Nature Communications is an open access journal.

As of January 2016, the journal only publishes open access content, and legacy subscription content has been made freely accessible alongside the open access articles published in *Nature Communications* prior to 2016.

### Creative Commons Licenses

Nature Communications articles are published open access under a [CC BY license](#) (Creative Commons Attribution 4.0 International License). The CC BY license allows for maximum dissemination and re-use of open access materials and is preferred by many research funding bodies. Under this license users are free to share (copy, distribute and transmit) and remix (adapt) the contribution including for commercial purposes, providing they attribute the contribution in the manner specified by the author or licensor ([read full legal code](#)).

Some historical papers have been published under a non-commercial license. Users may request permission to use the works for commercial purposes or to create derivative works by emailing [permissions@nature.com](mailto:permissions@nature.com).

Under Creative Commons, authors retain copyright in their articles.

Visit our [open research site](#) for more information about [Creative Commons licensing](#).

**THIEME LICENSE  
TERMS AND CONDITIONS**

Dec 12, 2017

This Agreement between Ryan Sawatzky ("You") and Thieme ("Thieme") consists of your license details and the terms and conditions provided by Thieme and Copyright Clearance Center.

License Number	4246471423495
License date	Dec 12, 2017
Licensed Content Publisher	Thieme
Licensed Content Publication	Synlett
Licensed Content Title	Thieme Chemistry Journals Awardees – Where Are They Now? Efficient Cross-Coupling of Secondary Amines/Azoles and Activated (Hetero)Aryl Chlorides Using an Air-Stable DPEPhos/Nickel Pre-Catalyst
Licensed Content Author	Ryan S. Sawatzky, Michael J. Ferguson, Mark Stradiotto
Licensed Content Date	Jan 1, 2017
Licensed Content Volume	28
Licensed Content Issue	13
Type of Use	Dissertation/Thesis
Requestor type	author of the original Thieme publication
Format	electronic
Portion	full article/document
Will you be translating?	no
Distribution quantity	4
Specified additional information	For use in my Ph.D. thesis
Order reference number	
Title of your dissertation / thesis	Advances in Palladium and Nick Catalyzed Cross-Coupling Reactions
Expected completion date	Dec 2017
Estimated size (number of pages)	125
Requestor Location	Ryan Sawatzky 5681 Rhuland st. Apt. # 804  Halifax, NS B3H 4J6 Canada Attn: Ryan Sawatzky
Publisher Tax ID	DE 147638607
Billing Type	Invoice
Billing Address	Ryan Sawatzky 5681 Rhuland st. Apt. # 804  Halifax, NS B3H 4J6 Canada Attn: Ryan Sawatzky
Total	0.00 USD
Terms and Conditions	

**Terms and Conditions**

**Introduction**

The publisher for this copyrighted material is **Georg Thieme Verlag KG**, in the following referred to as **Publisher**. By clicking "accept" in connection with completing this licensing transaction, you agree that the following terms and conditions apply to this transaction (along with the Billing and Payment terms and conditions established by Copyright Clearance Center, Inc. ("CCC"), at the time that you opened your CCC account and that are available at any time at <<http://myaccount.copyright.com>>).

**Limited License**

Publisher hereby grants to you a non-exclusive license to use this material. Licenses are for one-time use only with a maximum distribution equal to the number specified in the license. The first instance of republication or reuse granted by this license must be completed within 12 months of the date this license was granted (although copies prepared before the end date may be distributed thereafter).

Licences for reuse in a **dissertation/thesis** are limited to the depository copies that have to be delivered within the university system. Any further use and follow-up publications require separate permission.

If you are **the author requesting full use of your article** in an Institutional Repository, special rules apply. For more detailed information, please check

[https://www.thieme.de/statics/dokumente/thieme/final/de/dokumente/sw\\_%20autorenounge/final\\_Authors\\_Rights\\_SR\\_20150122.pdf](https://www.thieme.de/statics/dokumente/thieme/final/de/dokumente/sw_%20autorenounge/final_Authors_Rights_SR_20150122.pdf)

**Geographic Rights: Scope**

Licenses may be exercised anywhere in the world.

**Altering/Modifying Material: Not Permitted**

You may not alter or modify the material in any manner (except that you may use, within the scope of the license granted, one or more excerpts from the copyrighted material, provided that the process of excerpting does not alter the meaning of the material or in any way reflect negatively on the publisher or any writer of the material), nor may you translate the material into another language.

**Reservation of Rights**

Publisher reserves all rights not specifically granted in the combination of (i) the license details provided by you and accepted in the course of this licensing transaction, (ii) these terms and conditions and (iii) CCC's Billing and Payment terms and conditions.

**License Contingent on Payment**

While you may exercise the rights licensed immediately upon issuance of the license at the end of the licensing process for the transaction, provided that you have disclosed complete and accurate details of your proposed use, no license is finally effective unless and until full payment is received from you (either by publisher or by CCC) as provided in CCC's Billing and Payment terms and conditions. If full payment is not received on a timely basis, then any license preliminarily granted shall be deemed automatically revoked and shall be void as if never granted. Further, in the event that you breach any of these terms and conditions or any of CCC's Billing and Payment terms and conditions, the license is automatically revoked and shall be void as if never granted. Use of materials as described in a revoked license, as well as any use of the materials beyond the scope of an unrevoked license, may constitute copyright infringement and publisher reserves the right to take any and all action to protect its copyright in the materials.

**Copyright Notice: Disclaimer**

Must include the following copyright and permission notice in connection with any reproduction of the licensed material: "© Georg Thieme Verlag KG."

**Warranties: None**

Publisher makes no representations or warranties with respect to the licensed material and adopts on its own behalf the limitations and disclaimers established by CCC on its behalf in its Billing and Payment terms and conditions for this licensing transaction.

**Indemnity**

You hereby indemnify and agree to hold harmless publisher and CCC, and their respective officers, directors, employees and agents, from and against any and all claims arising out of your use of the licensed material other than as specifically authorized pursuant to this license.

**No Transfer of License**

This license is personal to you, but may be assigned or transferred by you to a business associate (or to your employer) if you give prompt written notice of the assignment or transfer to the publisher. No such assignment or transfer shall relieve you of the obligation to pay the designated license fee on a timely basis (although payment by the identified assignee can fulfill your obligation).

**No Amendment Except in Writing**

This license may not be amended except in a writing signed by both parties (or, in the case of publisher, by CCC on publisher's behalf).

**Objection to Contrary Terms**

Publisher hereby objects to any terms contained in any purchase order, acknowledgment, check endorsement or other writing prepared by you, which terms are inconsistent with these terms and conditions or CCC's Billing and Payment terms and conditions. These terms and conditions, together with CCC's Billing and Payment terms and conditions (which are incorporated herein), comprise the entire agreement between you and publisher (and CCC) concerning this licensing transaction. In the event of any conflict

between your obligations established by these terms and conditions and those established by CCC's Billing and Payment terms and conditions, these terms and conditions shall control.

**Jurisdiction:**

This license transaction shall be governed by and construed in accordance with the laws of the Federal Republic of Germany. You hereby agree to submit to the jurisdiction of the federal and state courts located in Berlin, Germany for purposes of resolving any disputes that may arise in connection with this licensing transaction.

**Special Terms:**

v 1.3

Questions? [customer@copyright.com](mailto:customer@copyright.com) or +1-855-239-3415 (toll free in the US) or +1-978-646-2777.

---